Creation of an organic acid production platform in Aspergillus niger using a system-level approach

Meijer, Susan Lisette; Nielsen, Jens; Olsson, Lisbeth

Publication date:
2008

Document Version
Publisher's PDF, also known as Version of record

Creation of an organic acid production platform in *Aspergillus niger* using a system-level approach

Susan Meijer

Ph.D. Thesis
April 2008

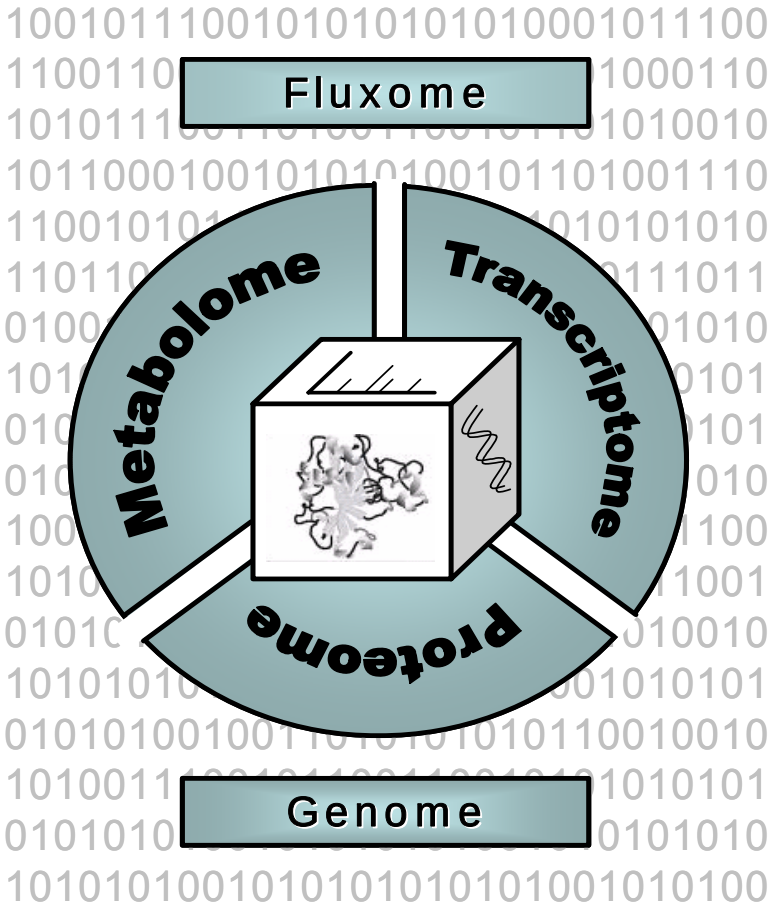

Center for Microbial Biotechnology
Department of Systems Biology

Acknowledgements

This thesis is based on experimental results carried out during my Ph. D. study at the Center of Microbial Biotechnology, Biocentrum, Technical University of Denmark in the period of September 2004 to September 2007. The study was financed by the Research School for Biotechnology (FOBI), the Royal Veterinary and Agricultural University (KVL) and Novozymes, for which I am grateful.

I wish to express my gratitude to my supervisors, Prof. Jens Nielsen and Prof. Lisbeth Olsson, for giving me the opportunity to carry out my Ph. D study at CMB. I am thankful for their excellent supervision and good scientific support. Also I would like to thank Gianni Panagiotou for his guidance and scientific input.

During my Ph. D project I entered the field of molecular biology and thanks to Michael Lynge Nielsen got familiar with this research area. Many thanks also to Arthur Ram (Leiden University), Peter Schaap (Wageningen University) and Wian de Jongh for providing some of the strains used in this study.
Since I had no experience in metabolic modelling several people helped me doing simulations. The help of Mikael Rørdam Andersen with the DNA microarray data was highly appreciated. Also the support for the flux calculations by Roberto Olivares and Manny Otero was most welcome.
The project also involved a fermentation part and I would like to thank Anne-Claire Chorin and Klaus Kinze for the hard work they put into running some of the cultivations. Furthermore, I would like to thank all the technicians for keeping the equipment up and running, which was not always an easy task.

To all my CMB colleagues, I would like to thank them for making CMB a fun and stimulating place to work. Especially ‘’Jakob’s lab’’ was always an interesting place to be. Of course, I would also express my appreciation to my office mates who socially and scientifically supported me all those years.

Finally, I would like to thank my family for their wonderful support and encouragement, especially in frustrating times.

Table of contents

Chapter 4

Chapter 5

Chapter 1

Outline of the thesis

Organic acids are important products that can be produced by multiple micro-organisms. Due to the growing demand for biological production platforms producing organic acids, several development programs have been initiated in order to create better cell factories. Chapter 2 gives a general introduction to biotechnological processes and techniques used in this area of research. Chapter 3 is focusing on cellular production platforms around succinic acid.

The aim of this work was to develop a cell factory for organic acid production, with the focus on succinate, and to gain more physiological knowledge of organic acid production using a system level approach. The micro-organism of choice for this research was the filamentous fungus *Aspergillus niger*. There are several reasons for choosing this particular micro-organism as cell factory for organic acid production:

1) it tolerates low pH (important when producing acids)
2) a wide variety of carbon sources can be used, including lignocellulose
3) it ensures high conversion rates of different substrates
4) high product yields can be achieved
5) it is a well studied micro-organism (lot of biochemical data available)
6) it has GRAS status (industrial production of e.g. citric acid and glucoamylase)

In order to create a better organic acid producer, we performed an in depth investigation on the effects of environmental factors in the central carbon metabolism of *Aspergillus niger* and assessed how they influence the organic acid production. Chapter 4 describes a medium optimisation study that determined the effect of different factors on the cellular behaviour of *Aspergillus niger*. A factorial design of experiments was used to determine the optimal medium composition for studying organic acid production. A separate study on the effect of oxygen on organic acid production was thereafter performed in well controlled fermentors. Chapter 5 is devoted to this oxygen effect on cellular behaviour, especially on the intra- and extra-cellular metabolite profiles, as well as the activities of several enzymes in the central carbon metabolism.

After these two physiological studies (described in chapter 4 and 5), different metabolic engineering strategies to improve succinate production were designed based on either metabolic model predictions or on rational thinking. Chapter 6 outlines two different gene deletions (Δ*sdh* and Δ*acl*) and gene targeting methods used to establish complete gene

deletions. The two deleted genes are involved in the primary metabolism of *A. niger* and have therefore a direct effect on the flux distribution, leading to different organic acid profiles. Also a batch characterisation of one of the deletion mutants is presented in this chapter. Chapter 7 gives a deeper inside into regulatory pathways that influence organic acid production. In this chapter a Δ*acuB* strain is characterised. AcuB is known to regulate genes involved in the glyoxylate pathway. This is one of the pathways leading to the organic acids succinate and malate, and therefore the influence of this regulatory node on the metabolic behaviour of the cells is expected to give us valuable information.

Instead of gene deletion, gene insertion also serves as a useful tool for metabolic engineering, and in chapter 8 and 9 two different gene insertion strategies are described and their influence on transcription, flux and organic acid production in the metabolic network is evaluated. In chapter 8 the isocitrate lyase (*icl*) gene was selected for overexpression, since this is expected to lead to an upregulation of the glyoxylate pathway. In chapter 9 two heterologous genes, fumarate reductase (*frds*) and fumarase (*fum*), have been inserted in the genome of *A. niger*, thereby creating a cytosolic reductive pathway towards succinate.

Finally, chapter 10 will summarize the results presented in this dissertation. It describes how the use of different –ome technologies can lead to a better understanding of the cell behaviour, which can lead to the development of better cell factories. Also a future outlook is given in chapter 10.

Chapter 2

Introduction

In this chapter the relevance of biotechnology and industrial applications is discussed. Additionally, an overview of techniques used for cell factory understanding and improvement is given.

2.1 Biotechnology

2.1.1 Biotechnological relevance

Biotechnology has developed rapidly during the last decades and has become one of the most promising future technologies. Especially industrial biotechnology, also called ‘’White biotechnology’’, has had a profound effect on the history of science and technology. Biochemical and microbiological processes belong to the oldest processes used by mankind. According to ancient history, bread making and beer brewing have already been established more than 6000 years ago (Boulton et al. 2004).

Major advances in molecular biology during the second half of the 20th century made biotechnology even more important and integrated it with industrial processes (Bud 1989). The technical improvements have made it possible for biotechnological processes to compete with the chemical industry. It is by no means new that biotechnology is applied in industry and environment. Biotech products are part of our daily live. Just think of the food industry (Beck and Ulrich 1993), where defined microbial cultures convert milk to yoghurt, yeasts produce bread, and pectinolytic enzymes remove cloudiness from fruit juices. Other examples of food products produced by biotechnological methods are: beer, wine, spirits, vinegar, cheese, sauerkraut, pickles and tea. Also in other parts of the world there are numerous biotechnologically produced foods such as sake, soya sauce, tempeh, tofu and kwas.

Biotechnology has also contributed to the environment in a variety of ways. Since the turn of the 19th to the 20th century the application of microbiological processes in waste water purification has led to a a major improvement on the purity of our drink water, but also rivers, lakes and other surface waters (Daims et al. 2006). Additionally, biotechnology offers methods for soil remediation. Micro-organisms are able to change the valency of inorganic

matter, e.g. uranium, thereby removing it from soil and groundwater. So biotechnology is closely connected to the environment.

2.1.2 Advantages and disadvantages of biotechnological processes

Biotechnology has contributed significantly to converting traditional production methods into modern, more effective ones and to increase the quality of the products. For example, beer brewing in the second half of the 20th century was switched from an open liquid surface production method to a closed submerged method. As a result many vats gave way for large fermentors with automatic control. Therefore, beer brewing processes nowadays use less than one tenth of the operating space compared to the early days, saving a lot equipment, manpower and additionally they ensure a consistent product quality (Boulton and Quain 2001).

Unfortunately, the use of biological systems also has a drawback compared to the use of physical or chemical processes. Biological systems often show a limited stability and have low productivities. One of the main goals in biotechnology is therefore to overcome the limits of biological systems. With the developments in molecular biology and systems biology we are able to improve the biological systems drastically. However, we must keep in mind that biotechnology is always competing with the petrochemical industry. In case a non-biotechnological method is developed fulfilling the qualitative requirements with a higher economic benefit than the biotechnological process, the former is still preferred. Products consisting of small molecules are considerably more susceptible to this economic selection than products consisting of large, specifically built molecules. For example, biotechnologically produced pharmaceuticals do not have the competitive pressure as for instance organic acids since no chemical process can produce the complex structure of the pharmaceutical economically, while organic acids can easily be produced by a handful of chemical reactions.

On the other hand, the products that are chemically synthesized are often accompanied by unwanted side products and their production processes imply unacceptable effects on the environment. This may result in choosing quantitatively submaximal production methods in order to stay in an acceptable range of quality. In this area biotechnological processes clearly have an advantage that eventually can lead to cost savings in e.g. the omission of environmental protection measures. Basically, this corresponds to the actual request of sustainability. Biotechnology has an advantage when sustainability becomes priority.

2.1.3 Future of biotechnology

The future of biotechnology lies in the increasing demand for environmental friendly processes, mainly driven by increasing political pressure. Biotechnological processes are believed to be a starting point in the battle against global warming. Furthermore, the prices of petroleum-derived carbon backbone molecules, used in chemical synthesis, are expected to increase in the near future (fossils become scarce), which will make biotechnology thrive. The future of biotechnology is very promising for improved processing, as well as healthier and higher quality products (e.g. rice with higher content of Vitamin A, allergen-free cashew nuts). Such advantageous properties of products could be achieved by metabolic engineering. Also technical advances, especially the upcoming nanotechnology, opens new possibilities for biotechnology, transferring the successful principles of application of machines into the molecular range.

The Biomass Program from the United States Government has identified a top ten of value-added chemicals, that can be produced from biomass, that would economically and technically be applicable in industry (Werpy and Petersen 2004). The top ten building blocks are shown in Table 2.1. Notice that the list contains eight low molecular weight organic acids. Even though these compounds suffer from a huge competition with the chemical industry, they are still believed to have potential for being manufactured in a biological way, indicating that biotechnology is getting more important over time.

Table 2.1 Top ten value added building blocks determined by the Biomass Program from the United States Government (Werpy and Petersen 2004).

Building Blocks
1,4 diacids (succinate, fumarate and malate)
2,5 furan dicarboxylic acid
3 hydroxy propionic acid
aspartic acid
glucaric acid
glutamic acid
itaconic acid
levulinic acid
3-hydroxybutyrolactone
glycerol

2.1.4 Biotechnologically important micro-organisms

In biotechnological processes different micro-organisms are being used for different purposes. It is important to find a suitable micro-organism for the biotechnological process in question. Bacteria and fungi are examples of organisms used in industry. However, fungi are definitely the main source of micro-organisms used in industrial application.

Fungi are a large and diverse group of eukaryotes having their own kingdom on equal footing with plants and animals (Bennett 1997). They distinguish themselves by spore formation, efficient secretion pathways and wide absorption spectra for different nutrients. Fungi have the most diverse and effective range of adaptation of all eukaryotes. They can stand severe dryness, extreme pH and are able to survive a range of other environmental stresses. Due to their versatile biochemical nature, fungi produce a wide array of acids and degradative enzymes to support their absorptive life style. This fungal variability in enzymes and metabolites is so astonishing, that we can exploit it for biotechnological purposes.

A large group of biotechnological products are enzymes. They are not only used in the food industry, like in meat and dairy production, or in fruit and vegetable processing, but also for bleaching paper, in washing powders, in the starch industry and in leather finishing. Another class of products produced in a biotechnological way are low molecular-weight organic chemicals, such as ethanol and citric acid. These chemicals are produced in bulk and have a wide area of application. Citric acid is widely used as an acidulant in soft drinks and many foods, as a buffer, and as an emulsifying agent. Ethanol is used as biofuel. Also complex molecules are made in a biotechnological way. Some fungal products are exploited as antibiotics (e.g. penicillin), immune response suppressants (e.g. cyclosporin A), blood pressure lowering agents (e.g. mevalonin), or other pharmaceuticals. Finally, many fungi are used directly as food and food flavoring agents. Asian food fermentations such as soy sauce, and tempeh are worldwide known as a food source.

2.1.5 Yeast versus filamentous fungi

The best studied fungus is the yeast *Saccharomyces cerevisiae,* not only because of its importance in baking, brewing, and fermentation processes, but also because it is one of the best understood species and most important eukaryotic model organism. Mark Adams once said: ‘‘Yeast is the unicellular human’’ (at the Oklahoma State University meeting). *S. cerevisiae* has been used not only as a model for studying human disease, but also as a model for all fungi. However, yeast is not as evolved as filamentous fungi. Filamentous fungi

have more genes and bigger genomes. They have more adaptation capabilities and form secondary metabolites unlike yeast. The genes controlling these functions can only be studied in organisms that possess them. That is why modelling of other filamentous fungi is so crucial in understanding their behaviour.

Two other well studied fungi are *Aspergillus nidulans* and *Neurospora crassa.* These filamentous organisms are often used as model organisms and were one of the first filamentous fungi to be sequenced. One of their big advantages is that more than 50 years of research data are available for these organisms in the area of classical genetics and biochemistry. Detailed genetic maps and hundreds of mutants are available for both species. Few experimental organisms have been so well characterised with respect to biological function. *Aspergillus* species are one of the most important fungal species used in industry.

Members of the genus *Aspergillus* biosynthesize a variety of economically important primary and secondary metabolites, including citric acid, mevalonin, and aflatoxin. They are able to secrete large amounts of their own proteins (‘‘homologous proteins’’), such as glucoamylase. Sophisticated technologies have been developed to handle large-scale *Aspergillus* fermentations. Although most of these fermentation processes are well established, the underlying genetics are still poorly understood (Cullen 2007). With the current increase in sequencing projects, making more complete genomic sequences available, we should be able to achieve a better physiological understanding and improve the production of chemicals and enzymes using these micro-organisms. The availability of genome data from related fungi gives us the possibility to compare genomes, their structure and get a feeling for evolutionary events. Nine *Aspergillus* species have been sequenced (Galagan et al. 2005; Machida et al. 2005; Nierman et al. 2005). An overview of the genome content and characteristics of four *Aspergillus* species is given in Table 2.2. Two genomes of *Aspergillus niger* are sequenced and have recently been released, the mutagenized CBS 513.88 strain (Pel et al. 2007) and the wild-type strain ATCC1015 (Baker 2006) (http:// genome.jgi-psf.org/Aspni1/Aspni1.home. html). The combination of sequence information and the existing biochemical, morphological, and genetic data, will make it easier to assign meaning to sequence data and help in designing new strategies for strain optimisation. So genomes are very important in the development of industrial production strains. However, genome information alone is not sufficient.

Table 2.2 Summary of four different Aspergillus genomes (data from Archer and Dyer 2004).

	A. niger	*A. nidulans*	*A. oryzae*	*A. fumigatus*
Genome size (Mb)	35.9	30.1	36.7	28.6
GC content (mole%)	50	50	48	50
Predicted genes	14097	9967	14063	9746
Coding sequences (% of total)	55.2	50.9	45.1	49.1
Mean gene length (bp)	1323	1536	1178	1442
Genes with introns (%)	87	89	81	76
Genes with Pfam hits	5306	4512	5306	4403

2.2 Biotechnological techniques

With the increase in biological applications and sequence information we also need to develop ways to better understand and control the microbial systems. The classical approach has been to analyse the role of individual components (genes or proteins) in the overall cell function. As a consequence of large sequencing programs, an increasing number of complete genomic sequences from different micro-organisms have become available. This led to substantial research efforts assigning function to all identified open reading frames, also referred to as functional genomics. Furthermore, there has been a significant development in molecular biology techniques, which have made it possible to optimise industrial fermentations through introduction of directed genetic modifications, an approach referred to as metabolic engineering. These two very important advances have changed the traditional way of looking at cellular behaviour (Nielsen and Olsson 2002).

Instead of looking at single cell components in the cell we now try to integrate data in order to retrieve a more holistic view on cell function. As a result we reach an increased understanding of the molecular mechanisms that make it possible to describe the interaction between all the components in the cell, which is called systems biology. However, to really establish a system-level understanding of the cell, information about the DNA sequence, RNA expression profiles, protein levels and metabolite levels is obligatory. But also information about the interaction between the different levels, such as protein-protein interactions, protein-DNA interactions and protein-metabolite interactions is needed. All these levels of information depend on each other and control the mechanisms in the cell, e.g. transcriptional control, control of mRNA degradation, translational control, protein activation/inactivation, and allosteric control of enzymes. We can divide the different levels of information into several classes namely: genome, transcriptome, proteome, interactome, metabolome and fluxome (Figure 2.1). Different strategies and technologies are used in the

different classes and an overview of the most used and advanced technologies is described below.

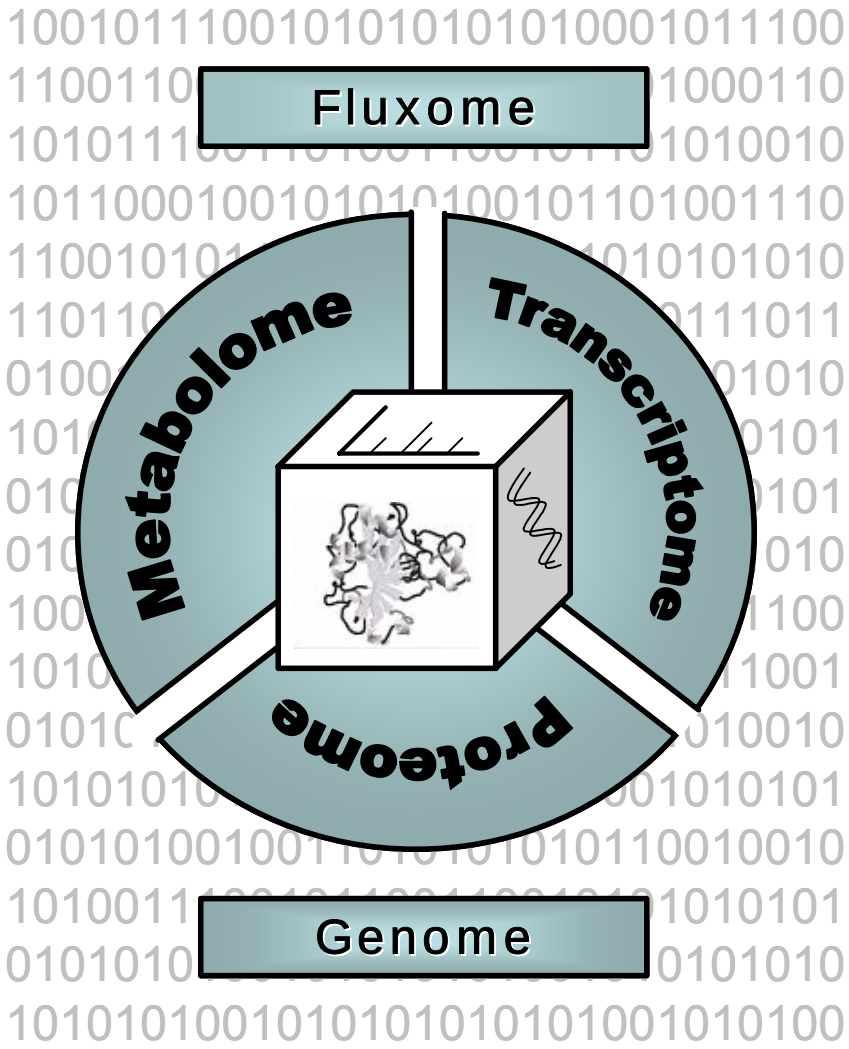

Figure 2.1 The different information levels in the cell that determine the functional behaviour of micro-organisms. Model integration of the different levels is required for enabling a systematic comprehension of the cells.

2.2.1 Genome analysis

In comparative sequence analysis the sequenced genomes of two or more organisms are compared, thereby facilitating annotation of protein coding genes and important functional sequences within proteins and in nonprotein-coding DNA, such as promoters (Casselton and Zolan 2002). As stated before, this field has gained a lot of attention since the introduction of high-throughput sequencing methods. There are many successful examples of comparative

sequence analysis among different organisms for annotation of protein coding sequences and functional sequences in proteins. However, identification of functional sequence elements not coding for proteins, e.g. sequences regulating gene expression, is much more complicated due to the relative rapid rate of change of non-protein-coding sequences in evolution and their relative simple structures (Archer and Dyer 2004; Cliften et al. 2001). Therefore, comparison of relative closely related organisms is more likely to identify potential non-protein-coding elements. These comparisons now become available, but only on a small scale in comparison to the protein coding comparisons.

2.2.2 Transcriptome analysis

Nowadays, DNA micro arrays are the common tool for transcriptome analysis and they are used in many laboratories. DNA microarrays measure relative expression levels of genes and have made it possible to estimate the level of expression of thousands of genes simultaneously (Butte 2002). This makes it possible to identify changes in expression between different biological states or when some genes are deleted or over-expressed.

Microarrays may give indications of gene function and regulation. Genes that participate in the same cellular processes often share similar transcription profiles. By mining expression data, using software applying clustering algorithms that group together genes with similar transcription profiles, genes with similar expression can be identified (Chou et al. 2007). Function of “orphan” genes may then be inferred from function of genes that have a similar transcription profile.

Genes with similar transcription might also be regulated by the same mechanisms, and therefore have similar regulatory elements in their promoters. Promoter analysis of such genes can reveal new regulatory elements and identify genes that are under regulation of a certain transcription factor. This has been demonstrated by Ideker et al. (2001a) in yeast, who identified potential Gal4 binding sites in nine new genes by promoter analysis of the genes in the same expression clusters as the genes with established Gal4-binding sites. Ideker et al. (2001b) also analysed the transcriptome of a number of mutants with deleted galactose genes against a reference strain. This yielded valuable information about the regulatory network of the galactose utilisation pathway. Apparently, transcriptome analysis can be used for reconstruction of regulatory pathways. Moreover, methods have been developed, in which the transcriptional responses have been correlated with metabolic networks, based on information from genome-scale metabolic models. This has resulted in

the discovery of so-called reporter metabolites, that are metabolites around which the most significant transcriptional changes occur (Patil and Nielsen 2005).

Microarrays seem to be promising, but it is an extremely difficult task. There are problems with sample taking, (m)RNA extraction and normalisation of the arrays. Sample taking and extraction of (m)RNA cause deviation in measurements. Normalisation is a process for removing variation in the arrays. This variation can stem from a variety of factors including physical properties of the dyes (heat and light sensitivity, relative half-life), efficiency of dye incorporation, experimental variability in probe coupling and processing procedures, and scanner settings at the data collection step. So it is difficult to retrieve representable data from the arrays due to all this variation, making it an elaborate and difficult process. Another question is how useful the information of mRNA is, if no information of other levels such as protein level and post transcriptional modification are taken into account.

In this dissertation microarray experiments have been used to analyse the metabolic pathway regulation on a gene expression level and the information is incorporated with other analyses to discover metabolic regulation mechanisms (Chapter 8 and 9).

2.2.3 Proteome analysis

Investigations of the correlation between mRNA and protein expression in *S. cerevisiae* have shown the difficulties of predicting the yeast proteome directly from the transcriptome (Ideker et al. 2001a; Gygi et al. 1999a). The correlation between mRNA and protein abundance is poor for some genes, suggesting that post-transcriptional regulation plays an important role.

Therefore, proteomics brings us one step closer in understanding gene function than transcriptome analysis, but the analysis is more difficult. Proteome analysis is aiming at the simultaneous large-scale analysis of the protein composition of an organism and covers many aspects of protein characterisation, such as identification, quantification, characterisation and identification of post-translational modifications, and cellular localisation (Gygi et al. 1999b). Two-dimensional (2D) gel electrophoresis has been used for analysis of the proteome since the late 1970's and is still an important technique for separation and quantification in proteomics today. The proteins resolved by 2D electrophoresis can be identified and analysed for e.g. post-translational modifications by mass spectroscopy combined with genomic information. However, specific classes of proteins (membrane or glycosylated proteins) and low abundance proteins are known to be absent or underrepresented in 2D gel patterns, moreover quantification in gels is very difficult. Due to

these limitations new methods for analysis of proteins in complex mixtures have been developed, avoiding the use of 2D gels (Kocher and Superti-Furga 2007). All these techniques rely on mass spectrometry for identification and quantification of the different proteins.

The focus of recent efforts in proteomics has shifted to quantitative methods that allow protein levels to be measured globally. Global analysis methods in proteomics are still under development. They are used for determination of protein biochemistry and cellular localisation, which gives important information about protein function and regulation.

2.2.4 Interactome analysis

Analysis of interactions between proteins and between proteins and DNA is very important for unravelling signal transduction pathways and can be used to generate functional annotations for proteins with unknown function. The yeast two-hybrid system, for example, identifies pairs of interacting proteins and has been used for genome-wide studies (Mukherjee et al. 2001). Future two-hybrid technologies might overcome some of the present-day limitations, but protein-protein interactions may also be analysed with protein chips (Phizicky et al. 2003).

Furthermore, with ultrasensitive mass spectrometric protein identification methods, it is possible to identify directly protein complexes on a proteome-wide scale. Two large-scale affinity tagging and mass spectroscopy analyses of protein complexes in yeast have been published (Gavin et al. 2002; Ho et al. 2002). These studies identified hundreds of novel protein-protein interactions and protein complexes and provide insight into the mechanisms by which protein complexes are co-ordinated into high-order networks responsible for many fundamental cellular processes.

Analysis of protein-DNA interactions gives valuable information about transcription factors and is required to construct a complete map of transcriptional regulation. A methodology, which can be applied genome-wide, has been developed. This method, which combines DNA arrays with chromatin immunoprecipitation, identifies sequences that are directly bound by a specific transcription factor of interest *in vivo*. It has discovered many new putative targets of some transcription factors (Iyer et al. 2001). Also protein chips have potential for studying protein-DNA interactions.

2.2.5 Metabolome analysis

The metabolome represents integrative information, and therefore, analysis of the metabolome may give further insight into the function of genes (Jewett et al. 2006; Wu et al. 2005). With the development of analytical technologies for separation, quantification, and identification, it is nowadays possible to measure hundreds of intracellular metabolites by using GC-MS (gas chromatography and mass spectroscopy) and LC-MS (Mashego et al. 2007).

The power of metabolomics has been illustrated by a study on *S. cerevisiae*. Raamsdonk et al. (2001) found that, even when mutation of a gene causes no obvious phenotype, metabolite profiling can still give clues to gene function. Raamsdonk et al. (2001) also showed that deletion mutants, having lost similar functions, have similar metabolite profiles. They propose that this can be used for assigning function to orphan genes by comparing the changes in metabolite profile, produced by deleting the gene, with a library of such profiles generated by individually deleting genes of known function.

Metabolome profiling has been used in order to find specific physiological states under different cultivation conditions and in different strains (see Chapter 5 and 7).

2.2.6 Fluxome analysis

Analysis of the fluxome (all fluxes in the cell) gives information about, which pathways are active and to what extent. In this way, a better understanding of what is occurring inside the cell at a given time is obtained. Fluxes cannot be measured directly *in vivo*, but some fluxes can be estimated from the uptake rates of substrates and secretion rates of metabolic products (Metabolic Flux Balance). Furthermore, an estimation of the flux distribution at metabolic branch points can be obtained using a mathematical model of the metabolism combined with the analysis of ^{13}C-labelling patterns of intracellular metabolites (Metabolic Network Analysis). The labelling pattern of ^{13}C in intracellular metabolites may be analysed using either GC-MS, LC-MS or NMR and has been proven very useful for identification of the metabolic network structures. From the labelling pattern and metabolite balancing a detailed analysis can be obtained, including flux estimation, identification of the network topology, metabolic channelling and subcellular compartmentation (Christensen and Nielsen 2000).

Metabolic Network Analysis has been used to get a better comprehension of the changes in primary metabolism instigated by metabolic engineering of *Aspergillus niger* (see Chapter 8 and 9).

2.2.7 Databases

Due to the development of all the above mentioned experimental techniques a lot of data are acquired in a short time. Therefore, comprehensive data sets are needed to grasp an entire picture of the organism of interest. Baxevanis (2003a+b) has given an overview of the available databases. Extensive computer databases first arose when the large-scale sequencing projects started. Although databases of nucleic acids and amino acids sequences, such as EMBL, Genbank and Swiss Prot, are still the largest, most utilised and best maintained, there is also a great interest in databases to store other types of molecular data. For instance, the Database of Interacting Proteins, BIND and MIPS contain searchable indices of known protein-protein interactions. TRANSFAC and SCPD catalogue interactions between proteins and DNA. Furthermore, databases of metabolic pathways have been established, such as EcoCyc (for *E. coli*), MetaCyc (different organisms), KEGG and WIT.

This recent explosion in both variety and amount of information poses two challenges to databases. Firstly, the information must be maintained systematically in a format that is compatible with both single queries and global searches. Secondly, the databases must be updated against the ever-increasing biological knowledge. It is also important to control the quality of the incoming data. Because conditions, under which experiments are performed, differ from lab to lab and even within labs, a reference point must be defined to which all the data can be compared and which can be used for simulation, modelling and system identification. This is a complicated task and means that many of the current experimental procedures must be automated to enable high-throughput experiments to be carried out with precise control of quality. This development is already seen in the collection of microarray data that have set some defined guidelines for the information on experiments (MIAME) (Maurer et al. 2005).

Because of the large amount of information, programs are developed using algorithms for database similarity searches. BLAST, FASTA and CLUSTAL are examples of these programs and make it possible to search through the databases.

Due to the rapid increase of information collected in the databases it is crucial not to neglect the importance of developing useful and reliable programs for updating and searching through the databases.

2.2.8 Modelling

With all technical advances mentioned above our understanding of the molecular mechanisms in biological systems is accelerating. Nevertheless, such knowledge does not provide us with an understanding of biological systems as systems (Kitano 2002a+b). Genes and proteins are components of the system. While an understanding of what constitutes the system is necessary for understanding the system, this is not sufficient. In order to understand biological systems, firstly the structures of the system need to be identified. This means that the regulatory relationships of genes and interactions of proteins that provides signal transduction and metabolic pathways, need to be identified. Besides, physical structures of organisms, cells, organelles, chromatin and other components need to be established. Secondly, we need a set of principles and methodologies that link the behaviour of molecules to system characteristics and functions. Different computer aided models have been developed that try to explain and predict cellular behaviour. Roughly, these models can be grouped into two kinds (Figure 2.2): stoichiometric models and kinetic models (Wiechert 2002). Each method has its own advantages and disadvantages.

Kinetic models are used for describing and predicting the dynamic behaviour of cells. However, building successful dynamic or kinetic models is heavily dependent on knowing or discovering the underlying biological mechanisms. Therefore, these models are severely constrained by the lack of enzymatic kinetic data and the discrepancy between *in vivo* and *in vitro* enzyme activities. Kinetic models try to simulate the physical and chemical processes (known or hypothesized) that take place in the biological system of interest. Mechanism and dynamics are closely related, and much of the value of kinetic modelling lies in the unique ability of dynamic experiments to reveal new and useful information about the complex biological systems. Kinetic models are able to extract more information about the dynamic behaviour of the cell compared to stoichiometric models that simulate steady state behaviour of the biological system.

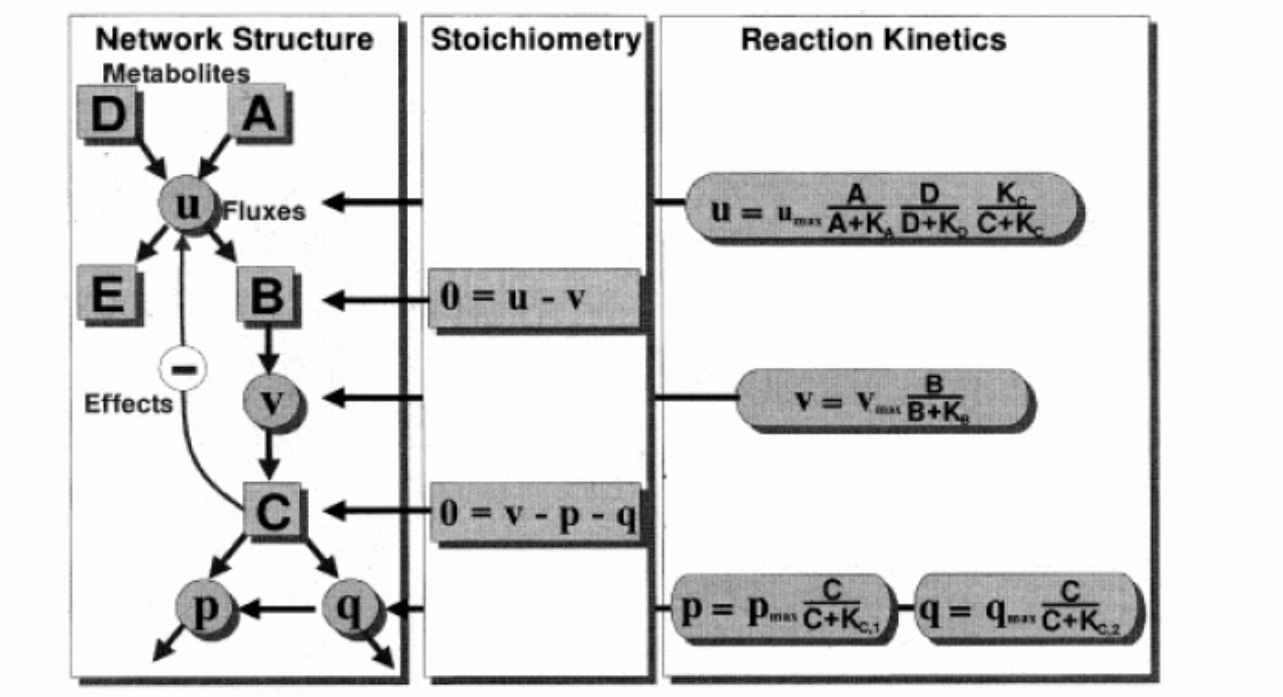

Figure 2.2 Schematic overview of a metabolic network structure and different kinds of models that are used to describe metabolic behaviour (Wiechert 2002).

Stoichiometric models are used to simulate a ‘’special’’ steady state in the biological system. They describe the biochemical reactions in the cell as a set of algebraic equations. The advantage of stoichiometric models is that they do not require any kinetic information about the biological system. Therefore, they can be used for large scale metabolic networks. For several micro-organisms these stoichiometric models are available, such as *E. coli*, *S. cerevisiae*, *A. niger*, *A. nidulans*, *S. coelicolor* (Pramanik and Keasling 1997; Foster et al. 2003; David et al. 2003; David et al. 2006, Borodina et al. 2005, respectively). They have already shown to be very useful in predicting cellular behaviour and discovering new genetic targets for optimisation of biological systems. Stoichiometric models are particularly useful in the field of Metabolic Engineering and were used in chapter 6, 8 and 9. The disadvantage of the stoichiometric model is that it cannot take into account the regulatory mechanisms that the cell possesses in contrast to the kinetic models.

Nevertheless, computer aided models are an important feature in understanding cellular behaviour. With the development of more advanced algorithms and models the behaviour of biological systems will be better understood and predicted.

2.3 References

Archer DB and Dyer PS 2004. From genomics to post-genomics in *Aspergillus*. *Current Opinion in Microbiology* **7** (5):499-504.

Baker SE 2006. *Aspergillus niger* genomics: Past, present and into the future. *Medical Mycology* **44**:S17-S21.

Baxevanis AD 2003a. Using genomic databases for sequence-based biological discovery. *Molecular Medicine* **9** (9-12):185-192.

Baxevanis AD 2003b. The molecular biology database collection: 2003 update. *Nucleic Acids Research* **31** (1):1-12.

Beck CI and Ulrich T 1993. Biotechnology in the food-industry - An invisible revolution is taking place. *Bio-Technology* **11** (8):895-&.

Bennett JW 1997. White paper: Genomics for filamentous fungi. *Fungal Genetics and Biology* **21** (1):3-7.

Borodina I, Krabben P and Nielsen J 2005. Genome-scale analysis of *Streptomyces coelicolor* A3(2) metabolism. *Genome Research* **15** (6):820-829.

Boulton CA and Quain D 2001. Brewing yeast and fermentation. By *Blackwell Sciences Ltd ,* London.

Boulton CA, Brookes PA, Stevens R and Briggs DE 2004. Brewing: Sciense and practice. editors *Woodhead Publishing Limited*, Abington Hall, Abington.

Bud R 1989. History of Biotechnology. *Nature* **337** (6202):10.

Butte A 2002. The use and analysis of microarray data. *Nature Reviews Drug Discovery* **1** (12):951-960.

Casselton L and Zolan M 2002. The art and design of genetic screens: Filamentous fungi. *Nature Reviews Genetics* **3** (9):683-697.

Chou JW, Zhou T, Kaufmann WK, Paules RS and Bushel PR 2007. Extracting gene expression patterns and identifying co-expressed genes from microarray data reveals biologically responsive processes. *Bmc Bioinformatics* **8**:427.

Christensen B and Nielsen J 2000. Metabolic network analysis of *Penicillium chrysogenum* using C^{13}-labeled glucose. *Biotechnology and Bioengineering* **68** (6):652-659.

Cliften PF, Hillier LW, Fulton L, Graves T, Miner T, Gish WR, Waterston RH and Johnston M 2001. Surveying *Saccharomyces* genomes to identify functional elements by comparative DNA sequence analysis. *Genome Research* **11** (7):1175-1186.

Cullen D 2007. The genome of an industrial workhorse. *Nature Biotechnology* **25** (2):189-190.

Daims H, Taylor MW and Wagner M 2006. Wastewater treatment: a model system for microbial ecology. *Trends in Biotechnology* **24** (11):483-489.

David H, Akesson M and Nielsen J 2003. Reconstruction of the central carbon metabolism of *Aspergillus niger*. *European Journal of Biochemistry* **270** (21):4243-4253.

David H, Hofmann G, Oliveira AP, Jarmer H and Nielsen J 2006. Metabolic network driven analysis of genome-wide transcription data from *Aspergillus nidulans*. *Genome Biology* **7** (11):R108.

Forster J, Famili I, Fu P, Palsson BO and Nielsen J 2003. Genome-scale reconstruction of the *Saccharomyces cerevisiae* metabolic network. *Genome Research* **13** (2):244-253.

Galagan JE, Calvo SE, Cuomo C, Ma LJ, Wortman JR, Batzoglou S, Lee SI, Basturkmen M, Spevak CC, Clutterbuck J, Kapitonov V, Jurka J, Scazzocchio C, Farman M, Butler J, Purcell S, Harris S, Braus GH, Draht O, Busch S, d'Enfert C, Bouchier C, Goldman GH, Bell-Pedersen D, Griffiths-Jones S, Doonan JH, Yu J, Vienken K, Pain A, Freitag M, Selker EU, Archer DB, Penalva MA, Oakley BR, Momany M, Tanaka T, Kumagai T, Asai K, Machida M, Nierman WC, Denning DW, Caddick M, Hynes M, Paoletti M, Fischer R, Miller B, Dyer P, Sachs MS, Osmani SA and Birren BW 2005. Sequencing of *Aspergillus nidulans* and comparative analysis with *A-fumigatus* and *A-oryzae*. *Nature* **438** (7071):1105-1115.

Gavin AC, Bosche M, Krause R, Grandi P, Marzioch M, Bauer A, Schultz J, Rick JM, Michon AM, Cruciat CM, Remor M, Hofert C, Schelder M, Brajenovic M, Ruffner H, Merino A, Klein K, Hudak M, Dickson D, Rudi T, Gnau V, Bauch A, Bastuck S, Huhse B, Leutwein C, Heurtier MA, Copley RR, Edelmann A, Querfurth E, Rybin V, Drewes G, Raida M, Bouwmeester T, Bork P, Seraphin B, Kuster B, Neubauer G and Superti-Furga G 2002. Functional organization of the yeast proteome by systematic analysis of protein complexes. *Nature* **415** (6868):141-147.

Gygi SP, Rist B, Gerber SA, Turecek F, Gelb MH and Aebersold R 1999b. Quantitative analysis of complex protein mixtures using isotope-coded affinity tags. *Nature Biotechnology* **17** (10):994-999.

Gygi SP, Rochon Y, Franza BR and Aebersold R 1999a. Correlation between protein and mRNA abundance in yeast. *Molecular and Cellular Biology* **19** (3):1720-1730.

Ho Y, Gruhler A, Heilbut A, Bader GD, Moore L, Adams SL, Millar A, Taylor P, Bennett K, Boutilier K, Yang LY, Wolting C, Donaldson I, Schandorff S, Shewnarane J, Vo M, Taggart J, Goudreault M, Muskat B, Alfarano C, Dewar D, Lin Z, Michalickova K, Willems AR, Sassi H, Nielsen PA, Rasmussen KJ, Andersen JR, Johansen LE, Hansen LH, Jespersen H, Podtelejnikov A, Nielsen E, Crawford J, Poulsen V, Sorensen BD, Matthiesen J, Hendrickson RC, Gleeson F, Pawson T, Moran MF, Durocher D, Mann M, Hogue CWV, Figeys D and Tyers M 2002. Systematic identification of protein complexes in *Saccharomyces cerevisiae* by mass spectrometry. *Nature* **415** (6868):180-183.

Ideker T, Galitski T and Hood L 2001a. A new approach to decoding life: Systems biology. *Annual Review of Genomics and Human Genetics* **2**:343-372.

Ideker T, Thorsson V, Ranish JA, Christmas R, Buhler J, Eng JK, Bumgarner R, Goodlett DR, Aebersold R and Hood L 2001b. Integrated genomic and proteomic analyses of a systematically perturbed metabolic network. *Science* **292** (5518):929-934.

Iyer VR, Horak CE, Scafe CS, Botstein D, Snyder M and Brown PO 2001. Genomic binding sites of the yeast cell-cycle transcription factors SBF and MBF. *Nature* **409** (6819):533-538.

Jewett MC, Hofmann G and Nielsen J 2006. Fungal metabolite analysis in genomics and phenomics. *Current Opinion in Biotechnology* **17** (2):191-197.

Kitano H 2002a. Looking beyond the details: a rise in system-oriented approaches in genetics and molecular biology. *Current Genetics* **41** (1):1-10.

Kitano H 2002b. Systems biology: A brief overview. *Science* **295** (5560):1662-1664.

Kocher T and Superti-Furga G 2007. Mass spectrometry-based functional proteomics: from molecular machines to protein networks. *Nature Methods* **4** (10):807-815.

Machida M, Asai K, Sano M, Tanaka T, Kumagai T, Terai G, Kusumoto KI, Arima T, Akita O, Kashiwagi Y, Abe K, Gomi K, Horiuchi H, Kitamoto K, Kobayashi T, Takeuchi M, Denning DW, Galagan JE, Nierman WC, Yu JJ, Archer DB, Bennett JW, Bhatnagar D, Cleveland TE, Fedorova ND, Gotoh O, Horikawa H, Hosoyama A, Ichinomiya M, Igarashi R, Iwashita K, Juvvadi PR, Kato M, Kato Y, Kin T, Kokubun A, Maeda H, Maeyama N, Maruyama J, Nagasaki H, Nakajima T, Oda K, Okada K, Paulsen I, Sakamoto K, Sawano T, Takahashi M, Takase K, Terabayashi Y, Wortman JR, Yamada O, Yamagata Y, Anazawa H, Hata Y, Koide Y, Komori T, Koyama Y, Minetoki T, Suharnan S, Tanaka A, Isono K, Kuhara S, Ogasawara N and Kikuchi H 2005. Genome sequencing and analysis of *Aspergillus oryzae*. *Nature* **438** (7071):1157-1161.

Mashego MR, Rumbold K, De Mey M, Vandamme E, Soetaert W and Heijnen JJ 2007. Microbial metabolomics: past, present and future methodologies. *Biotechnology Letters* **29** (1):1-16.

Maurer M, Molidor R, Sturn A, Hartler J, Hackl H, Stocker G, Prokesch A, Scheideler M and Trajanoski Z 2005. MARS: Microarray analysis, retrieval, and storage system. *Bmc Bioinformatics* **6**:101.

Mukherjee S, Bal S and Saha P 2001. Protein interaction maps using yeast two-hybrid assay. *Current Science* **81** (5):458-464.

Nielsen J and Olsson L 2002. An expanded role for microbial physiology in metabolic engineering and functional genomics: moving towards systems biology. *Fems Yeast Research* **2** (2):175-181.

Nierman WC, Pain A, Anderson MJ, Wortman JR, Kim HS, Arroyo J, Berriman M, Abe K, Archer DB, Bermejo C, Bennett J, Bowyer P, Chen D, Collins M, Coulsen R, Davies R, Dyer PS, Farman M, Fedorova N, Fedorova N, Feldblyum TV, Fischer R, Fosker N, Fraser A, Garcia JL, Garcia MJ, Goble A, Goldman GH, Gomi K, Griffith-Jones S, Gwilliam R, Haas B, Haas H, Harris D, Horiuchi H, Huang J, Humphray S, Jimenez J, Keller N, Khouri H, Kitamoto K, Kobayashi T, Konzack S, Kulkarni R, Kumagai T, Lafton A, Latge JP, Li WX, Lord A, Majoros WH, May GS, Miller BL, Mohamoud Y, Molina M, Monod M, Mouyna I, Mulligan S, Murphy L, O'Neil S, Paulsen I, Penalva MA, Pertea M, Price C, Pritchard BL, Quail MA, Rabbinowitsch E, Rawlins N, Rajandream MA, Reichard U, Renauld H, Robson GD, de Cordoba SR, Rodriguez-Pena JM, Ronning CM, Rutter S, Salzberg SL, Sanchez M, Sanchez-Ferrero JC, Saunders D, Seeger K, Squares R, Squares S, Takeuchi M, Tekaia F, Turner G, de Aldana CRV, Weidman J, White O, Woodward J, Yu JH, Fraser C, Galagan JE, Asai K, Machida M, Hall N, Barrell B and Denning DW 2005. Genomic sequence of the pathogenic and allergenic filamentous fungus *Aspergillus fumigatus*. *Nature* **438** (7071):1151-1156.

Patil KR and Nielsen J 2005. Uncovering transcriptional regulation of metabolism by using metabolic network topology. *Proceedings of the National Academy of Sciences of the United States of America* **102** (8):2685-2689.

Pel HJ, de Winde JH, Archer DB, Dyer PS, Hofmann G, Schaap PJ, Turner G, de Vries RP, Albang R, Albermann K, Andersen MR, Bendtsen JD, Benen JAE, van den Berg M, Breestraat S, Caddick MX, Contreras R, Cornell M, Coutinho PM, Danchin EGJ, Debets AJM, Dekker P, van Dijck PWM, van Dijk A, Dijkhuizen L, Driessen AJM, d'Enfert C, Geysens S, Goosen C, Groot GSP, de Groot PWJ, Guillemette T, Henrissat B, Herweijer M, van den Hombergh JPTW, van den Hondel CAMJ, van der Heijden RTJM, van der Kaaij RM, Klis FM, Kools HJ, Kubicek CP, van Kuyk PA, Lauber J, Lu X, van der Maarel MJEC, Meulenberg R, Menke H, Mortimer MA, Nielsen J, Oliver SG, Olsthoorn M, Pal K, van Peij NNME, Ram AFJ, Rinas U, Roubos JA, Sagt CMJ, Schmoll M, Sun JB, Ussery D, Varga J, Vervecken W, de Vondervoort PJJV, Wedler H, Wosten HAB, Zeng AP, van Ooyen AJJ, Visser J and Stam H 2007. Genome sequencing and analysis of the versatile cell factory *Aspergillus niger* CBS 513.88. *Nature Biotechnology* **25** (2):221-231.

Phizicky E, Bastiaens PIH, Zhu H, Snyder M and Fields S 2003. Protein analysis on a proteomic scale. *Nature* **422** (6928):208-215.

Pramanik J and Keasling JD 1997. Stoichiometric model of *Escherichia coli* metabolism: Incorporation of growth-rate dependent biomass composition and mechanistic energy requirements. *Biotechnology and Bioengineering* **56** (4):398-421.

Raamsdonk LM, Teusink B, Broadhurst D, Zhang NS, Hayes A, Walsh MC, Berden JA, Brindle KM, Kell DB, Rowland JJ, Westerhoff HV, van Dam K and Oliver SG 2001. A functional genomics strategy that uses metabolome data to reveal the phenotype of silent mutations. *Nature Biotechnology* **19** (1):45-50.

Werpy T and Petersen G 2004. Top value added chemicals from biomass. *http://www nrel gov/docs/fy04osti/35523 pdf* (27-03-2008).

Wiechert W 2002. Modelling and simulation: tools for metabolic engineering. *Journal of Biotechnology* **94** (1):37-63.

Wu LA, van Winden WA, van Gulik WM and Heijnen JJ 2005. Application of metabolome data in functional genomics: A conceptual strategy. *Metabolic Engineering* **7** (4):302-310.

Chapter 3

Succinic acid

Improving the organic acid production in *A. niger* will be assessed in a targeted approach. Since it is not possible to increase all organic acid yields at the same time succinate was used as model organic acid. It was attempted to divert fluxes toward succinate production. A short introduction to succinate and its relevance for biotechnology is presented in this chapter.

3.1 Industrial relevance of succinic acid

Succinic acid can be seen as a platform chemical from which several other industrially relevant compounds can be produced. Succinic acid and its derivatives are widely used as specialty chemicals with applications in polymers, foods, pharmaceuticals and cosmetics. This acid is a valuable four-carbon intermediate that can be converted by catalytic processes into a number of compounds, such as 1,4 – butanediol, tetrahydrofuran, and γ-butyrolactone. The chemistry of succinic acid to the primary families of derivatives is shown in Figure 3.1.

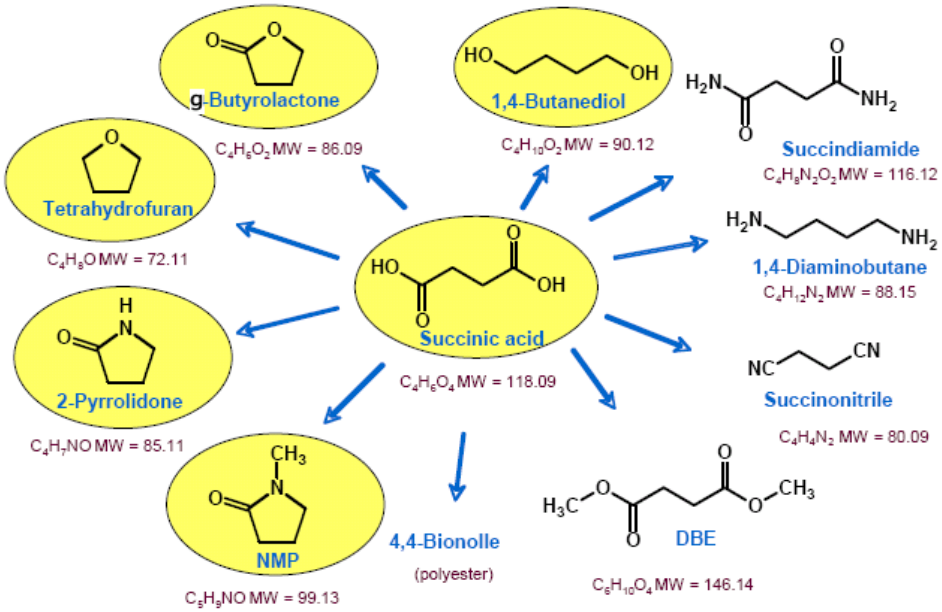

Figure 3.1 The platform chemical succinic acid and its primary families of derivatives that are widely used in industry (Werpy and Petersen 2004).

Nowadays there are four major markets for succinic acid:

- The first and largest is as a surfactant/detergent/foaming agent. Succinic acid can be esterified to dimethyl succinate, which is marketed as an environmentally friendly solvent.
- The second market is as an ion chelator, where it is used in electroplating to prevent corrosion of metals.
- The third is the food market, where it is used as an acidulant/pH modifier, as flavouring agent or as an anti-microbial agent.
- The fourth market is the production of health related agents, including pharmaceuticals, antibiotics, amino acids and vitamins.

Biotechnologically produced succinic acid has the potential to become a large-volume commodity chemical that would form the basis for supplying many important intermediate and specialty chemicals for the consumer product industry. As a commodity chemical, succinic acid can replace many commodities based on benzene and intermediate petrochemicals, resulting in a large reduction in pollution of the environment. The development of low-cost routes would have a significant impact on the demand for succinic acid. It would expand current markets and open up new markets for the acid. If the price can be reduced, the total succinic acid production could be bigger than the citric acid production and will come in the range of ethanol production. In 2004 the total trade market for succinic acid was $ 1.3 billion dollars and is still expanding (Werpy and Petersen 2004). The total production requirement was around $2.72 * 10^8$ kgs of succinic acid per year in 1999 (Zeikus et al. 1999).

Succinic acid is an expensive compound and attempts are made to lower the production costs. Currently, succinic acid is manufactured by the hydrogenation of maleic anhydride to succinic anhydride, followed by hydration to succinic acid. A fermentation process for succinic acid production is desirable because in such processes, renewable resources such as starchy crops and other agricultural products can be used as feedstock. The cost price for succinic acid produced petrochemically ranged from $5.90 to $8.80 per kgs in the year 1999, which was 10 times more than the costs of citric acid (Zeikus et al. 1999). Due to advances in fermentation and separation technology for the biological process, the production costs have been reduced to $ 2/kgs and, therefore, it is attractive to produce it biochemically (Potera 2005). However, in order to compete with other petrochemical derived products and to open up new specialty and commodity markets for succinic acid, the fermentation costs need to be at or below $0.5/kgs (Werpy and Petersen 2004). This is a significant technical challenge that could be met by further advances in the biobased succinic acid process.

3.2 Process improvements regarding succinic acid production

There are several key areas for improvement in the fermentation process for succinic acid. First of all, the productivity is an important factor for improvement. This will reduce the capital and operating costs of fermentation. We need to achieve a productivity of at least 2.5 g/L/hr in order for the process to be economically competitive with the petrochemical industry. Most likely this will be achieved by metabolic engineering strategies. A second key area for improvement is the medium composition. Medium designs for commercial fermentations can save a lot of money, since for bulk chemical production the medium costs have a large influence on the cost price. There is a thrive towards a minimal amount of nutrients. Furthermore, expensive nutrient components, such as yeast extract and biotin, must be avoided. Waste materials like molasses, corn steep liquor or equivalents are desirable. The final titer is also a point for reducing the overall process costs. Although this is not the most important aspect, a high final titer will drastically reduce the downstream processing costs. The separation and concentration of succinic acid will be simplified immensely if high product titers are achieved. Since downstream processing costs are often substantial this will affect the total production costs. Finally, the fermentation conditions can be optimised. The fermentation should be run at a low pH, and preferably without requiring any neutralisation. Both the cost of neutralisation and the conversion of the succinic acid salt to the free acid add significant costs to the fermentation process. This can be avoided when the fermentation process is run at a low pH, as can be achieved with *Aspergillus*.

3.3 Metabolic pathways leading to succinic acid

There are three possible metabolic pathways leading towards succinate: the oxidative part of the TCA cycle, the reductive part of the TCA cycle, and the glyoxylate bypass (Figure 3.2) (Magnuson and Lasure 2004). Metabolism by either the oxidative part of the TCA cycle or the glyoxylate bypass pathway conserves only four of the six carbons from glucose in the four-carbon succinic acid product. On the other hand, the reductive part of the TCA cycle produces two four-carbon acids for every glucose molecule metabolised via glycolysis, operating in conjunction with the caboxylation reaction catalysed by pyruvate carboxylase (Figure 3.2). Thus, anaerobic metabolism is preferred for succinic acid production, since it can theoretically generate a very high yield of 2 mol succinic acid / mol glucose. Under anaerobic conditions NAD^+ can be regenerated by reducing fumarate to succinate, which is

also called fumarate respiration. This strategy is used by several anaerobic bacteria that naturally produce a lot of succinate.

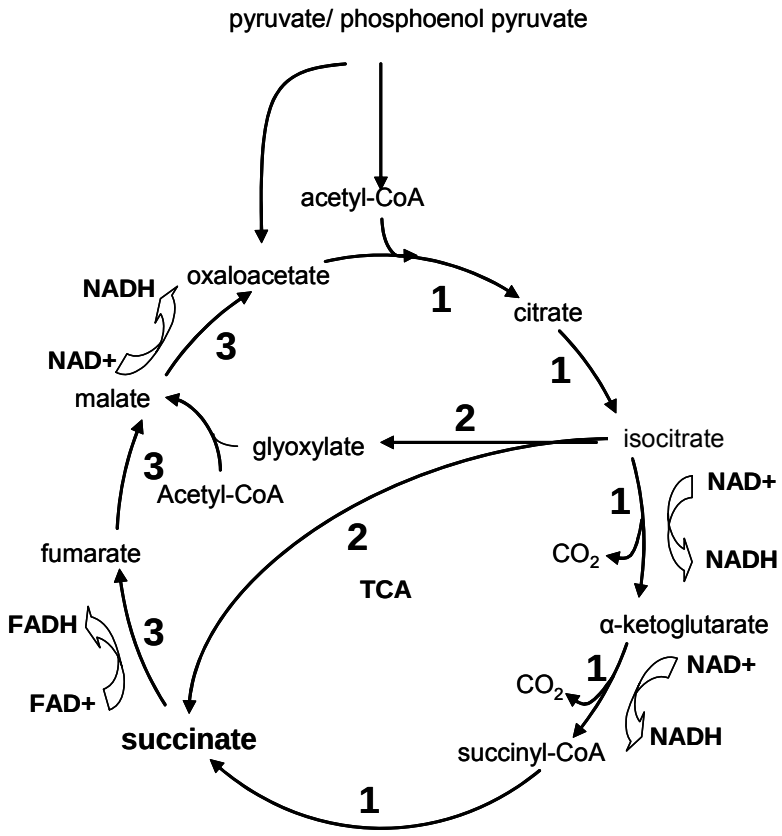

Figure 3.2 The metabolic pathways leading to succinate. 1 = oxidative TCA cycle, 2 = glyoxylate bypass, 3 = reductive TCA cycle.

The disadvantage of using these anaerobic bacteria is that they are not tolerant to acidic conditions and the fermentation needs to be neutralised. The fermentations are operated at pH values around 6.5 and the pK_a values for succinate are 4.21 and 5.64 at 22 ºC. Therefore in bacterial fermentations the succinic acid salt is produced (Datta 1992). However, the free acid is required to manufacture commodity and specialty chemicals. This raises the costs of fermentation immensely, because a lot of base is needed to neutralise the medium, thereby producing succinic acid salt. During the downstream processing the succinic acid needs to be separated from the fermentation broth and acidification is required to retrieve again the acid form of succinic acid. Normally, the downstream processing costs account for 60-70% of the product costs (Baniel and Eyal 1995). Therefore, the major cost inefficiencies associated with product recovery, concentration, acidification and purification have made it unattractive to create a fermentation-based succinate production process in these anaerobic bacteria.

Over the past 5-10 years there has been considerable research in order to develop improved micro-organisms and separation technologies to reduce the overall cost of biobased succinic acid. All these advances have made the production of succinic acid based chemicals from carbohydrates via fermentation practical and economically feasible. Therefore, it has been designated to one of the top ten value-added compounds for which a biological process route is more desirable than the traditional chemical production route (Werpy and Petersen 2004). However, more improvements are needed to make the biological process out-compete the chemical process. The two main areas of improvement are:

- the development of better succinic acid producing micro-organisms
- the development of better downstream processing technologies

3.4 Micro-organisms producing succinic acid

Until now most emphasis has been on bacterial fermentations for biological succinic acid production, as relatively efficient processes have been developed for anaerobic bacteria (see McKinlay et al 2007, for a recent review). However, some eukaryotic micro-organisms are also known to produce succinic acid. The yeast *Saccharomyces cerevisiae*, for example, produces succinate when the CO_2 concentration is held at high levels during the fermentation (Aguilera et al 2005). Arikawa et al. (1999) studied the effect of TCA cycle enzymes on succinic acid production and found that in *S. cerevisiae* succinic acid is mainly produced by the reductive part of the TCA cycle, fumarate respiration. Also filamentous fungi are known to produce succinic acid in small amounts as by-product. *Fusarium* spp. (Foster 1949), *Aspergillus* spp. (Bercovitz et al. 1990), and *Penicillium simplicissimum* (Gallmetzer et al. 2002) are known to produce and secrete the acid in low concentrations. Nowadays, succinic acid is produced biochemically from glucose using several bacteria like an engineered *Anaerobiospirillum succiniciproducens,* an engineered *Eschericia coli*, and most recently via an engineered *Mannheimia succiniciproducens.* For a comparison between their production capabilities see Table 3.1.

Table 3.1 The succinic acids yields and productivities achieved in two naturally producing micro-organisms and in metabolically engineered *E. coli*.

Organism	Yield (g/g)	Productivity (g/L/h)
Anaerobiospirullum succiniciproducens	0.98	0.6
Mannheimia succiniciproducens	0.7	1.2
Escherichia coli (anaerobic)	1.1	1.3
Escherichia coli (aerobic)	0.94	1.1

3.4.1 Bacterial micro-organisms naturally producing succinic acid

The natural over-producers *A. succiniciproducens* and *M. succiniciproducens* produce succinate at relatively high rates and concentrations during anaerobic fermentation at pH 7 (Zeikus et al. 1999; Song et al. 2006). However, a wide range of fermentation by-products, such as ethanol, acetic, formic and lactic acids are also formed. This leads to reduced succinate yield and increases the complexity of the purification process. It has been observed that *M. succiniciproducens* and *A. succiniciproducens* mainly use the phosphoenolpyruvate carboxykinase (PEPCK) and the reductive TCA cycle route for succinate production. Therefore, phosphoenolpyruvate is an important branching point in the formation of succinate. Two pathways originate here: one towards succinate and another towards the major by-products. PEPCK is a carboxylating enzyme fixating CO_2, making the CO_2 availability a critical parameter for the enzyme kinetics. The dissolved CO_2 concentration should ideally be as close to its maximum as possible. This can be ensured by CO_2 sparging and/or addition of carbonate to the fermentation media (Lee et al. 1999; Zeikus et al. 1999; Song et al. 2006). Also the addition of external electron donors e.g. hydrogen have shown to positively influence the cell growth and productivity of succinate. These electron donors seem to improve NAD^+/NADH regeneration leading to an increased succinate yield, since succinate production is a redox consuming process (Lee et al. 1999). The redox balance is an important factor in the succinate process. Lin et al. (2005a) showed that also the oxidation state of the carbon source had a significant impact on succinate production.

The two species mentioned above are both good candidates for succinate production, as they produce succinate with high productivity and with high yield on a broad range of carbon sources. However, the by-product formation needs to be decreased before the strains can be used in an economic feasible process.

The *M. succiniciproducens* genome has recently been sequenced, which made genomic-based metabolic engineering possible. Disruptions of the genes lactate dehydrogenase (LDH), pyruvate:formate lyase (PFL), phosphotransacetylase (PTA) and acetate kinase (ACK) have been conducted, with a nearly complete elimination of the by-products acetate, formate and lactate as a result (Song et al. 2006). These disruptions together with fermentation optimisation (batch → fed batch) have increased the succinate yield from 0.7 to 0.76 g/g and the productivity from 1.2 to 1.8 g/L/h. The highest product titer achieved was 52.8 g/L. Unfortunately, this approach is impossible for *A. succiniciproducens* as its genome has not yet been sequenced.

3.4.2 Metabolically engineered *E. coli* for succinic acid over-production

E. coli is not a natural succinate over-producer. Under anaerobic conditions, it produces succinate as a minor by-product, while under aerobic conditions succinate is not accumulated at all. However, because *E. coli* has a well-studied metabolism and many molecular tools are available, research has been done on succinate production in this micro-organism. In literature three methods for succinate production by *E. coli* have been exploited: anaerobic-, aerobic- and dual-phase fermentation. During anaerobic fermentation only one metabolic pathway leads towards succinate, which is the reductive part of the TCA cycle. In aerobic fermentations there are two additional metabolic pathways that make succinate production possible. These pathways are the glyoxylate cycle and the oxidative portion of the TCA cycle (Magnuson and Lasure 2004). Because of this difference in metabolic pathways being used also different metabolic engineering strategies are needed for product optimisation.

To enhance succinate production and minimise by-product formation under anaerobic fermentation of *E. coli*, numerous metabolic engineering approaches have been tested with different degrees of success. Increasing flux towards succinate by over-expression of enzymes has been one approach. PEP carboxylase, pyruvate carboxykinase (PYCK) and fumurate reductase (FRDS) are examples of enzymes that result in increased succinate production when being overexpressed (Goldberg et al. 1983; Gokarn et al. 2000). PEP carboxylase catalyses the formation of oxaloacetate (OAA) from PEP, but without the gain of ATP as with PEP carboxykinase. A 50 fold higher activity of PEP carboxylase gave a 3.5 fold increase in the succinate concentration, making it one of the major fermentation products achieving a final yield of 0.45 mol/mol glucose (Millard et al. 1996). Increasing PEP carboxykinase activity had no effect in *E. coli*. PYCK catalyses the formation of OAA from pyruvate in a similar reaction as PEP carboxykinase, and insertion of the PYCK gene from *Rhizobium etli* (PYCK is not indigenous in *E. coli)* raised the succinate concentration to a final yield of 0.23 mol/mol glucose and it was sufficient to restore succinate production in a PEPCK deletion strain (Gokarn et al. 2000). Finally, also multiple copies of native FRDS have shown to improve the conversion rate of fumarate to succinate (Goldberg et al. 1983; Wang et al. 1998).

A second strategy for improving succinate production is deleting by-product forming pathways. The genes coding for pyruvate:formate lyase (PFL) and lactate dehydrogenase (LDH) have been deleted. This has shown to result in an increased malate yield at the expense of ethanol-, acetate-, formate- and lactate yields (Stols and Donnelly 1997). An additional side effect of these deletions is that pyruvate is accumulated, which seriously

reduced growth due to inadequate NADH regeneration (Hong and Lee 2001). In order to reduce the accumulation of pyruvate a number of approaches have been investigated, including over-expression of the gene *sfcA* encoding for malic enzyme (ME) (Hong and Lee 2001). At normal conditions ME catalyses the conversion of malate to pyruvate, but at elevated pyruvate concentrations the reaction is reversed and reduces the pyruvate pool. Another approach is to delete the *ptsG* gene. *PtsG* is a glucose-specific membrane-bound permease that catalyses a glucose phosphotransferase system, responsible for the transport of glucose across the cell membrane. During the process glucose is phosphorylated to glucose-6-P with the concomitant dephosphorylation of PEP to pyruvate. A *ptsG* deletion therefore eliminates the cell's ability to combine glucose uptake with pyruvate formation. This has shown to result in a reduced pyruvate pool. This strategy was discovered from investigations of a derivate of the *Δpfl Δldh* strain that had restored cell growth due to a mutation in the *ptsG* gene and led to a yield of 1 mol succinic acid / mol glucose (Donnelly et al. 1998; Chatterjee et al. 2001).

The over-expression and deletion strategies mentioned above can also be combined. A strain with an over-expression of the *pyck* and *sfcA* genes and a deletion of the *ptsG, ldh,* and *pfl* genes, operated in a dual-phase fermentation, has shown to be one of the most efficient methods for succinate production in *E. coli*, giving a succinic acid yield of 1.7 mol/mol glucose (Lin et al. 2005a; Vemuri et al. 2002). This process is not completely anaerobic, but uses an initial aerobic phase to build up biomass, followed by an anaerobic phase, where succinate production occurs. At anaerobic conditions the production of biomass is not very efficient, which subsequently limits the succinate productivity due to a low specific growth rate and a low NADH regeneration rate.

In order to initiate an accumulation of succinate under aerobic conditions, inactivation of succinate dehydrogenase (SDH) is important. Two mutated strains, one with five gene deletions and one with four gene deletions, were investigated. The construct with five deletions (Δ*sdhAB*, Δ*icd*, Δ*iclR*, Δ*poxB* and Δ*ackA-pta*) created a strain in which the glyoxylate cycle was the only metabolic route able to produce succinate, yielding 0.95 mol/mol glucose (Lin et al. 2005b). It was the first platform in *E. coli* that has shown a feasible production of succinate entirely under aerobic conditions. The disadvantage of this approach is the simultaneous accumulation of pyruvate, citrate and isocitrate. To prevent these accumulations a second production system was constructed, in which *sdhAB*, *iclR*, *poxB* and *ackA-pta* were deleted. This has created a two route system with the glyoxylate cycle and the oxidative branch of the TCA cycle producing succinate (Lin et al. 2005c). Both pathways branch from isocitrate and reduce the accumulation of the C_6 intermediates from the TCA cycle. A final strategy to further reduce the accumulation of by-products was made

by introducing a *ptsG* deletion and an over-expression of *pepC*. This strain finally achieved the maximum aerobic theoretical succinate yield of 1.0 mol / mol glucose (Lin et al. 2005c+d).

Although *E. coli* is not a natural succinate producer a large spectrum of metabolic engineering strategies has drastically improved the succinate yield. By genetically engineering *E. coli* it is possible to reach economically interesting succinate yields, showing the potential of metabolic engineering.

3.5 References

Aguilera J, Petit T, de Winde JH and Pronk JT 2005. Physiological and genome-wide transcriptional responses of *Saccharomyees cerevisiae* to high carbon dioxide concentrations. *Fems Yeast Research* **5** (6-7):579-593.

Arikawa Y, Kuroyanagi T, Shimosaka M, Muratsubaki H, Enomoto K, Kodaira R and Okazaki M 1999. Effect of gene disruptions of the TCA cycle on production of succinic acid in *Saccharomyces cerevisiae*. *Journal of Bioscience and Bioengineering* **87** (1):28-36.

Baniel AM and Eyal AM 1995. Citric acid extraction. *US patent: 5426220*.

Bercovitz A, Peleg Y, Battat E, Rokem JS and Goldberg I 1990. Localisation of pyruvate carboxylase in organic acid producing *Aspergillus* strains. *Applied and Environmental Microbiology* **56** (6):1594-1597.

Chatterjee R, Millard CS, Champion K, Clark DP and Donnelly MI 2001. Mutation of the *ptsC* gene results in increased production of succinate in fermentation of glucose by *Escherichia coli*. *Applied and Environmental Microbiology* **67** (1):148-154.

Datta R 1992. A process for the production of succinic acid by anaerobic fermentation. *US patent 5143833*.

Donnelly MI, Millard CS, Clark DP, Chen MJ and Rathke JW 1998. A novel fermentation pathway in an *Escherichia coli* mutant producing succinic acid, acetic acid, and ethanol. *Applied Biochemistry and Biotechnology* **70-2**:187-198.

Foster JW 1949. Chemical activities of fungi. *Academic Press, New York*.

Gallmetzer M, Meraner J and Burgstaller W 2002. Succinate synthesis and excretion by *Penicillium simplicissimum* under aerobic and anaerobic conditions. *Fems Microbiology Letters* **210** (2):221-225.

Gokarn RR, Eiteman MA and Altman E 2000. Metabolic analysis of *Escherichia coli* in the presence and absence of the carboxylating enzymes phosphoenolpyruvate carboxylase and pyruvate carboxylase. *Applied and Environmental Microbiology* **66** (5):1844-1850.

Goldberg I, Lonbergholm K, Bagley EA and Stieglitz B 1983. Improved conversion of fumarate to succinate by *Escherichia coli* strains amplified for fumarate reductase. *Applied and Environmental Microbiology* **45** (6):1838-1847.

Hong SH and Lee SY 2001. Metabolic flux analysis for succinic acid production by recombinant *Escherichia coli* with amplified malic enzyme activity. *Biotechnology and Bioengineering* **74** (2):89-95.

Lee PC, Lee WG, Kwon S, Lee SY and Chang HN 1999. Succinic acid production by *Anaerobiospirillum succiniciproducens*: effects of the H_2/CO_2 supply and glucose concentration. *Enzyme and Microbial Technology* **24** (8-9):549-554.

Lin H, Bennett GN and San KY 2005a. Effect of carbon sources differing in oxidation state and transport route on succinate production in metabolically engineered *Escherichia coli*. *Journal of Industrial Microbiology & Biotechnology* **32** (3):87-93.

Lin H, Bennett GN and San KY 2005c. Metabolic engineering of aerobic succinate production systems in *Escherichia coli* to improve process productivity and achieve the maximum theoretical succinate yield. *Metabolic Engineering* **7** (2):116-127.

Lin H, Bennett GN and San KY 2005b. Genetic reconstruction of the aerobic central metabolism in *Escherichia coli* for the absolute aerobic production of succinate. *Biotechnology and Bioengineering* **89** (2):148-156.

Lin H, Bennett GN and San KY 2005d. Fed-batch culture of a metabolically engineered *Escherichia coli* strain designed for high-level succinate production and yield under aerobic conditions. *Biotechnology and Bioengineering* **90** (6):775-779.

Magnuson JK and Lasure LL 2004. Organic acid production by filamentous fungi. Chapter 12 in *ADVANCES IN FUNGAL BIOTECHNOLOGY FOR INDUSTRY, AGRICULTURE, AND MEDICINE,* editors J S Tkacz and L Lange, pp 307-340 Kluwer Academic/Plenum Publishers, New York, NY.

McKinlay JB, Vieille C and Zeikus JG 2007. Prospects for a bio-based succinate industry. *Applied Microbiology and Biotechnology* **76** (4):727-740

Millard CS, Chao YP, Liao JC and Donnelly MI 1996. Enhanced production of succinic acid by overexpression of phosphoenolpyruvate carboxylase in *Escherichia coli*. *Applied and Environmental Microbiology* **62** (5):1808-1810.

Potera C 2005. Making succinate more successful. *Environmental Health Perspectives* **113** (12):A832-A835.

Song H and Lee SY 2006. Production of succinic acid by bacterial fermentation. *Enzyme and Microbial Technology* **39** (3):352-361.

Stols L and Donnelly MI 1997. Production of succinic acid through overexpression of NAD(+)-dependent malic enzyme in an *Escherichia coli* mutant. *Applied and Environmental Microbiology* **63** (7):2695-2701.

Vemuri GN, Eiteman MA and Altman E 2002. Succinate production in dual-phase *Escherichia coli* fermentations depends on the time of transition from aerobic to anaerobic conditions. *Journal of Industrial Microbiology & Biotechnology* **28** (6):325-332.

Wang XH, Gong CS and Tsao GT 1998. Bioconversion of fumaric acid to succinic acid by recombinant *E. coli*. *Applied Biochemistry and Biotechnology* **70**:919-928.

Werpy T and Petersen G 2004. Top value added chemicals from biomass. *http://www nrel gov/docs/fy04osti/35523 pdf* (27-03-2008).

Zeikus JG, Jain MK and Elankovan P 1999. Biotechnology of succinic acid production and markets for derived industrial products. *Applied Microbiology and Biotechnology* **51** (5):545-552.

Chapter 4

The effect of medium composition on growth and organic acid production in *Aspergillus niger*

4.1 Abstract

The medium composition has a significant impact on the physiology of *Aspergillus niger*. The effect of different medium components has been intensively studied for the citric acid process. By modifying the medium composition, it is possible to produce certain morphologies of *A. niger* and also to change the product formation spectrum produced by the micro-organism. In this study, it was attempted to create an optimal medium composition for succinate production in *A. niger*. Several salt and trace element combinations were tested, using a fractional factorial design of experiments. It was observed that the experiments resulted in very distinct outcomes. A well defined optimum medium composition could not be determined under the cultivation conditions used. It was hypothesized that the oxygen transfer rate had a significant influence on the physiology of *A. niger* using the cultivation conditions applied in this study. Therefore, the effect of the oxygen availability needs to be studied in more detail under controlled cultivation conditions using a medium composition assessed by this medium optimisation study.

Keywords: *Aspergillus niger*, medium optimisation, Design of Experiments, organic acids

4.2 Introduction

Aspergillus niger is a morphologically complex organism, showing different morphologies at different times of its life cycle, differing in form between surface and submerged growth and also differing with the nature of the growth medium and physical environment (Papagianni 2004). When grown in submerged culture, *A. niger* can exhibit different morphological forms, ranging from dispersed mycelial filaments to densely packed mycelial spheres better known as pellets (Figure 4.1).

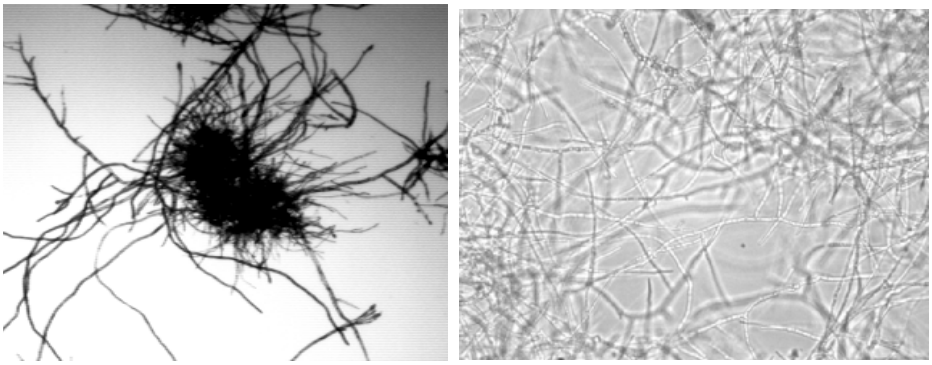

Figure 4.1 The two extreme shapes of *Aspergillus niger* : pellet morphology (left) and filamentous morphology (right) (Diano 2007).

The different morphological states have a significant effect on the rheology of the fermentation medium. Filamentous growth results in very viscous media, leading to a significant change in the mass transfer properties of the medium, specially the gas-liquid mass transfer. Pelleted growth exhibits low viscosity and therefore achieves better agitation and oxygen transfer compared to filamentous growth. However, the central region of larger pellets is prone to autolysis as a result of nutrient and oxygen deficiency. This autolysis can have a significant effect on the cellular behaviour and product synthesis (Phillips 1966; Elmayerg and Scharer et al. 1973). The morphological form is very important to achieve the maximal performance. For example, filamentous growth of *A. niger* is preferred for pectic enzyme production, whereas the pelleted form is preferred for citric acid production (Steel et al. 1954; Kristiansen and Bullock 1988).

The particular form exhibited is not only stipulated by the genetic material in the cell, but also by other factors. Factors affecting the fungal morphology include the nature of the inoculum, the type and concentration of the carbon source, the levels of nitrogen and phosphate, the

levels of trace minerals, and the concentrations of dissolved oxygen and carbon dioxide. At least 13 elements are essential for growth of *Aspergillus niger*, namely oxygen, carbon, hydrogen, nitrogen, phosphorus, potassium, sulfur, magnesium, manganese, iron, zinc, copper and molybdenum (Papagianni 2004). The first eight are macronutrients, needed in relatively large quantities (in the order of g/L). The latter five are micronutrients, which are required in small amounts (in the order of mg/L). Also physical factors affect the morphology like agitation, pH, temperature and culture mode. These will not be discussed here, as we only focused on the composition of a succinate production medium for *A.niger*.

Since *A. niger* is used as production organism for citric acid production a lot of research has been done on medium optimisation. Clear medium requirements are defined for the citric acid fermentation process. Because *A. niger* has a wide range of organic compounds that it can use for its metabolism, a lot of research has been focused on the carbon source usage for citric acid production. Not only the type of carbon source, but also the concentration is important (Xu et al. 1989). In general, it is believed that only carbon sources allowing fast growth (sucrose, glucose, etc.) lead to rates of carbon catabolism necessary for citrate overflow (Wolschek and Kubicek 1999). Additionally, the carbon source exerts a strong effect on the levels of enzymes in the TCA cycle, leading to high final molar yields of citric acid (Hossain et al. 1984). It is known that carbon concentrations higher than 50 g/L are needed in order to produce citric acid (Papagianni 2007). Another important feature in the citric acid process by *A. niger* is that growth needs to be restricted, although it is still not clear whether phosphate or nitrogen is the necessary limiting factor (Shu and Johnson 1984; Kubicek and Rohr 1977; Kristiansen and Sinclair 1979).

Oxygen availability is a critical parameter for *A. niger*, since it is unable to grow without it. The oxygen availability in the reactor is measured by the dissolved oxygen tension (DOT). There are critical DOT levels for growth, but also for product formation. This indicates a general role of oxygen in metabolic regulation. In the case of citric acid production, the influence of oxygen has been well established (Clark and Lentz 1961). Interruptions of aeration do not reduce the viability of the cells, but result in complete loss of ability to produce citric acid (Kubicek et al. 1980).

Carbon dioxide fixation has also a major role in the production of commercially important organic acids. The formation of citric acid from hexoses by *A. niger* proceeds via the glycolysis that splits into two C_3 compounds, one of which is decarboxylated to C_2 and the other is carboxylated to C_4. Condensation of the C_2 and C_4 products then occurs to form citric acid (Bentley and Thiessen 1957; Kubicek and Rohr 1989). In order to increase the

carboxylation reaction in the cells and thereby increasing the product yield, carbon dioxide can both be added via the gas phase to the bioreactor or in a liquid form as $NaHCO_3$ (Bushell and Bull 1981).

Furthermore, it is well known that for fungal growth certain essential metals are required. Once taken up some trace metals, like iron and zinc, are incorporated into enzymes that catalyse biochemical transformations occurring at key points in the carbon cycle. The effect of trace metals on growth and citric acid production in *A. niger* has been extensively investigated. Zinc (Zn), manganese (Mn), copper (Cu) and iron (Fe) have been shown to affect both fungal morphology and citric acid production (Papagianni 2004). It is thought that the levels of Fe and Zn are related to the split of carbon between biomass and citric acid (Mattey 1992). It has been shown that addition of zinc during the citric acid production phase resulted in a reversion to growth (Wold and Suzuki 1976). Also copper ions have been reported to effect the morphology and citric acid production. The copper ions induced a loose pelleted form of growth, reduced biomass levels and increased the volumetric productivity of citric acid (Haq et al. 2002). Manganese is known to drastically inhibit citric acid production. Mn^{2+} ions have shown to be specifically involved in many cellular processes, such as cell wall synthesis and sporulation (Kisser et al. 1980). The influence of Mn on *de novo* protein synthesis seems to play an important role in citric acid production. Under Mn deficiency it is believed that there is relatively more protein breakdown resulting in a high intracellular NH_4^+ concentration. As a consequence there is a release of the inhibition of phosphofructokinase, leading to a flux through glycolysis and the formation of citric acid (Kubicek and Rohr 1977; Habison et al. 1979).

Finally, the pH is an important parameter in the cultivation of micro-organisms. It is a measure of the concentration of H^+ ions present in the medium. *A. niger* can grow over a wide range of pH ranging from 1.5 to 8. However, its metabolite production profile changes completely at different pH. At pH < 3 the major acid produced is citrate (Papagianni et al. 1994), while at a pH between 3 - 6 mainly oxalate is produced (Kubicek and Rohr 1986; Ruijter et al. 1999). When pH values reach 5.5 or higher gluconate production may occur (Rohr et al. 1983; Mattey 1992)). This indicates that the pH has a major impact on the flux distributions inside the cell as well as on the *in vitro* enzyme activities. The pH also influences the solubility of compounds, like CO_2, that will dissolve better at higher pH in the form of bicarbonate.

It is obvious that the medium composition can have a huge influence on the production profiles of metabolites. Therefore, the influence of different medium components and their

effect on growth and succinate production was investigated, as a basis for more detailed studies on the physiology of wild-type and metabolically engineered strains.

4.3 Materials and Methods

4.3.1 Cultivation conditions

Conidiospores were propagated on solid medium at 37°C in darkness for 5-7 days. The medium consisted of 10 g/L glucose, 6 g/L $NaNO_3$, 0.5 g/L KCl, 0.5 g/L $MgSO_4 \cdot 7H_2O$, 1.5 g/L KH_2PO_4, 2.2 mg/L $ZnSO_4 \cdot 7H_2O$, 1.1 mg/L H_3BO_3, 0.5 mg/L $MnCl_2 \cdot 4H_2O$, 0.5 mg/L $FeSO_4 \cdot 7H_2O$, 0.17 mg/L $CoCl_2 \cdot 6H_2O$, 0.16 mg/L $CuSO_4 \cdot 5H_2O$, 0.15 mg/L $Na_2MoO_4 \cdot 2H_2O$, 5 mg/L Na_4EDTA and 18 g/L agar.

Spores were harvested from the agar plates using 0.01% Tween-80 (v/v). The shake flasks were filled with 100 ml of appropriate medium and adjusted to the correct pH (see Appendix 1, 3 and 4) after which they were inoculated with spores to a final concentration of 10^9 spores/L. The cultures were grown at 30°C and 80 rpm in 500 ml baffled shake flasks.

4.3.2 Cell dry weight determination

The concentration of biomass was determined on a dry weight basis. Filters were dried in a microwave oven at 150W for ten minutes, cooled for 2 hours in a desiccator and finally the dry weight of each filter was determined. A known quantity of culture broth was taken and vacuum filtered. The filtrate was frozen for quantification of extracellular metabolites. The filter cake was dried at 150W in the microwave oven for 15 minutes before being cooled for 2 hours in a desiccator and finally weighed to determine the dry cell weight.

4.3.3 Extracellular metabolites quantification

Acetate, pyruvate, oxalate, malate, fumarate, glycerol, ethanol, citrate, succinate and xylose were separated by high pressure liquid chromatography (HPLC). The HPLC system (Dionex, Rødovre, Denmark) used was equipped with an ion exclusion column Aminex HPX-87H (Biorad, Hercules, CA). The column was kept at 65°C and eluted at 0.6 ml/min with a mobile phase consisting of 5mM H_2SO_4. Acetate, oxalate, citrate, fumarate and succinate were detected by an UV detector (Waters 486 turnable absorbance detector) at 210 nm. Ethanol, glycerol and xylose were detected by a differential refractive index (RI) detector (Waters 410). For acquisition and analysis of the data, the software Chromoleon 3D (Dionex, Rødovre, Denmark) was used.

4.3.4 Design of experiments for medium optimisation

In order to investigate the effect that medium components have on growth and succinate production in *A. niger*, a reference medium had to be chosen as starting point for the medium optimisation. Two reference media, that have been developed for different purposes, were selected. One medium is applied for enzyme production in *A. niger* (Pedersen et al. 2000) and the other medium is used for citric acid production (Kristiansen and Sinclair 1979). The composition of both media is shown in Table 4.1.

Table 4.1 Reference media used for media optimisation of succinate production.

Medium	Pedersen et al. (2000)		Kristiansen and Sinclair (1979)	
Carbon source (g/L)	Glucose	20	Glucose	50
Nitrogen source (g/L)	$(NH_4)_2SO_4$	7.3	NH_4NO_3	0.5
Salts (g/L)	KH_2PO_4	1.5	KH_2PO_4	0.1
	$MgSO_4 \cdot 7H_20$	1	$MgSO_4 \cdot 7H_20$	0.1
	NaCl	1	KCl	0
	$CaCl_2 \cdot 2H_2O$	0.1	$CaCl_2 \cdot 2H_2O$	0
Trace elements (mg/L)	$ZnSO_4 \cdot 7H_20$	7.2	$ZnSO_4 \cdot 7H_20$	0.1
	$CuSO_4 \cdot 5H_2O$	1.3	$CuSO_4 \cdot 5H_2O$	0.1
	$NiCl_2 \cdot 6H_2O$	0.3	$NiCl_2 \cdot 6H_2O$	0
	$MnCl_2 \cdot 4H_2O$	3.5	$MnCl_2 \cdot 4H_2O$	0
	$FeSO_4 \cdot 7H_2O$	6.9	$(NH_4)_2SO_4Fe_2(SO_4)_2 \cdot 24H_2O$	0.1
Limitation		N		N

After choosing the reference media, a set of experiments was developed to determine the effect of the medium components on growth and succinate production. The design of experiments and statistical analysis of the response on biomass (Rs,x) and succinate (Rs,suc) yield (C-mol/C-mol) was carried out using a modelling and design program (Modde version 7.0, UMETRICS, UMETRI AB, Umeå, SWEDEN).

In Figure 4.2 the experimental design is schematised and shows the in- and output of the system. In this study, *A. niger* is the black box system and by changing the environmental conditions (input), we want to predict the growth and succinate yields (output). The Design Of Experiments (DOE) method permits us to determine the effect of the factors on the response and thereby minimising the variance of the effects with a minimal number of experiments. In this design set-up multiple factors are changed simultaneously in an ordered fashion, enabling a statistical analysis of the effect of factors on the response and identification of interactions between the different factors.

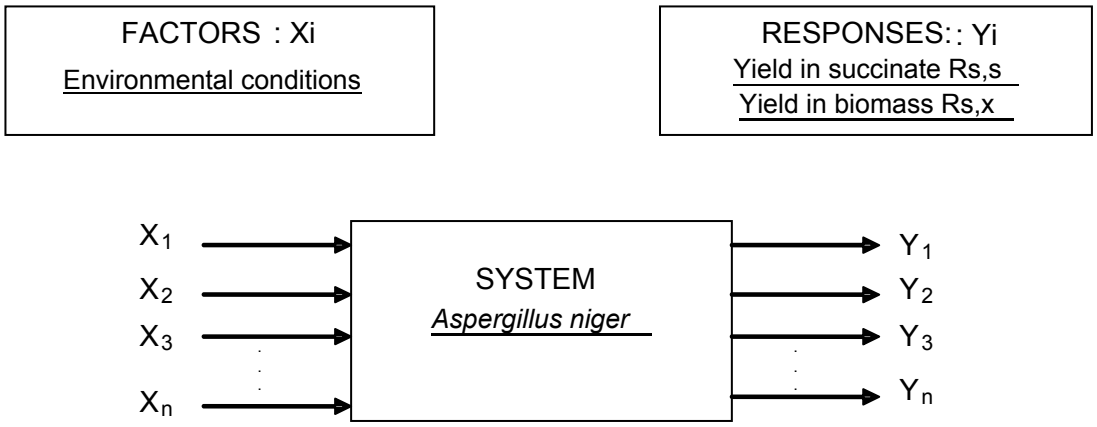

Figure 4.2 Schematised design of experiment set-up for medium optimisation.

The procedure applied in this statistical experimental design for process optimisation is divided into three steps:

1) identification of the media components that have most influence on the response ("screening")
2) optimum determination (''RSM'')
3) verification of the model (''checking experiment'')

4.3.4.1 Screening

For the identification of the most important media components, a fractional factorial design was used. A complete factorial design would be most accurate, but requires too many experiments. With statistical programming methods it is possible to determine the effect of factors and the interaction between factors using the fractional factorial design. When it is likely that there are some important interactions between the factors, the appropriate design to use for the screening experiment is a fractional factorial design of resolution IV. This

design permits to describe the data by a linear model of the 1st order with interactions of the 1st order (eq.1).

$$\hat{y} = a_0 + a_1 X_1 + a_2X_2 + \ldots\ldots a_kX_k + a_{12} X_1X_2 + \ldots\ldots + a_{jk} X_jX_k \qquad \text{eq. 1}$$

The design of resolution IV determines the main effects, but the effects of the interactions between factors are confounded. The global effect of all the confounded interactions can be calculated, but the ability to determine the effect of each interaction is lost.

4.3.4.2 Response surface modelling - RSM

Factors that influence the response the most are selected by the screening experiment. The optimal point found by screening is then used for a more thorough study. This second investigation is done with a design at three levels, like a Box Benhken design or central composite design. This step is called “response surface modelling” (RSM) and permits to describe the response by a quadratic model detecting curvature in the response (eq. 2).

$$\hat{y}= a_o + a_1X_1 + a_2X_2 + a_3X_3 + a_{12}X_1X_2 + a_{13}X_1X_3 + a_{23}X_2X_3 + a_{11}X_1^2 + a_{22} X_2^2 + a_{33} X_3^2 \qquad \text{eq.2}$$

In the Box Benhken Factorial (BBF) design, the treatment combinations are at the midpoints of edges of the process space and at the center (Figure 4.3). This design requires 3 levels of each factor but the third factor is determined from the two first levels (the low and high level).

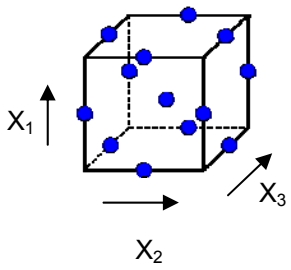

Figure 4.3 Box Benhken design for surface modelling of the optimal medium composition. The cube indicates the process space. Each direction corresponds to a factor. A point indicates a treatment combination.

A Central Composite Factorial (CCF) design contains an imbedded factorial or fractional factorial design with center points that are augmented with a group of ‘’star points'' allowing estimation of curvature. In the CCF the star points are at the center of each face of the process space (Figure 4.4).

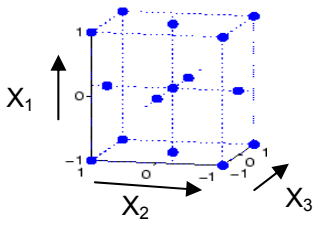

Figure 4.4 Central Composite Factorial design for surface modelling of the optimal medium composition. The cube indicates the process space. Each direction corresponds to a factor. A point indicates a treatment combination.

4.3.4.3 Model performance

After running the factorial design (both for screening and optimum search experiments) the results were analysed according to the flowchart below (Figure 4.5). First of all, it was verified if the normal assumption holds for the residuals. Residuals are estimates of experimental error obtained by subtracting the observed responses from the predicted responses. The predicted response is calculated from the chosen model after all the unknown model parameters have been estimated from the experimental data. Residuals are elements of variation unexplained by the fitted model. Since this is a form of error, the same general assumptions apply as to errors in general, meaning one expects them to be (roughly) normal and (approximately) independently distributed with a mean of 0 and some constant variance. After removing outliers the model is statistically validated.

For the statistical validation of the model three values are important:

- the R^2 is the percentage of the response variation explained by the model. R^2 is a measure of fit. It means how well the model fits the data.
- the Q^2 is the percentage of the response variation predicted by the model according to cross validation. Q^2 tells you how well the model predicts new data.
- the validity of the model, meaning it compares the model error with the pure error. The pure error is a measure of the reproducibility of the experiments.

Finally, the confidence interval is calculated for each coefficient based on the residual standard deviation and determines if an effect is statistically significant. The coefficient is significant (different from noise) when the confidence interval does not cross zero.

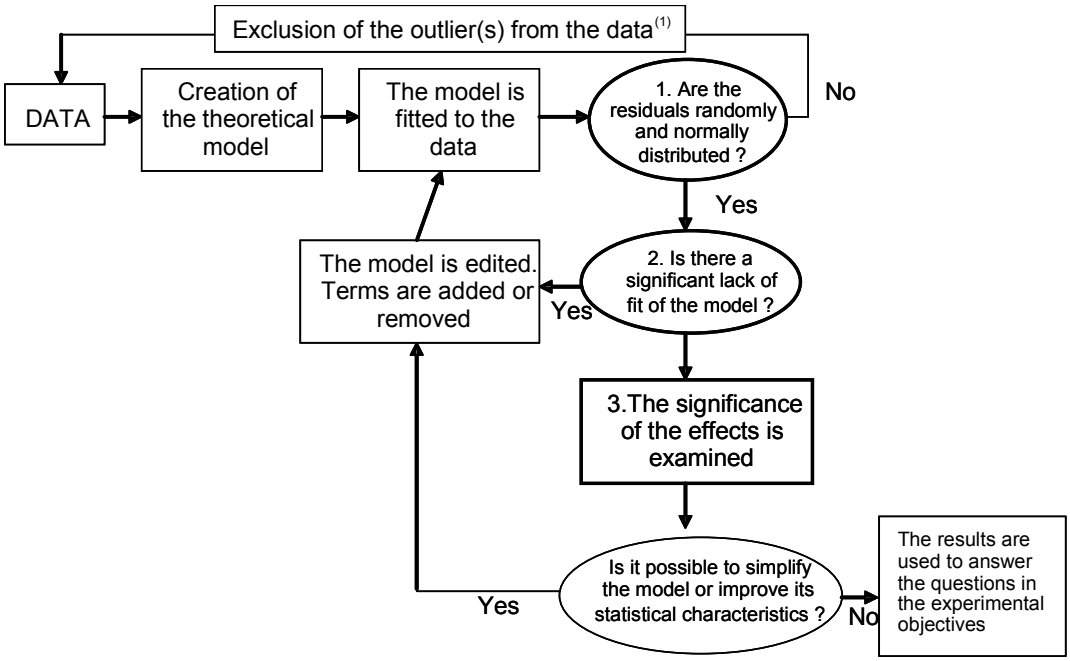

(1) An outlier is an experimental point which does not verify the normality assumption of the residual.

Figure 4.5 Flowchart of model development for response surface modelling experiment. The thin-lined boxes indicate the model development and the bold-lined boxes represent the model performance check.

4.3.4.4 Checking

The model needs to be validated. This is done by checking the reproducibility of the experiments. Some conditions are randomly selected and replicated for testing the reproducibility and thus the reliability of the model.

4.4 Results and discussion

4.4.1 Definition of standard medium and operating ranges

The reference media taken from literature (Table 4.1) were slightly adjusted towards the testing conditions that were relevant in this study (Table 4.2). The carbon source was changed from glucose to xylose. The most common organic compounds that support growth, and thereby supply a lot of carbon and energy to the cells, are sugars like glucose and sucrose, which are rapidly taken up. However, *A. niger* has a wide range of organic compounds that can be used for its metabolism, including xylose. We changed the carbon source from glucose to xylose, since it is the second most abundant carbon source in nature and we believe that the pathway from xylose towards succinate might contribute positively to the redox balance in the cell, thereby favouring succinate production. A second reason for using xylose is that it has been shown that different carbon sources can induce certain enzymes in the Embden-Meyerhof-Parnas (EMP) and pentose phosphate (PP) pathway, thereby redirecting fluxes in the cells (Papagianni 2004). However, not only metabolic pathways are influenced by the carbon source, but also signal transduction pathways like carbon catabolite repression are affected by the carbon source (Ruijter and Visser 1997). Therefore the carbon source is an important factor regulating the cellular behaviour. By using xylose we change the regulatory circuits that might benefit the succinate production. The concentration of the carbon source is important, as stated before. Therefore, a high concentration (50g/L) of carbon source was used to achieve a carbon overflow towards succinate production.

A second change made in the medium was the nitrogen source. Nitrogen may be supplied as ammonia, as nitrate or in organic compounds, such as amino acids, proteins or yeast extract. In this study $NaNO_3$ was used as nitrogen source, since in a previous experiment (data not shown) it was shown that more growth could be achieved under oxygen limited conditions. This illustrates that nitrate might give more reducing power to the cells under oxygen limited conditions. Since in shake flask cultivations the air supply is sub-optimal, nitrate is believed to reduce oxygen limiting effects.

With these factors (carbon and nitrogen source) set, an experimental space was designed, where the influence of certain salts and trace elements on the growth and succinate production was determined. The aim was to increase succinate production and limit by-

product formation, which mainly occurs in the form of citrate and oxalate at pH<5 using xylose as carbon source. The levels of nitrogen and phosphate have been chosen to be either in phosphate or nitrogen limitation. Table 4.3 describes the variables used in this study and their operating ranges.

Table 4.2 Adjusted media compositions of the two reference media used as starting media for the medium optimisation study.

Medium		1	2
Carbon source (g/L)	Xylose	50	50
Nitrogen source (g/L)	$NaNO_3$	2	2
Salts (g/L)	KH_2PO_4	0.4	1.5
	$MgSO_4 \cdot 7H_20$	0.4	1
	NaCl	0	1
	$CaCl_2 \cdot 2H_2O$	0	0.1
Antifoam (μL)	sb2121	50	50
Trace elements (mg/L)	$ZnSO_4 \cdot 7H_20$	0.4	7.2
	$CuSO_4 \cdot 5H_2O$	0.4	1.3
	$NiCl_2 \cdot 6H_2O$	0	0.3
	$MnCl_2 \cdot 4H_2O$	0	3.5
	$FeSO_4 \cdot 7H_2O$	0.2	6.9

4.4.2 Screening experiment

The screening experiment was carried out with a two level fractional factorial design and the 11 variables that are presented in Table 4.3. A resolution IV design was used containing 3 center points and a total of 35 runs. In Appendix 1 the complete worksheet is presented and in Appendix 2 the confoundings are listed.

The *A. niger* cultivations on the different media gave distinct biomass and succinic acid yields (Appendix 5) as well as varying physiologies. Some conditions showed large pellet morphologies, while under other conditions mycelia were observed.

Table 4.3 Factors and experimental ranges used in the screening experiment.

Factor's name	Abbreviation	Unit	Factor type	Level -	Level +
$MgSO_4 \cdot 7H_20$	Mg	g/L	Quantitative	0.2	2
NaCl	NaCl	g/L	Quantitative	0.1	10
$CaCl_2 \cdot 2H_2O$	$CaCl_2$	g/L	Quantitative	0.1	1.5
$ZnSO_4 \cdot 7H_20$	Zn	mg/L	Quantitative	0.08	8
$CuSO_4 \cdot 5H_2O$	Cu	mg/L	Quantitative	0.2	5
$NiCl_2 \cdot 6H_2O$	Ni	Mg/L	Quantitative	0	0.5
$FeSO_4 \cdot 7H_2O$	Fe	mg/L	Quantitative	0.2	10
$NaNO_3$	N	g/L	Quantitative	2	10
KH_2PO_4	P	g/L	Quantitative	0.1	2.5
$MnCl_2 \cdot 4H_2O$	Mn	mg/L	Quantitative	0	16
pH	pH	pH units	Quantitative	2	3.5

The biomass yield ranged from 19 % to 57 % (C-mol/ C-mol of xylose). One response has been removed because it did not conform to the normal distribution of residuals (outlier see Table 4.4 A). The succinate yield ranged from 0.01 % to 0.63 % (maximal concentration reached 0.30 g/L). Another outlier was removed based on this yield's normal distribution of the residuals (Table 4.4 B).

Table 4.4 Terms of the optimal models for biomass and succinic acid response.

A. Biomass response modelling, B. Succinic acid response modelling

A.

Biomass response modelling		
Terms of the model		Outliers removed
Main effects	Interactions(1)	Experiment nr.
Mg	$CaCl_2$*Cu	18
Cu	Mg*$CaCl_2$/Mn*N	
$CaCl_2$	Mg*Zn	
Fe	NaCl*Zn	
N	Mg*Fe	
P	Mg*N	
Mn	Mg*P	
	Mg*Mn	

B.

Succinic acid response modelling		
Terms of the model		Outliers removed
Main effects	Interactions(1)	Experiment nr.
Mg	Cu*Mn	4
Cu	Fe*N	
$CaCl_2$	CaCl*N	
Fe	Cu*N	
N	Zn*Fe	
P	N*Mn	
Mn		
Zn		

(1) The couples of factors indicated are the ones associated to the interaction coefficients after simplification of the table of confoundings.

During the cultivation different morphological growth forms were observed, ranging from loosely packed hyphae forming viscous medium to compact pellets of different sizes and colors. These different kinds of morphologies indicate the importance of the medium composition on cellular aggregation, which has consequences on nutrient and oxygen diffusion and therefore a consequence on growth and metabolite production.

4.4.2.1 Modelling and statistical analysis

After exclusion of the two outliers detected by the normality plot the residuals were evenly distributed. Two models were designed to describe on one hand succinic acid production and on the other hand biomass production. They have been fitted by multiple linear regression (MLR). Both models showed a good ability to describe the data (good R^2), but a poor ability to predict them (weak Q^2) (Table 4.5 A and B). There appeared to be a lack of reproducibility of the results in case of the succinate production. With regard to the biomass the weak validity of the model was due to a very good reproducibility of the centre points (the validity of the model was calculated comparing the residual standard deviation to the standard deviation of the centre points). Nevertheless, the regression was significant in the two cases (see Table 4.5 A and B).

Table 4.5 Statistical characteristics of the models fitted by multiple linear regressions.
A. Characteristics of the biomass model, B. Characteristics of the succinic acid model.

A.

MLR	
	Biomass
R^2	0.77
Q^2	0.07
p-value regression	0.00
Model validity	0.27
reproducibility	0.97

B.

MLR	
	succinic acid
R^2	0.67
Q^2	-0.03
p-value regression	0.02
Model validity	0.96
reproducibility	-0.13

The experimental design chosen (fractional factorial design IV) permitted to obtain models of the first order with interactions of the first order with confoundings among the interactions. However, by using the following two assumptions it is possible to considerably simplify the confoundings making it possible to associate one or two couples of factors to one term of interactions (see Table 4.4 A and B).

The assumptions are:

- if the main effect of a factor does not appear in the model then an interaction, which implies this factor, can be neglected
- the couple of factors that has the strongest probability to interact is the one with the strongest main effects.

4.4.2.2 Effects of factors on biomass and succinate production

Although a high residual standard deviation was observed in the experiments, it was still possible to retrieve five factors from the biomass model and three factors from the succinic acid model that were significant. In the biomass model (Figure 4.6) both magnesium and phosphate had a positive effect on growth that was statistically significant. This result is coherent with literature, since Shu and Johnson (1984) have shown that excess phosphate is increasing growth. Phosphate is a convenient and readily used source of phosphorus, while organic forms are also used in industrial processes. Both phosphate and magnesium play an important role in metabolite overproduction and effect fungal morphology. Magnesium is known to be a cofactor for a number of enzymes and also favours growth this way (Bowes and Mattey 1979).

Manganese on the contrary has a strong negative effect on growth. Manganese also inhibits the positive effect of phosphate, since there is a negative interaction between phosphate and manganese. Manganese is known to be involved in a number of processes in the cell. It stimulates cell wall synthesis and sporulation and is therefore essential for growth (Kisser et al. 1980). Because of these properties, manganese has also a major influence on the morphology of the cells and that might be one of the reasons for observing several different morphological states in the experiments.

In this model it was not possible to distinguish between the effects of phosphate or nitrogen limitation. No significant effects of nitrogen and interactions between N and P were detected that influenced biomass formation. Although other studies showed that nitrogen limitation resulted in induced pellet formation (Braun and Vecht-Lifshitz 1991), or that excess phosphate reduced pellet formation (Katz et al. 1972), none of these phenomena were observed in the shake flask cultivations performed in the screening experiment. Although nitrogen had no significant effect, its negative interaction with manganese was significant. It appeared that a high concentration of nitrogen increased the negative effect of manganese. However, this result has to be confirmed, because the interaction shown by the model can be due to other interactions, since this interaction is confounded in the design.

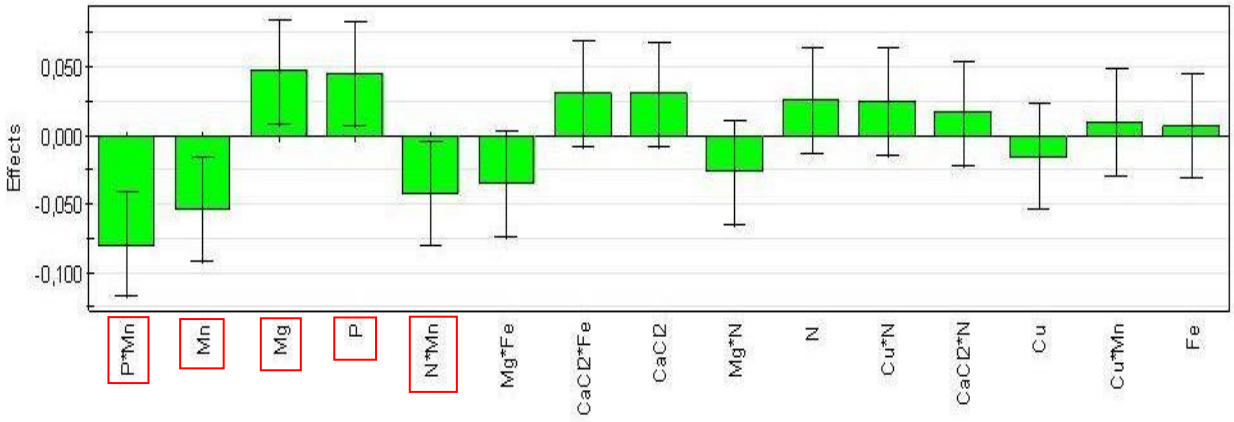

Figure 4.6 Standardised and centered effects of medium compounds on biomass yield (ordered by decreasing effects from left to right) according to optimal biomass yield modelling. The effects that are surrounded by lines are the significant effects found by the model.
Residual Standard Deviation (RSD) = 0.0499; Degree of Freedom (DF)= 18; Confidence level (1-α) = 0.95

Looking at the succinate model (Figure 4.7) it was observed that none of the compounds, showing a significant effect on growth, had a significant effect on succinic acid production. Only Mn belonged to one of the 5 major effects in the succinate model and was also significant in the biomass model.

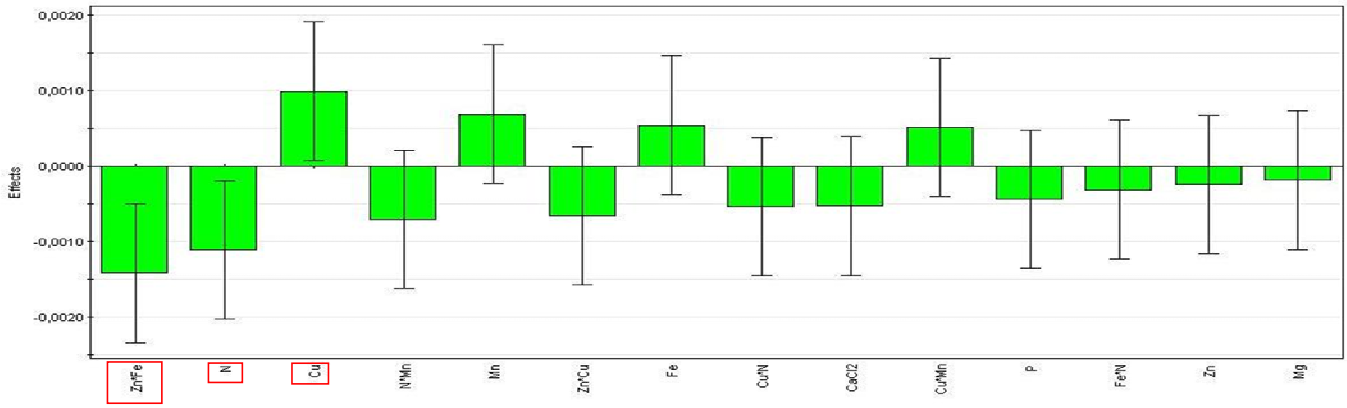

Figure 4.7 Standardised and centered effects of medium compounds on succinic acid yield (ordered by decreasing effects from left to right) according to optimal succinic acid yield modelling. The effects that are surrounded by lines are the significant effects found by the model.
Residual Standard Deviation (RSD) = 0.0012; Degree of Freedom (DF)= 19; Confidence level (1-α) = 0.95

The succinate model showed a negative effect for nitrate, meaning that high levels of nitrate decrease the succinic acid production significantly. It was not possible to conclude if either nitrogen or phosphate limitation was favourable, because there was no significant effect of phosphate concentration and no term of interaction between nitrogen and phosphate in the model. However, combining both models and knowing phosphate has a positive effect on growth and nitrate has a negative effect on succinate, it may be assumed that nitrogen limitation is more favourable.

In the succinate model Zn and Fe had no significant effect independently, but at high levels both factors decreased the yield of succinate significantly. This indicates again the importance of a balanced medium composition.

Copper had a positive effect on succinic acid production. Such a positive effect on organic acid production has already been shown by Haq et al. (2002) with citric acid production. Copper is known to reduce the iron concentration in the cell, thereby counteracting its growth inhibiting effect. The copper ions also induce pelleted growth and have a negative effect on biomass formation.

From the screening experiment four factors seem to be interesting for use in further studies. These factors are copper, nitrogen, manganese and iron. Copper and nitrogen had a significant effect on succinic acid production. Manganese and iron did not have a significant effect in the succinate model, but manganese did have a significant effect in the biomass model. Iron had in both models not a significant but a relative important effect. Based on the results of this screening experiment, it was decided to continue in further studies with nitrogen limitation and phosphate in excess.

4.4.3 The RSM experiment

After the screening experiment four factors were selected that influenced the succinate production most. These factors, Cu, Fe, $NaNO_3$ and Mn, were used for further study by a response surface modelling experiment. For the selected factors concentrations levels were chosen around the optimal zone found in the screening experiment. Other components were fixed to their low level, except phosphate. Phosphate was fixed at 2 g/L in order to achieve a nitrogen limitation in all the flasks. The experimental ranges of the four remaining factors were widened in order to better fine tune the optimal medium condition (Table 4.6). The design chosen for the response surface modelling experiment is the BBF design with 24 runs plus 3 center points (detailed worksheet in Appendix 3).

Table 4.6 Components and their experimental ranges for the RSM design. The factors in bold are the 4 compounds varied during this experiment.

Factor	Abbreviation	Unit	Factor type	Condition	Range of values
$MgSO_4 \cdot 7H_2O$	Mg	g/L	Quantitative	Constant	0.2
NaCl	NaCl	g/L	Quantitative	Constant	0.1
$CaCl_2 \cdot 2H_2O$	$CaCl_2$	g/L	Quantitative	Constant	0.1
$ZnSO_4 \cdot 7H_2O$	Zn	mg/L	Quantitative	Constant	0.08
$CuSO_4 \cdot 5H_2O$	**Cu**	**mg/L**	**Quantitative**	**Controlled**	**2 to 16**
$NiCl_2 \cdot 6H_2O$	Ni	mg/L	Quantitative	Constant	0
$FeSO_4 \cdot 7H_2O$	**Fe**	**mg/L**	**Quantitative**	**Controlled**	**8 to 30**
$NaNO_3$	**N**	**g/L**	**Quantitative**	**Controlled**	**0.5 to 3**
KH_2PO_4	P	g/L	Quantitative	Constant	0.2
$MnCl_2 \cdot 2H_20$	**Mn**	**mg/L**	**Quantitative**	**Controlled**	**10 to 35**
pH	pH	pH units	Quantitative	Constant	2

The biomass yield ranged from 28% to 67% in this modelling experiment. The succinate yield varied from 0.03 % to 0.41% (a maximum concentration of 0.20 g/L was achieved) and, unfortunately, is lower than the maximum yields reached during the screening experiment. In Appendix 6 the results of the BBF RSM experiment are listed. After exclusion of one outlier detected by the normality plot (for both biomass and succinic acid response) (Table 4.7 A and B), the residuals were randomly and normally distributed.

4.4.3.1 Modelling and statistical analysis

Models for biomass and succinic acid yields have been fitted by MLR. The models resulting from the optimised statistical characteristics appeared good models for both description and prediction of values. The reproducibility was better than during the screening experiment and also a good validity of the model was achieved (8 A and B).

Table 4.7 Terms of the optimal models for biomass and succinic acid response in the RSM experiment.

A. Biomass response modelling. B. Succinic acid response modelling

A.

Biomass RSM			
Terms of the model			Outliers removed
Main effects	Interactions	Quadratic terms	Experiment nr.
Fe	Fe*Mn	Fe*Fe	19
N		N*N	
Mn			

B.

Succinic acid RSM		
Terms of the model		Outliers removed
Main effects	Interactions	Experiment nr.
Mg	Cu*Fe	19
Cu	Fe*N	
Fe		
N		

The models found in this experiment were more simple than for the screening experiment. In these models only six terms were selected for describing each model (Table 4.7 A and B). No terms of curvature appeared in the succinic acid model, meaning that the potential optimum was not in the parameter range studied. In the biomass model two quadratic terms were determined, resulting in a curvature in the model. Looking at the significance of effects, it was observed that nitrogen and iron were significant factors for biomass in the RSM (Figure 4.8), which they were not after the screening experiment. Fe had a positive curve effect, whereas nitrogen had a negative curve effect. The manganese effect on biomass was found positive in this experiment, compared to a negative effect in the screening experiment. A maximum biomass yield was found using [Fe]= 30 mg and [Mn]=35 mg (respectively high levels) and an intermediary concentration in nitrogen of 2g/L.

Table 4.8 Statistical characteristics of the models fitted by multiple linear regressions.

A. Characteristics of the biomass model. B. Characteristics of the succinic acid model.

A.

MLR	
	Biomass
R^2	0.75
Q^2	0.34
p-value regression	0.00
Model validity	0.43
reproducibility	0.96

B.

MLR	
	Succinic acid
R^2	0.78
Q^2	0.60
p-value regression	0.00
Model validity	0.91
reproducibility	0.68

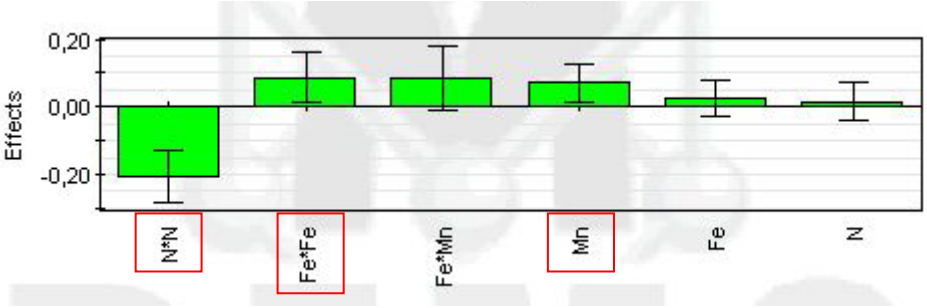

Figure 4.8 Standardised and centered effects of medium compounds on biomass yield (ordered by decreasing effects from left to right) according to optimal biomass yield modelling. The effects that are surrounded by lines are the significant effects found by the model.
Residual Standard Deviation (RSD) = 0.046; Degree of Freedom (DF)= 19; Confidence level (1-α) = 0.95

In the succinate model the only significant effect found was nitrogen (Figure 4.9). In contrast to the screening experiment the effect was found to be positive. It was also observed that in this model Fe alone had no significant effect. Nevertheless, iron increased the succinic acid yield in synergy with copper and inhibited the positive effect of nitrogen significantly. The response surface, created by succinic acid yield modelling, had a plane shape and, therefore, no optimum could be found in the experimental design space tested in this experiment (Figure 4.10). The optimum medium composition found for biomass yielded high nitrogen and copper levels and a low iron level. This result is in contradiction with the screening experiment. Even if the RSM model would predict a well defined optimum, the problem of the reproducibility between the two blocks of experiments (screening and RSM) still remains. An unknown factor seems to have a larger influence on succinate production than the medium components that have been varied in the two blocks of experiments.

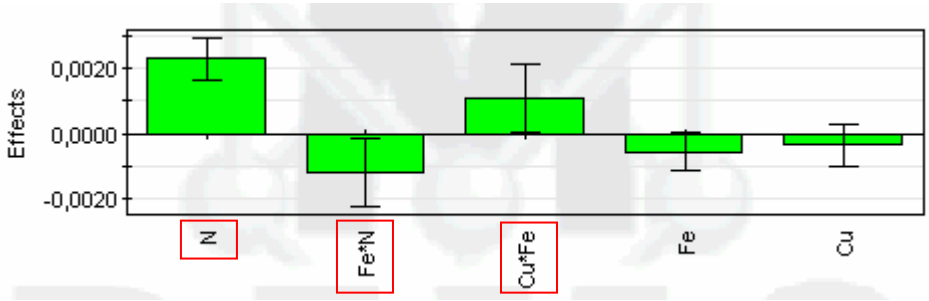

Figure 4.9 Standardised and centered effects of medium compounds on succinic acid yield (ordered by decreasing effects from left to right) according to optimal succinic acid yield modelling. The effects that are surrounded by lines are the significant effects found by the model.
Residual Standard Deviation (RSD) = 0.0005; Degree of Freedom (DF)= 20; Confidence level (1-α) = 0.95

4.4.3.2 Checking experiment

Finally, the models needed to be validated by analysing the reproducibility of the results. Replicates of cultures from the screening and from the Box-Benhken design were made and compared, based on their biomass yield and succinic acid yield (Table 4.9). There were significant differences between the yields reached in the two replicates (Table 4.9). In most cases the relative standard deviation is larger than 10% (especially large variations were observed in the succinic acid yield). Furthermore, different morphologies (presence of pellets, pellet size, color of supernatant) could be distinguished in this experiment. The large variability in the relative standard deviations indicates that the experiments are difficult to repeat and this is most likely the main reason for the limited quality of the medium optimisation models.

Table 4.9 Comparison of the yields reached in two replicate made of different experimental conditions.

Experiment nr.	Design of Experiment	Biomass			Succinic acid		
		Yield (g/g)		STDEV	Yield (mg/g)		STDEV
		1	2		1	2	
30	Screening	0.36	0.23	31	15.0	23.0	30
31	Screening	0.34	0.32	4	6.2	8.9	25
32	Screening	0.40	0.35	9	1.3	0.7	40
33	RSM	0.39	0.27	26	4.1	5.0	14
34	RSM	0.30	0.26	10	4.1	2.7	29

STDEV is the relative standard deviation expressed in percentage, 1 and 2 are the replicates of each experiment.

4.4.4 CCF modelling

Since the BBF RSM experiment did not result in a clear optimum and the reproducibility test was performing poorly, it was decided to run a second RSM experiment. The design chosen was a CCF design in 26 runs plus 3 centre points (detailed worksheet in Appendix 4).

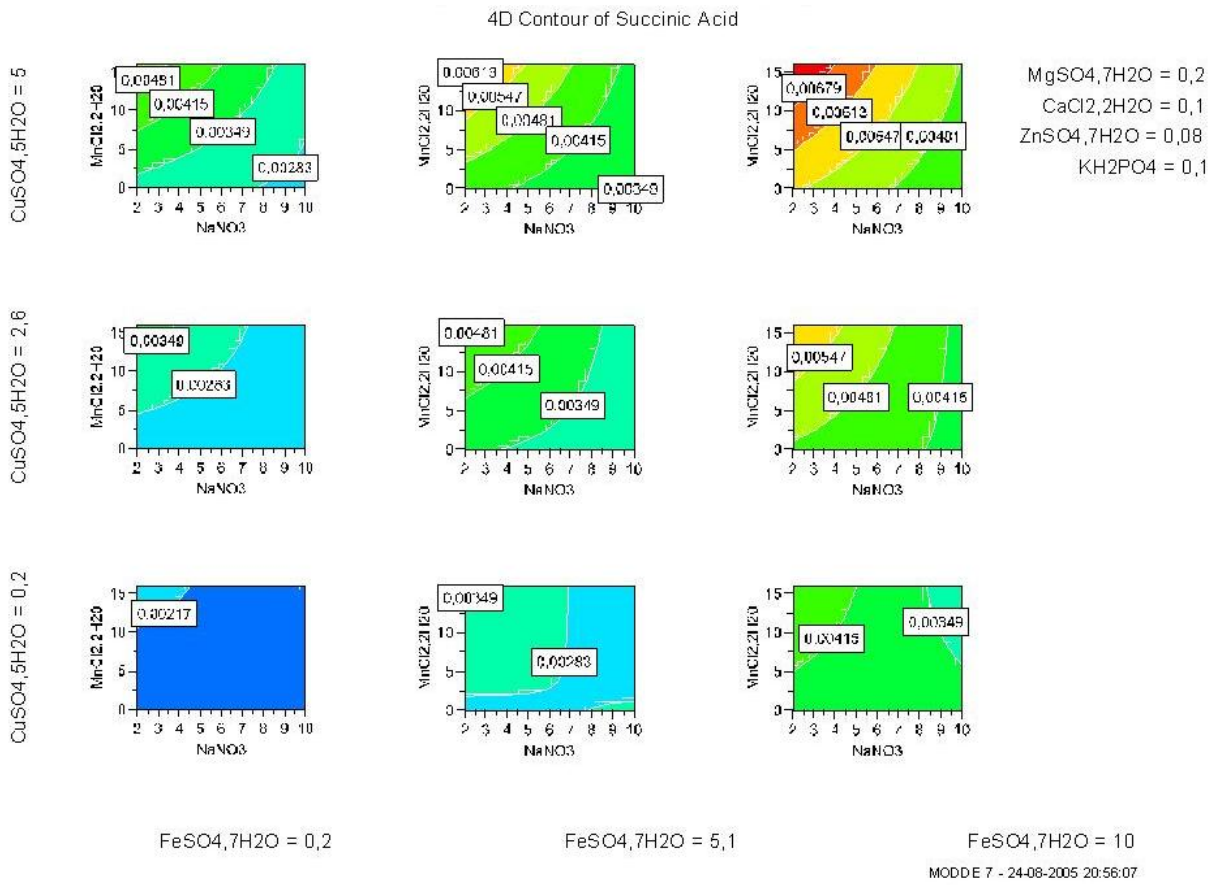

Figure 4.10 4D contour plot of succinic acid yield in the Box Benhken RSM experiment space.

4.4.4.1 Modelling and statistical analysis of the CCF design

By using this CCF design it was attempted to detect a curvature, which could explain the two different directions of optimisation found by the fractional factorial screening design and the BBF design. The variable and concentration ranges used in this CCF experiment can be found in Table 4.10. Zinc was added as variable, because the compound appeared three times in the screening experiment for succinic acid modelling (see Figure 4.7). This indicates that it may have an effect on succinate production and that the effect is often through interactions with other metals like Fe and Cu. These interactions are already known from literature (Papagianni 2004). Literature states that media lacking Zn^{2+} result in a lower glycolytic capacity, as aldolase is Zn^{2+} dependent (Mattey 1992). This shifts metabolism mainly towards gluconic acid production, but might also stimulate the PPPP, leading to different organic acid profiles. By using xylose the PPPP is already stimulated, but additional regulation by metals might be beneficial.

Table 4.10 Concentration values of the components for the CCF design : [Cu],[Fe],[$NaNO_3$],[Mn] and [Zn] are considered as variables and are presented in bold.

Factor	Abbreviation	Unit	Factor type	Condition	Range of values
$MgSO_4 \cdot 7H_2O$	Mg	g/L	Quantitative	Constant	0.2
NaCl	NaCl	g/L	Quantitative	Constant	0.1
$CaCl_2 \cdot 2H_2O$	CaCl2	g/L	Quantitative	Constant	0.1
$ZnSO_4 \cdot 7H_2O$	**Zn**	**mg/L**	**Quantitative**	**Controlled**	**0 to 0.16**
$CuSO_4 \cdot 5H_2O$	**Cu**	**mg/L**	**Quantitative**	**Controlled**	**2 to 9**
$NiCl_2 \cdot 6H_2O$	Ni	Mg/L	Quantitative	Constant	0
$FeSO_4 \cdot 7H_2O$	**Fe**	**mg/L**	**Quantitative**	**Controlled**	**7 to 11**
$NaNO_3$	**N**	**g/L**	**Quantitative**	**Controlled**	**2 to 5**
KH_2PO_4	P	g/L	Quantitative	Constant	0.2
$MnCl_2 \cdot 2H_20$	**Mn**	**mg/L**	**Quantitative**	**Controlled**	**10 to 16**
pH	pH	pH units	Quantitative	Constant	2

The simulated model resulted in biomass yields varying from 21% to 40%, which is a narrow and low range compared to the screening and BBF RSM experiments.

The succinate yield retrieved in this experiment covered a larger range than the BBF experiment and varied from 0.01 % to 0.67 % (maximum concentration of 0.33 g/L). This was highest succinate yield achieved, compared to the other two experiments. An overview of the results of the CCF responses can be found in Appendix 7.

After having removed the outliers (Table 4.11 B), the residuals were again randomly and normally distributed. The optimal model for succinic acid response fitted by MLR had very good statistical characteristics (Table 4.11 A) and the center points were reproducible.

Table 4.11 Characteristics of the optimal CCF model for succinic acid yield.
A. Statistical characteristics of the model. B. Terms of the model.

A.

MLR	
	succinic acid
R^2	0.97
Q^2	0.42
p-value regression	0.00
Model validity	0.67
reproductibility	0.97

B.

Succinic acid			
terms of the model			outliers removed
Main effects	interactions	quadratic terms	experiment n°
Zn	Zn*Cu	Zn*Zn	23
Cu	Zn*N	N*N	24
Fe	Zn*Mn		25
N	Cu*Fe		
Mn	Cu*N		
	Cu*Mn		
	Fe*Mn		
	N*Mn		

The residual standard deviation was very low and a lot of factors were significant. The terms of the model and their interactions are shown in Table 4.11 B, in which also two quadratic effects are integrated in the model.

The results showed that the concentration of nitrogen presented a positive curve effect on the domain of values (2-5g/L) and negative interactions with metals (Cu, Fe, Zn and Mn) (Figure 4.11). Zinc had a strong negative effect and therefore a total deficiency in Zn seems suitable for succinic acid production. Iron had a significant negative effect. Furthermore, it could be seen that positive interactions appeared between the metals added. Metals have a huge impact on enzyme activities and can serve as electron donors or acceptors, Lewis acids or structural regulators (Riordan et al. 1977). A good balance between the metals is therefore necessary for achieving an optimal medium composition for succinate production.

Unfortunately, in this experiment the response surface had again a plane shape and no optimum appeared. Therefore, it was not possible to define a real optimum medium composition. In the range of values studied in this second RSM experiment, the optimal levels for the factors would lead in the direction of a high concentration of nitrogen (5g/L) and low concentrations of metals: Zn (deficiency), Mn (10 mg/L), Cu (2mg/L), Fe (7mg/L).

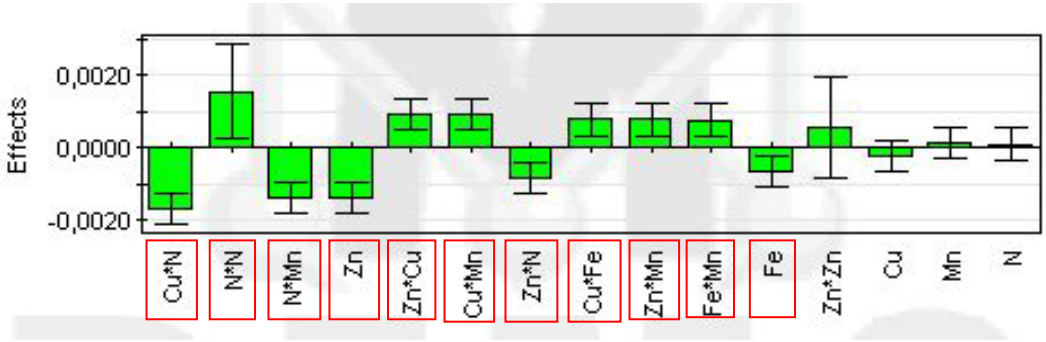

Figure 4.11 Standardised and centered effects of medium compounds on succinic acid yield (ordered by decreasing effects from left to right) according to optimal succinic acid yield modelling. The effects that are surrounded by lines are the significant effects found by the model.
Residual Standard Deviation (RSD) = 0.0004 Degree of Freedom (DF)= 10 Confidence level (1-α) = 0.95

4.5 Conclusion

The strategy of medium optimisation by DOE (screening and response surface modelling) did not result in a clearly defined optimum for succinic acid production by *A. niger*. The yield in succinic acid has not significantly been improved by changing the medium components. However, a great variation in the succinate yields, reached in the different experiments, was detected. The main problem encountered in the design strategy was the reproducibility between the experiments and above all between the screening and response surface modelling experiments. These problems might be caused by a factor that can not be controlled in the shake flask cultivations and might have a major influence on the succinic acid yield. A possible candidate is the oxygen transfer rate.

The aeration and shaking conditions in the flasks can easily induce metabolic and morphological changes that might have major influences on succinic acid production. If this is the case, it will be difficult to define a clear effect of the medium compounds, since the oxygen transfer capacity variation is too prominently present and thereby overshadowing the effect of the medium components. Different optimal medium compositions were retrieved in all the experiments performed in this study. For example, in the BBF design the optimum concentration of Fe and Mn was 30 and 35 mg/L respectively, while in the CCF design this was 7 and 10 mg/L respectively. It was decided to use medium 2 for further studies (shown in Table 4.2) and perform a more controlled experiment in fermentors, where the influence of different oxygen levels on the physiology of *A. niger* is determined (Chapter 5).

Additionally, it was observed that the concentration of succinic acid strongly increases when autolysis of the biomass occurs. It would be interesting to study the secretion of succinic acid more carefully and to compare the intra- and extra-cellular profiles of succinic acid. Unfortunately, only little information is available on organic acid transporters in *A. niger*, but a comparison between intra- and extracellular metabolite concentrations of succinate has been made in a physiological experiment as mentioned above (see Chapter 5).

4.6 References

Bentley R and Thiessen CP 1957. Biosynthesis of itaconic acid in *Aspergillus terreus*: Traces studies with C^{14}-labeled substrates. *Journal of Biological Chemistry* **226**:673-687.

Bowes I and Mattey M 1979. Effect of manganese and magnesium-ions on mitochondrial NADP+-dependent isocitrate dehydrogenase from *Aspergillus niger*. *Fems Microbiology Letters* **6** (4):219-222.

Braun S and Vechtlifshitz SE 1991. Mycelial morphology and metabolite production. *Trends in Biotechnology* **9** (2):63-68.

Bushell ME and Bull AT 1981. Anaplerotic metabolism of *Aspergillus nidulans* and its effect on biomass synthesis in carbon limited chemostats. *Archives of Microbiology* **128** (3):282-287.

Clark DS and Lentz CP 1961. Submerged citric acid fermentation of sugar beet molasses - Effect of pressure and recirculation of oxygen. *Canadian Journal of Microbiology* **7** (4):447-&.

Diano A 2007. Physiology of *Aspergillus niger* in oxygen limitation. *Ph D thesis*:Center of Mircobial Biotechnology, Biocentrum-DTU, Technical University of Denmark, Denmark.

Elmayerg H and Scharer JM 1973. Physiological studies on *Aspergillus niger* fermentation with polymer additive. *Journal of General and Applied Microbiology* **19** (5):385-392.

Habison A, Kubicek CP and Rohr M 1979. Phosphofructokinase as a regulatory enzyme in citric acid producing *Aspergillus niger*. *Fems Microbiology Letters* **5** (1):39-42.

Haq IU, Ali S, Qadeer MA and Iqbal J 2002. Effect of copper ions on mould morphology and citric acid productivity by *Aspergillus niger* using molasses based media. *Process Biochemistry* **37** (10):1085-1090.

Hossain M, Brooks JD and Maddox IS 1984. The effect of the sugar source on citric acid production by *Aspergillus niger*. *Applied Microbiology and Biotechnology* **19** (6):393-397.

Katz D, Goldstei D and Rosenber RF 1972. Model for branch initiation in *Aspergillus nidulans* based on measurements of growth parameters. *Journal of Bacteriology* **109** (3):1097-&.

Kisser M, Kubicek CP and Rohr M 1980. Influence of manganese on morphology and cell-wall composition of *Aspergillus niger* during citric acid fermentation. *Archives of Microbiology* **128** (1):26-33.

Kristiansen B and Sinclair CG 1979. Production of citric acid in continuous culture. *Biotechnology and Bioengineering* **21** (2):297-315.

Kristiansen B and Bullock JD 1988. Developments in industrial fungal biotechnology. In *"Fungal biotechnology"* Smith J.E., Berry D.R., Kristiansen B., editors. London: Academic press, p.203-223.

Kubicek CP and Rohr M 1977. Influence of manganese on enzyme synthesis and citric acid accumulation in *Aspergillus niger*. *European Journal of Applied Microbiology* **4** (3):167-175.

Kubicek CP, Zehentgruber O, Elkalak H and Rohr M 1980. Regulation of citric acid production by oxygen - Effect of dissolved oxygen tension on adenylate levels and respiration in *Aspergillus niger*. *European Journal of Applied Microbiology and Biotechnology* **9** (2):101-115.

Kubicek CP and Rohr M 1986. Citric acid fermentation. *Critical Reviews in Biotechnology* **3** (4):331-373.

Kubicek CP and Rohr M 1989. Citric acid fermentation. *Critical Reviews in Biotechnology* **4**:331-373.

Mattey M 1992. The production of organic acids. *Critical Reviews in Biotechnology* **12** (1-2):87-132.

Papagianni M, Mattey M and Kristiansen B 1994. Morphology and citric acid production of *Aspergillus niger*. *Biotechnology Letters* **16** (9):929-934.

Papagianni M 2004. Fungal morphology and metabolite production in submerged mycelial processes. *Biotechnology Advances* **22** (3):189-259.

Papagianni M 2007. Advances in citric acid fermentation by *Aspergillus niger*: Biochemical aspects, membrane transport and modelling. *Biotechnology Advances* **25** (3):244-263.

Pedersen H, Beyer M and Nielsen J 2000. Glucoamylase production in batch, chemostat and fed-batch cultivations by an industrial strain of *Aspergillus niger*. *Applied Microbiology and Biotechnology* **53** (3):272-277.

Phillips DH 1966. Oxygen transfer into mycelial pellets. *Biotechnology and Bioengineering* **8** (3):456-460.

Riordan JF 1977. Role of metals in enzyme activity. *Annals of Clinical and Laboratory Science* **7** (2):119-129.

Röhr M, Kubicek CP and Kominek J 1983. Citric acid. In: Reed G, Rehm HJ (eds) *Biotechnology*, vol 3 Verlag Chemie, Weinheim, pp 420-454.

Ruijter GJG and Visser J 1997. Carbon repression in *Aspergilli*. *Fems Microbiology Letters* **151** (2):103-114.

Ruijter GJG, van de Vondervoort PJI and Visser J 1999. Oxalic acid production by *Aspergillus niger*: an oxalate-non-producing mutant produces citric acid at pH 5 and in the presence of manganese. *Microbiology* **145**:2569-2576.

Shu P and Johnson MJ 1984. Citric acid production by submerged fermentation with *Aspergillus niger*. *Industrial and Engineering Chemistry* **40**:1202-1205.

Steel R, Martin SM and Lentz CP 1954. A standard inoculum for citric acid production in submerged culture. *Canadian Journal of Microbiology* **1** (3):150-157.

Wold WSM and Suzuki I 1976. Citric acid fermentation by *Aspergillus niger* - Regulation by zinc of growth and acidogenesis. *Canadian Journal of Microbiology* **22** (8):1083-1092.

Wolschek M and Kubicek CP 1999. Biochemistry of cirtic acid accumulation by *A. niger* . In: Kristiansen B , Mattey M , Linden J , editors *Citric acid biotechnology* London, PA: Taylor & Francis, pp 11-32.

Xu DB, Madrid CP, Rohr M and Kubicek CP 1989. The Influence of type and concentration of the carbon source on production of citric acid by *Aspergillus niger*. *Applied Microbiology and Biotechnology* **30** (6):553-558.

APPENDIX 1

Worksheet of the screening experiment design

Exp Nr.	Run Order	$MgSO_4 \cdot 7H_2O$	NaCl	$CaCl_2 \cdot 2H_2O$	$ZnSO_4 \cdot 7H_2O$	$CuSO_4 \cdot 5H_2O$	$NiCl_2 \cdot 6H_2O$	$FeSO_4 \cdot 7H_2O$	$NaNO_3$	KH_2PO_4	$MnCl_2 \cdot 2H_20$	pH
1	1	0.2	0.1	0.1	0.08	0.2	0	0.2	2	0.1	0	2
35	2	1.1	5.05	0.8	4.04	2.6	0.25	5.1	6	1.3	8	2.75
32	3	2	10	1.5	8	5	0.5	10	10	2.5	16	3.5
9	4	0.2	0.1	0.1	8	0.2	0	10	10	2.5	16	3.5
33	5	1.1	5.05	0.8	4.04	2.6	0.25	5.1	6	1.3	8	2.75
7	6	0.2	10	1.5	0.08	0.2	0	0.2	10	2.5	0	3.5
11	7	0.2	10	0.1	8	0.2	0.5	0.2	10	2.5	16	2
12	8	2	10	0.1	8	0.2	0	0.2	10	0.1	0	2
10	9	2	0.1	0.1	8	0.2	0.5	10	10	0.1	0	3.5
23	10	0.2	10	1.5	0.08	5	0	0.2	2	2.5	16	2
4	11	2	10	0.1	0.08	0.2	0	10	2	2.5	16	3.5
19	12	0.2	10	0.1	0.08	5	0.5	10	10	0.1	16	2
26	13	2	0.1	0.1	8	5	0.5	10	2	0.1	16	2
31	14	0.2	10	1.5	8	5	0	10	10	0.1	0	3.5
25	15	0.2	0.1	0.1	8	5	0	10	2	2.5	0	2
21	16	0.2	0.1	1.5	0.08	5	0.5	10	2	2.5	16	3.5
5	17	0.2	0.1	1.5	0.08	0.2	0.5	10	10	2.5	0	2
18	18	2	0.1	0.1	0.08	5	0.5	0.2	10	2.5	0	3.5
2	19	2	0.1	0.1	0.08	0.2	0.5	0.2	2	2.5	16	2
16	20	2	10	1.5	8	0.2	0.5	10	2	2.5	0	2
24	21	2	10	1.5	0.08	5	0.5	0.2	2	0.1	0	2
8	22	2	10	1.5	0.08	0.2	0.5	0.2	10	0.1	16	3.5
15	23	0.2	10	1.5	8	0.2	0	10	2	0.1	16	2
29	24	0.2	0.1	1.5	8	5	0.5	0.2	10	0.1	0	2
14	25	2	0.1	1.5	8	0.2	0	0.2	2	2.5	0	3.5
27	26	0.2	10	0.1	8	5	0.5	0.2	2	2.5	0	3.5
20	27	2	10	0.1	0.08	5	0	10	10	2.5	0	2
13	28	0.2	0.1	1.5	8	0.2	0.5	0.2	2	0.1	16	3.5
30	29	2	0.1	1.5	8	5	0	0.2	10	2.5	16	2
28	30	2	10	0.1	8	5	0	0.2	2	0.1	16	3.5
17	31	0.2	0.1	0.1	0.08	5	0	0.2	10	0.1	16	3.5
34	32	1.1	5.05	0.8	4.04	2.6	0.25	5.1	6	1.3	8	2.75
6	33	2	0.1	1.5	0.08	0.2	0	10	10	0.1	16	2
3	34	0.2	10	0.1	0.08	0.2	0.5	10	2	0.1	0	3.5
22	35	2	0.1	1.5	0.08	5	0	10	2	0.1	0	3.5

$MgSO_4 \cdot 7H_2O$; NaCl; $NaNO_3$; KH_2PO_4 and $CaCl_2 \cdot 2H_2O$ are expressed in g/L.

$ZnSO_4 \cdot 7H_2O$; $CuSO_4 \cdot 5H_2O$; $NiCl_2 \cdot 6H_2O$; $FeSO_4 \cdot 7H_2O$ and $MnCl_2 \cdot 2H_20$ are expressed in mg/L.

Appendix 2

Confoundings of factors in screening experiment

	Confounded with	Confounded with	Confounded with
Mg*NaCl	CaCl2*Ni	Fe*P	Mn*pH
Mg*CaCl2	NaCl*Ni	Zn*P	N*Mn
Mg*Zn	CaCl2*P	Cu*Mn	Ni*Fe
Mg*Cu	Zn*Mn	N*P	
Mg*Ni	NaCl*CaCl2	Zn*Fe	N*pH
Mg*Fe	NaCl*P	Zn*Ni	
Mg*N	CaCl2*Mn	Cu*P	Ni*pH
Mg*P	NaCl*Fe	CaCl2*Zn	Cu*N
Mg*Mn	NaCl*pH	CaCl2*N	Zn*Cu
Mg*pH	NaCl*Mn	Ni*N	
NaCl*CaCl2	Mg*Ni	Zn*Fe	N*pH
NaCl*Zn	CaCl2*Fe	Cu*pH	Ni*P
NaCl*Cu	Zn*pH	Fe*N	
NaCl*Ni	Mg*CaCl2	Zn*P	N*Mn
NaCl*Fe	Mg*P	CaCl2*Zn	Cu*N
NaCl*N	CaCl2*pH	Cu*Fe	Ni*Mn
NaCl*P	Mg*Fe	Zn*Ni	
NaCl*Mn	Mg*pH	Ni*N	
NaCl*pH	Mg*Mn	CaCl2*N	Zn*Cu
CaCl2*Zn	Mg*P	NaCl*Fe	Cu*N
CaCl2*Cu	Zn*N	Fe*pH	P*Mn
CaCl2*Ni	Mg*NaCl	Fe*P	Mn*pH
CaCl2*Fe	NaCl*Zn	Cu*pH	Ni*P
CaCl2*N	Mg*Mn	NaCl*pH	Zn*Cu
CaCl2*P	Mg*Zn	Cu*Mn	Ni*Fe
CaCl2*Mn	Mg*N	Cu*P	Ni*pH
CaCl2*pH	NaCl*N	Cu*Fe	Ni*Mn
Zn*Cu	Mg*Mn	NaCl*pH	CaCl2*N

A * B represent the interaction between A and B.

	Confounded with	Confounded with	Confounded with
Zn*Ni	Mg*Fe	NaCl*P	
Zn*Fe	Mg*Ni	NaCl*CaCl2	N*pH
Zn*N	CaCl2*Cu	Fe*pH	P*Mn
Zn*P	Mg*CaCl2	NaCl*Ni	N*Mn
Zn*Mn	Mg*Cu	N*P	
Zn*pH	NaCl*Cu	Fe*N	
Cu*Ni	Fe*Mn	P*pH	
Cu*Fe	NaCl*N	CaCl2*pH	Ni*Mn
Cu*N	Mg*P	NaCl*Fe	CaCl2*Zn
Cu*P	Mg*N	CaCl2*Mn	Ni*pH
Cu*Mn	Mg*Zn	CaCl2*P	Ni*Fe
Cu*pH	NaCl*Zn	CaCl2*Fe	Ni*P
Ni*Fe	Mg*Zn	CaCl2*P	Cu*Mn
Ni*N	Mg*pH	NaCl*Mn	
Ni*P	NaCl*Zn	CaCl2*Fe	Cu*pH
Ni*Mn	NaCl*N	CaCl2*pH	Cu*Fe
Ni*pH	Mg*N	CaCl2*Mn	Cu*P
Fe*N	NaCl*Cu	Zn*pH	
Fe*P	Mg*NaCl	CaCl2*Ni	Mn*pH
Fe*Mn	Cu*Ni	P*pH	
Fe*pH	CaCl2*Cu	Zn*N	P*Mn
N*P	Mg*Cu	Zn*Mn	
N*Mn	Mg*CaCl2	NaCl*Ni	Zn*P
N*pH	Mg*Ni	NaCl*CaCl2	Zn*Fe
P*Mn	CaCl2*Cu	Zn*N	Fe*pH
P*pH	Cu*Ni	Fe*Mn	
Mn*pH	Mg*NaCl	CaCl2*Ni	Fe*P

APPENDIX 3

Worksheet of the Box-Benhken design for response surface modelling

Exp Nr.	Run Order	$MgSO_4 \cdot 7H_2O$	NaCl	$CaCl_2 \cdot 2H_2O$	$ZnSO_4 \cdot 7H_2O$	$CuSO_4 \cdot 5H_2O$	$NiCl_2 \cdot 6H_2O$	$FeSO_4 \cdot 7H_2O$	$NaNO_3$	KH_2PO_4	$MnCl_2 \cdot 2H_20$	pH
17	1	0.2	0.1	0.1	0.08	2	0	19	0.5	0.2	22.5	2
8	2	0.2	0.1	0.1	0.08	9	0	19	3	0.2	35	2
2	3	0.2	0.1	0.1	0.08	16	0	8	1.75	0.2	22.5	2
16	4	0.2	0.1	0.1	0.08	9	0	30	3	0.2	22.5	2
9	5	0.2	0.1	0.1	0.08	2	0	19	1.75	0.2	10	2
11	6	0.2	0.1	0.1	0.08	2	0	19	1.75	0.2	35	2
26	7	0.2	0.1	0.1	0.08	9	0	19	1.75	0.2	22.5	2
15	8	0.2	0.1	0.1	0.08	9	0	8	3	0.2	22.5	2
25	9	0.2	0.1	0.1	0.08	9	0	19	1.75	0.2	22.5	2
20	10	0.2	0.1	0.1	0.08	16	0	19	3	0.2	22.5	2
10	11	0.2	0.1	0.1	0.08	16	0	19	1.75	0.2	10	2
23	12	0.2	0.1	0.1	0.08	9	0	8	1.75	0.2	35	2
1	13	0.2	0.1	0.1	0.08	2	0	8	1.75	0.2	22.5	2
4	14	0.2	0.1	0.1	0.08	16	0	30	1.75	0.2	22.5	2
12	15	0.2	0.1	0.1	0.08	16	0	19	1.75	0.2	35	2
3	16	0.2	0.1	0.1	0.08	2	0	30	1.75	0.2	22.5	2
18	17	0.2	0.1	0.1	0.08	16	0	19	0.5	0.2	22.5	2
22	18	0.2	0.1	0.1	0.08	9	0	30	1.75	0.2	10	2
6	19	0.2	0.1	0.1	0.08	9	0	19	3	0.2	10	2
5	20	0.2	0.1	0.1	0.08	9	0	19	0.5	0.2	10	2
27	21	0.2	0.1	0.1	0.08	9	0	19	1.75	0.2	22.5	2
13	22	0.2	0.1	0.1	0.08	9	0	8	0.5	0.2	22.5	2
7	23	0.2	0.1	0.1	0.08	9	0	19	0.5	0.2	35	2
19	24	0.2	0.1	0.1	0.08	2	0	19	3	0.2	22.5	2
21	25	0.2	0.1	0.1	0.08	9	0	8	1.75	0.2	10	2
14	26	0.2	0.1	0.1	0.08	9	0	30	0.5	0.2	22.5	2
24	27	0.2	0.1	0.1	0.08	9	0	30	1.75	0.2	35	2

$MgSO_4 \cdot 7H_2O$; NaCl; $NaNO_3$; KH_2PO_4 and $CaCl_2 \cdot 2H_2O$ are expressed in g/L.

$ZnSO_4 \cdot 7H_2O$; $CuSO_4 \cdot 5H_2O$; $NiCl_2 \cdot 6H_2O$; $FeSO_4 \cdot 7H_2O$ and $MnCl_2 \cdot 2H_20$ are expressed in mg/L.

The gray colums represent the compounds that are found in the screening experiment and are varied in concentration in order to find an optimal medium composition

APPENDIX 4

Worksheet of the

CCF design for response surface modelling

Exp Nr.	Run Order	$MgSO_4 \cdot 7H_2O$	NaCl	$CaCl_2 \cdot 2H_2O$	$ZnSO_4 \cdot 7H_2O$	$CuSO_4 \cdot 5H_2O$	$NiCl_2 \cdot 6H_2O$	$FeSO_4 \cdot 7H_2O$	$NaNO_3$	KH_2PO_4	$MnCl_2 \cdot 2H_20$	pH
11	1	0.2	0.1	0.1	0	9	0	7	5	0.2	16	2
26	2	0.2	0.1	0.1	0.08	5.5	0	9	3.5	0.2	16	2
1	3	0.2	0.1	0.1	0	2	0	7	2	0.2	16	2
3	4	0.2	0.1	0.1	0	9	0	7	2	0.2	10	2
27	5	0.2	0.1	0.1	0.08	5.5	0	9	3.5	0.2	13	2
23	6	0.2	0.1	0.1	0.08	5.5	0	9	2	0.2	13	2
15	7	0.2	0.1	0.1	0	9	0	11	5	0.2	10	2
9	8	0.2	0.1	0.1	0	2	0	7	5	0.2	10	2
2	9	0.2	0.1	0.1	0.16	2	0	7	2	0.2	10	2
7	10	0.2	0.1	0.1	0	9	0	11	2	0.2	16	2
29	11	0.2	0.1	0.1	0.08	5.5	0	9	3.5	0.2	13	2
13	12	0.2	0.1	0.1	0	2	0	11	5	0.2	16	2
17	13	0.2	0.1	0.1	0	5.5	0	9	3.5	0.2	13	2
21	14	0.2	0.1	0.1	0.08	5.5	0	7	3.5	0.2	13	2
18	15	0.2	0.1	0.1	0.16	5.5	0	9	3.5	0.2	13	2
28	16	0.2	0.1	0.1	0.08	5.5	0	9	3.5	0.2	13	2
22	17	0.2	0.1	0.1	0.08	5.5	0	11	3.5	0.2	13	2
24	18	0.2	0.1	0.1	0.08	5.5	0	9	5	0.2	13	2
6	19	0.2	0.1	0.1	0.16	2	0	11	2	0.2	16	2
10	20	0.2	0.1	0.1	0.16	2	0	7	5	0.2	16	2
14	21	0.2	0.1	0.1	0.16	2	0	11	5	0.2	10	2
5	22	0.2	0.1	0.1	0	2	0	11	2	0.2	10	2
25	23	0.2	0.1	0.1	0.08	5.5	0	9	3.5	0.2	10	2
12	24	0.2	0.1	0.1	0.16	9	0	7	5	0.2	10	2
4	25	0.2	0.1	0.1	0.16	9	0	7	2	0.2	16	2
20	26	0.2	0.1	0.1	0.08	9	0	9	3.5	0.2	13	2
19	27	0.2	0.1	0.1	0.08	2	0	9	3.5	0.2	13	2
8	28	0.2	0.1	0.1	0.16	9	0	11	2	0.2	10	2
16	29	0.2	0.1	0.1	0.16	9	0	11	5	0.2	16	2
30*	30	0.2	0.1	0.1	0.08	0.2	0	10	2	2.5	16	3.5
31*	31	0.2	10	0.1	0.08	5	0.5	10	10	0.1	16	2
32*	32	2	0.1	1.5	8	5	0	0.2	10	2.5	16	2
33*	33	0.2	0.1	0.1	0.08	9	0	8	3	0.2	22.5	2
34*	34	0.2	0.1	0.1	0.08	9	0	19	3	0.2	10	2

* These experiments do not belong to the CCF design. The grey columns represent the compounds that are varied in concentration to find the medium optimum
$MgSO_4 \cdot 7H_2O$; NaCl; $NaNO_3$; KH_2PO_4 and $CaCl_2 \cdot 2H_2O$ are expressed in g/L.
$ZnSO_4 \cdot 7H_2O$; $CuSO_4 \cdot 5H_2O$; $NiCl_2 \cdot 6H_2O$; $FeSO_4 \cdot 7H_2O$ and $MnCl_2 \cdot 2H_20$ are expressed in mg/L.

APPENDIX 5

Screening experiment responses

Experiment Nr.	Run order	Culture time [1] (d)	Xylose consumed (C-mol/L)	Biomass yield [2] (C-mol/C-mol)	Succinic acid yield (mC-mol/C-mol)
1	1	11.0	1.37	0.28	0.11
35[3]	2	13.9	1.66	0.35	1.81
32	3	13.9	1.66	0.31	1.92
9	4	13.9	1.66	0.19	0.28
33[3]	5	13.9	1.66	0.33	1.84
7	6	13.9	1.66	0.44	2.03
11	7	11.0	1.66	0.34	3.15
12	8	13.9	1.58	0.35	4.09
10	9	11.0	1.66	0.34	2.57
23	10	13.9	1.50	0.22	4.37
4	11	13.9	1.57	0.36	15.46
19	12	13.9	1.66	0.34	6.25
26	13	13.9	1.64	0.35	4.12
31	14	11.0	1.66	0.47	1.28
25	15	13.9	1.63	0.38	5.01
21	16	13.9	1.39	0.35	5.79
5	17	11.0	1.66	0.57	2.38
18	18	11.0	1.66	0.75	2.30
2	19	13.9	1.55	0.39	2.68
16	20	11.0	1.66	0.50	1.16
24	21	13.9	1.16	0.35	2.47
8	22	13.9	1.35	0.36	0.11
15	23	13.9	1.66	0.32	3.35
29	24	13.9	1.19	0.27	2.59
14	25	11.0	1.59	0.47	1.72
27	26	13.9	1.59	0.31	2.38
20	27	13.9	1.66	0.45	2.63
13	28	13.9	1.57	0.37	3.90
30	29	11.0	1.66	0.40	1.31
28	30	13.9	1.57	0.40	5.91
17	31	13.9	1.50	0.31	3.30
34[3]	32	13.9	1.66	0.35	4.76
6	33	11.0	1.66	0.38	3.36
3	34	13.9	1.45	0.28	3.80
22	35	13.9	1.39	0.28	4.73

[1] Yields are calculated before a significant decrease of biomass (1g/L) and when xylose concentration is below 2 g/L.

[2] Yields in biomass calculated with the following formula of the biomass: $CH_{1.72}O_{0.55}N_{0.17}P_{0.005}$

[3] These results are the centre points

APPENDIX 6

Box Benhken experiment responses

Experiment Nr.	Run order	Culture time [1] (d)	Xylose consumed (C-mol/L)	Biomass yield [2] (C-mol/C-mol)	Succinic acid yield (mC-mol/C-mol)
17	1	13.7	0.90	0.30	0.79
8	2	10.9	1.66	0.33	2.54
2	3	13.7	1.66	0.42	1.77
16	4	10.9	1.66	0.38	1.81
9	5	10.9	1.66	0.46	2.73
11	6	10.9	1.66	0.47	1.76
26[3]	7	13.7	1.65	0.46	1.56
15	8	7.9	1.66	0.39	4.06
25[3]	9	13.7	1.66	0.43	2.24
20	10	11.1	1.66	0.38	2.41
10	11	13.7	1.66	0.40	1.71
23	12	13.7	1.62	0.49	2.12
1	13	13.7	1.63	0.44	2.93
4	14	13.7	1.66	0.44	2.78
12	15	13.7	1.66	0.46	1.54
3	16	13.7	1.63	0.43	1.73
18	17	13.7	0.94	0.28	0.93
22	18	13.7	1.60	0.43	1.14
6	19	7.9	1.66	0.30	4.14
5	20	13.7	1.14	0.32	0.33
27[3]	21	13.7	1.65	0.44	1.18
13	22	13.7	0.92	0.41	0.83
7	23	13.7	0.94	0.32	0.72
19	24	10.9	1.66	0.41	0.85
21	25	13.7	1.66	0.42	1.89
14	26	13.72	1.12	0.39	0.93
24	27	13.72	1.66	0.67	1.93

[1] Yields are calculated before a significant decrease of biomass (1g/L) and when xylose concentration is below 2 g/L.

[2] Yields in biomass calculated with the following formula of the biomass: $CH_{1.72}O_{0.55}N_{0.17}P_{0.005}$

[3] These results are the centre points

APPENDIX 7

CCF experiment responses

Experiment Nr.	Run order	Culture time [1] (d)	Xylose consumed (C-mol/L)	Biomass yield [2] (C-mol/C-mol)	Succinic acid yield (C-mol/C-mol)
11	1	7.8	1.66	0.29	0.31
26	2	7.8	1.66	0.29	0.36
1	3	10.6	1.66	0.26	1.43
3	4	10.6	1.66	0.40	1.18
27[3]	5	10.6	1.66	0.21	0.75
23	6	10.6	1.66	0.25	4.12
15	7	7.8	1.63	0.35	1.27
9	8	10.6	1.66	0.31	6.77
2	9	7.8	1.63	0.34	0.27
7	10	10.6	1.66	0.36	3.38
29[3]	11	7.8	1.66	0.30	0.27
13	12	10.6	1.66	0.30	2.07
17	13	7.8	1.64	0.28	1.05
21	14	7.8	1.66	0.25	0.00
18	15	7.8	1.66	0.29	0.20
28[3]	16	7.8	1.63	0.30	0.55
22	17	7.8	1.66	0.26	0.25
24	18	7.8	1.66	0.26	0.39
6	19	7.8	1.62	0.26	0.23
10	20	7.8	1.64	0.32	0.75
14	21	7.8	1.66	0.24	0.09
5	22	10.6	1.66	0.30	0.62
25	23	no results	no results	no results	no results
12	24	7.8	1.66	0.24	0.24
4	25	10.6	1.66	0.25	3.39
20	26	7.8	1.66	0.29	0.29
19	27	7.8	1.66	0.31	0.37
8	28	7.8	1.65	0.26	0.33
16	29	7.8	1.66	0.24	0.20
30*	30	10.6	1.66	0.23	2.26
31*	31	10.6	1.66	0.32	0.89
32*	32	10.6	1.66	0.35	0.73
33*	33	7.8	1.66	0.27	0.50
34*	34	10.6	1.67	0.26	2.68

[1] Yields are calculated before a significant decrease of biomass (1g/L) and when xylose concentration is below 2 g/L.

[2] Yields in biomass calculated with the following formula of the biomass: $CH_{1.72}O_{0.55}N_{0.17}P_{0.005}$

[3] These results are the centre points

* These experiments do not belong to the CCF design but are the replicates for the checking experiment

Chapter 5

Physiological characterisation of xylose metabolism in *Aspergillus niger* under oxygen limited conditions

Meijer S., Panagiotou G., Olsson L. and Nielsen J.
Biocentrum-DTU, Center for Microbial Biotechnology, Denmark

Biotechnology and Bioengineering (2007) **98** (2):462-475

5.1 Abstract

The physiology of *Aspergillus niger* was studied under different aeration conditions. Five different aeration rates were investigated in batch cultivations of *A. niger* grown on xylose. Biomass, intra- and extra-cellular metabolites profiles were determined and ten different enzyme activities in the central carbon metabolism were assessed. The focus was on organic acid production with a special interest in succinate production. The fermentations revealed that oxygen limitation significantly changes the physiology of the micro-organism. Changes in extra cellular metabolite profiles were observed, i.e there was a drastic increase in polyol production (erythritol, xylitol, glycerol, arabitol and mannitol) and to a lesser extent in the production of reduced acids (malate and succinate). The intracellular metabolite profiles indicated changes in fluxes, since several primary metabolites, like the intermediates of the TCA cycle accumulated during oxygen limitation (on average 3 fold increase). Also the enzyme activities showed changes between the exponential growth phase and the oxygen limitation phase. In general, the oxygen availability has a significant impact on the physiology of this fungus causing dramatic alterations in the central carbon metabolism that should be taken into account in the design of *A. niger* as a succinate cell factory.

Keywords: *Aspergillus niger*, organic acids, oxygen limitation, metabolome profiling

5.2 Introduction

The filamentous fungus *Aspergillus niger* is widely used in industry for the production of citric acid and many different enzymes. In nature this fungus is found in soils, where it plays a central role in the global carbon cycle (Lewis et al. 1994). The natural ability to break down lignocellulose from plants, by production of hydrolytic and oxidative extracellular enzymes, makes it an interesting micro-organism for creating high sugar syrups (Pedersen et al. 1999). However, its ability to efficiently produce citric acid (Kubicek et al. 1986), makes it an obvious candidate for development of an efficient cell factory for the production of other organic acids. In particular its ability to use complex feedstocks as nutrients, allows this organism to be used for production of chemicals from biomass. These products can be further processed for use as plastic monomers, solvents, detergents, pharmaceuticals or fuels (Potera 2005), reducing the dependence on petroleum that constitutes the traditional source for synthesis of chemical building blocks used in these products.

The US DOE Office of Energy Efficiency and Renewable Energy has started a Biomass Program, in which they aim for developing biorefineries producing multiple biobased products, including higher-value chemicals as well as fuels and power. The program has identified the top ten value-added chemicals from biomass that would economically and technically support the production of fuels and power in an integrated biorefinery (Werpy and Petersen 2004). One of these chemicals is the four-carbon dicarboxylic acid succinate (Potera 2005; Zeikus et al. 1999). Several production micro-organisms for succinate production are already under investigation.

There are some naturally producing organisms like *Mannheimia succiniciproducens* and *Actinobacillus succinogenes* that produce large amounts of this acid (Lee et al. 2006). However, they are cultivated at pH values around 6, and the product is therefore the succinic acid salt, and obtaining the free acid adds costs to the downstream processing. Several research groups have also metabolically engineered *E.coli* to produce succinic acid (Lee et al. 2005; Lin et al. 2005; Millard et al. 1996; Sanchez et al. 2005; Vemuri et al. 2002), but the productivities obtained do still not allow to compete with the chemical process, and an *E. coli* based process will also only enable production of the succinate salt. The highest productivity obtained with *E. coli* is around 1.8 g/L/h, but it has been estimated that this needs to be increased to 2.5 g/L/h to become compatible with the chemical process (Lee et al. 2006; Werpy and Petersen 2004).

In the present study we wanted to evaluate the use of *A. niger* as production organism for organic acids, including succinic acid. The advantage of using this organism is that it can grow at low pH,

thereby producing succinic acid instead of its salt. It also has been shown that *A. niger* is able to produce high yields and final titers of organic acids especially in the form of citric acid (Kubicek et al. 1986). However, contrary to how much is known about the fermentation process for citric acid production, relatively little is known about the molecular mechanisms controlling the metabolism of *A. niger* (Karaffa et al. 2001). The effects of various environmental factors on suppressing or triggering the export of various biomass degrading enzymes, molecular mechanisms critical to fermentation process development, and mechanisms involved in the control of fungal morphology, have been studied (Papagianni 2004; Grimm et al. 2005). Nevertheless, a thorough understanding of the molecular mechanisms controlling carbon flux in this fungus is still lacking. The creation of a stoichiometric metabolic model of *A. niger* (David et al. 2003) has contributed to a better understanding of the central carbon metabolism and even more insight will be gained from the study of the *A. niger* genome. As more fungal genomes are sequenced, scientists will even be able to use comparative genomics to find commonalities and differences in the molecular circuits that control carbon flux in fungi (Archer and Dyer 2004; Nielsen and Olsson 2002). All these data can be integrated with metabolite profiling and finally with transcriptome data to retrieve a comprehensible system approach for engineering *A. niger* (Jewett et al. 2006).

Here we investigated the effect of oxygen limitation on the phenotype of *A.niger* and the metabolic profiles in the central carbon metabolism. Oxygen limitation, occurring in industrial processes, has been shown to result in reduced productivity of citric acid and has a significant influence on the morphology of *A. niger* (Kubicek et al. 1980). Furthermore, it has an effect on the redox and energy state of the micro-organism. Simulation of the oxygen limitation with a stoichiometric model indicated that carbon fluxes were redirected towards different metabolic pathways, resulting in a changed metabolic profile (David et al. 2003). We therefore focused on micro-aerobic cultivation conditions, since in micro-organisms that naturally produce succinate, this acid is produced most efficiently under anaerobic conditions, probably due to the use of the reductive part of the TCA-cycle to balance the redox state within the cell (also referred to as fumarate respiration). *A. niger* is an aerobic organism, but we approached anaerobic conditions by limiting the oxygen supply and studied the physiological response of *A. niger* to these micro-aerobic conditions and especially the effects on succinate production.

The cultivations were performed on xylose, the second most abundant carbon source in nature, that is fermented relatively easy by *A. niger*. Xylose enters the metabolism in the reductive part of the Pentose Phosphate Pathway (PPP) and it is therefore necessary that there is a flux back to glucose-6-phosphate in order to ensure use of the oxidative part of the PPP for NADPH production (Diano et al. 2006).

As nitrogen source we used nitrate, as nitrate consumption results in an increase in the reducing power that supports cellular metabolism during oxygen limited conditions. Nitrate uptake and conversion releases NADP that delivers extra reducing power to the cells especially under oxygen limited condition where the NAD(P)H/NAD(P) ratio is high and cellular reducing power is low.

5.3 Materials and Methods

5.3.1 Strain

The laboratory strain *Aspergillus niger* N402 was used in this study. This strain is also known as A733 at the fungal genetics stock center and is a short-conidiophore derivative (cspA1 mutation) of the N400 strain which is an *Aspergillus niger* wild type strain.

5.3.2 Media

A minimal medium adjusted to pH 6.5 was used for the pre-culture. Spores were propagated on agar plates containing 10 g/L D-glucose, 50 ml salt solution, 1 ml trace element solution 1 and 18 g/L agar. The salt solution consisted of 120 g/L $NaNO_3$, 10.4 g/L KCl, 10.4 g/L $MgSO_4 \cdot 7\ H_2O$ and 30.4 g/L KH_2PO_4. The trace element solution 1 consisted of 22 g/L $ZnSO_4 \cdot 7\ H_2O$, 11 g/L H_3BO_3, 5 g/L $MnCl_2 \cdot 2\ H_2O$, 5 g/L $FeSO_4 \cdot 7\ H_2O$, 1.7 g/L $CoCl_2 \cdot 6\ H_2O$, 1.6 g/L $CuSO_4 \cdot 5\ H_2O$, 1.5 g/L $Na_2MoO_4 \cdot 2\ H_2O$ and 50 g/L Na_4EDTA.

A chemically defined medium adjusted to pH 2.5 was used for the batch cultivations containing 50 g/L xylose, 10 g/L $NaNO_3$, 1.5 g/L KH_2PO_4, 1 g/L $MgSO_4 \cdot 7\ H_2O$, 2 g/L NaCl, 0.1 g/L $CaCl_2 \cdot 2H_2O$, 0.5 ml/L antifoam (sb2121) and 1 ml/L trace element solution 2. The trace element solution 2 consisted of 0.4 g/L $ZnSO_4 \cdot 7\ H_2O$, 5 g/L $CuSO_4 \cdot 5\ H_2O$, 0.25 g/L $NiCl_2 \cdot 6\ H_2O$, 35 g/L $MnCl_2 \cdot 2\ H_2O$ and 30 g/L $FeSO_4 \cdot 7\ H_2O$.

5.3.3 Cultivation conditions

During the pre-culture spores were propagated on agar plates at 37 ºC for 4-7 days and harvested with 0.01% Tween-80.

The batch cultivations were inoculated with a volume of spore solution to yield a spore concentration of 10^9 spores/L bioreactor. These cultivations were carried out in 3 L-Braun fermenters with a working volume of 2 L. The bioreactors were equipped with temperature control, pH control and two Rushton four-blade disc turbines. No baffles were incorporated in the reactors, thereby reducing the surface area available for wall growth. Air was used for sparging and the concentrations of oxygen and carbon dioxide in the exhaust gas were monitored by an acoustic

gas analyser (Brüel & Kjær, Nærum, Denmark). The dissolved oxygen tension (DOT) was measured with an oxygen probe (Mettler Toledo sensors). During the cultivation the temperature was maintained at 30 ºC. The pH was controlled by automatic addition of 2 M NaOH and 2 M HCl. The pH was initially set to 2.5 to prevent spore aggregation and was gradually increased to 3.5 as soon as spore germination started. After inoculation the agitation was shortly (10 s) increased to 1000 rpm to avoid spore aggregation and thereafter kept at 150 rpm until the spores started to germinate. The agitation was in two steps increased to 700 rpm as soon as the spores started to germinate. Five different aeration levels, 0.01, 0.02, 0.05, 0.1 and 1 vvm, respectively, were applied to simulate oxygen-limited and aerobic conditions. The mass flow controller is sufficiently precise to enable differentiation between the different flow rates.

5.3.4 Sampling

For the quantification of cell dry weight a known cell culture volume was filtered through a pre-weighed nitrocellulose filter (pore size 45 µm, Pall Corporation). The filtrate was frozen immediately and later used for the determination of substrate and extracellular metabolites. The filter was washed with 0.9% w/v NaCl, dried for 15 min in a microwave oven at 150 W and weighed again to determine the biomass concentration.

For the quantification of intracellular metabolites 10 mL of cell culture was immediately quenched in 20 mL of cold 72% methanol (- 40 ºC). After quenching the cells were separated from the quenching solution by centrifugation at 10000g for 20 min at -20 ºC and the intracellular metabolites were extracted as described by Koning et al (1992). Finally, the samples were lyophilised and stored at - 80 ºC until further analysis.

For determination of *in vitro* enzyme activities the samples were filtered through a nitrocellulose filter (pore size 45 µm, Pall Corporation), washed with 0.9% w/v NaCl and the filter cake (± 1 g) was immediately frozen in liquid nitrogen and stored at -80 ºC.

5.3.5 Quantification of substrate and extracellular metabolites

The concentrations of sugars, organic acids and polyols in the extracellular environment were determined by using high-performance liquid chromatography. Xylose, acetate, pyruvate, citrate, ethanol, succinate, fumarate, malate, glycerol, and oxalate concentrations were measured on an Aminex HPX-87H cationic exchange column (BioRad, Hercules, California), eluted at 60 ºC with 5 mM H_2SO_4 at a flow rate of 0.6 mL/min. Metabolites were detected with both a refractive index

detector and a UV detector. The polyols arabitol, erythritol, glycerol, mannitol and xylitol were analysed using a CarboPac MA1 anionic exchange column (Dionex, Rødovre, Denmark) that was eluted at 60 ºC with 612 mM NaOH at a flow rate of 0.4 mL/min and an electrochemical detector (ED 40) was employed.

5.3.6 Determination of intracellular metabolites

The lyophilised samples were derivatised using methyl chloroformate as described by Villas-Boas et al. (2003). The resulting dry organic solutions were transferred to silanised GC vials and analysed. The GC-MS analysis of amino and non-amino organic acids was performed with a Hewlett–Packard system HP 6890 gas chromatograph coupled to a HP 5973 quadrupole mass selective detector (EI) operated at 70 eV. The column used for all analysis was a J&W1701 (Folsom, CA) 30 m long; 250 µm inner diameter; 0.10 µm film thickness. The MS was operated in scan mode (start after 5 min, mass range 38–550 atomic mass unit at 2.88 s/scan) (Villas-Boas et al. 2003).

5.3.7 Preparation of cell extracts

The frozen samples were thawed on ice and 0.5 g was suspended in 2 mL of 0.1 M sodium phosphate (pH 7.4), 5 mM $MgCl_2$, 1 mM EDTA and 2.6 mM dithiothreitol buffer. This solution was transferred to 2-mL FastPrep tubes containing 0.5 mL glass beads (0.75-1 mm). The FastPrep tubes were processed 3 times 10 s on a FastPrep FP120 Instrument (Savant Instruments, Holbrook, NY), at speed setting 5, with cooling on ice in between. After disruption, samples were centrifuged at 13,000 g at 4 ºC for 10-20 min, and the supernatants were analysed for enzyme activity.

5.3.8 Analysis of in vitro enzyme activities

Enzyme assays were performed at 30°C with a HP8453 UV-visible light spectrophotometer. In order to test the linearity of the assays, the reactions were performed with 2-3 different dilutions of cell extract. For succinate dehydrogenase and pyruvate carboxylase the activity measurements were, however, determined only once. The specific enzyme activities are expressed as micromoles $minute^{-1}$ $milligram^{-1}$ (U/mg). The amount of protein was determined by the Bradford method (Bradford 1979) with bovine serum albumin as the standard.

The enzymes measured and reaction mixtures used are listed in Table 5.1. All the assays were tested with pure enzyme before quantification of the enzyme activities in the cell extracts, but for

succinate dehydrogenase, malic enzyme and pyruvate carboxylase no pure enzymes were available.

Table 5.1 Enzyme assay methods

Enzyme	Reaction mixture	Ref.
Glucose-6P dehydrogenase (EC 1.1.1.49)	50 mM Tris-HCl (pH 8.2), 2 mM D-glucose 6-phosphate, 0.67 mM ß-nicotinamide adenine dinucleotide phosphate, 10 mM magnesium chloride and cell extract. (340 nm; ε = 6.22 mM^{-1} cm^{-1})	1(m)
Malic dehydrogenase (EC 1.1.1.37)	100 mM potassium phosphate (pH 7.5), 0.13 mM ß-nicotinamide adenine dinucleotide (reduced form), 0.25 mM oxalacetic acid and cell extract. (340 nm; ε = 6.22 mM^{-1} cm^{-1})	1
Malic enzyme (EC 1.1.1.40)	67 mM Tris-HCl (pH 7.4), 3.3 mM L-malic acid, 0.3 mM β-nicotinamide adenine dinucleotide phosphate, 5.0 mM manganese chloride and cell extract. (340 nm; ε = 6.22 mM^{-1} cm^{-1})	1
Pyruvate decarboxylase (EC 4.1.1.1)	187 mM citric acid (pH 6), 33 mM sodium pyruvate, 0.11 mM ß-nicotinamide adenine dinucleotide (reduced form), 10 units alcohol dehydrogenase, and cell extract. (340 nm; ε = 6.22 mM^{-1} cm^{-1})	1
Pyruvate carboxylase (EC 6.4.1.1)	134 mM Tris-HCl (pH 7.8), 5 mM magnesium sulfate, 7 mM pyruvic acid, 0.12% (w/v) bovine serum albumin, 0.23 mM β-nicotinamide adenine dinucleotide (reduced form), 0.05 mM acetyl coenzyme A, 2.63 units malic dehydrogenase, 1 mM adenosine 5'-triphosphate, 15 mM potassium bicarbonate and cell extract. (340 nm; ε = 6.22 mM^{-1} cm^{-1})	1(m)
Pyruvate dehydrogenase (EC 1.2.4.1)	51 mM Tris-HCl (pH 7.4), 0.20 mM magnesium chloride, 0.01 mM calcium chloride, 0.30 mM Thiamine pyrophosphate, 0.12 mM coenzyme A, 2.0 mM β-NAD, 2.64 mM L-cysteine hydrochloride, 20.4 mM pyruvate and cell extract. (340 nm; ε = 6.22 mM^{-1} cm^{-1})	1(m)
Citrate synthase (EC 2.3.3.1)	46 mM Tris (pH 8), 0.42 mM Acetyl-CoA, 1 mM OAA, 5.3 mM KCl, 0.6 mM DTNB and cell extract. (412 nm; ε = 13.6 mM^{-1} cm^{-1})	1(m)
Isocitrate lyase (EC 4.1.3.1)	30 mM Tris-HCl (pH 6.8), 5 mM magnesium chloride, 1 mM ethylenediaminetetraacetic acid, 4 mM phenylhydrazine, 1 mM DL-isocitric acid, and cell extract. (324 nm; ε = 16.8 mM^{-1} cm^{-1})	1(m)
Succinate dehydrogenase (EC 1.3.99.1)	0.8 M Tris-HCl (pH 7.6), 0.15 M sucrose, 0.4 M succinate, 8 mM sodium azide, 6.4 mM INT and cell extract. (458 nm; ε = 22 mM^{-1} cm^{-1})	2
Fumarase (EC 4.2.1.2)	96.7 mM potassium phosphate (pH 7.6), 48.3 mM L-malic acid and cell extract. (240 nm; ε = 2.44 mM^{-1} cm^{-1})	1

1. http://www.sigmaaldrich.com/Area_of_Interest/Biochemicals/Enzyme_Explorer/Key_Resources/Assay_Library/Assays _by_En zyme_Name_III (06-10-2006)
2. Green and Narahara (1980).

m. modified assay

5.4 Results and discussion

5.4.1 Physiology

The fermentation performance of *A. niger* was studied under different aeration conditions. Five batch cultivations were performed using different levels of aeration (0.01, 0.02, 0.05, 0.1 and 1 vvm) and the effects of oxygen limitation on the specific growth rate, biomass and product yields, and enzyme activities were determined. The carbon source used in all fermentations was xylose, which was supplied at a high concentration (50 g/L) at the beginning of the cultivation to ensure a high glycolytic flux needed for organic acid production (Kubicek et al. 1986). This high sugar concentration is likely to cause carbon catabolite repression in the beginning of the fermentation. This carbon catabolite repression is mainly via the CreA transcription factor (Kelly 1994; Drysdale et al. 1993). In all our fermentations we performed analyses at approximately the same sugar concentration, and any possible effects of CreA repression are therefore likely to be the same in the fermentations, and this issue was not considered any further. Nitrate was used as nitrogen source, as this enables better growth conditions under oxygen limitation by supplying more reducing power (Takasaki et al. 2004). All batch fermentations were characterised by a lag phase, an exponential growth phase and an oxygen limitation phase. An extended lag phase was observed when less oxygen was supplied during the cultivation. However, this was not reflected in the specific growth rate (Table 5.2). When the cells reached the exponential growth phase the specific growth rate was found to be independent of the oxygen supply and ranged between 0.13 and 0.15 h^{-1}. A log plot of the biomass profiles (Figure 5.1) shows a clear distinction between the exponential growth phase and the oxygen limitation phase. From the growth curves we could also conclude that at lower airflow the oxygen limitation sets in slightly sooner.

Changes in the carbon uptake rate were followed and it increased with increasing aeration from 3.4 to 13.0 mmol/L/h. The xylose was completely consumed in all fermentations, except for the fermentation with the lowest aeration (0.01 vvm), where only 46% of the initial amount was consumed. The biomass yields were fairly constant, indicating more by-product formation at higher aeration. By-product formation could be detected already in the exponential growth phase and continued in the oxygen limitation phase. The main by-products produced were polyols (glycerol, erythritol, xylitol) and some organic acids (succinate and malate).

Table 5.2 Growth characteristics and product yield coefficients for different cultivation conditions of *Aspergillus niger*.

(vvm)	Acids (mmol/mol xylose)				Polyols (mmol/mol xylose)						(g/g xylose)	(h^{-1})	(mmol/L/h)
aeration	succinate	fumarate	malate	oxalate	ethanol	erythritol	glycerol	xylitol	mannitol	arabitol	biomass	μ	q_s
0.01	3.51	0.63	4.61	n.a.	n.a.	27.99	5.80	24.79	10.93	8.77	0.28	0.13	3.4
0.02	0.52	0.33	0.91	n.a.	275.83 [a]	9.92	9.24	9.05	5.18	2.82	0.30	0.13	7.8
0.05	1.38	5.29	1.09	12.74	n.a.	14.32	6.69	9.63	2.33	2.47	0.23	0.15	9.2
0.10	0.45	0.31	0.73	57.19	n.a.	7.08	16.50	12.13	1.62	1.86	0.35	0.15	13.0
1.00	n.a.	n.a.	0.51	86.77	n.a.	7.03	2.30	3.20	0.29	0.28	0.27	0.15	13.0

The yields determined are the maximal yields achieved during the different cultivations

[a] only small amount formed within 15 h after inoculation

Table 5.3 Enzyme activities measured in U/mg protein for different cultivation conditions.

	0.01 vvm		0.02 vvm		0.05 vvm		0.1 vvm		1 vvm	
	Growth	O2-lim	Growth	O2-lim	Growth	O2-lim	Growth	O2-lim	Growth	lim
Glucose-6-P dehydrogenase	0.86 ± 0.33	0.58 ± 0.13	0.79 ± 0.28	0.54 ± 0.17	1.01 ± 0.29	0.59 ± 0.16	1.00 ± 0.19	0.95 ± 0.22	1.81 ± 0.53	0.51 ± 0.09
Pyruvate carboxylase	0.021	0.018	0.029	0.023	0.013	0.000	0.036	0.017	0.019	0.016
Malic enzyme	1.20 ± 0.17	1.49 ± 0.34	2.2 ± 0.45	1.56 ± 0.43	1.83 ± 0.61	1.57 ± 0.36	7.03 ± 0.79	1.65 ± 0.50	3.61 ± 1.15	1.69 ± 0.53
Citrate synthase	0.96 ± 0.20	0.75 ± 0.23	0.89 ± 0.11	0.27 ± 0.03	0.79 ± 0.13	0.57 ± 0.09	0.35 ± 0.08	0.25 ± 0.03	0.43 ± 0.11	0.19 ± 0.03
Isocitrate lyase	0.40 ± 0.08	0.37 ± 0.01	0.75 ± 0.19	0.39 ± 0.10	0.33 ± 0.12	0.25 ± 0.04	0.48 ± 0.22	0.38 ± 0.12	0.83 ± 0.14	0.16 ± 0.05
Succinate dehydrogenase	0.008	0.000	0.016	0.018	0.019	0.077	0.019	0.023	0.100	0.012
Fumarase	1.18 ± 0.07	1.29 ± 0.15	1.29 ± 0.23	1.43 ± 0.31	0.72 ± 0.14	1.43 ± 0.13	4.42 ± 1.17	0.82 ± 0.02	3.27 ± 2.08	0.80 ± 0.12
Malic dehydrogenase	1.88 ± 0.35	2.32 ± 0.22	3.52 ± 0.55	2.25 ± 0.79	2.2 ± 0.29	2.73 ± 0.47	4.21 ± 1.13	2.48 ± 0.43	3.65 ± 0.36	2.61 ± 0.39

All enzyme activities are the average of 3 independent measurements except for succinate dehydrogenase and pyruvate carboxylase.

The activities are expressed in U/mg protein and the lower case numbers are the standard deviations.

Figure 5.2 gives a typical profile of the extracellular metabolites being produced. It is obvious that the polyol production drastically increases when the oxygen limitation sets in. At the end of the fermentation, when the carbon source is exhausted, these polyols are consumed again. This activation of polyol consumption pathways provides the cells with more carbon for metabolism.

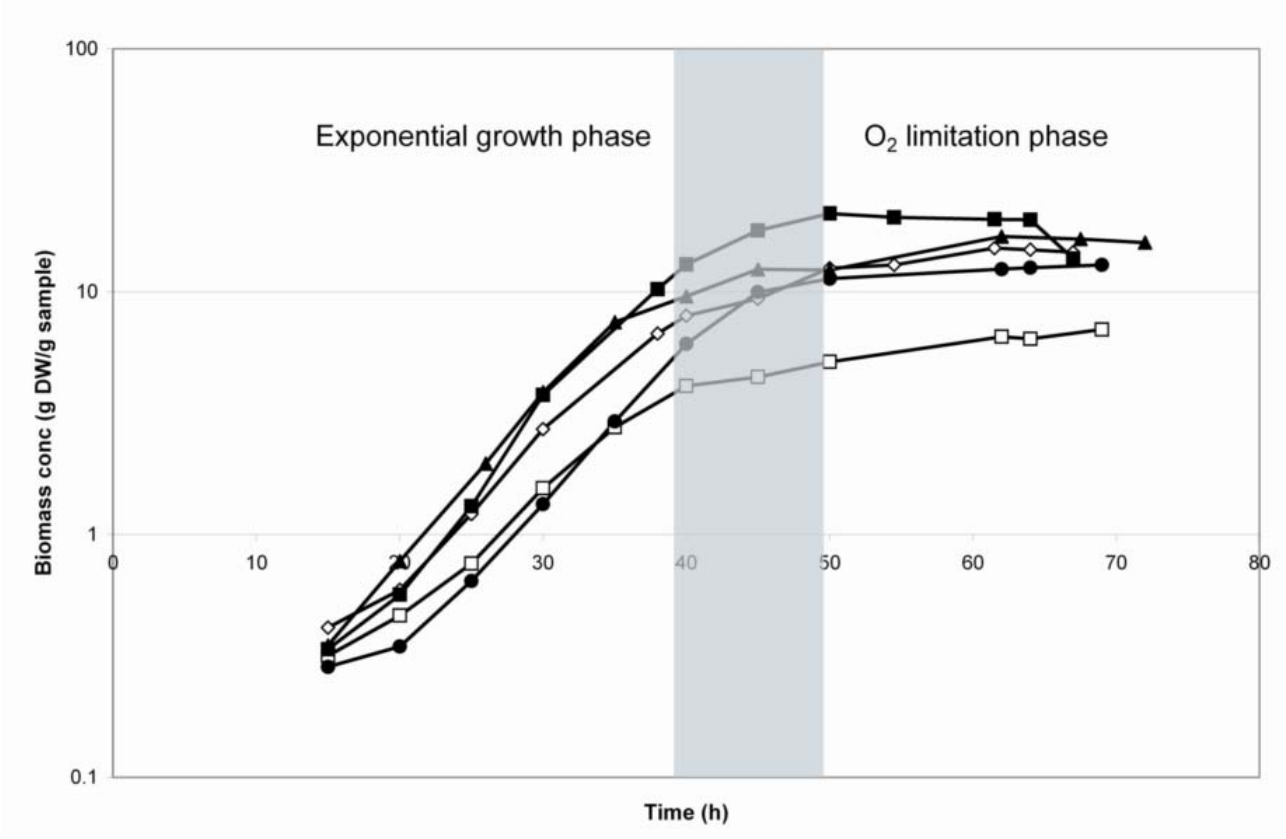

Figure 5.1 Logarithmic plot of the biomass profiles under different aeration levels. ■: 1 vvm; ▲: 0.1 vvm; ●: 0.05vvm; ◇: 0.02 vvm; □: 0.01 vvm. The gray area is where the transition from exponential growth phase to oxygen limitation phase occurs.

5.4.2 Extracellular metabolites

The yields of both polyol and organic acid production on consumed substrate increased as the oxygen supply decreased (Figure 5.2). It was observed that erythritol and glycerol were the first polyols being produced (20-25 hours), followed by xylitol (25-30 hours). Furthermore, the erythritol and glycerol production stopped before the production of xylitol. Arabitol and mannitol production started later in all cultivations, but the production stopped approximately at the same time as for the other polyols. The arabitol production was higher than the mannitol production (0.08 g/L and 0.01g/L, respectively) and the total amount of these polyols decreased with an increasing airflow.

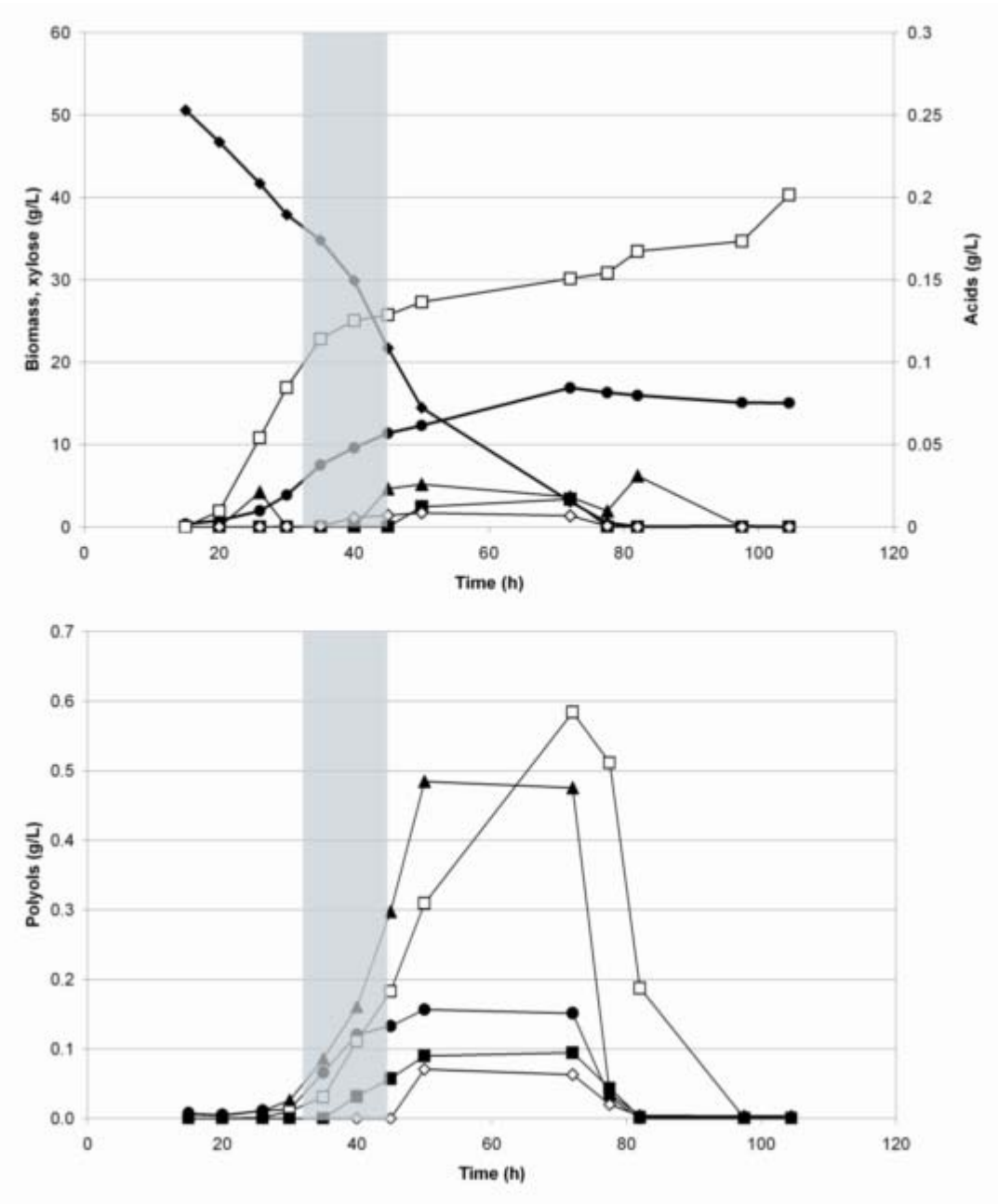

Figure 5.2 A typical batch production profile (0.1 vvm) with a clear increase in acid and in polyol during the oxygen limitation phase. A) ♦: xylose; •: biomass; ▲: malate; ■: succinate; ◇: fumarate; □: oxalate. B) ◇: mannitol; □: xylitol; ■: arabitol; ▲: erythritol; •: glycerol. The gray area is where the transition from exponential growth phase to oxygen limitation phase occurs.

Polyols are known to be involved in carbohydrate reserves, osmoregulation, storing reducing power and translocation processes in the metabolism of *A. niger* (Witteveen and Visser 1995; Beever and Laracy 1986). Due to the use of xylose as carbon source, significant amounts of xylitol were produced during all cultivations (Table 5.2). Xylitol production is known to be regulated by the NADH levels in the cell. Under oxygen limited conditions the NADH pool increases, thereby limiting the NAD dependent xylitol dehydrogenase, xylitol production will increase under these conditions (Jeffries et al. 2004). In fungi xylose is metabolised via xylitol to xylulose and further to xylulose-5-phosphate from where it enters the reductive part of the PPP. Xylitol production requires the cofactor NADPH and this demand is satisfied by a backflux from the reductive part of the PPP to the oxidative part of the PPP (Diano and Nielsen 2006).

With nitrate as nitrogen source, we further increase the NADPH requirement leading to a high flux through the PPP (Ruijter et al. 2005). This was also reflected by high activity of the G6PDH and high production of erythritol (Table 5.2 and Table 5.3). Also arabitol is produced from the PPP, but the production was not as high as erythritol (0.08 g/L and 0.48 g/L, respectively). Furthermore, the results obtained in this study are in agreement with Poulsen et al. (2005), who showed that by using nitrate as nitrogen source enzymes in the PPP were upregulated, leading to a PPP overflow, resulting in erythritol production. The high flux through the PPP results in a reduced flux through the EMP pathway and this leads to less glycerol production (Table 5.2). At aeration conditions allowing a high oxygen availability we observe oxalate production, which is a well known product produced by *A. niger* under certain conditions (Ruijter and Visser 1999). With lower aeration a drastic decrease in oxalate production (from 0.4 g/L to 0) is measured and a small increase in the production of succinate and malate (0.07 and 0.05 g/L, respectively) is found. These results indicate that more reduced organic acids are being produced when the oxygen availability is lower and could be an indication that the reductive part of the TCA cycle is slightly active under oxygen limited conditions. This is in contradiction with the results of Diano et al. (2006), who observed a significant succinate production under the same cultivation conditions, namely when *A. niger* was grown on xylose and nitrate and oxygen limitation was posed on the system. The reason for this is not clear, but could be explained by strain differences (Diano et al. used an industrial strain). In another filamentous fungus, *Fusarium oxysporum*, an increase in ethanol and acetate was observed at anaerobic growth conditions when xylose was the carbon source, indicating that there are differences in the by-product spectrum in different fungi and even different strains (Panagiotou and Christakopoulos 2004).

5.4.3 Intracellular metabolites

Since metabolites represent the reactants of the metabolic network, quantification of metabolite concentrations offers a direct access to the identification of the intracellular kinetics of metabolism (Buchholz et al. 2002; Jewett et al. 2006). Intracellular metabolite profiles give new insights in how the cellular metabolism and regulation change in response to growth conditions, thereby providing a greater comprehension of flux dynamics and metabolic control.

Table 5.4 Intracellular metabolite profiles determined during both the exponential growth phase and the oxygen limitation phase in all cultivations. The values are expressed in relative area normalised by dryweight.

	0.01 vvm		0.02 vvm		0.05 vvm		0.1 vvm		1 vvm	
Metabolite	growth	O2-limitation	growth	O2-limitation	growth	O2-limitation	growth	O2-limitation	growth	O2-limitation
Pyruvate metabolism										
pyruvate	37	205	12	44	37	51	0	3	7	0
lactate	24	350	38	162	311	122	0	46	27	1
2-oxovalerate	1	9	2	3	4	8	0	0	0	0
2-isopropylmalate	7	20	0	5	17	9	0	0	8	0
TCA cycle										
citrate	967	7816	1839	3698	844	2798	379	1403	1030	1993
2-oxoglutarate	24	142	71	29	50	93	0	31	19	12
cis-aconitate	6	117	8	44	14	26	8	9	14	26
succinate	77	435	67	167	112	297	18	14	33	3
malate/fumarate	233	1713	292	398	718	687	0	32	54	15
2-aminobutyrate	2	34	32	25	38	20	0	10	33	12
4-amino-n-butyrate (GABA)	0	73	4	209	22	631	0	28	15	6
Amino acid metabolism										
histidine	0	0	4	43	0	9	0	42	25	187
glutamate	857	1831	5873	4057	2745	1524	1842	1734	9213	2000
glutamine	0	0	9	37	0	0	0	3	21	61
pyroglutamate	54	248	916	305	796	245	0	213	636	324
asparagine	55	118	166	146	37	97	38	183	183	742
aspartate	235	773	1561	757	1193	185	501	902	3070	1998
threonine	0	0	125	133	36	48	0	57	102	175
lysine	6	109	208	150	36	71	0	307	90	925
proline	132	2469	181	432	430	657	43	390	178	817
D-2-amino adipate	0	4	13	17	19	8	0	15	27	17
ornithine	34	215	161	238	102	288	126	263	268	190
phenylalanine	1	86	53	88	33	71	0	124	55	225
tyrosine	0	38	5	27	4	14	0	69	11	76
alanine	1839	9262	6889	7042	9395	9325	626	1707	4931	427
leucine	69	568	121	363	143	153	30	243	136	326
valine	52	633	280	894	340	551	63	329	430	298
methionine	0	9	20	48	18	13	0	21	23	89
glycine	0	244	107	142	121	117	16	33	58	93
serine	0	0	9	7	4	5	0	15	12	26
Other metabolites										
citramalate	11	48	18	9	15	34	0	2	6	1
malonate	0	0	1	5	0	2	0	0	0	0
myristate	0	0	10	3	0	0	0	0	7	7

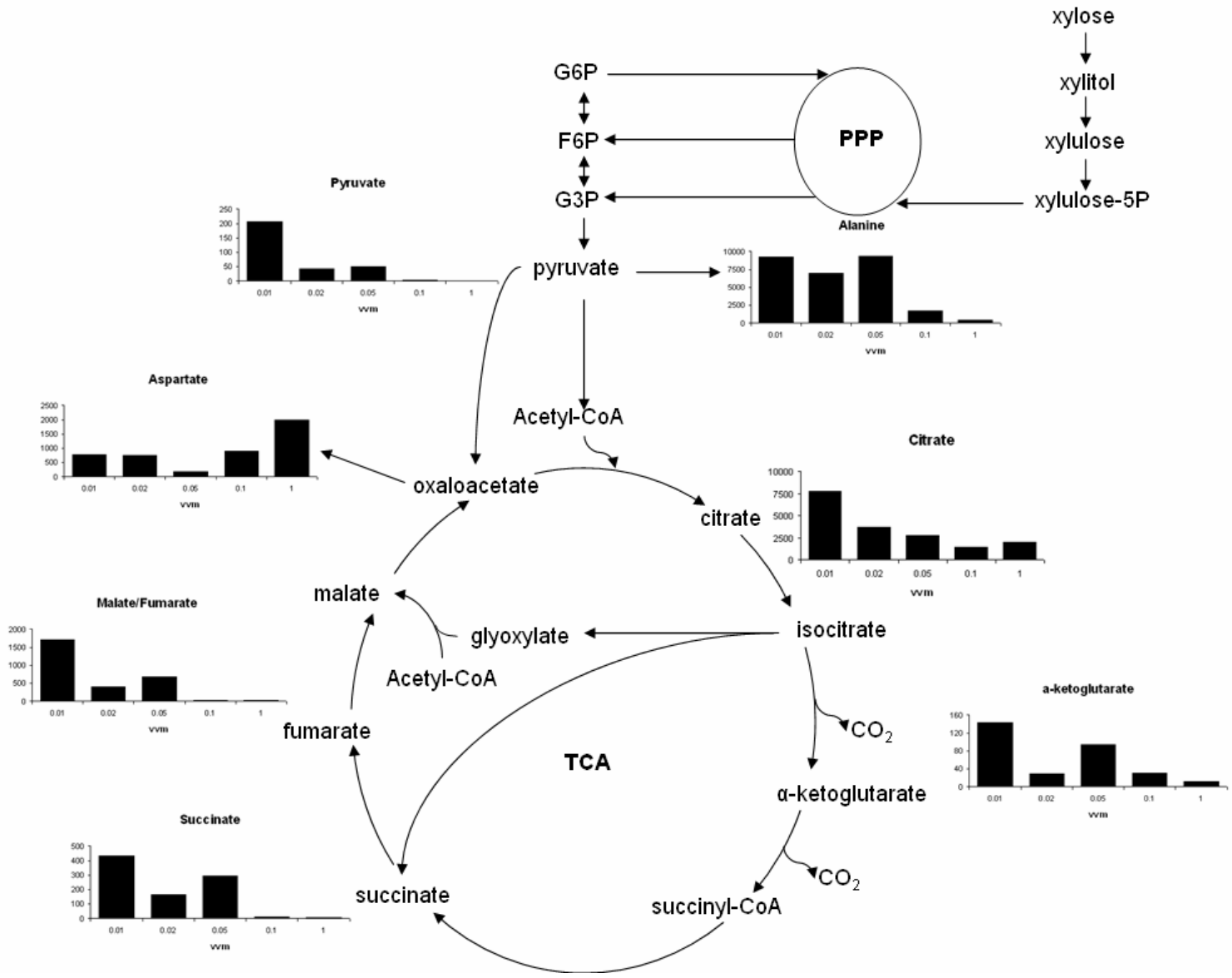

Figure 5.3 Intracellular metabolites levels in the oxygen limitation phase measured under the different cultivation conditions (0.01 vvm, 0.02 vvm, 0.05 vvm, 0.1 vvm and 1 vvm). Malate and fumarate could not be separated by the applied method. All values are expressed as relative area normalised by dryweight.

In the present study, the profile of intracellular amino and non-amino organic acids was expressed as peak areas normalised by the biomass concentration both during the exponential growth phase and in the oxygen limitation phase. By using an in house metabolite library, consisting of 74 metabolites, 49% of these metabolites could be detected during the GC-MS analysis. High levels of alanine, leucine, valine, proline, ornithine, aspartate, glutamate and citrate were measured in both the exponential growth phase and the oxygen limitation phase (Table 5.4). A number of compounds were detected that had higher levels in the oxygen limitation phase compared to the exponential growth phase. Amino acids in this category are: glycine, valine, leucine, threonine, proline, asparagine, methionine, phenylalanine, ornithine, tyrosine and lysine (Table 5.4). Also histidine showed the same profile, but for this amino acid the level was found to increase with the aeration level in the fermentations, which is opposite as observed for the other amino acids.

Analysis of organic acids showed that citrate, pyruvate, lactate, malate, fumarate and succinate had increased levels in the oxygen limitation phase and we also observed that the levels increased when the aeration level in the fermentations decreased (Table 5.4). Furthermore, cis-aconitate and 4-amino-n-butyrate were present in higher levels during oxygen limitation than during exponential growth (Table 5.4). These results indicate that metabolites of the TCA cycle accumulate during oxygen limitation. Furthermore, amino acids directly derived from TCA cycle intermediates show the same trend, e.g. asparagine, threonine, isoleucine, proline and lysine (Table 5.4). The accumulation of TCA cycle intermediates is accompanied with accumulation of upstream metabolites, e.g. pyruvate, lactate, tyrosine and alanine (Table 5.4). This further points to difficulties in oxidation of NADH resulting in accumulation of pathway intermediates. Figure 5.3 gives a schematic overview of how a selection of intracellular metabolites varies in the fermentations.

A few unusual metabolites were also detected (Table 5.4). The detection of pyroglutamate (Panagiotou et al. 2005), for example, is an indication of active glutathione metabolism, which seems to be more active in the growth phase compared to the oxygen limitation phase. The metabolite citramalate was also measured, but in very low amounts at all aeration levels. This metabolite has been found in several micro-organisms, for example in the filamentous fungus *Fusarium oxysporum* (Panagiotou et al. 2005), but also in bacteria like the *Rhodobacter sphaeroides* (Filatova et al. 2005a). Citramalate can be formed by condensation of acetyl-CoA and pyruvate or via the itaconate pathway. The first pathway is only identified in bacteria and is called the citramalate pathway (Filatova et al. 2005a), whereas the second pathway is also found in fungi (Bonnarme et al. 1995). The citramalate pathway (CM) is thought to be an alternative to the glyoxylate cycle (Filatova et al. 2005b). The CM pathway converts the citramalate formed, via

several intermediate products, to glyoxylate and propionyl-CoA. The glyoxylate can then enter the TCA cycle again by malate synthase creating malate. Citramalic acid is chemically related to the TCA cycle compound malic acid. Presumably, citramalate may interfere with the production of malic acid in the TCA cycle (http://www.gpl4u.com/test1comp2.html). However, further characterisation of citramalate production is necessary to reveal the biochemical pathway and functional properties of this pathway in filamentous fungi. Especially its competitive nature with the glyoxylate pathway is interesting in relation to succinate production. In our study no clear conclusion could be made on the activity of the glyoxylate pathway, as the intracellular glyoxylate measurements were contradicting the activity of the isocitrate lyase.

We also detected 4-amino-n-bytyric acid (GABA) and glutamate. These compounds are intermediates of the GABA shunt, a pathway that bypasses certain steps in the TCA cycle (Balazs et al. 1970). In this alternative pathway, 2-ketoglutarate is aminated to form glutamate instead of being oxidatively decarboxylated to succinate like in the TCA cycle. The glutamate is subsequently decarboxylated to GABA, by glutamate decarboxylase. GABA is then irreversibly transaminated to succinic semialdehyde by 4-aminobutyrate transaminase. Finally, the TCA cycle is entered again by oxidation of succinic semialdehyde to succinate by NAD(P)H dependent succinic semialdehyde dehydrogenase. The activation of this GABA shunt is mainly caused by the $NADH/NAD^+$ ratio, that has been shown to regulate the 2-ketoglutarate dehydrogenase complex (Streeter and Salminen 1990). Therefore, under oxygen limited conditions a redox imbalance could be expected, leading to activation of the GABA shunt and indeed we observed an increase in the GABA levels under oxygen limitation. GABA can also be produced by catabolism of ornithine and lysine and in our study we measured elevated levels of ornithine and lysine (Kumar et al. 2000). The exact function of the GABA shunt has not yet been unravelled, but the intermediate conversion towards succinate is interesting. Other filamentous fungi like *Neurospora crassa*, *Aspergillus nidulans* and *Fusarium oxysporum* are also known to produce GABA as an intracellular metabolite (Kumar and Punekar 1997; Schmit and Brody 1975; Panagiotou et al. 2005). In *Neurospora crassa* it is thought to be involved in spore germination (Schmit and Brody 1975). In *Aspergillus niger* an unusual accumulation of GABA during acidogenesis has been documented (Kubicek et al. 1979), showing that the GABA levels increased in parallel with citric acid accumulation, while under normal conditions it was virtually undetectable. What kind of function GABA performs under oxygen limitation, after being activated by the high $NADH/NAD^+$ ratio, is still unclear.

5.4.4 Enzyme assays

Ten enzymes related to the xylose to succinate flux were investigated in the different fermentations, both in the exponential growth phase and in the oxygen limitation phase. We measured glucose-6P dehydrogenase, pyruvate dehydrogenase, pyruvate decarboxylase, pyruvate carboxylase, malic enzyme, malic dehydrogenase, fumarase, succinate dehydrogenase, isocitrate lyase and citrate synthase. No activity could be detected for two of these enzymes, pyruvate dehydrogenase (PDH) and pyruvate decarboxylase (PDC). The activities of the other eight enzymes, expressed in Units per mg of protein, are shown in Table 5.3 together with the reactions they catalyse. As a general trend we observed that the activity of the enzymes decreased during the oxygen limitation phase compared to the exponential growth phase (Figure 5.4). This is probably due to a general reduction in metabolic activity caused by a decrease in substrate uptake and specific growth rate.

5.4.4.1 Glucose-6-P dehydrogenase

All cultivations have been performed using a high concentration of xylose as carbon source. The detection of glucose-6-phosphate dehydrogenase indicates a backflux of carbon from the reductive part of the pentose phosphate pathway via the glycolysis to the oxidative part of the pentose phosphate pathway. This is necessary for replenishing NADPH required for biosynthesis and also for uptake of xylose and nitrate. The conversion of xylose to xylitol by the xylose reductase is NADPH dependent thereby increasing the cellular demand for NADPH. This NADPH requirement is elevated by the consumption of nitrate, the nitrogen source used in the cultivations. The uptake of one mole of nitrate requires another 2 moles of NADPH. The G6PDH activity correlated with the xylose consumption rate at all levels of aeration. A clear increase in G6PDH activity is detected with increasing aeration (Figure 5.4). Therefore, if more oxygen is available more sugar can be consumed and more NADPH should be available requiring a higher G6PDH activity.

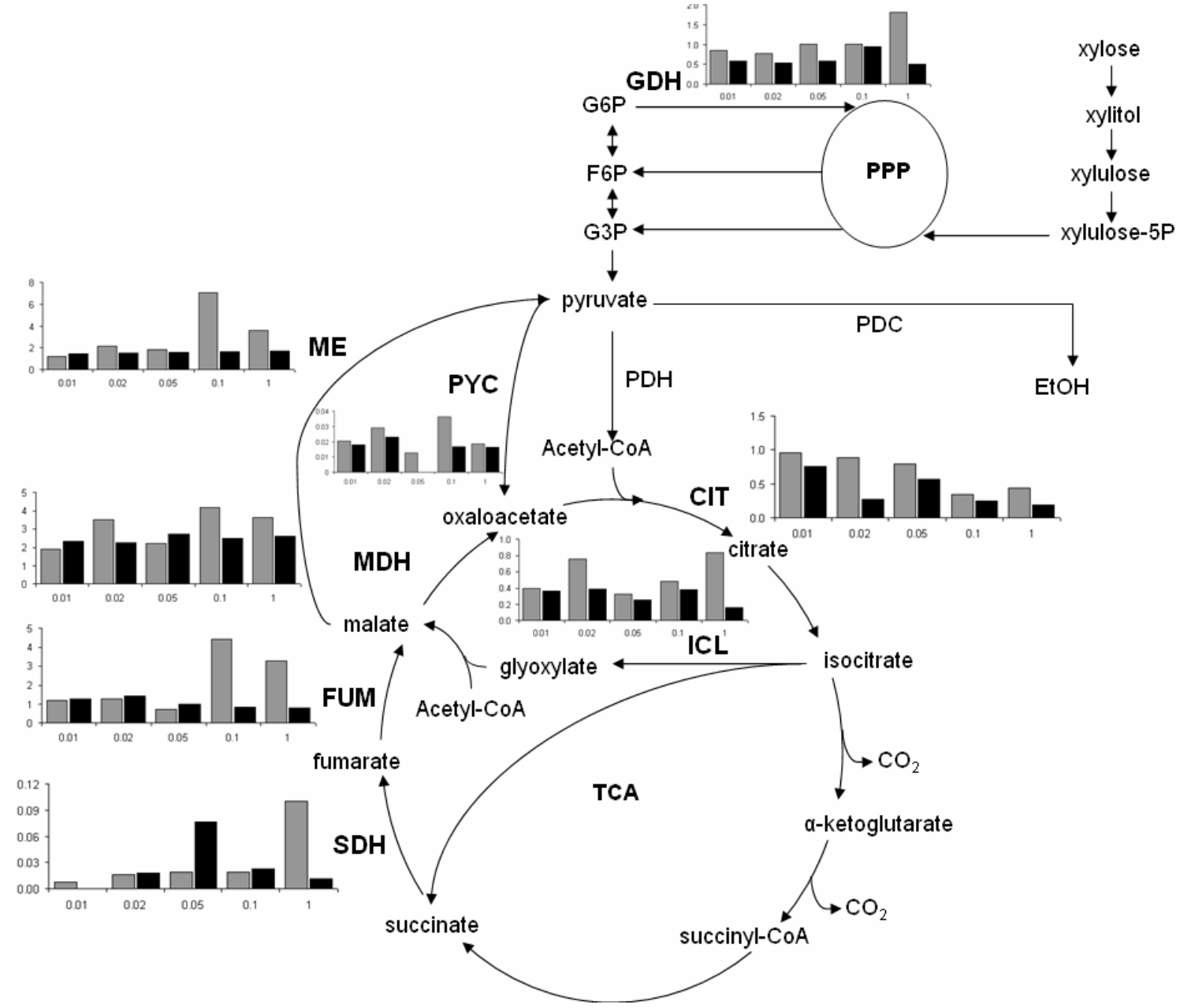

Figure 5.4 Enzyme activities measured under the different cultivation conditions (0.01 vvm, 0.02 vvm, 0.05 vvm, 0.1 vvm and 1 vvm). Light grey bars are the enzyme measurements in the exponential growth phase. Black bars are the enzyme activities measured in the oxygen limitation phase. No PDH and PCD activity could be detected. GDH: Glucose-6-P dehydrogenase, PYC: pyruvate carboxylase, PDH: pyruvate dehydrogenase, PDC: pyruvate decarboxylase, PDH: pyruvate dehydrogenase, PDC: pyruvate decarboxylase, ME: malic enzyme, ICL: isocitrate lyase, CIT: citrate synthase, MDH: malic dehydrogenase, FUM: fumarase and SDH: succinate dehydrogenase.

5.4.4.2 Pyruvate carboxylase, pyruvate decarboxylase and pyruvate dehydrogenase

The pyruvate branchpoint is an important point of regulation in the metabolism of micro-organisms and plays and important role in succinate production. Recently, Lee et al. (2005) showed *in silico* that the metabolic flux to pyruvate is crucial for an efficient succinate production in *E. coli*. However, in high succinate producing micro-organisms the phosphoenolpyruvate carboxylase plays a fundamental role in succinic acid production. In yeast, the pyruvate node has been extensively studied as well as the interplay between pyruvate dehydrogenase, pyruvate decarboxylase and pyruvate carboxylase (Pronk et al. 1996). It is an important junction between assimilatory and dissimilatory reactions. However, this pathway may not be active in *A. niger*, since no activity could be measured and only seldom small quantities of acetate or ethanol are produced. This indicates that this fungus is not as efficient as other fungi in producing ethanol or other metabolites for redox balancing and this may also explain why this fungus cannot grow anaerobically.

Thus, *A. niger* seems to be dependent on the energetically more favourable respiratory pathway, which is coupled to the TCA cycle. The TCA cycle has both a dissimilatory and an assimilatory function for energy and redox balancing, and for producing biosynthetic precursors, respectively. Pyruvate can enter the TCA cycle in two ways. One is as a 2-carbon metabolite by oxidative decarboxylation of pyruvate to acetyl-CoA by pyruvate dehydrogenase. The other one is by CO_2 fixation producing oxaloacetate from pyruvate by pyruvate carboxylase. We have measured activity of pyruvate carboxylase in our cell extracts but could not measure pyruvate dehydrogenase activity (Table 5.3). Since there is a requirement for both acetyl-CoA and oxaloacetate to have a functional TCA cycle, it is believed that there must be an *in vivo* pyruvate dehydrogenase activity. However, this enzyme consists of a multimeric complex that is difficult to measure in crude cell extracts due to proteolytic degradation and interference with other enzymes. Localisation and substrate affinity of the three enzymes competing for pyruvate is also an important issue considering the competitive nature they share for the same substrate. Jaklitsch et al. (1991) have done extensive studies to determine the localisation of these enzymes and they observed that in *A. niger* the pyruvate dehydrogenase is located in the mitochondria, thereby requiring transport of pyruvate from the cytosol to the mitochondria by an unknown transport process. Pyruvate decarboxylase on the other hand is only located in the cytosol, while pyruvate carboxylase is present in both the mitochondria and the cytosol. Unfortunately, no kinetic data are available for *Aspergillus* species restricting a reasonable model for competition between these three enzymes for the substrate pyruvate. There is also not a clear trend visible in the pyruvate carboxylase activity measured in all cultivations at

different aeration rates. The activity does, however, follow the general trend of being less active during the oxygen limitation than in the exponential growth phase.

5.4.4.3 Isocitrate lyase and malic enzyme

Isocitrate lyase is part of the glyoxylate cycle. The primary function of the glyoxylate cycle is to permit growth when C_2 compounds, such as ethanol and acetate, are the only sources of carbon (Kornberg et al. 1966a+b). The glyoxylate cycle consists of two steps. In the first, isocitrate is hydrolysed to succinate and glyoxylate by isocitrate lyase. In the second step, acetyl-CoA is condensed with glyoxylate to produce malate by malate synthase. Malate is an intermediate of the TCA cycle and can be metabolised further. The activity of the glyoxylate cycle has been shown to be under carbon catabolite repression (Stemple et al. 1998; Prathumpai et al. 2004). However, recently Panagiotou et al. (2006) detected glyoxylate intracellularly during xylose fermentations using *Fusarium oxysporum*, and ^{13}C-labelling experiments verified that the pathway was active under anaerobic conditions. We initially hypothesized that isocitrate lyase was inactive using high xylose concentrations in the cultivations. However, in this study we measured activity of isocitrate lyase, indicating that the carbon catabolite repression can somehow be overcome (Table 5.3). The activity of isocitrate lyase increased with increasing aeration indicating that the glyoxylate cycle was more active at higher aeration (Figure 5.4). Since we did not detect any two-carbon metabolites, nor did we detect any intracellular glyoxylate, the physiological significance of this enzyme is not clear. Because succinate is produced via the glyoxylate cycle, a very active cycle would likely increase succinate production.

Malic enzyme is known for its function in fatty acid biosynthesis (Wynn et al. 1999). However, malic enzyme can also be a part of the gluconeogenesis together with isocitrate lyase. This might be the reason why isocitrate lyase and malic enzyme show similar enzyme profiles in the exponential phase (Figure 5.4). It is hard to explain the increase in activity, since gluconeogenesis is normally repressed by the high concentrations of xylose used is this study. We would expect an increasing glycolytic flux with increasing air supply resulting in an inhibition of the gluconeogenesis pathways. In the oxygen limitation phase the enzyme seems to be constitutively expressed without any changes in the activity between the different aeration levels.

5.4.4.4 TCA cycle enzymes

The citrate synthase showed an opposite activity profile compared to fumarase in the growth phase (Figure 5.4). Citrate is known to be the main product produced in fully aerated cultivations at low pH. The decrease in citrate synthase and increase in fumarase might attribute to the increase in extracellular oxalate being produced at high aeration conditions. The lack of citrate excretion is

probably due to the selected medium, which contains manganese that is known to drastically inhibit citrate production by a yet unknown mechanism (Kubicek et al. 1979). Therefore, it seems that under the studied conditions oxalate production is preferred at higher aeration rates.

Under oxygen limited conditions, the citrate synthase activity was always lower than in the exponential growth phase and showed a decreasing trend with increasing aeration (Table 5.3). From literature we know that oxygen is crucial for citrate production (Horitzu and Clark 1966; Kubicek et al. 1980). If oxygen is limited this can have major influences on the citrate synthase activity, but the molecular mechanism of how oxygen limitation negatively influences citrate production is not known.

A general trend in the activities of malic dehydrogenase and succinate dehydrogenase was not found (Figure 5.4). Oxygen therefore seems to have no effect on their activity level.

From the enzyme activity measurements it is difficult to conclude on whether there is a relationship between the gluconeonenesis pathways and the TCA cycle during the exponential growth phase. Thus, our analysis points to that both malic enzyme and isocitrate lyase are active at the same time as pyruvate carboxylase. This indicates that both the gluconeogenesis and the TCA are upregulated at the same time. Co-operation of these pathways has also been found in yeast based on transcriptome analysis (Regenberg et al. 2006).

Under oxygen limitation the increase in TCA cycle intermediates (and derivatives hereof) suggests a lower TCA activity, which can also be seen by the enzyme activities of the citrate synthase and fumarase. This is probably caused by the higher NADH/NAD^+ ratio occurring at oxygen limitation. The extracellular metabolite profiles together with the intracellular metabolite profiles could also indicate a low activity of the reductive TCA cycle, which might be regulated by the NADH/NAD+ ratio.

5.5 Conclusion

In this study we have investigated the effect of different oxygen levels on *A. niger* metabolism. The aim was to study micro-aerobic growth conditions and the effect on organic acid production, with a special interest in succinic acid. Poor production of organic acids was found, which is in agreement with *A. niger*'s absolute aerobic nature, suggesting a poor performance of the reductive TCA cycle. Nevertheless, a slight increase in organic acid production, mostly fumarate and malate, was measured at oxygen limited conditions. However, the largest changes were depicted in polyol production, indicating a redox imbalance in the cell due to the lack of oxygen. The oxygen level has less effect on the specific growth rate, but influences the substrate uptake rate drastically.

Additionally, intracellular metabolite profiles were determined, giving some indications of which pathways might be activated or deactivated at different oxygen levels. For example citramalate, GABA and pyroglutathione were measured (mainly under oxygen limited conditions) indicating activity of the citramalate pathway, GABA shunt and glutathione metabolism, respectively. Also in the central carbon metabolism (TCA cycle intermediates) different metabolite levels were determined, indicating a shift in the flux pattern. The enzymes measured, showed a lower activity of the TCA cycle under oxygen limited conditions, which is consistent with earlier findings. Furthermore, the G6PDH showed higher activities when more oxygen was available indicating a higher glycolytic flux, which is also consistent with earlier studies.

5.6 References

Archer DB and Dyer PS 2004. From genomics to post-genomics in *Aspergillus*. *Current Opinion in Microbiology* **7** (5):499-504.

Balazs R, Machiyama Y, Hammond BJ, Julian T and Richter D 1970. The operation of the gamma-aminobutyrate bypath of the tricarboxylic acid cycle in brain tissue *in vitro*. *Biochemisrty Journal* **116** :445-461.

Beever RE and Laracy E 1986. Osmotic adjustment in the filamentous fungus *Aspergillus nidulans*. *Journal of Bacteriology* **168**(1):1358-1365.

Bonnarme P, Gillet B, Sepulchre AM, Role C, Beloeil JC and Ducrocq C 1995. Itaconate biosynthesis in *Aspergillus terreus*. *Journal of Bacteriology* **177** (12):3573-3578.

Bradford M 1979. A rapid and sensitive for the quantitation of microgram quantitites of protein utilizing the principle of protein-dye binding. *Analytical Biochemistry* **72**:248-254.

Buchholz A, Hurlebaus J, Wandrey C and Takors R 2002. Metabolomics: quantification of intracellular metabolite dynamics. *Biomolecular Engineering* **19** (1):5-15.

David H, Akesson M and Nielsen J 2003. Reconstruction of the central carbon metabolism of *Aspergillus niger*. *European Journal of Biochemistry* **270** (21):4243-4253.

Diano A and Nielsen J 2006. Polyol synthesis in *Aspergillus niger*: influence of oxygen availability, carbon and nitrogen sources on the metabolism. *Biotechnology and Bioengineering* **94** (5):899-908.

Drysdale MR, Kolze SE and Kelly JM 1993. The *Aspergillus niger* carbon catabolite repressor encoding gene, creA. *Gene* **130** (2):241-245.

Filatova LV, Berg IA, Krasil'nikova EN and Ivanovskii RN 2005a. The mechanism of acetate assimilation in purple nonsulfur bacteria lacking the glyoxylate pathway: enzymes of the citramalate cycle in *Rhodobacter sphaeroides*. *Mikrobiologiia* **74** (3):319-328.

Filatova LV, Berg IA, Krasil'nikova EN, Tsygankov AA, Laurinavichene TV and Ivanovskii RN 2005b. The mechanism of acetate assimilation in purple nonsulfur bacteria lacking the glyoxylate pathway: acetate assimilation in *Rhodobacter sphaeroides* cells] *Mikrobiologiia* **74** (3):313-318.

Green JD and Narahara HT 1980. Assay of succinate dehydrogenase activity by the tetrazolium method: evaluation of an improved technique in skeletal muscle fractions. *Journal of Histochemistry and Cytochemistry* **28** (5):408-412

Grimm LH, Kelly S, Krull R and Hempel DC 2005. Morphology and productivity of filamentous fungi. *Applied Microbiology and Biotechnology* **69** (4):375-384.

Horitsu H and Clark DS 1966. Effect of ferrocyanide on growth and citric acid production by *Aspergillus niger*. *Canadian Journal of Microbiology* **12** (5):901-907.

Jaklitsch WM, Kubicek CP and Scrutton MC 1991. Intracellular location of enzymes involved in citrate production by *Aspergillus niger*. *Canadian Journal of Microbiology* **37** (11):823-827.

Jeffries TW and Jin YS 2004. Metabolic engineering for improved fermentation of pentoses by yeasts. *Applied Microbiology and Biotechnology* **63** (5):495-509.

Jewett MC, Hofmann G and Nielsen J 2006. Fungal metabolite analysis in genomics and phenomics. *Current Opinion in Biotechnology* **17**:191-197

Karaffa L, Sandor E, Fekete E and Szentirmai A 2001. The biochemistry of citric acid accumulation by *Aspergillus niger*. *Acta Microbiologica et Immunologica Hungarica* **48** (3-4):429-440.

Kelly JM 1994. Carbon catabolite repression. In *Aspergillus*: 50 years on, pp 355-367. Edited by Martinelli SD, Kinghorn JR. Amsterdam: Elsevier Science B.V.

Koning W and Dam KAv 1992. A method for the determination of changes of glycolytic metabolites in yeast on a subsecond time scale using extraction at neutral pH. *Analytical Biochemistry* **204** (1):118-123

Kornberg HL and Smith J 1966a. Temperature-sensitive synthesis of isocitrate lyase in *Escherichia coli*. *Biochimica Biophysica Acta* **123** (3):654-657

Kornberg HL 1966b. The role of and control of the glyoxylate cycle in *Escherichia coli*. *Biochemistry Journal* **99**:1-11

Kubicek CP, Zehentgruber O, El-Kalak H and Röhr M 1980. Regulation of citric acid production by oxygen:Effect of dissolved oxygen tension on adenylate levels and respiration in *Aspergillus niger*. *European Journal of Applied Microbiology and Biotechology* **9**:101-115.

Kubicek CP and Röhr M 1986. Citric acid fermentation. *Critical Reviews Biotechnology* **3**:331-374.

Kubicek CP, Hampel W and Röhr M. 1979. Manganese deficiency leads to elevated amino acid pools in citric acid accumulating *Aspergillus niger*. *Archives of Microbiology* **123**:73-79.

Kumar S, Punekar NS, SatyaNarayan V and Venkatesh KV. 2000. Metabolic fate of glutamate and evaluation of flux through the 4-aminobutyrate (GABA) shunt in *Aspergillus niger*. *Biotechnology and Bioengineering* **67** (5):575-584.

Kumar S and Punekar NS 1997. The metabolism of 4-aminobutyrate (GABA) in fungi. *Mycological Research* **4**:403-409.

Lee SJ and Song H 2006. Genome-based metabolic engineering of *Mannheimia succiniciproducens* for succinic acid production. *Applied Environmental Microbiology* **72** (3):1939-1948.

Lee SJ, Lee DY, Kim TY, Kim BH, Lee J and Lee SY 2005. Metabolic engineering of *Escherichia coli* for enhanced production of succinic acid, based on genome comparison and in silico gene knockout simulation. *Applied Environmental Microbiology* **71** (12):7880-7887.

Lewis C, AJ and Smith JE 1994. Health related aspects of the genus *Aspergillus*. *Biotechnology Handbooks* **7**:219-261.

Lin H, Bennett GN and San KY 2005. Fed-batch culture of a metabolically engineered *Escherichia coli* strain designed for high-level succinate production and yield under aerobic conditions. *Biotechnology and Bioengineering* **90** (6):775-779.

Millard CS, Chao YP, Liao JC and Donnelly MI 1996. Enhanced production of succinic acid by overexpression of phosphoenolpyruvate carboxylase in *Escherichia coli*. *Applied Environmental Microbiology* **62** (5):1808-1810.

Nielsen J and Olsson L 2002. An expanded role for microbial physiology in metabolic engineering and functional genomics: moving towards systems biology. *FEMS Yeast Research* **2** (2):175-181.

Panagiotou G, Christakopoulos P, Grotkjær T and Olsson L 2006. Engineering of the redox balance of *Fusarium oxysporum* enables anaerobic growth on xylose. *Metabolic Engineering* **8**:474-482

Panagiotou G, Villas-Boas SG, Christakopoulos P, Nielsen J and Olsson L 2005. Intracellular metabolite profiling of *Fusarium oxysporum* converting glucose to ethanol. *Journal of Biotechnology* **115** (4):425-434.

Panagiotou G and Christakopoulos P 2004. NADPH-dependent D-aldose reductases and xylose fermentation in *Fusarum oxysporum*. *Journal of Bioscience Bioengineering* **97** (5):299-304

Papagianni M 2004. Fungal morphology and metabolite production in submerged mycelial processes. *Biotechnology Advances* **22** (3):189-259.

Pedersen H, Carlsen M and Nielsen J 1999. Identification of enzymes and quantification of metabolic fluxes in the wild type and in a recombinant *Aspergillus oryzae* strain. *Applied Environmental Microbiology* **65** (1):11-19.

Potera C 2005. Making succinate more successful. *Environmental Health Perspectives* **113** (12):832-835.

Poulsen BR, Nohr J, Douthwaite S, Hansen LV, Iversen JJ, Visser J and Ruijter GJ 2005 Increased NADPH concentration obtained by metabolic engineering of the pentose phosphate pathway in *Aspergillus niger*. *FEBS Journal* 272 (6):1313-1325

Prathumpai W, McIntyre M and Nielsen J 2004. The effect of CreA in glucose and xylose catabolism in Aspergillus nidulans. *Applied Microbiology and Biotechnology* **63** (6):748-753

Pronk JT, Steensma H and Van Dijken JP 1996. Pyruvate metabolism in *Saccharomyces cerevisiae*. *Yeast* **12**:1607-1633.

Regenberg B, Grotkjær T, Winther O, Fausbøll A, Åkesson M, Bro C, Hansen LK, Brunak S and Nielsen J 2006. Growth-rate regulated genes have profound impact on interpretation of transcriptome profiling in *Saccharomyces cerevisiae*. *Genome Biology* **7** (11):R107

Ruijter GJ, Nohr J, Douthwaite S, Hansen LV, Iversen JJ and Visser J 2005. Increased NADPH concentration obtained by metabolic engineering of the pentose phosphate pathway in *Aspergillus niger*. *FEBS Journal* **272** (6):1313-1325.

Ruijter GJ and Visser J 1999. Oxalic acid production by *Aspergillus niger*: an oxalate-non-producing mutant produces citric acid at pH 5 and in the presence of manganese. *Microbiology* **145** (Pt 9):2569-2576.

Sanchez AM, Bennett GN and San KY 2005. Efficient succinic acid production from glucose through overexpression of pyruvate carboxylase in an *Escherichia coli* alcohol dehydrogenase and lactate dehydrogenase mutant. *Biotechnology Progress* **21** (2):358-365.

Schmit JC and Brody S 1975. *Neurospora crassa* conidial germination: role of endogenous amino acid pools. *Journal of Bacteriology* **124**:232-242.

Stemple CJ, Davis MA and Hynes MJ 1998. The *facC* gene of *Aspergillus nidulans* encodes an acetate-inducible carnitine acetyltransferase. *Journal of Bacteriology* **180** (23):6242-6251

Streeter JG and Salminen SO 1990. Periplasmic metabolism of glutamate and aspartate by intact *Bradyrhizobium japonicum* bacteroids. *Biochimica Biophysica Acta* **1035**:257-263.

Takasaki K, Shoun H, Yamaguchi M, Takeo K, Nakamura A, Hoshino T and Takaya N 2004. Fungal ammonia fermentation, a novel metabolic mechanism that couples the dissimilatory and assimilatory pathways of both nitrate and ethanol. Role of acetyl CoA synthetase in anaerobic ATP synthesis. *Journal of Biological Chemistry* **279** (13):12414-12420.

Vemuri GN, Eiteman MA and Altman E 2002. Succinate production in dual-phase *Escherichia coli* fermentations depends on the time of transition from aerobic to anaerobic conditions. *Journal of Industrial Microbiology and Biotechnology* **28** (6):325-332.

Villas-Boas SG, Delicado DG, Akesson M and Nielsen J 2003. Simultaneous analysis of amino and nonamino organic acids as methyl chloroformate derivatives using gas chromatography-mass spectrometry. *Analytical Biochemistry* **322** (1):134-138.

Witteveen CF and Visser J 1995. Polyol pools in *Aspergillus niger*. *FEMS Microbiology Letters* **134** (1):57-62.

Werpy T and Petersen G 2004. Top value added chemicals from biomass. *http://www.nrel.gov/docs/fy04osti/35523.pdf* (27-03-2007).

Wynn JP, bin Abdul Hamid A and Ratledge C 1999. The role of malic enzyme in the regulation of lipid accumulation in filamentous fungi. *Microbiology* **145**:911-917.

Zeikus J, Jain M and Elankovan P 1999. Biotechnology of succinic acid production and markets for derived industrial products. *Applied Microbiology and Biotechnology* **51**:545-552.

Chapter 6

Gene deletion strategies for rearranging organic acid production profiles in *Aspergillus niger*

Meijer S., Nielsen M.L., Olsson L. and Nielsen J.
Biocentrum-DTU, Center for Microbial Biotechnology, Denmark

Acl deletion aimed at *Applied Environmental Microbiology*

6.1 Abstract

With the availability of the genome sequence of the filamentous fungus *Aspergillus niger*, the use of targeted genetic modifications has become easier. This makes this fungus an attractive micro-organism for creating a cell factory platform for production of chemicals. Using different molecular biology techniques, this study focused on metabolic engineering of *A. niger* to improve its organic acid production in the direction of succinic acid. Two gene targets were determined for complete gene deletion, ATP-citrate lyase (*acl*) and succinate dehydrogenase (*sdh*). It was attempted to delete these genes using several bi-partite gene targeting methods. Only the *acl* gene was successfully deleted and was characterised in batch cultivations. It was found that the succinic acid yield was threefold improved by deleting the *acl* gene. Additionally, the total amount of organic acids produced in this strain was significantly increased. The fact that the *sdh* gene could not be deleted might be due to poor transformation performance or the possibility that *sdh* is an essential gene.

Keywords: *Aspergillus niger*, organic acids, ATP: citrate lyase, succinate dehydrogenase

6.2 Introduction

The release of the genomic sequence of *Aspergillus niger* in 2006 has opened a window of opportunities in the field of biotechnology (Baker 2006; Pel et al. 2007). However, while a genomic sequence can yield a great deal of information, genome sequencing is only the first step towards understanding a microbe's biological capability. It is still a challenge how genomic information can be transferred to information on the functions of genes and further to the role of the individual genes on overall cellular function. Due to several sequencing projects and intensive annotating programs we are now able to compare genomes among different species. The comparison helps us in identifying genes and additionally make it possible to assign putative function to genes. With the genome sequence available for *A. niger* it has also become possible to perform target deletion of genes, which is often the key to redirect fluxes towards desirable pathways.

Tools for predicting the effect of a gene deletion *in silico* have already been developed for *A. niger*. David et al. (2003) created a detailed stoichiometric metabolic model of the central carbon metabolism. They used the model to identify metabolic engineering targets for increased succinate production. Hereby they predicted that it should be possible to obtain an increased succinate yield in a double deletion mutant (pyruvate decarboxylase and ATP:citrate lyase) when grown under oxygen limiting conditions. Although this stoichiometric model does not contain any regulatory information, it has shown to give us a good indication of metabolic changes in the cell (Ideker et al. 2001; Stephanopoulos et al. 2004; Price et al. 2003; Patil et al. 2004). However, model predictions still need to be verified experimentally, which may lead to a revision of the model. In the present study, an attempt was made to replicate the results from the stoichiometric model prediction. Because the molecular biology tools in *A. niger* are not as reliable as in e.g. *E. coli*, mainly due poor homologous recombination in this filamentous fungus, an altered strategy was used. In a previous study (Meijer et al. 2007) it was shown that the pyruvate decarboxylase (PDC) enzyme was not active under oxygen limiting conditions. Therefore, instead of making a double deletion, only a single deletion mutant was created in which ATP:citrate lyase (ACL) was knocked out.

Because an improvement in the organic acid yield of succinate has already been attempted in several other micro-organisms (Lee et al 2006; Lin et al. 2005a; Vermuri et al. 2002; Arikawa et al. 1999), also a rational approach was undertaken in the present study. This would allow a comparison of this approach with the model predicted strategy. In different microbial cell factories, evaluated for succinate production it has been found that an

important gene involved in improving succinate production is the gene encoding succinate dehydrogenase (*sdh*). This gene encodes an enzyme that is part of the TCA cycle and is catalysing the conversion of succinate to fumarate. If this gene is deleted, the TCA cycle is interrupted and 3 pathways remain that can form succinate as the end product (the oxidative and the reductive TCA cycle and the glyoxylate pathway). We therefore also deleted the *sdh* gene in *A. niger*. However, the impact of this gene deletion on the overall metabolism of *A. niger* is not known. In other micro-organisms, like *E. coli,* the stoichiometric model already predicted that *sdh* deletion would improve the succinate yield. This is not the case for the *A. niger* model. SDH is an enzyme that is part of the respiratory chain and uses as cofactor $FADH_2$ (David et al. 2003). Due to a lack of detailed knowledge about the possible active $FADH_2$ contributing pathways in *A. niger*, the deletion of this gene might have a major impact on the redox balance of FAD/$FADH_2$ in the cell. Another concern is the fact that *A. niger* is unable to grow anaerobically in contrast to the other micro-organisms in which *sdh* has been deleted. These species use the reductive TCA cycle (fumarate respiration) as the main pathway for redox balancing and produces succinate via this route during anaerobic conditions.

In order to construct the two deletion strains (*⊿acl* and *⊿sdh*), the bipartite gene targeting method was used (Nielsen et al. 2006). Since homologous recombination is a rare event compared to non-homologous end joining in *A. niger*, this fragmented marker method reduces the background signal (ectopic integrations of the marker) during transformations. As stated above genetic targeting techniques in *A. niger* are challenging and therefore several strategies concerning the deletion were performed simultaneously. For example, the bipartite method with and without pop-out possibilities was used and also the transient marker system developed by Nielsen et al. (2007) was evaluated. The latter method incorporates the marker gene in its native locus in the genome, thereby not disturbing any other gene expression levels except for the targeted gene. In case of the normal bipartite gene targeting method a strain stays either auxotrophic for the marker gene or has the marker gene inserted in the genome locus of the deleted target gene. This may result in a changed expression level of the marker gene and influence the metabolic state of the cells.

6.3 Materials and Methods

6.3.1 Strains

The *Aspergillus* strains used in this study were:

- A742 derived from strain N402 containing a mutation in *pyrA5*.
- AB4.1 derived from strain N402 containing a mutation in *pyrG1* (van Hartingsveldt et al. 1987).
- pyrG-tr constructed by Nielsen et al. (2007) containing a transient *pyrG* mutation (IBT28739. IBT Culture Collection at BioCentrum-DTU, Lyngby. Denmark).
- As reference the N402 strain (*cspA1* mutation) was used (A733 at the fungal genetics stock center).

6.3.2 Deletion strategies

The first deletion strategy (D1) tested was the deletion of the target genes (*sdh* and *acl*, respectively) in the A742 strain, where *pyr4* from *Neurospora crassa* is used as marker gene (Ballance et al. 1983). Protoplasting and gene targeting procedures for *A. niger* were used as described previously for A*. nidulans* (Nielsen et al. 2006). A schematic overview of the gene targeting method is shown in Figure 6.1

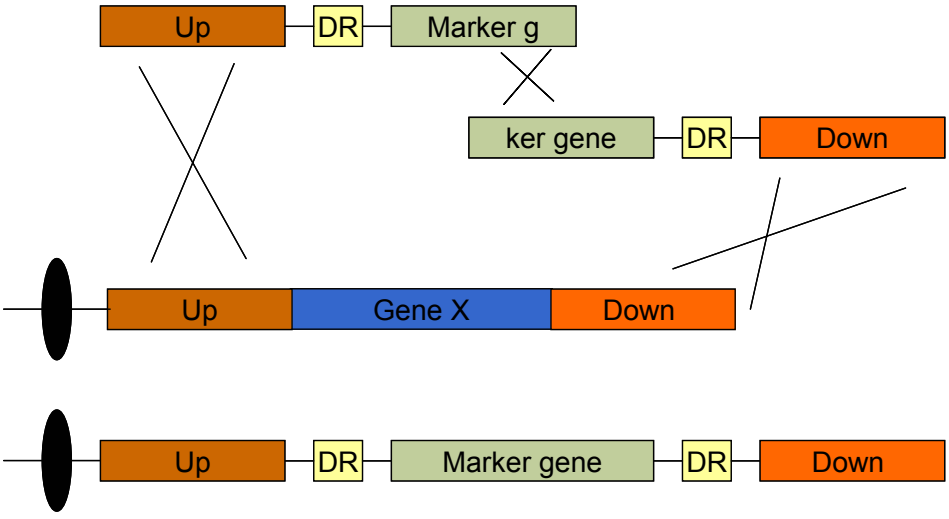

Figure 6.1 Schematic representation of the bipartite gene targeting method. We used different ACL and SDH gene fragments for up and downstream homologous sequences. As marker gene we used the *pyr4* gene from *N. crassa* and we performed transformations with and without direct repeats (DR).

The deletion strains were constructed using PCR generated bipartite gene targeting substrates. Each part of the bipartite substrate consists of a targeting fragment and a marker fragment, which are individually amplified by PCR using the primer pairs presented in Table 6.1.

In order to achieve adequate sequence overlap to favour homologous recombination,1.5 kb flanking regions were used, flanking both sites of the coding region. The upstream region of the gene was fused to the *pyr4* upstream marker fragment and the downstream region of the gene to the downstream part of *pyr4*. The *pyr4* fragments were made with and without direct repeats (see primers Table 6.1). The fusion is facilitated by using oligonucleotides that have fusion tags (adaptamers) (Erdeniz et al. 1997; Nielsen et al. 2006). 2 – 3 µg of each purified fusion PCR fragment was used for the transformation in 100 µL protoplast solution of *A. niger*. The transformation was performed as described by Nielsen et al. (2005). Selection of transformants was done on minimal medium plates (MM).

As a second strategy (D2) the flanking regions were elongated (2.5 kb) and the AB4.1 was used for transformation. We performed this transformation, like the first strategy, both with and without direct repeats.

At the same time the transient marker system was used for transformation of the marker gene (with direct repeats) into the pyrG-tr strain (Nielsen et al. 2007).

Table 6.1 Primers used for bipartite PCR fragments

Primer name (a)	Sequence (b)	D1 (c)	D2 (c)	D3 (c)
pDEL1-pyr4				
Upst-pDEL1-F-Ad	cat ggc aat tcc cgg gga tc TGG ATA ACC GTA TTA CCG CC	x	x	x
Dst-pDEL1-R-Ad	cat ggt ggt cag ctg gaa tt TGC CAA GCT TAA CGC GTA CC	x	x	x
pyr4-IF	GTT GTC TGC TTG CGC TTC TTC	x	x	x
pyr4-IR	CCA GAA GCA GTA CAC GGC	x	x	x
pyr_F2	cat ggc aat tcc cgg gga tc GCC GGC AAT TCT TTT T	x	x	
pyr_R	cat ggt ggt cag ctg gaa tt CCT CCG CCA TTT CTT A	x	x	
SDH				
SDH_fl_F	TGT TCT TCT ATG CGG GCG A	x		
SDH_fl_R	CCG TGA ACT TTT GGT CTT CC	x		
SDH_edge_F	aat tcc agc tga cca cca tg AGA TAC TAA TGC CAT AGC CGC	x	x	x
SDH_edge_R2	gat ccc cgg gaa ttg cca tg CAA GAG ATA GTG AGA GGC TG	x	x	x
SDH_fl_F3	GGT GCA TGG AAG CGA GAT AC		x	x
SDH_Fl_R3	CCA ATG AAC CAA GTT GCC GC		x	x
ACL				
ACL2_fl_F	GCA TCA GCA CAG AAA CCC AA	x		
ACL2_fl_R	CCG ATG ATG TAA TGG GTT GG	x		
ACL2_edge_R*	aat tcc agc tga cca cca tg GCC TGT TTT CTT TTC ACC CA	x	x	x
ACL2_edge_F2*	gat ccc cgg gaa ttg cca tg GGC TGA ATA CTC TGT GAA TCG	x	x	x
ACL_fl_F3	CGG GAA GTC AAC CTA CTG CA		x	x
ACL_fl_R3	GAA TCG ACT TGG CGG ACA TG		x	x

a) Pyr_F2 and pyr_R are the primers used when no direct repeats are wanted in the transformation.

b) The capital letters are the homologous regions with the target DNA, the small letters are the adaptamer sequences used for the fusion PCR.

c) D1 = transformation in the A742 strain, D2 = transformation in the AB4.1 strain, D3 = transformation in the pyrG-tr strain.

6.3.3 Southern blot analysis of transformants

For each strain, approximately 2 µg of genomic DNA was isolated and digested with appropriate restriction enzymes. Sequence information for restriction digest of the target loci (*acl* or *sdh*) were obtained from the *A. niger* ATCC 1015 genome sequence from the US Department of Energy Joint Genome Institute (http://genome.jgi-psf.org/Aspni1/). Blotting was done according to the method described by Sambrook and Russell (2001) and using RapidHyb™ hybridisation buffer (Amersham Pharmacia) for probing. The target locus was detected by probing with the labelled upstream target gene PCR fragment. The probes were radioactively labelled with α-32P-dCTP by random priming using Rediprime II™ kit (GE Healthcare).

6.3.4 Characterisation of deletion mutant

The deletion strain was tested in batch fermentations with 50 g/L glucose and 50 g/L xylose, respectively, as initial carbon concentrations and compared to the wild type strain N402. The medium composition used was the same as described in Meijer et al. (2007) and was also used for the pre-culture.

Before inoculation of the batch fermentors, spores were harvested with 0.01% Tween-80 from pre-culture plates that were incubated for 4-7 days at 30 ºC. Subsequently, 10^9 spores/L were added to the bioreactors. All strains were cultivated under oxygen limitation (0.1 vvm) in 5 L in-house manufactured bioreactors with a working volume of 4 L. The bioreactors were equipped with two disk turbine impellers rotating at 700 rpm. The initial pH was set at 2.5 and after 16 hours increased to 5 with $NaCO_3$. The temperature was maintained constant at 30 ºC and the pH was controlled by automatic addition of 1 M $NaCO_3$ and 2 M HCl.

6.3.5 Cell dry weight determination

The cell mass concentration on a dry weight basis was determined by the use of nitrocellulose filters with a pore size of 0.45 µm (Osmonics, Minnetonka, MN). Initially, the filters were pre-dried in a microwave oven at 150 W for 10 minutes, and then weighed. A known weight of cell culture was filtered, and the residue was washed with distilled water. Finally, the filter was dried in the microwave at 150 W for 15 minutes and the dry weight was determined.

6.3.6 Extracellular metabolite quantification

For determination of the extracellular metabolites, a culture sample was taken and immediately filtered through a 0.45 µm-pore-size nitrocellulose filter (Osmonics, Minnetonka, MN). The filtrate was frozen and kept at -20°C until analysis. Glucose, acetate, pyruvate, citrate, ethanol, succinate, fumarate, malate, glycerol, and oxalate concentrations were determined on an Aminex HPX-87H cationic exchange column (BioRad, Hercules, California) eluted at 60 ºC with 5 mM H_2SO_4 at a flow rate of 0.6 mL/min. Metabolites were detected with both a refractive index detector and a UV detector.

6.4 Results and Discussion

To divert carbon fluxes into the direction of succinate, several metabolic engineering strategies were tested in this study. Two different gene loci were targeted for complete gene deletion in order to divert the fluxes of the primary metabolism towards succinate.

6.4.1 Strain construction

In an attempt to redirect fluxes towards C_4 precursor compounds two different gene deletion strategies were designed. One of the strategies is based on an *in silico* model prediction, that has shown an increase in succinate production when both *pdc* and *acl* were deleted (David et al. 2003). In a previous study it has been shown that PDC has no detectable activity under the cultivation conditions posed on the system, so it was decided to delete only *acl* (Meijer et al. 2007).
The second target for deletion is *sdh*. This is based on a rational understanding of the carbon metabolism. Deletion of this target has demonstrated higher C_4 organic acid levels in other micro-organisms like *E. coli* (Lin et al. 2005b).

The methods used for deleting these genes (*acl* and *sdh*) were similar, with the only differences being in the primers and flanking regions used during the transformation. In the first transformation design the PCR fragments were directly transformed in the A742 strain (D1). This transformation was performed with and without direct repeats. When direct repeats are involved a second selection step is required, and this complicates the already difficult transformation protocol. With direct repeats the unstable marker replacement needs to be popped out. Selection of transformants was done on minimal medium plates (MM), since transformants should have lost their auxotrophic behaviour. The auxotrophic A742 strain on the other hand needs 10 mM of both uracil and uridine for survival. This strain is used as negative control as it is unable to grow on MM.
The results of this transformation were surprising. On the Southern blots both the WT and the transformed band sizes could be detected (Figure 6.2 A and B). This indicates that multiple chromosomes are present in the transformants. A heterokaryon could be an explanation for this observation. However, heterokaryons are believed to occur only in mycelia and not in spores. Spores are believed to be haploid. Since these transformants were purified by streaking (4x), it was suggested that we might deal with a diploid strain. However, diploidity in *A. niger* strains was never mentioned in the literature.

To ensure that two transformants were not co-purified accidentally, single spores were picked and analysed on Southern blots. In Figure 6.2 the results of these single spore picked transformants are displayed. Even the differences between transformations with and without direct repeats can be detected on these blots. A 600 bp size difference was seen between the two transformations (Figure 6.2 A). Again, this is an indication that the band really is the band from the correct target locus and not a random background band. Another remarkable observation is that this phenomenon is seen in both genomic target regions (both for *acl* and *sdh* genome locus). It can be concluded that the A742 strain has multiple copies of the chromosomes and is not a good strain for doing deletions. The chances of homologous recombination in *A. niger* are already very small ($1:10^6$). If the gene has to be deleted on 2 different chromosomes to achieve a complete deletion, the chances are even smaller.

It was not possible to show that the strain was diploid by using benomyl as haplodizing agent. Benomyl is a microtubule destabilizing agent that will generate haploid cells out of diploid cells (Yu et al. 1999). Diploid cells are very sensitive to benomyl and are not able to survive in this medium. However, the haploidization effect of benomyl is extremely concentration dependent. The correct concentration could not be determined.

Instead, another *pyr* negative strain, AB4.1, was used that is also related to the N402 wild-type strain (see deletion strategy D2). The AB4.1 strain has been used for multiple transformations and is believed to be a haploid strain (Ram et al. 2004; Denherder et al. 1992). The flanking regions were increased in these transformations from 1.5 kb to 2.5 kb in order to improve the homologous recombination efficiency. Again, the transformations were performed with and without direct repeats. The recovery of transformants was high in these transformations, but only 1 correct deletion mutant could be retrieved (over 400 were checked). The Southern blot (Figure 6.3) clearly shows that the *acl* gene is replaced by the marker. This mutant was transformed without direct repeats so we were unable to pop-out the heterologous *pyr4* marker. The other transformants that were retrieved from these transformations still showed a high number of ectopic integrations of the bipartite fragments, resulting in several bands on the Southern blots (data not shown).

Although it was tried to delete the *acl* and *sdh* in the pyrG-tr strain as well (see deletion strategy D3), this strategy was unsuccessful. It contains the most elaborate transformation protocol used in this study and when successful, it would result in the most reliable deletion strain with the native marker gene located at its original place in the genome.
The transformation efficiency in *A. niger* is very poor and a synthetic marker selection on hygromycin (used in D3) complicates the method. Hygromycin selection is not as efficient as

auxotrophic selection, thereby causing a lot of background noise in the form of non-specific transformants. This background noise can be decreased by using sorbitol as osmotic stabilizing agent instead of sucrose. Even though this turned out to be a major improvement, no desired deletions could be retrieved with this method.

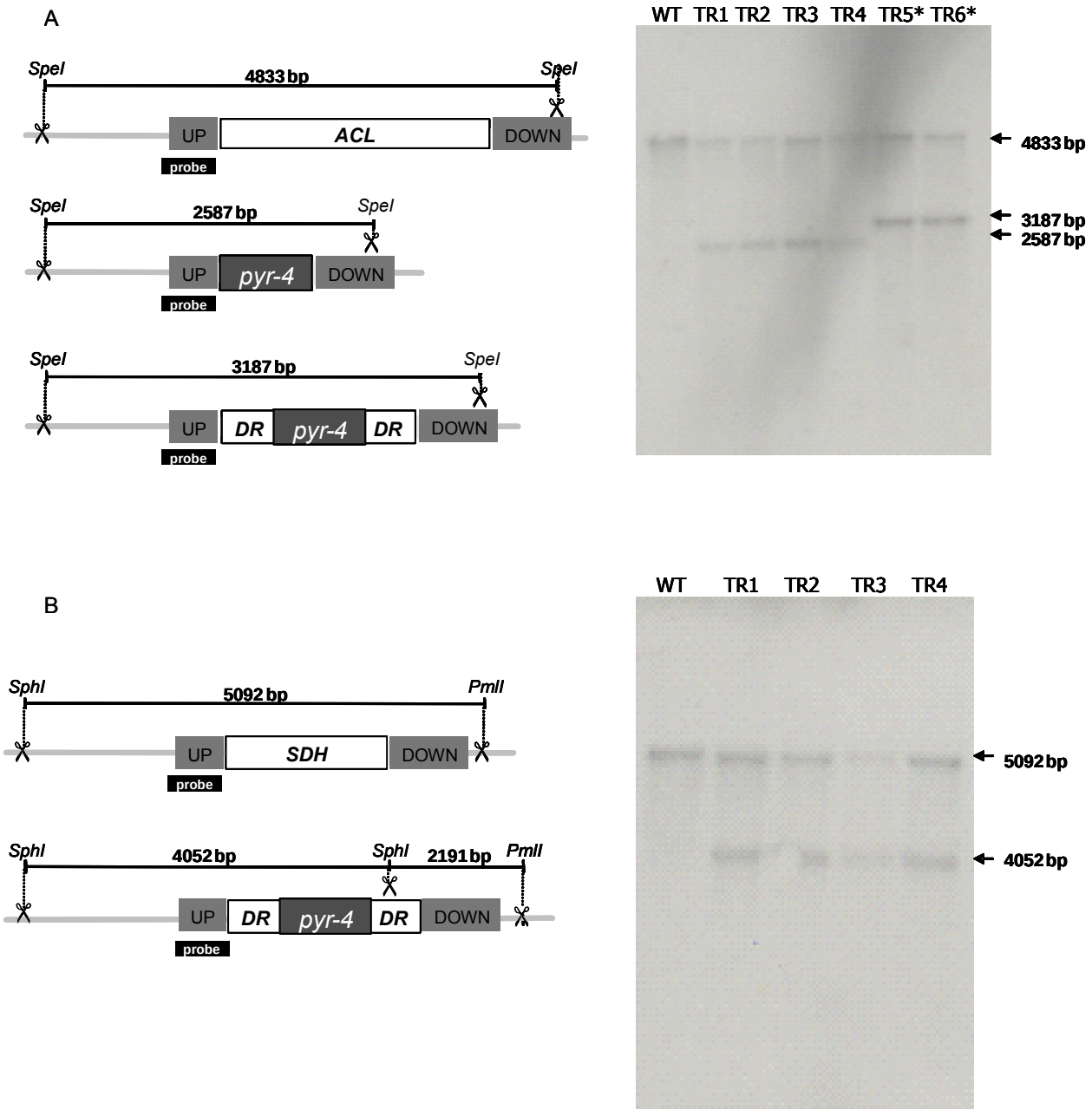

Figure 6.2 On the left side the restricted genomic regions, their length and the restriction enzymes used in the different strains are presented. On the right side the Southern blots are shown. A are the deletion results from *acl* deletion in the A742 strain. B shows the deletion results for *sdh* deletion in the A742 strain. WT = wild-type, TR = transformant,* = with direct repeats.

The fact that many different deletion strategies have been tried and only one transformant was successfully deleted in the target locus, indicates that the transformation protocols in *A. niger* are far from optimal. Efforts towards deleting the non-homologous end joining pathways are being made (Meyer et al. 2007). This might give promising new strategies for deleting target specific genes in the future. When the transformation efficiency has been improved, the deletion of *sdh* should be tested again. It is still possible that *sdh* is an essential gene, but the poor transformation results in this study may imply that the transformation method failed.

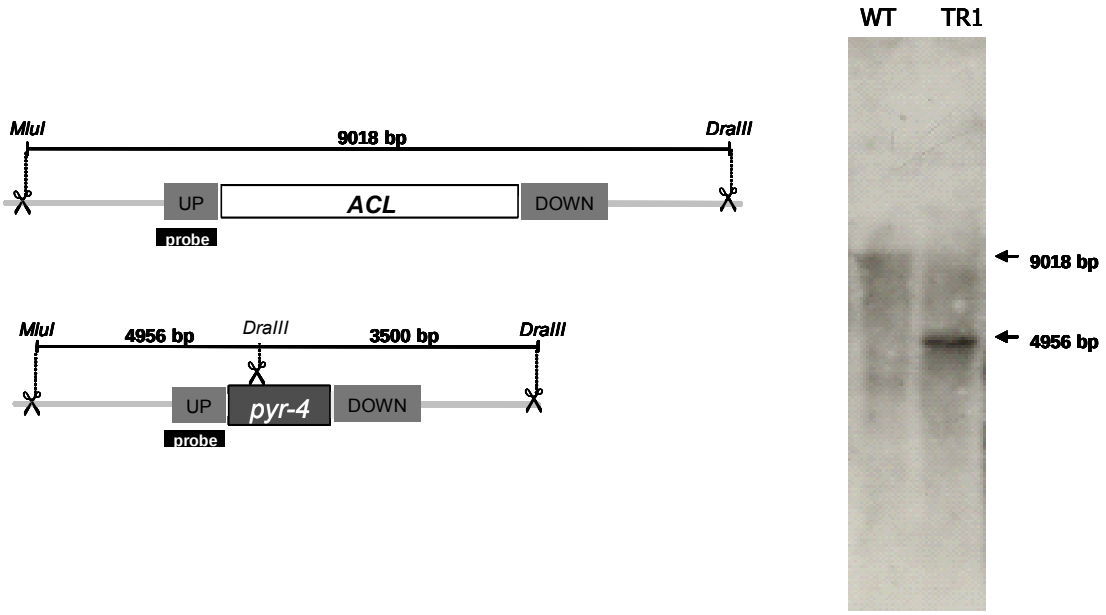

Figure 6.3 On the left side the genomic region of the target locus, its length and the restriction enzymes used for Southern blot analysis, is shown before and after the deletion. No direct repeats are used in this deletion. On the right hand side the Southern blot is presented with the first lane containing the WT band and the second lane containing the deletion band.

6.4.2 Strain characterisation

The *acl* deletion strain was compared to the wild-type N402 strain in 2 different batch set-ups. The carbon sources tested were glucose and xylose and the cultivations were run under oxygen limiting conditions. An overview of the batch profiles of the different fermentations is shown in Figure 6.4. The first observation during the fermentation was that the Δ*acl* strain consumed two times more base compared to the wild-type on both glucose and xylose. This indicated that more acids were being produced. The increased acid production could be verified by the HPLC method analysing several extracellular acids. Table 6.2 shows the acids

measured in the different fermentations. It was observed that the ratio between the different acids changed when the carbon source has been changed.

Table 6.2 Organic acid yields in C-mmol/C-mol carbon source.

	Succinate	Acetate	Glycerol	Citrate	Fumarate	Oxalate	Pyruvate
WT xylose	n.a.	n.a.	14	1	0.18	27	1.1
Δ*acl* xylose	n.a.	n.a.	16	5	0.74	24	2.3
WT glucose	2.1	n.a.	12	25	0.40	26	n.a.
Δ*acl* glucose	7.1	51	11	40	0.30	29	n.a.

n.a. means not analysed.

Additionally, the total amount of acid being produced differed between the different strains. Looking at the total amount of organic acid produced, it was observed that on xylose the *Δacl* strain produced slightly more acids compared to the wild-type (48 and 43 C-mmol, respectively). On glucose the difference was more pronounced. Here a total acid production of about 66 C-mmol was seen in the wild-type compared to 138 C-mmol in the *Δacl* strain. Thus, glucose as carbon source increased the acid production in the deletion strain more than two-fold. With glucose as C-source no pyruvate could be detected, indicating that there is no bottleneck at this point in the glycolysis, which might have resulted in the production of organic acids. One of the organic acids produced was citrate, which is known to be preferably produced during growth on glucose. The *acl* deletion seemed to stimulate citrate production also on xylose, but the yield was significantly lower than the yields achieved on glucose. During growth on xylose, pyruvate could be measured indicating that there is flux control at the entry into the TCA cycle, and this may explain the reduced amount of total organic acid production compared to cultivation on glucose.

It was observed that succinate was not produced when xylose was used as carbon source. On the other hand, using glucose as C-source resulted in production of small amounts of succinate (0.10 – 0.25 g/L). The deletion of *acl* increased the succinate yield more than 3 times, supporting the stoichiometric model prediction. Even though the model predicted a double deletion and not a single *acl* deletion, the experimental finding of an inactive PDC enzyme (Meijer et al. 2007) combined with this single deletion strain seems to confirm the model predictions quite well. The succinate yield was significantly increased, but it did not reach the maximum yields (>0.7 g/g) predicted by the model. An explanation might be that

some reactions are under-estimated and that regulatory effects influence the metabolic state, which is not incorporated in the stoichiometric model. Modelling is therefore an iterative process, i.e. the model needs to be adjusted to the obtained experimental results in order to get a more realistic view on cellular function.

Finally, during growth on xylose the fumarate yield increased significantly in the deletion strain compared to the wild-type strain, which was not observed on glucose. This is an unexpected result, since in other cases (*E. coli* or *M. succiniciproducens*) succinate and fumarate production are closely related. If succinate is produced through the reductive TCA cycle, fumarate must be produced before succinate. In this study it is observed that fumarate and succinate production are not correlated at all, indicating that *A. niger* does not use the reductive TCA cycle for succinate production. More likely it will use the oxidative TCA cycle or the glyoxylate shunt. Fumarate production is possibly obtained by the reductive pathway. The fumarate reductase is most likely missing or not active in *A. niger*, making it impossible to produce succinate via the reductive pathway under these experimental conditions. No large differences in glycerol and oxalate yield were observed between the different carbon sources and strains. The most prominent change seems to occur in the TCA cycle and not in other pathways. The flux has clearly been redirected by deleting *acl*. The stoichiometric model needs to be fine tuned by incorporating these experimental results. New simulations should be performed in order to define a new strategy for further optimising succinate production in *A. niger*.

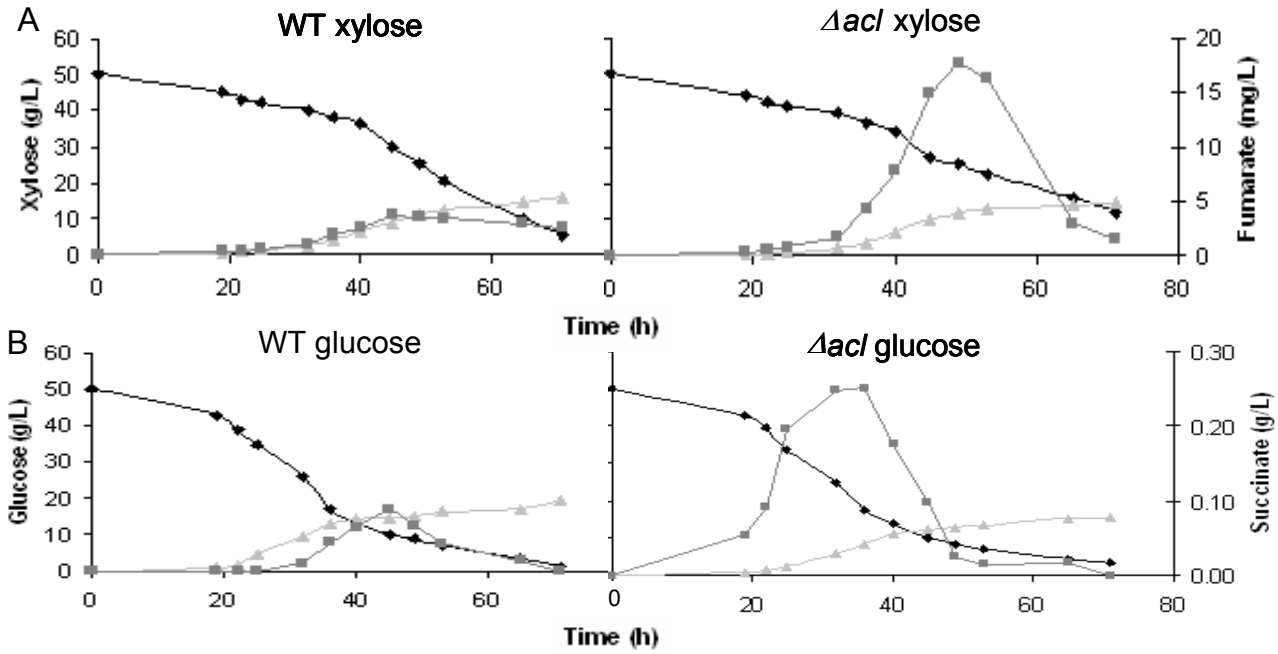

Figure 6.4 Batch profiles of carbon source consumption, biomass and organic acid production. A. ♦ = xylose consumption, ▲ = biomass production, ■ = fumarate production. B. ♦ = glucose consumption, ▲ = biomass production, ■ = succinate production

6.5 Conclusion

Two deletion strategies were tested in an attempt to increase the succinate production in *A. niger*. One strategy (*acl* deletion) is based on stoichiometric metabolic model predictions under oxygen limited conditions. The other strategy (*sdh* deletion) was chosen as it has been successfully used in other micro-organisms. Several approaches were tested to achieve complete gene deletions of these two target genes. However, the different gene targeting methods used in this study did not result in a high deletion success rate. Only one of the two target genes was successfully deleted. There is still an urgent need for improved gene targeting methods in *A. niger*.

In the *acl* deletion strain there was an increased organic acid production on both glucose and xylose as carbon-sources. On glucose a three-fold higher succinate yield was detected in the deletion strain. This might indicate that the stoichiometric model is a good tool for defining target genes.

Although *A. niger* can be used as a cell factory for succinate production, further optimisation is needed in order to reach levels of industrial relevance. Additionally, there is still a lack of physiological knowledge, which complicates the optimisation process. This can only be overcome by more research on the metabolism of *A. niger*.

6.6 References

Arikawa Y, Kuroyanagi T, Shimosaka M, Muratsubaki H, Enomoto K, Kodaira R and Okazaki M 1999. Effect of gene disruptions of the TCA cycle on production of succinic acid in *Saccharomyces cerevisiae*. *Journal of Bioscience and Bioengineering* **87** (1):28-36.

Baker SE 2006. *Aspergillus niger* genomics: Past, present and into the future. *Medical Mycology* **44**:S17-S21.

Ballance DJ, Buxton FP and Turner G 1983. Transformation of *Aspergillus nidulans* by the orotidine-5'-phosphate decarboxylase gene of *Neurospora crassa*. *Biochemical and Biophysical Research Communications* **112** (1):284-289.

David H, Akesson M and Nielsen J 2003. Reconstruction of the central carbon metabolism of *Aspergillus niger*. *European Journal of Biochemistry* **270** (21):4243-4253.

Denherder IF, Rosell AMM, Vanzuilen CM, Punt PJ and Vandenhondel AMJJ 1992. Cloning and expression of a member of the *Aspergillus niger* gene family encoding alpha-galactosidase. *Molecular & General Genetics* **233** (3):404-410.

Erdeniz N, Mortensen UH and Rothstein R 1997. Cloning-free PCR-based allele replacement methods. *Genome Research* **7** (12):1174-1183.

Ideker T, Galitski T and Hood L 2001. A new approach to decoding life: Systems biology. *Annual Review of Genomics and Human Genetics* **2**:343-372.

Lee SJ, Song H and Lee SY 2006. Genome-based metabolic engineering of *Mannheimia succiniciproducens* for succinic acid production. *Applied and Environmental Microbiology* **72** (3):1939-1948.

Lin H, Bennett GN and San KY 2005a. Effect of carbon sources differing in oxidation state and transport route on succinate production in metabolically engineered *Escherichia coli*. *Journal of Industrial Microbiology & Biotechnology* **32** (3):87-93.

Lin H, Bennett GN and San KY 2005b. Genetic reconstruction of the aerobic central metabolism in *Escherichia coli* for the absolute aerobic production of succinate. *Biotechnology and Bioengineering* **89** (2):148-156.

Meijer S, Panagiotou G, Olsson L and Nielsen J 2007. Physiological characterisation of xylose metabolism in *Aspergillus niger* under oxygen-limited conditions. *Biotechnology and Bioengineering* **98** (2):462-475.

Meyer V, Arentshorst M, El-Ghezal A, Drews AC, Kooistra R, van den Hondel CAMJ and Ram AFJ 2007. Highly efficient gene targeting in the *Aspergillus niger kusA* mutant. *Journal of Biotechnology* **128** (4):770-775.

Nielsen ML, Albertsen L and Mortensen U 2005. Genetic stability of direct and inverted repeats in *Aspergillus nidulans*. *Journal of Biotechnology* **118**:S13.

Nielsen ML, Albertsen L, Lettier G, Nielsen JB and Mortensen UH 2006. Efficient PCR-based gene targeting with a recyclable marker for *Aspergillus nidulans*. *Fungal Genetics and Biology* **43** (1):54-64.

Nielsen ML, de Jongh WA, Meijer SL, Nielsen J and Mortensen UH 2007. Transient marker system for iterative gene targeting of a prototrophic fungus. *Applied and Environmental Microbiology* **73** (22):7240-7245.

Patil KR, Akesson M and Nielsen J 2004. Use of genome-scale microbial models for metabolic engineering. *Current Opinion in Biotechnology* **15** (1):64-69.

Pel HJ, de Winde JH, Archer DB, Dyer PS, Hofmann G, Schaap PJ, Turner G, de Vries RP, Albang R, Albermann K, Andersen MR, Bendtsen JD, Benen JAE, van den Berg M, Breestraat S, Caddick MX, Contreras R, Cornell M, Coutinho PM, Danchin EGJ, Debets AJM, Dekker P, van Dijck PWM, van Dijk A, Dijkhuizen L, Driessen AJM, d'Enfert C, Geysens S, Goosen C, Groot GSP, de Groot PWJ, Guillemette T, Henrissat B, Herweijer M, van den Hombergh JPTW, van den Hondel CAMJ, van der Heijden RTJM, van der Kaaij RM, Klis FM, Kools HJ, Kubicek CP, van Kuyk PA, Lauber J, Lu X, van der Maarel MJEC, Meulenberg R, Menke H, Mortimer MA, Nielsen J, Oliver SG, Olsthoorn M, Pal K, van Peij NNME, Ram AFJ, Rinas U, Roubos JA, Sagt CMJ, Schmoll M, Sun JB, Ussery D, Varga J, Vervecken W, de Vondervoort PJJV, Wedler H, Wosten HAB, Zeng AP, van Ooyen AJJ, Visser J and Stam H 2007. Genome sequencing and analysis of the versatile cell factory *Aspergillus niger* CBS 513.88. *Nature Biotechnology* **25** (2):221-231.

Price ND, Papin JA, Schilling CH and Palsson BO 2003. Genome-scale microbial in silico models: the constraints-based approach. *Trends in Biotechnology* **21** (4):162-169.

Ram AFJ, Arentshorst M, Damveld RA, vanKuyk PA, Klis FM and van den Hondel CAMJ 2004. The cell wall stress response in *Aspergillus niger* involves increased expression of the glutamine : fructose-6-phosphate amidotransferase-encoding gene (*gfaA*) and increased deposition of chitin in the cell wall. *Microbiology-Sgm* **150**:3315-3326.

Sambrook J and Russell DW 2001. Molecular cloning a laboratory manual. *Cold Spring Harbor Laboratory Press,* Cold Spring Harbor, NY.

Stephanopoulos G, Alper H and Moxley J 2004. Exploiting biological complexity for strain improvement through systems biology. *Nature Biotechnology* **22** (10):1261-1267.

Vanhartingsveldt W, Mattern IE, Vanzeijl CMJ, Pouwels PH and Vandenhondel CAMJ 1987. Development of a homologous transformation system for *Aspergillus niger* based on the *pyrG* gene. *Molecular & General Genetics* **206** (1):71-75.

Vemuri GN, Eiteman MA and Altman E 2002. Succinate production in dual-phase *Escherichia coli* fermentations depends on the time of transition from aerobic to anaerobic conditions. *Journal of Industrial Microbiology & Biotechnology* **28** (6):325-332.

Yu JH, Rosen S and Adams TH 1999. Extragenic suppressors of loss-of-function mutations in the *Aspergillus* FlbA regulator of G-protein signaling domain protein. *Genetics* **151** (1):97-105.

Chapter 7

Physiological characterisation of *acuB* deletion in *Aspergillus niger*

Meijer S., Jongh de W.A., Olsson L. and Nielsen J.
Biocentrum-DTU, Center for Microbial Biotechnology, Denmark

Aimed at *Journal of Biotechnology*

7.1 Abstract

The *acuB* gene of *A. niger* is an autolog of *facB* in *A. nidulans*. It encodes a positively acting regulatory protein, which is involved in acetate induction of ACS (*acuA*), ICL (*acuD*) and MS (*acuE*). Mutants lacking AcuB function are unable to grow on acetate as sole carbon source. *AcuB* is also known to be directly repressed by CreA. Under carbon repression conditions *acuB* is repressed, thereby preventing acetate metabolism as long as the repressing carbon source is present. Even though a*cuB* is reported to be repressed directly by the main glucose repression gene *creA*, it is believed that there is a basic level of AcuB activity under glucose repressive conditions.

In the present study the effect of the deletion of the *acuB* gene on the physiology of *A. niger* was assessed. The differences in organic acid and acetate production, enzyme activities and extracellular amino and non-amino organic acid production were determined under glucose repressing and derepressing conditions. Furthermore, the consumption of alternative carbon sources (e.g. xylose, citrate, lactate and succinate) was investigated.

It was shown that AcuB has pleiotropic effects on the physiology of *A. niger*. The results indicate that metabolic pathways, that are not directly involved in acetate metabolism, are influenced by *acuB* deletion. Clear differences in organic acid consumption and production were detected between the *∆acuB* and reference strain. However, the hypothesis that AcuB is responsible for some basic *acuA* activity necessary for activation of the acetate metabolic pathways, even during growth on glucose, could not be confirmed.

Keywords: *AcuB* deletion, signal transduction pathways, organic acids, acetate

7.2 Introduction

The biochemically versatile fungus *Aspergillus niger* produces a wide array of acids and degradative enzymes to support its absorptive life style. This metabolic diversity and its capability to use a large amount of different carbon sources, makes *A. niger* a valuable cell factory for use in many different industrial processes (Bennett 1997). The diverse carbon catabolism of *A. niger* is, like many other micro-organisms, regulated by several mechanisms providing adaptation to prevailing conditions. One of these regulatory processes is carbon catabolite repression, ensuring that readily metabolisable carbohydrates repress the synthesis of enzymes related to the catabolism of alternative carbon sources. This preferential utilization of the most favoured carbon source is beneficial for two reasons. Firstly, the energetically easiest metabolisable carbon source is used first, and secondly, no energy is wasted on the synthesis of other catabolic systems (Ruijter and Visser 1997a).

Carbon repression in *Aspergilli* has been the focus of several studies, in particular for the model organism *A. nidulans* (for review see Arst 1977; Kelly and Hynes 1982; Ruijter and Visser 1997b; Scazzocchio et al. 1995). The major regulatory gene controlling carbon repression is *creA* (Agger et al. 2002; Ruijter et al. 1997b; Shroff et al. 1997). The carbon repression regulated by the CreA protein can be divided into three groups based on their metabolic function. The first and main group consists of genes encoding enzymes that catabolize less preferred carbon sources (Prathumpai et al. 2004). The second group comprises genes that are involved in secondary metabolism (Espeso and Penalva 1992). The third group includes genes encoding gluconeogenic and glyoxylate cycle enzymes (Sandeman and Hynes 1989; Bowyer et al. 1994; Kelly and Hynes 1981; David et al. 2005). The regulatory impact of CreA on metabolism is complex and encompasses a diverse range of signal transduction pathways (Veen et al. 1995; Dowzer and Kelly 1991).

AcuB, the focus of this study, is a global regulator in acetate metabolism and is directly repressed by CreA (Katz and Hynes 1989). Under carbon repression conditions *acuB* is repressed, thereby preventing induction of acetate metabolism as long as the repressing carbon source is present. However, it is believed that AcuB has a basic level of activity under carbon repressing conditions, since the glyoxylate bypass genes induced by AcuB, showed a low level of expression under glucose repressive conditions (Ruijter et al. 1999). Also the lack of acetate formation during oxalate production, formed by the enzymatic cleavage of oxaloacetate (OAA) to oxalate and acetate in medium with a high glucose concentration, has been thought to be caused by basic level activity of AcuB. These data led to the hypothesis

that acetyl CoA synthetase (ACS) is induced by AcuB, and metabolises all acetate formed. It has already been shown that ACS has detectable enzyme activity levels under glucose repressing conditions in *A. niger*, but not in *A. nidulans* (Sealy-Lewis and Fairhurst 1998).

The *acuB* gene of *A. niger* is an autolog of *facB* in *A. nidulans* (Papadopoulou and Sealy-Lewis 1999). It encodes a positively acting regulatory protein, which is involved in acetate induction of acetyl-CoA synthase (*AcuA*), isocitrate lyase (*AcuD*), malate synthase (*AcuE*) and NADP-specific isocitrate dehydrogenase (IDH) (Hynes 1977; Todd et al. 1997a; Kelly 1980). In *A. nidulans* FacB also induces acetamidase (*AmdS*). AcuB can take over this function but, in contrast to *A. nidulans, amdS* is not a natural occurring gene in *A. niger* (Sealy-lewis and Fairhurst 1998; Todd et al. 1998). AcuB contains a Zn(II)2Cys6 DNA-binding motif that shows high similarity to the Cat8 and Sip4 proteins in *S. cerevisiae* (Todd et al. 1997b). Cat8 is thought to be the central regulator of gluconeogenesis (Hedges et al. 1995), while Sip4 is involved in regulation of carbon metabolism via its interaction with Snf1 (Lesage et al. 1996).

Mutants lacking AcuB function have been shown to be unable to grow on acetate as the sole carbon source (Sealy-Lewis and Fairhurst 1998). The two-carbon compound acetate is capable to function as sole carbon source for many micro-organisms. In eukaryotes, acetate utilisation occurs in three different subcellular localisations (Stemple et al. 1998). First the acetate is activated to acetyl-CoA in the cytosol by acetyl-CoA synthase (ACS). Acetyl-CoA is subsequently transported by the acetylcarnitine shuttle to the mitochondria, where it is metabolised via the TCA cycle. Such a shuttle also transfers the acetyl-CoA from the cytosol to the glyoxysomes, where acetyl-CoA is metabolised via the glyoxylate pathway (Kornberg 1966). However, when growing on acetate, gluconeogenesis is required for energetic and structural cell viability. Gluconeogenesis leads to depletion of the citric acid cycle (TCA) intermediates, that are replenished via the glyoxylate pathway. The glyoxylate pathway consists of two reactions producing the TCA cycle intermediates malate and succinate from isocitrate and acetyl-CoA. The two enzymes catalysing these reactions are isocitrate lyase (ICL) and malate synthase (MS), which are both under AcuB regulation. The AcuB mediated induction of these enzymes is regulated at two levels: induction of *acuB* levels and increased activity of AcuB caused by acetate itself (Todd et al. 1997a; Katz and Hynes 1989).

In this study the effect of complete deletion of the *acuB* gene on the physiology of *A. niger* was characterised. The differences in organic acid production and extracellular amino acid secretion under glucose repressing and derepressing conditions were determined. Furthermore, the consumption of alternative carbon sources in solid state and submerged

cultures was investigated and the enzyme activities of four key enzymes in the TCA cycle and glyxoylate pathway were determined.

7.3 Material and Methods

7.3.1 Strains

As reference strain (WT) the laboratory strain N402 of *Aspergillus niger* was used. This strain is also known as A733 at the fungal genetics stock center and is a short-condiophore derivative of the N400 strain. The N402 strain is closely related to the ATCC1015 strain that is sequenced by DOE (Department of Energy, USA) (http://genome.jgi-psf.org/Aspni1/Aspni1.home.html, Sept 2007).

The other strain used was a Δ*acuB* strain in which the complete coding region of *acuB* has been deleted from the N402 strain by using the reversible auxotrophic marker strategy decribed in Nielsen et al. (2007).

7.3.2 Cultivation media

For the pre-culture a defined medium was used, containing 10 g/L D-glucose, 50 mL/L salt solution, 1 mL trace element solution 1 and 18 g/L agar. The salt solution consisted of 120 g/L $NaNO_3$, 10.4 g/L KCl, 10.4 g/L $MgSO_4 \cdot 7\ H_2O$ and 30.4 g/L KH_2PO_4. The trace element solution 1 consisted of 22 g/L $ZnSO_4 \cdot 7\ H_2O$, 11 g/L H_3BO_3, 5 g/L $MnCl_2 \cdot 2\ H_2O$, 5 g/L $FeSO_4 \cdot 7\ H_2O$, 1.7 g/L $CoCl_2 \cdot 6\ H_2O$, 1.6 g/L $CuSO_4 \cdot 5\ H_2O$, 1.5 g/L $Na_2MoO_4 \cdot 2\ H_2O$ and 50 g/L Na_4EDTA. Spores were propagated on plates containing this medium at pH 6.5.

The growth phenotype of the Δ*acuB* strain on different carbon sources was compared to the reference strain N402 on agar plates containing the same medium as described above. As carbon source were used glucose (10 g/L), fumarate (10 g/L), citrate (10 g/L), succinate (10 g/L), acetate (10 g/L), propionate (4 %, 0.1 % glucose) and propionate (1.6 %, 0.1 % glucose), respectively.

The batch cultivations were carried out in a chemically defined medium adjusted to pH 2.5 containing 0.5 g/L $NaNO_3$, 3 g/L KH_2PO_4, 2 g/L $MgSO_4 \cdot 7\ H_2O$, 2 g/L NaCl, 0.2 g/L $CaCl_2 \cdot 2H_2O$, 0.5 ml/L antifoam (sb2121) and 1 ml/L trace element solution 2. The trace element solution 2 consisted of 14.3 g/L $ZnSO_4 \cdot 7\ H_2O$, 2.5 g/L $CuSO_4 \cdot 5\ H_2O$, 0.5 g/L $NiCl_2 \cdot 6\ H_2O$, 7 g/L $MnCl_2 \cdot 2\ H_2O$ and 13.8 g/L $FeSO_4 \cdot 7\ H_2O$. The carbon sources were varied in these cultivations and are listed in Table 7.1.

Table 7.1 Carbon sources and concentrations used in the batch fermentations of both WT and *ΔacuB* strains.

Carbon source	Concentration
Glucose	100 g/L
Glucose	50 g/L
Glucose	10 g/L
Xylose	10 g/L
Glucose - succinate	10 g/L - 10 g/L
Glucose - citrate	10 g/L - 10 g/L
Glucose - lactate	10 g/L - 10 g/L

7.3.3 Cultivation conditions

The pre-culture plates were incubated for 4-7 days at 30 ºC after which the spores were harvested with 0.01 % w/w Tween-80. For the phenotypic growth characterisation the agar plates were incubated at 30 ºC and checked regularly to assess the growth differences.

All batch cultivations were carried out in 3 L Braun bioreactors with a working volume of 2 L. The temperature was maintained constant at 30 ºC and the pH was controlled by automatic addition of 2 M NaOH and 2 M HCl. Two Rushton four-blade disc turbines were used for homogeneous mixing. No baffles were incorporated in the reactors, thereby reducing the surface area available for biofilm formation. All cultivations were inoculated with spores to an initial concentration of $5*10^8$ spores/L. The initial aeration rate, agitation and pH were 0.2 vvm, 200 rpm and pH 2.5, respectively. These were gradually increased after germination (approx. 15 hours) to 1 vvm, 700 rpm and pH 5 respectively, after which these parameters were kept constant throughout the rest of the cultivation. Air was used for sparging and the concentrations of oxygen and carbon dioxide in the exhaust gas were monitored by an acoustic gas analyser (Brüel & Kjær, Denmark). The dissolved oxygen tension (DOT) was measured with an oxygen probe (Mettler Toledo sensors).

7.3.4 Sampling

Biomass samples were taken manually from the reactor. For dry weight measurements, a known cell culture volume was filtered through a pre-weighed nitrocellulose filter (pore size 45 µm, Pall Corporation). The filtrate was frozen immediately and later used for

determination of substrate and extracellular metabolites. The filter was washed with 0.9 % w/v NaCl, dried for 15 min in a microwave oven at 150 W and weighed again to determine the biomass concentration.

For determination of *in vitro* enzyme activities biomass samples were filtered through a nitrocellulose filter (pore size 45 µm, Pall Corporation) and washed with 0.9 % w/v NaCl. Thereafter, the filter cake (± 1 g) was immediately frozen in liquid nitrogen and stored at -80 ºC.

7.3.5 Substrate and extracellular metabolite quantification

High-performance liquid chromatography (Dionex, Rødovre, Denmark) was used for quantification of extracellular sugars and organic acids. Glucose, xylose, acetate, pyruvate, citrate, ethanol, succinate, fumarate, malate, glycerol, lactate and oxalate concentrations were measured on an Aminex HPX-87H cationic exchange column (BioRad, Hercules, California) eluted at 60 ºC with 5 mM H_2SO_4 at a flow rate of 0.6 mL/min. Metabolites were detected with both a refractive index detector and a UV detector. We calculated the maximum obtained yields for all these organic acids based on their substrate consumption.

Extracellular amino and non-amino organic acids were analysed using GC-MS analysis. The filtrate (1 mL) was lyophilised and derivatised using methyl chloroformate as decribed by Vilas-Boas et al. (2003). The resulting dry organic solutions were transferred to silanised GC vials and analysed with a Hewlett–Packard system HP 6890 gas chromatograph coupled to a HP 5973 quadrupole mass selective detector (EI) operated at 70 eV. The column used for all analyses was a J&W1701 (Folsom, CA) 30 m long; 250 µm inner diameter; 0.10 µm film thickness. The MS was operated in scan mode (start after 5 min, mass range 38–550 atomic mass unit at 2.88 s/scan) (Villas-Boas et al. 2003). Principal component analysis (PCA) was performed on the extracellular amino and non-amino organic acids in order to better visualise the differences between the two strains and their cultivation conditions.

7.3.6 Analysis of in vitro enzyme activities

The frozen samples were crushed in liquid nitrogen with a mortar. The crushed biomass (0.5 g) was solved in 2 ml of extraction buffer containing 25 mM MES-NaOH, 0.1 mM EDTA, 0.1 mM DTT, 0.1 mM phenylmethylsulfonyl fluoride, 0.1 mM NaN_3. This solution was transferred to 2-mL FastPrep tubes containing 0.5 mL glass beads (0.75-1 mm). The FastPrep tubes were processed 3 times 10 s on a FastPrep FP120 Instrument (Savant Instruments, New York), at speed setting 5, with cooling on ice in between. After disruption, samples were

centrifuged at 13000 g at 4 ºC for 10-20 min, and the supernatants were analysed for enzyme activity.

Enzyme assays were performed at 30 °C using a HP8453 UV-visible light spectrophotometer for detection of respective reactions. In order to test the linearity of the assays, the reactions were performed with 2-3 different dilutions of cell extract. The specific enzyme activities are expressed as micromoles minute^{-1} substrate consumed milligram^{-1} protein (U/mg). The amount of protein was determined by the Bradford method (Bradford 1976) with bovine serum albumin as the standard. We measured four different enzyme activities in the exponential growth phase: citrate synthase (CIT), malate dehydrogenase (MDH), isocitrate lyase (ICL) and malate synthase (MS) (Meijer et al. 2007; http://www.sigmaaldrich.com/sigma/enzyme%20assay/malatesynthase.pdf).

7.4 Results and Discussion

Since AcuB has been shown to have a wide regulatory role, we performed a detailed physiological characterisation of the *ΔacuB* strain constructed by Nielsen et al. (2007). The phenotypic behaviour of the *ΔacuB* strain was compared to the wild-type *A.niger* strain (N402). The focus of our study was on determining the influence of the *acuB* gene in the utilisation of certain di- and tricarboxylic acids and its effect on carbon repression.

7.4.1 Solid state growth characterisation

As a first screening test the solid state growth performance of both WT and *ΔacuB* on different carbon sources, as well as on the toxic compound propionate, were compared (Table 7.2). Results from literature have illustrated that mutants, that are hampered in their acetate metabolism, are able to grow on propionate concentrations at which the WT cannot (Sealy-Lewis 1994). The results of this screening experiment show that both strains can grow equally well on glucose, as on the organic acids fumarate, citrate and succinate. At these growth conditions deletion of the *acuB* gene has no detectable influence on the growth phenotype. Apparently, the role of AcuB on the physiology was more subtle and a more detailed characterisation is needed for identifying the physiological state of the strains.

On the other hand, we observed that the solid state growth of the *ΔacuB* strain was affected in its acetate metabolism and that it was more resistant to the toxic compound propionate. These last two observation correlate well with the literature showing that AcuB is responsible for regulating acetate uptake and metabolism (Hynes 1977; Todd et al. 1997a; Kelly 1980). An unknown mechanism makes the *ΔacuB* strain less susceptible to propionate. This resistance is most likely caused by the inability of the *ΔacuB* strain to metabolise certain compounds and thereby incapable to produce certain toxic intermediates like propionyl-CoA and methylisocitrate that are formed from propionate (Brock and Buckel 2004). This plate screening test is, however, a rough method for comparing strains. On other carbon sources like citrate, succinate and fumarate the differences between the *ΔacuB* and the WT strains were minimal.

Table 7.2 Growth phenotype of the *ΔacuB* strain on different carbon sources compared to the WT. Tested by point inoculating spores of the WT and *ΔacuB* onto MM plates with the indicated carbon source.

Carbon source	Growth of ΔacuB	Growth of the WT
Glucose	+++	+++
Fumarate	+++	+++
Citrate	+++	+++
Succinate	+++	+++
Acetate	---	+
Propionate 4%, 0.1 % glucose	--	0
Propionate 1.6%, 0.1 % glucose	-	---

+++ Normal growth
+ Slower growth
- Slow growth. altered morphology. delayed sporulation. Faun coloured spores
-- Very slow growth. altered morphology. delayed sporulation. Faun coloured spores
--- Very slow growth. altered morphology. no sporulation observed.
0 No growth

7.4.2 Uptake and specific growth rates

To get more insight into the role of AcuB, controlled batch cultivations of *ΔacuB* and WT were performed. Growth on several different carbon sources was tested (see Table 7.1), and also the effect of high sugar concentrations, since *acuB* expression is known to be influenced by carbon repression. Additionally, an attempt was made to grow the strains on acids as the sole carbon source. Several different intermediates of the TCA cycle were tested as carbon source to determine what effect *acuB* deletion has on these compounds and their gluconeogenesis pathways. An additional carbon source (lactate) was tested in these batch cultivations, since in *S. cerevisiae* it has been shown that deletion of an *acuB* homologue restricts lactate usage (Bojunga et al. 1998; Soares et al. 2004). It was found that in submerged cultures both strains were unable to germinate on media containing organic acids as the sole carbon source. This is in contrast with the observations on solid media.

Therefore, it was decided to add glucose to the medium allowing germination and initial growth, after which the micro-organism could switch to metabolising the alternative carbon source.

An illustration of these batch fermentations is shown in Figure 7.1. The volumetric carbon uptake rates of all carbon sources are presented in Table 7.3, together with the specific growth rates. These values show that the glucose uptake rate was slightly lower when a second carbon source was present. In the exponential phase (phase 1) the uptake rate of the second carbon source was less than the uptake rate in the glucose depleted phase (phase 2) for all substrates. For both strains lactate was the least favourable carbon source, and the Δ*acuB* strain was clearly more impaired in lactate uptake than the WT strain. The lactate uptake rates were 0.43 and 0.13 mmol/L/h, respectively. This is consistent with observations made in *C. albicans* and *S. cerevisiae*, where a *cat8* deletion (the homolog of *acuB* in *C. albicans* and *S. cerevisiae*) restricts the micro-organisms to consume lactate (Bojunga et al. 1998; Soares et al. 2004). Lactate is a non-fermentable carbon source, whose consumption is regulated by carbon repression. When *cat8* is deleted, the lactate permease *jen1* is expressed at a low level, leading to reduced lactate uptake.

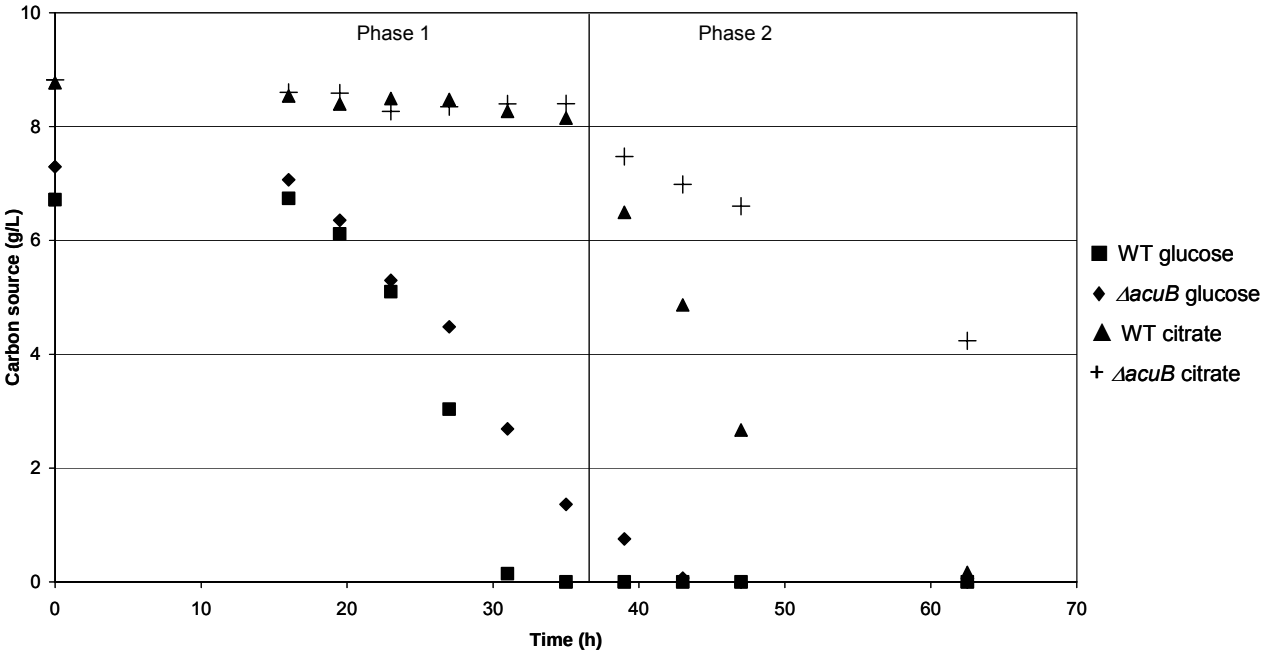

Figure 7.1 Typical carbon consumption profile for both the WT and Δ*acuB* strain when 2 carbon sources are present in the medium. Phase 1 is the exponential phase in which the glucose (most favourable carbon source) is consumed. In phase 2 the glucose is depleted and the second carbon source is consumed.

It should also be noted that uptake of citrate is almost absent in both strains when glucose is present in the medium (0.04 – 0.10 mmol/L/h), while succinate is consumed at similar rates by the WT strain in the presence and absence of glucose (0.70 versus 0.77 mmol/L/h). A clear difference is observed between the succinate uptake rate in the exponential phase in the Δ*acuB* and WT strains, with the uptake rate being lower in the mutant (0.21 versus 0.70 mmol/L/h). In contrast, the succinate uptake rate is similar in the Δ*acuB* strain and the WT strain when glucose is exhausted. The lower succinate uptake rate of the mutant in the exponential phase is surprising, since the *acuB* gene is known to be under carbon repression. Katz and Hynes (1989) showed that in an *A. nidulans* strain, carrying a *creA* mutation, *facB* induction was alleviated compared to the wild-type strain. Papadopoulou and Sealy-Lewis (1999) showed that *facB* is the homolog of *acuB* and that their functions could be interchanged. Although AcuB is not known to regulate the succinate uptake system directly, it could have an influence under carbon repressing conditions. It seems that carbon repression does not have a major impact on succinate consumption in the WT strain. On the contrary, a carbon repression effect can be postulated in the Δ*acuB* strain. However, this regulation will be influenced by a regulatory circuit that is not influenced by AcuB. It is possible that a basic level of *acuB* expression relieves the carbon repressive effect on succinate consumption in the WT strain, suggesting a new regulatory role for AcuB.

Another interesting observation is that, when glucose is depleted, the Δ*acuB* strain has a higher citrate consumption rate compared to the WT. There is no clear explanation for this observation. Possibly, when *acuB* is deleted a plethora of regulatory circuits are affected that stimulate organic acid uptake systems. Another possibility is that AcuB limits the transport systems of organic acids.

Table 7.3 illustrates that when more carbon source is added to the culture medium the volumetric carbon uptake rate increases, which correlates well to the higher biomass concentrations in the reactor. The specific growth rates are fairly constant at the different conditions, except for a few outliers (Table 7.3). This indicates that the available carbon concentration regulates the carbon uptake rates, but does not affect the specific growth rates of the micro-organism.

7.4.3 Enzyme activities

AcuB is known to be a regulatory protein that induces several enzymes (such as ICL, MS, ACS) and *acuB* is in itself again regulated by the global carbon repression gene *creA*. Because of both the carbon regulation and the enzyme regulation, the effect of *acuB* deletion on the activity of four different enzymes was determined (CIT, MDH, ICL and MS). ICL and

MS are known to be directly regulated by AcuB (Sealy-Lewis and Fairhurst 1998), while deletion of *acuB* might have an indirect effect on CIT and MDH.

Table 7.3: Carbon uptake rate and specific growth rate for all different cultivation conditions in both WT and Δ*acuB* strains.

	WT			**Δ*acuB***		
	q_s 1. phase	q_s 2. phase	μ	q_s 1. phase	q_s 2. phase	μ
Single carbon source						
Glucose	4.18		0.12	4.31		0.10
Glucose (50)	7.90		0.13	8.89		0.17
Glucose (100)	14.11		0.17	12.21		0.14
Xylose	5.56		0.13	4.37		0.12
Glucose+Citrate			0.14			0.16
Glucose	2.50			2.86		
Citrate	0.04	0.79		0.10	2.38	
Glucose+Lactate			0.16			0.16
Glucose	2.07			2.95		
Lactate	0.27	0.43		0.17	0.13	
Glucose+Succinate			0.15			0.21
Glucose	3.24			4.09		
Succinate	0.70	0.77		0.21	1.85	

q_s is expressed in mmol/L/h and μ in h^{-1}.
(50) and (100) means 50 and 100 g/L, respectively, when nothing is stated the concentration is 10 g/L

It was also tested which effect *acuB* deletion had on the physiology, when the sugar concentrations in the batch fermentations were changed (10, 50 and 100 g/L). Figure 7.2 shows the enzyme activities measured (U/mg protein). Comparing the three different sugar concentrations it appears that CIT and ICL show an increasing activity level with increasing sugar concentration (Pearson correlation of 0.95 and 0.99, respectively), while MDH and MS activity levels do not show much change. For CIT this increase is found for both Δ*acuB* and WT, while for ICL the increase in activity in Δ*acuB* is significantly higher than for WT. This is peculiar because literature states that *acuB* is not induced under carbon repression, resulting in un-induced glyoxylate enzymes like ICL and MS (Hynes 1977: Katz and Hynes 1989). This favours the hypothesis of a basic level of AcuB under glucose repressing conditions. ICL clearly shows the opposite profile, suggesting that more regulating systems are influencing

ICL under carbon repressing conditions or that AcuB might have an inhibiting effect on ICL activity. The MS profile indicates a decrease in activity in the Δ*acuB* strain. This profile could be expected due to carbon repression in the WT strain, but it should not be present in the Δ*acuB* strain.

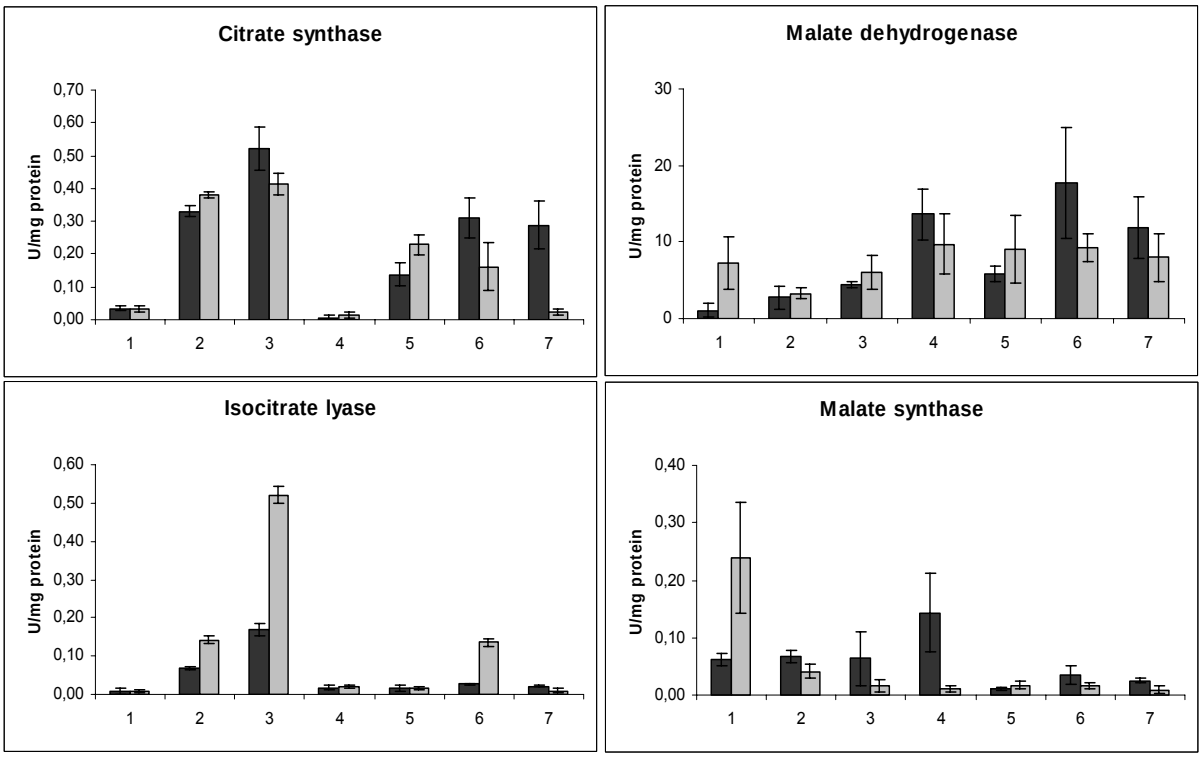

Figure 7.2 Enzyme activities are expressed in U/mg protein. The WT activities are expressed in the dark grey bars and the enzyme activities of *Δacu*B in the light grey bars. Levels 1 till 7 express the different fermentation conditions used in the fermentation. 1) glucose 10 g/L, 2) glucose 50 g/L, 3) glucose 100 g/L, 4) xylose 10 g/L, 5) glucose 10 g/L + citrate 10 g/L, 6) glucose 10 g/L + lactate 10 g/L and 7) glucose 10 g/L + succinate 10 g/L. All enzyme activities were determined in the exponential growth phase.

The inconsistencies between the enzyme activity measured and the current knowledge suggest that more regulatory pathways influence the enzyme activities in *A. niger*. The enzyme activities are not completely repressed by high sugar concentrations, which has been shown earlier for ICL (Meijer et al. 2007; Ruijter et al. 1999).

7.4.4 Organic acid production

The yields of excreted organic acids for the 7 different cultivation conditions of both strains are illustrated in Table 7.4 and Figure 7.3. The organic acid produced at the highest level in all fermentations is oxalate (0.7 – 4.7 g/L). Oxalate is one of the organic acids known to be produced in *A. niger* under certain conditions (Ruijter et al. 1999). The formation of organic acids is dependent on the pH of the medium. At pH < 3 the major acid produced is citrate, while at a pH between 3 - 6 mainly oxalate is produced (Kubicek and Rohr 1986; Ruijter et al. 1999). When pH values reach 5.5 or higher gluconate production may occur (Rohr et al. 1983).

Table 7.4 Maximal product yields in mmol/mol substrate for the different fermentation conditions and both WT and Δ*acuB* strains.

	Biomass		Succinate		Citrate		Fumarate		Oxalate		Pyruvate		Glycerol	
	WT	ΔacuB	WT	ΔacuB	WT	ΔacuB	WT	ΔacuB	WT	ΔacuB	WT	ΔacuB	WT	ΔacuB
glucose 10 g/L	1.9	1.9	3.5	0.0	14.7	19.8	0.0	0.2	251	203	18.0	2.5	22.8	8.2
glucose 50 g/L	1.6	1.7	6.0	0.9	15.7	3.0	0.8	0.1	153	103	5.3	10.9	26.4	4.8
glucose 100 g/L	1.4	1.3	2.1	1.4	43.2	39.5	1.5	1.3	130	89	0.0	0.0	52.7	38.4
xylose	2.2	2.2	1.0	1.4	3.5	4.2	1.1	0.6	199	142	0.3	0.6	1.1	0.9
gluc + cit	4.5	5.0	5.3	0.0	0.0	0.0	0.8	0.8	226	239	0.0	2.6	13.1	36.7
gluc + lac	4.2	4.5	46.1	46.7	60.7	70.4	0.6	1.2	219	210	1.8	16.8	22.6	25.9
gluc + succ	4.1	4.3	0.0	0.0	57.9	42.0	4.1	2.8	206	178	3.1	1.0	18.9	13.5

It should also be noted that, under all growth conditions, no acetate was detected in neither of the strains. This indicates that, although *acuB* is deleted, the cells are still able to metabolise acetate that may be formed. Ruijter et al. (1999) have demonstrated that an equimolar acetate / oxalate yield was achieved upon cleavage of oxaloacetate by a partially purified oxaloacetate hydrolase (OAH). The lack of acetate production by *A. niger* during oxalate production was explained by the fact that a Δ*acuA* (no acetylCoA synthase) strain did transiently produce acetate. Sealy-Lewis and Fairhurst (1998) discovered that AcuB is the regulatory enzyme that induces *acuA*. Lacking this induction would lead to acetate production, as there would be no acetylCoA synthase (ACS) activity. Sealy-Lewis and Fairhurst (1998) also demonstrated that ACS is not completely repressed by glucose, even though CreA has been shown to repress it directly. It seems that under glucose derepressed conditions *acuA* is induced by AcuB. When *acuB* is deleted, there is still a basic level of activity of ACS, as is found during glucose repressing conditions. Other pathways are likely to take over the regulation of AcuB and/or the enzymes that are normally induced by AcuB. These alternative pathways will then lead to a basic level of ACS activity. This basic level of activity seems to be sufficient to ensure that the acetate, produced by the oxaloacetate hydrolase, is metabolised.

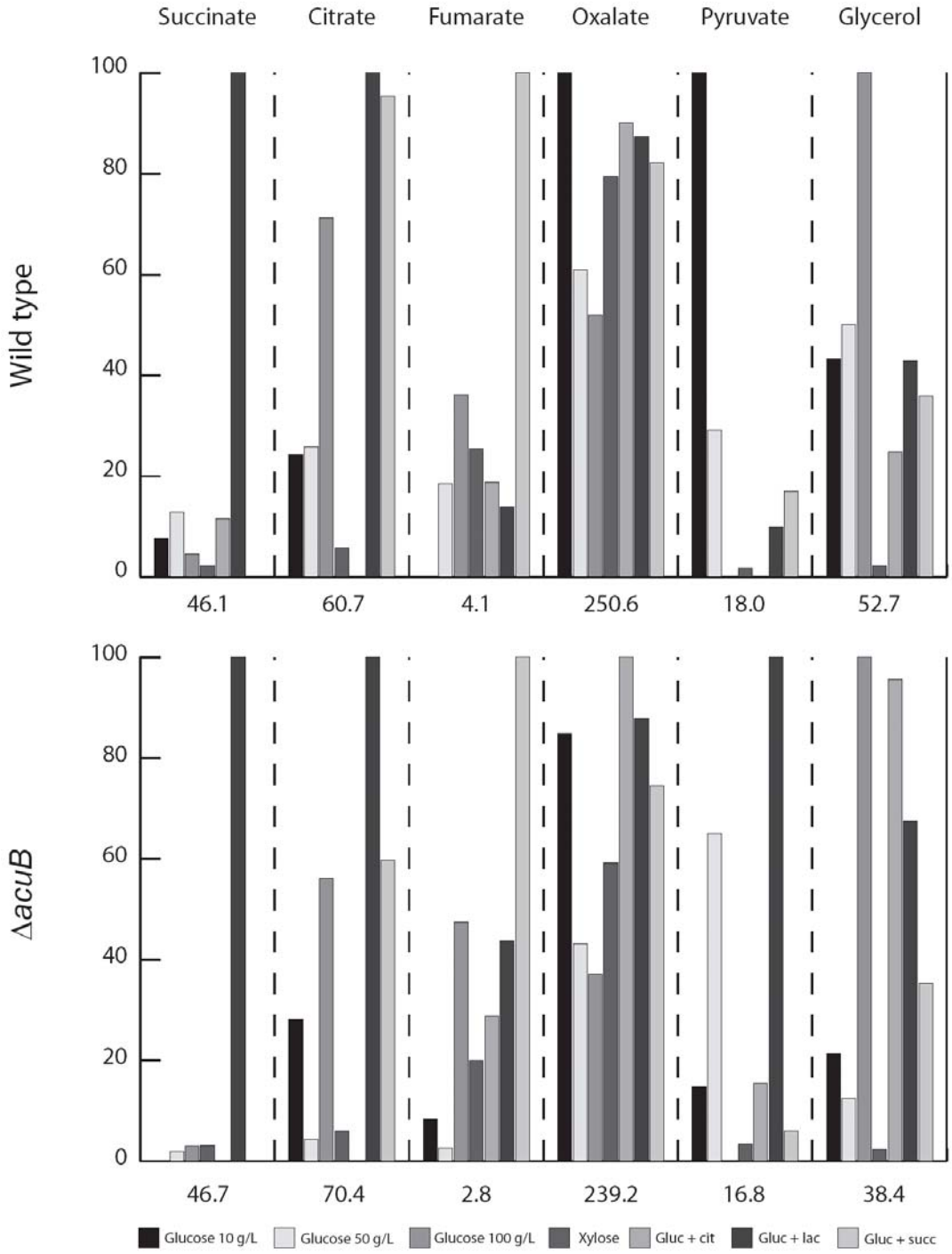

Figure 7.3 Comparison of maximal product yields for succinate, citrate, fumarate, oxalate, pyruvate and glycerol normalised to the highest yield. The top graph represents the yields for the WT, while the bottom graph respresents the *ΔacuB* yields. The colours of the bars represent the fermentation conditions used as presented directly under the graph. The values shown underneath both figures indicate the highest maximal yields to which the other yields are normalised.

Additionally, slightly higher citrate production was detected in fermentations with high sugar concentration compared to lower sugar concentration in both the WT and Δ*acuB* strain (average of WT and Δ*acuB* is 17 mM and 41 mM, respectively). This has been extensively documented in literature and is known as the overflow metabolism of *A. niger* that starts producing citrate at glucose concentrations of 50 g/L and higher (Papagianni 2007). Moreover, in fermentations where a second carbon source (lactate and succinate) is used, the production of citrate is even higher (average of WT and Δ*acuB* 65 mM for lactate or 49 mM for succinate). When lactate is used as a second carbon source also a significant amount of succinate is produced, while when succinate is used as second carbon source a lot of fumarate is produced, indicating a change in TCA cycle kinetics (Table 7.4). Glycerol is mainly produced in fermentations with high sugar concentrations (38-52 mM). For the Δ*acuB* strain there is also higher production of glycerol when citrate is used as second carbon source (37 and 13 mM in the Δ*acuB* and WT, respectively). It seems that the balance between oxalate and glycerol changes when the sugar concentration increases (decrease in oxalate production and increase in glycerol production). This might be caused by the fact that in cultivations with high sugar concentrations, the flux switches from the pentose phosphate pathway towards glycolysis (Legisa and Mattey 2007). When a second carbon source is added the product profile seems to become dependent on the source of the second compound (citrate, lactate or succinate).

7.4.5 Amino and non-amino organic acids

Looking at the extracellular amino and non-amino organic acid profiles we were not able to separate the Δ*acuB* strain from the WT strain by PCA analysis (data not shown). It appears that the fermentation conditions have a higher influence on the extracellular metabolite profiles than the effect of the gene deletion. The sugar concentration in particular has a large impact on the secretion pattern. The PCA plot (Figure 7.4) clearly shows that at high sugar concentrations (100 g/L glucose), more organic acids are produced compared to the low sugar concentration (10 g/L). At the intermediate sugar concentration (50 g/L) a higher production of amino acids is detected. These results correspond well to other investigations, which indicate that high sugar concentrations lead to an overflow metabolism producing high titers of organic acids. Karaffa and Kubicek (2003) showed that high amounts of citric acid are produced when the sugar concentration is high. At lower concentration glucose is mainly used for biomass production (Karaffa and Kubicek 2003; Ruijter and Visser 1997b).

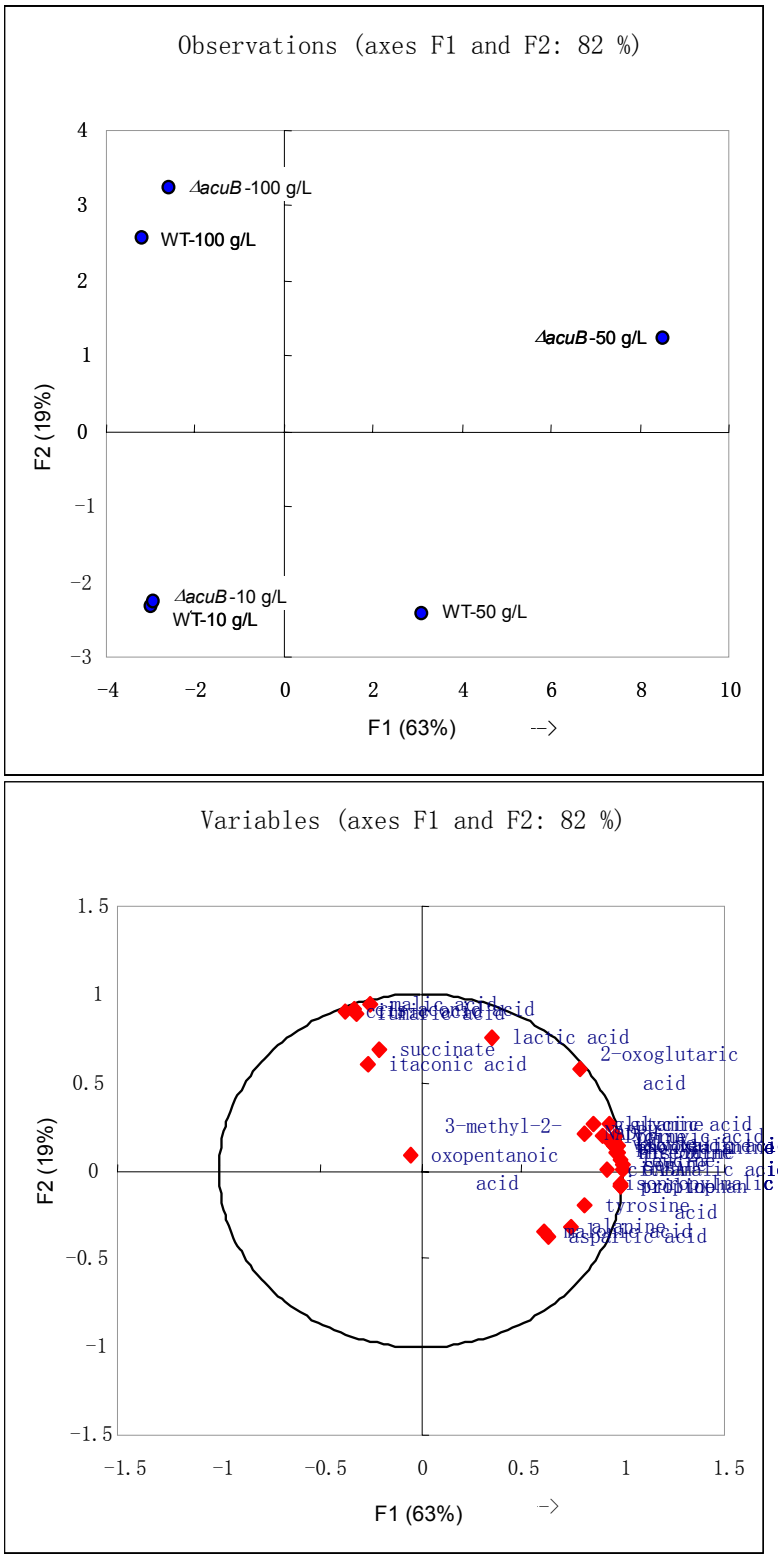

Figure 7.4 PCA analysis of ΔacuB and WT using 10, 50, 100 g/L glucose, respectively. The PCA is based on the extracellular amino and non-amino organic acids.

7.5 Conclusion

We conclude that the Δ*acuB* strain was limited in its acetate metabolism. This is clearly observed during the growth on solid media. The increased resistance of Δ*acuB* to propionate was confirmed in our experiments. In the submerged batch cultivations the differences between Δ*acuB* and WT were more subtle than expected. Especially under carbon repressing conditions we did not see the expected effect of Δ*acuB* on the enzyme activities that, in *A. nidulans*, are known to be regulated by AcuB (ICL and MS). Therefore, it seems that *A. niger* possesses more regulatory systems that ensure robustness in terms of metabolism of different carbon sources compared with *A. nidulans*. Thus, Δ*acuB* had an altered consumption and production of organic acids, but its effect is likely to be limited due to the presence of other processes involved in controlling the general state of metabolism in *A. niger*.

7.6 References

Agger T, Petersen JB, O'Connor SM, Murphy RL, Kelly JM and Nielsen J 2002. Physiological characterisation of recombinant *Aspergillus nidulans* strains with different *creA* genotypes expressing *A. oryzae* alpha-amylase. *Journal of Biotechnology* **92** (3):279-285.

Arst HN and Jr & Bailey CR 1977. The regulation of carbon metabolism in *Aspergillus nidulans*. *Genetics in Physiology of Aspergillus* 131-146.

Bennett JW 1997. White paper: Genomics for filamentous fungi. *Fungal Genetics and Biology* **21** (1):3-7.

Bojunga N, Kotter P and Entian KD 1998. The succinate/fumarate transporter Acr1p of Saccharomyces cerevisiae is part of the gluconeogenic pathway and its expression is regulated by Cat8p. *Molecular and General Genetics* **260** (5):453-461.

Bowyer P, Delucas JR and Turner G 1994. Regulation of the expression of the isocitrate lyase gene (*acuD*) of *Aspergillus nidulans*. *Molecular & General Genetics* **242** (4):484-489.

Bradford MM 1976. Rapid and sensitive method for quantitation of microgram quantities of protein utilizing principle of protein-dye binding. *Analytical Biochemistry* **72** (1-2):248-254.

Brock M and Buckel W 2004. On the mechanism of action of the antifungal agent propionate - Propionyl-CoA inhibits glucose metabolism in *Aspergillus nidulans*. *European Journal of Biochemistry* **271** (15):3227-3241.

David H, Krogh AM, Roca C, Akesson M and Nielsen J 2005. CreA influences the metabolic fluxes of *Aspergillus nidulans* during growth on glucose and xylose. *Microbiology-Sgm* **151**:2209-2221.

Dowzer CEA and Kelly JM 1991. Analysis of the *creA* gene, a regulator of carbon catabolite repression in *Aspergillus nidulans*. *Molecular and Cellular Biology* **11** (11):5701-5709.

Espeso EA and Penalva MA 1992. Carbon catabolite repression can account for the temporal pattern of expression of a *Penicillin* biosynthetic gene in *Aspergillus nidulans*. *Molecular Microbiology* **6** (11):1457-1465.

Hedges D, Proft M and Entian KD 1995. *Cat8*, a new zinc cluster encoding gene necessary for derepression of gluconeogenic enzymes in the yeast *Saccharomyces cerevisiae*. *Molecular and Cellular Biology* **15** (4):1915-1922.

Hynes MJ 1977. Induction of acetamidase of *Aspergillus nidulans* by acetate metabolism. *Journal of Bacteriology* **131** (3):770-775.

Karaffa L and Kubicek CP 2003. *Aspergillus niger* citric acid accumulation: do we understand this well working black box? *Applied Microbiology and Biotechnology* **61** (3):189-196.

Katz ME and Hynes MJ 1989. Isolation and analysis of the acetate regulatory gene, *facB*, from *Aspergillus nidulans*. *Molecular and Cellular Biology* **9** (12):5696-5701.

Kelly JM 1980. Pleiotropic mutants of *Aspergillus nidulans* affected in carbon metabolism. *Ph D thesis* La Trobe University, Bundoora, Victoria, Australia.

Kelly JM and Hynes MJ 1981. The regulation of phosphoenolpyruvate carboxykinase and the NADP-linked malic enzyme in *Aspergillus nidulans*. *Journal of General Microbiology* **123**:371-375.

Kelly JM and Hynes MJ 1982. The regulation of NADP-linked isocitrate dehydrogenase in *Aspergillus nidulans*. *Journal of General Microbiology* **128**:23-28.

Kornberg HL 1966. Role and control of glyoxylate cycle in *Escherichia coli* - First Colworth Medal Lecture. *Biochemical Journal* **99** (1):1-11

Kubicek CP and Rohr M 1986. Citric acid fermentation. *Critical Reviews in Biotechnology* **3** (4):331-373.

Legisa M and Mattey M 2007. Changes in primary metabolism leading to citric acid overflow in *Aspergillus niger*. *Biotechnology Letters* **29** (2):181-190.

Lesage P, Yang XL and Carlson M 1996. Yeast SNF1 protein kinase interacts with SIP4, a C-6 zinc cluster transcriptional activator: A new role for SNF1 in the glucose response. *Molecular and Cellular Biology* **16** (5):1921-1928.

Meijer S, Panagiotou G, Olsson L and Nielsen J 2007. Physiological characterisation of xylose metabolism in *Aspergillus niger* under oxygen-limited conditions. *Biotechnology and Bioengineering* **98** (2):462-475.

Nielsen ML, Jongh WA, Meijer SL, Nielsen J and Mortensen UH 2007. Transient marker system for iterative gene targeting of a prototrophic fungus. *Applied and Environmental Microbiology* **73** (22):7240-7245.

Papadopoulou S and Sealy-Lewis HM 1999. The *Aspergillus niger acuA* and *acuB* genes correspond to the *facA* and *facB* genes in *Aspergillus nidulans*. *Fems Microbiology Letters* **178** (1):35-37.

Papagianni M 2007. Advances in citric acid fermentation by *Aspergillus niger*: Biochemical aspects, membrane transport and modelling. *Biotechnology Advances* **25** (3):244-263.

Prathumpai W, McIntyre M and Nielsen J 2004. The effect of CreA in glucose and xylose catabolism in *Aspergillus nidulans*. *Applied Microbiology and Biotechnology* **63** (6):748-753.

Röhr M, Kubicek CP and Kominek J 1983. Citric acid. In: Reed G, Rehm HJ (eds) *Biotechnology*, vol 3 Verlag Chemie, Weinheim, pp 420-454.

Ruijter GJG and Visser J 1997b. Carbon repression in *Aspergilli*. *Fems Microbiology Letters* **151** (2):103-114.

Ruijter GJG, Vanhanen SA, Gielkens MMC, vandeVondervoort PJI and Visser J 1997a. Isolation of *Aspergillus niger creA* mutants and effects of the mutations on expression of arabinases and L-arabinose catabolic enzymes. *Microbiology-Uk* **143**:2991-2998.

Ruijter GJG, van de Vondervoort PJI and Visser J 1999. Oxalic acid production by *Aspergillus niger*: an oxalate-non-producing mutant produces citric acid at pH 5 and in the presence of manganese. *Microbiology-Sgm* **145**:2569-2576.

Sandeman RA and Hynes MJ 1989. Isolation of the *facA* (Acetyl-Coenzyme-A synthetase) and *acuE* (Malate synthase) genes of *Aspergillus nidulans*. *Molecular & General Genetics* **218** (1):87-92.

Scazzocchio C, Gavrias V, Cubero B, Panozzo C, Mathieu M and Felenbok B 1995. Carbon catabolite repression in *Aspergillus nidulans* - A review. *Canadian Journal of Botany-Revue Canadienne de Botanique* **73**:S160-S166.

Sealy-Lewis HM and Fairhurst V 1998. Isolation of mutants deficient in acetyl-CoA synthetase and a possible regulator of acetate induction in *Aspergillus niger*. *Microbiology-Uk* **144**:1895-1900.

Sealy-Lewis HM 1994. A new selection method for isolating mutants defective in acetate utilization in *Aspergillus nidulans*. *Current Genetics* **25** (1):47-48.

Shroff RA, OConnor SM, Hynes MJ, Lockington RA and Kelly JM 1997. Null alleles of *creA*, the regulator of carbon catabolite repression in *Aspergillus nidulans*. *Fungal Genetics and Biology* **22** (1):28-38.

Soares-Silva I, Paiva S, Kotter P, Entian KD and Casal M 2004. The disruption of JEN1 from Candida albicans impairs the transport of lactate. *Molecular Membrane Biology* **21** (6):403-411.

Stemple CJ, Davis MA and Hynes MJ 1998. The *facC* gene of *Aspergillus nidulans* encodes an acetate-inducible carnitine acetyltransferase. *Journal of Bacteriology* **180** (23):6242-6251.

Todd RB, Kelly JM, Davis MA and Hynes MJ 1997a. Molecular characterisation of mutants of the acetate regulatory gene *facB* of *Aspergillus nidulans* . *Fungal Genetics and Biology* **22** (2):92-102.

Todd RB, Murphy RL, Martin HM, Sharp JA, Davis MA, Katz ME and Hynes MJ 1997b. The acetate regulatory gene *facB* of *Aspergillus nidulans* encodes a Zn(II)2Cys6 transcriptional activator. *Molecular & General Genetics* **254** (5):495-504.

Todd RB, Andrianopoulos A, Davis MA and Hynes MJ 1998. *FacB*, the *Aspergillus nidulans* activator of acetate utilization genes, binds dissimilar DNA sequences. *Embo Journal* **17** (7):2042-2054.

Veen P van der, Ruijter GJG and Visser J 1995. An extreme c*reA* mutation in *Aspergillus nidulans* has severe effects on D-glucose utilization. *Microbiology-Uk* **141**:2301-2306.

Villas-Boas SG, Delicado DG, Akesson M and Nielsen J 2003. Simultaneous analysis of amino and nonamino organic acids as methyl chloroformate derivatives using gas chromatography-mass spectrometry. *Analytical Biochemistry* **322** (1):134-138.

Chapter 8

Overexpression of Isocitrate lyase – Glyoxylate bypass influence on metabolism in *Aspergillus niger*

Meijer S., Otero J., Olivares R., Andersen MR., Olsson L. and Nielsen J.
Biocentrum-DTU, Center for Microbial Biotechnology, Denmark

Aimed at *Metabolic Engineering*

8.1 Abstract

In order to improve the production of succinate and malate by the filamentous fungus *Aspergillus niger* the activity of the glyoxylate bypass pathway was increased by over-expression of the isocitrate lyase (*icl*) gene. The hypothesis was that when isocitrate lyase was up-regulated the flux towards glyoxylate would increase, leading to excess formation of malate and succinate compared to the wild-type. However, metabolic network analysis showed that an increased *icl* expression did not result in an increased glyoxylate bypass flux. The analysis did show a global response with respect to gene expression, leading to an increased flux through the oxidative part of the TCA cycle. Instead of an increased production of succinate and malate, a major increase in fumarate production was observed.
The effect of malonate, a competitive inhibitor of succinate dehydrogenase (SDH), on the physiological behaviour of the cells was investigated. Inhibition of SDH was expected to lead to succinate production, but this was not observed. There was an increase in citrate and oxalate production in the wild-type strain. Furthermore, in the strain with over-expression of *icl* the organic acid production shifted from fumarate towards malate production when malonate was added to the cultivation medium.
Overall, the *icl* over-expression and malonate addition had a significant impact on metabolism and on organic acid production profiles. Although the expected succinate and malate formation was not observed, a distinct and interesting production of fumarate and malate was found.

Keywords: isocitrate lyase over-expression, glyoxylate bypass, reduced organic acids, Metabolic Network Analysis, gene expression.

8.2 Introduction

For decades microbial citric acid production has been an important industrial process. The main source for citric acid production is the filamentous fungus *Aspergillus niger*. Medium composition and technical parameters have been extensively characterised and adapted to create an optimal production process (Kristiansen et al. 1999; Papagianni 2007). With advances in molecular biology and functional genomics during the last years it has become possible to study metabolism at a global level. One important breakthrough has been the sequencing of the *A. niger* genome (Baker 2006; Pel et al. 2007) and the subsequent design of DNA microarrays (Andersen et al. 2008). Another important and powerful method is metabolic network analysis, which has proven to be an important tool for analysis of the metabolic network and cellular physiology. This method has been developed by Christensen and Nielsen (1999) and others (Schmidt et al. 1997; Zupke and Stephanopoulos 1994). For quantifying metabolic fluxes, measurements of the amino acid labelling patterns by GC-MS or NMR are required, using ^{13}C- labelled carbon sources. Quantification of the fluxes provides a direct measure of the degree of engagement of various pathways on the overall cellular function.

Using DNA microarrays and flux analysis it is possible to get an in-depth knowledge about which molecular and biochemical pathways play a key role in product formation. Especially, in the quest to develop generic cell factories used for the production of a wide range of products, it is necessary to obtain detailed knowledge of the working mechanism of metabolic networks. The main focus of the present study is on the central carbon metabolism and the organic acid production in *A. niger*. With the ability of this fungus to produce high amounts of citric acid, it represents an attractive cell factory for the production of other organic acids like malic, fumaric and succinic acid. They are all considered valuable for the chemical industry (Werpy and Petersen 2004). For the production of these four-carbon organic acids it is quite natural to study the role of the glyoxylate pathway, as this pathway leads to malic acid and succinic acid production. Therefore, it was attempted to redirect fluxes towards the glyoxylate pathway by over-expressing the isocitrate lyase (ICL). Isocitrate lyase is the first enzyme of the glyoxylate pathway, with malate synthase being the second enzyme. The effect of adding malonic acid to the medium was also investigated. Malonic acid is known to be an inhibitor of succinate dehydrogenase (SDH). By disrupting the TCA cycle we tried to produce more organic acids in the form of succinic acid and malic acid.

The influence of *icl* over-expression and malonic acid addition on cellular performance was determined by transcript levels using DNA microarrays and metabolic flux analysis. Additionally, activities of key enzymes in the pathways leading to organic acids, as well as extracellular metabolite levels were measured. Our goal was to link the different information levels (genome, transcriptome, enzyme activities, metabolome and fluxome) to obtain a system-level understanding of the effect of *icl* over-expression on the cellular physiology. This provided us with new insights into the metabolism that can be used for improving the organic acid production of succinate and malate in the filamentous fungus *A. niger*.

8.3 Materials and Methods

8.3.1 Strains

As reference strain the laboratory strain N402 of *Aspergillus niger* was used. The *icl* over-expression was made in the *pyrA*- strain AB4.1, which is auxotrophic for uridine and uracil. The *icl* gene was put on a high copy number plasmid. The vector used was pCR2.1-AfpyrG (kindly provided by Axel Brakhage), which carries *pyrG* from *A. fumigatus* (Vanhartingsveldt et al. 1987). *Icl* was fused to the *A. nidulans gpdA* promoter using fusion PCR. PCR was performed using the Expand High Fidelity PCR kit (Roche) according to the manufacturer's recommendations. The primers used are shown in Table 8.1. The fusion PCR product of *gpdA* and *icl* was cut with SbfI, and the pCR2.1-AfpyrG vector was cut with PsiI. Both these enzymes are blunt-end cutting restriction enzymes and therefore the pCR2.1-AfpyrG vector and *icl* fusion gene product can be ligated using T4 DNA ligase. The ICL over-expression plasmid pCR2.1-AfpyrG_ICL was transformed into the AB4.1 strain using the protoplast and transformation procedures for *A. niger* as described previously for *A. nidulans* (Nielsen et al. 2006).

Table 8.1 Primers used for fusion PCR to over-express *icl* in *A. niger*

Primer name	Sequence
GpdA_up	AATAT **CCTGCAGG** GCT GAT TCT GGA GTG ACC CAG AG
GpdA_down	CTT CTT CTT CAA AGG AAG CCA T ACA CCG GGC GGA CAG ACG
ICL_up	ATG GCT TCC TTT GAA GAA GAA G
ICL_down	ATTA **CCTGCAGG** ATT CCC CTC CAT TCC CAT GC

The underlined letters are the overlapping genetic elements used for fusion PCR. The bold letters code for the restriction enzyme Sbf1 that is used for restriction of the fusion PCR product, before insertion in the pCR2.1-AfpyrG plasmid.

8.3.2 Cultivation media

For the pre-culture a defined medium was used containing 10 g/L D-glucose, 50 ml salt solution, 1 ml trace element solution 1 and 18 g/L agar. The salt solution contained 120 g/L $NaNO_3$, 10.4 g/L KCl, 10.4 g/L $MgSO_4 \cdot 7\ H_2O$ and 30.4 g/L KH_2PO_4. The trace element solution 1 contained 22 g/L $ZnSO_4 \cdot 7\ H_2O$, 11 g/L H_3BO_3, 5 g/L $MnCl_2 \cdot 2\ H_2O$, 5 g/L $FeSO_4 \cdot$

7 H_2O, 1.7 g/L $CoCl_2 \cdot 6\ H_2O$, 1.6 g/L $CuSO_4 \cdot 5\ H_2O$, 1.5 g/L $Na_2MoO_4 \cdot 2\ H_2O$ and 50 g/L Na_4EDTA. Spores were propagated on agar plates containing this medium at pH 6.5.

The batch cultivations were carried out in a chemically defined medium adjusted to pH 2.5 containing 10 g/L glucose, 10 g/L $NaNO_3$, 3 g/L KH_2PO_4, 2 g/L $MgSO_4 \cdot 7\ H_2O$, 2 g/L NaCl, 0.2 g/L $CaCl_2 \cdot 2H_2O$, 0.5 ml/L antifoam (sb2121) and 1 ml/L trace element solution 2. The trace element solution 2 contained 14.3 g/L $ZnSO_4 \cdot 7\ H_2O$, 2.5 g/L $CuSO_4 \cdot 5\ H_2O$, 0.5 g/L $NiCl_2 \cdot 6\ H_2O$, 7 g/L $MnCl_2 \cdot 2\ H_2O$ and 13.8 g/L $FeSO_4 \cdot 7\ H_2O$.

For the flux experiments 5 g/L of 1-^{13}C glucose was used as sole carbon source. The rest of the medium components were the same as described above. The same reactor was used in all other experiments, only the working volume was reduced to 200 mL for the flux experiment.

8.3.3 Cultivation conditions

Before spore harvesting with 0.01% w/w Tween-80 the pre-culture plates were incubated for 4-7 days at 30 ºC. Subsequently, 10^9 spores were inoculated in 3 L Braun bioreactors with a working volume of 2 L. The temperature was maintained constant at 30 ºC and the pH was controlled by automatic addition of 1 M $NaCO_3$ or 2 M HCl. Two Rushton four-blade disc turbines were used for homogeneous mixing. No baffles were used in the reactors thereby reducing the surface area available for biofilm formation. The initial aeration rate, agitation and pH were 0.2 vvm, 200 rpm and pH 2.5, respectively. They were gradually changed after germination (that takes place after approximately 15 hours) to 0.02 vvm, 700 rpm and pH 5, respectively. These parameters were kept constant throughout the rest of the batch cultivation. Air was used for sparging and the concentrations of oxygen and carbon dioxide in the exhaust gas were monitored by an acoustic gas analyser (Brüel & Kjær, Nærum, Denmark). The dissolved oxygen tension (DOT) was measured with an oxygen probe (Mettler Toledo sensors).

8.3.4 Sampling

Biomass samples were taken manually from the reactor. For dry weight measurements, a known cell culture volume was filtered through a pre-weighed nitrocellulose filter (pore size 45 µm, Pall Corporation). The filtrate was frozen immediately and later used for the determination of the concentrations of substrate and extracellular metabolites. The filter was washed with 0.9 % w/v NaCl, dried for 15 min in a microwave oven at 150 W and weighed again to determine the biomass concentration.

For determination of *in vitro* enzyme activities, flux analysis and microarray analysis, biomass samples were filtered through a nitrocellulose filter (pore size 45 µm, Pall Corporation) and washed with 0.9% w/v NaCl. The filter cake (± 1 g) was immediately frozen in liquid nitrogen and stored at -80 ºC.

8.3.5 Substrate and extracellular metabolite quantification

High-performance liquid chromatography was used for the quantification of extracellular sugars and organic acids. Glucose, acetate, pyruvate, citrate, ethanol, succinate, fumarate, malate, glycerol and oxalate concentrations were measured on an Aminex HPX-87H cationic exchange column (BioRad, Hercules, California) eluted at 60 ºC with 5 mM H_2SO_4 at a flow rate of 0.6 mL/min. Metabolites were detected with both a refractive index detector and a UV detector.

8.3.6 Analysis of *in vitro* enzyme activities

The frozen samples were crushed on liquid nitrogen with a mortar. The crushed biomass (0.5 g) was solved in 2 ml of extraction buffer containing 25 mM MES-NaOH, 0.1 mM EDTA, 0.1 mM DTT, 0.1 mM phenylmethylsulfonyl fluoride and 0.1 mM NaN_3. This solution was transferred to 2 mL FastPrep tubes containing 0.5 mL glass beads (0.75-1 mm). The FastPrep tubes were processed 3 times 10 s on a FastPrep FP120 Instrument (Savant Instruments, New York), at speed setting 5, with cooling on ice in between. After disruption, samples were centrifuged at 13,000 g at 4 ºC for 10-20 min, and the supernatants were analysed for enzyme activity.

Enzyme assays were performed at 30 °C using a HP8453 UV-visible light spectrophotometer. In order to test the linearity of the assays, the reactions were performed with 2-3 different dilutions of cell extract. The specific enzyme activities were expressed in micromoles $minute^{-1}$ $milligram^{-1}$ (U/mg). The amount of protein was determined by the Bradford method with bovine serum albumin as the standard (Bradford 1976). Four different enzyme activities were measured: citrate synthase (CIT), malate dehydrogenase (MDH), isocitrate lyase (ICL) and pyruvate carboxylase (PYC) as described by Meijer et al. (2007).

8.3.7 Determination of intracellular flux distribution

8.3.7.1 Sample preparation and derivatisation for flux analysis

35-50 mg of biomass was dissolved in 600 µl 6M HCl and kept overnight at 105 ºC for hydrolysis. The hydrolysate was then centrifuged for 5 minutes at 15,000 rpm and the supernatant was transferred into new vials. The supernatant was dried for 3 hours at 105 ºC and dissolved in 200 µl milliQ water.

In the mean time, the resin bed for solid phase extraction was prepared by weighing 1 g of Dowex cation exchange resin and mixed with 15 mL of 50 % w/w glycerol. One mL of resin solution was added to a syringe containing a frit on a SPE workstation. When the resin was settled at the bottom of the syringe, the excess of glycerol was drained and a second frit was added on top of the resin. Two mL of biomass hydrolysate was added on the SPE column. After the biomass had trickled through the column, 1 mL of 50 % v/v ethanol solution was added followed by 200 µl 1M NaOH solution, which washed the remaining unbound compounds off the column. Finally, the amino acids were eluted with 1 mL of solution containing 1 % v/v NaOH in saline (0.9 % w/v NaCl), ethanol and pyridine in a ratio of 9:5:1, respectively. The eluted amino acids were derivatised by two separate methods.

1) ethylchloroformate (ECF) derivatisation
2) dimethylformamide dimethylacetal (DMF/DMA) derivatisation

In the ECF derivatisation 50 µl ECF was added to 500 µl amino acid solution and mixed in two sequential rounds of 30 s. Next, 200 µl propylacetate was added and finally 50 µl 1M HCl. The upper organic layer was removed and analysed by GC-MS.

The DMF/DMA derivatisation required the addition of 300 µl 1M HCl to 500 µl amino acid solution followed by a 2-4 hours drying period at 105 ºC. 200 µl DMF/DMA and 200 µl acetonitrile were then added to dissolve the dried substance and mixed well for 30 s. This solution was kept at 100 ºC for 20 minutes and was subsequently transferred to -20 ºC for 10 minutes to ensure proper derivatisation. This solution was finally analysed by the GC-MS.

8.3.7.2 GC-MS analysis

GC-MS analysis was performed on an Agilent (Palo Alto, CA, USA) HP 6890 gas chromatograph coupled to a HP 5973 quadrupole mass selective detector in positive electron impact ionization (EI^+) operated at an electron energy of 70 eV. The GC was equipped with a 4.0 mm i.d. Siltek gooseneck splitless deactivated liner (Restek, Bellefonte, PA, USA), and a Supelco (Bellefonte, PA, US) SLB-5 MS column, 15 m, 0.25 mm i.d., 0.25 µm film. Helium of

a purity of 99.999% was used as carrier gas at a constant linear gas velocity of 35 cm/s. Transfer line temperature was 280 ºC, quadrupole temperature 150 ºC and MS source 200 ºC. The GC-MS system was controlled from Agilent MSD Chemstation v. D.01.02.16. For both methods (ECF and DMF/DMA) 1 µL sample was injected in the splitless (30 sec, split 1:20) mode at 200 ºC using a hot needle. The MS scan range was m/z 40-400 with 2.88 s/scan. To avoid sample carry-over the syringe was cleaned using five times 5 µL acetone, then five times 5 µL dichloromethane and finally 3 times rinsing with 3 µL sample.

8.3.7.2.1 ECF derivatives

The oven temperature was initially held at 75 °C for one min. Hereafter, the temperature was raised with a gradient of 40 °C/min until 165 °C, after which the temperature increase was 4 °C/min until 190 °C and followed by an increase of 40 °C/min up to 240 °C. Finally, the temperature was increased to 260 °C with a gradient of 4 °C/min and held constant for 4 minutes. The flow through the column was held constant at 1.3 mL He/min. The temperature of the inlet was 200 °C, of the interface 280 °C and of the quadrupole 105 °C.

8.3.7.2.2 DMF/DMA derivatives

Initially, the oven temperature was held at 60 °C for one min. Hereafter, the temperature was raised with a gradient of 20 °C/min until 130 °C, after which the temperature increase was 4 °C/min until 150 °C and followed by an increase of 40 °C/min up to 260°C. Next, this the temperature was held constant for 4.25 minutes. The flow through the column was held constant at 1 mL He/min. The temperature of the inlet was 230 °C, of the interface 270 °C and of the quadrupole 105 °C.

8.3.7.3 Metabolic network analysis

The flux analysis was based on the labelling patterns of derivatives of glucose and amino acids obtained from acid hydrolysis of the biomass. The mass spectra obtained from the GC-MS were converted into summed fractional labelling (SFL) patterns with the aid of the XCMS library operating within the R programming language environment (Smith et al. 2006). The SFL of a molecule or a fragment is identical to the sum of the fractional labelling of the carbon atoms contained in the molecule or fragment.

The metabolic network consisted of 52 reactions, 6 of them are reversible and 25 balanced metabolites (see supplementary material S2). The fluxes were determined using an in-house program code in Matlab V 7.0.4 (Grotkjær et al. 2005), which implements the metabolic network analysis framework from Wiechert (2001). The algorithm minimises the differences between measured fluxes and calculated fluxes by least square minimisation, as well as measured and calculated SFL using the non-linear Levenberg-Marqueartd algorithm.

Measured fluxes were weighed with a standard deviation of 10 %. Multiple initial guesses were generated with a genetic algorithm to verify the existence of a global minimum. A sensitivity analysis was done by adding 10 % of Gaussian noise to the measured SFL data in 50 simulations followed by calculating the standard deviation of the estimated fluxes.

8.3.8 Analysis of transcription data

8.3.8.1 Total RNA extraction

Total RNA was extracted from 40-50 mg frozen mycelia. The mycelia were transferred to pre-cooled 2 ml Eppendorf tubes containing steel balls (2x ∅2mm, 1x ∅5mm) and shaken in a Mixer Mill for 10 minutes at 4 °C. The resulting powder was used for total RNA extraction using the Qiagen RNA easy kit, according to the protocol for isolation of total RNA from plant and fungi.

The quality of the extracted total RNA of each sample was analysed using the Bioanalyser 2100 (Agilent technologies Inc., Santa Clara, CA, USA) and the quantity of the extracted total RNA was determined spectrophotometrically (Amersham Pharmacia Biotech, GE Healthcare Biosciences AB, Uppsala, Sweden). The total RNA was stored at -80 °C until further processing.

8.3.8.2 Biotin labelled cRNA and microarray processing

5 μg of total RNA was used for making 15 μg of fragmented biotin labelled cRNA that was hybridised to the 3AspergDTU gene chip (Affymetrix) according to the Affymetrix GeneChip Expression Analysis Technical Manual (Affymetrix 2007). The cRNA quality and quantity were analysed in the same way as the total RNA described above. A GeneChip fluidics Station FS-400 and a GeneChip scanner were used for hybridisation and scanning of the microarrays. The scanned probe array images were converted to .CEL files using the GeneChip Operating Software (Affymetrix). Affymetrix CEL-data files were pre-processed using the statistical language and environment R (R Development Core Team 2007). The probe intensities were normalised for background using the robust multiarray average (RMA) method (Irizarry et al. 2003) only using perfect match (PM) probes. Subsequently, normalisation was performed using the quantiles algorithm (Bolstad et al. 2003). Gene expression values were calculated from the PM probes with the medianpolish summary method (Irizarry et al. 2003). All statistical pre-processing methods were used by invoking them through the Affymetrix package (Gautier et al. 2004).

Statistical analysis was applied to determine genes subject to differential transcriptional regulation. The limma package (Smyth 2004) was used for all statistical analyses. Moderated t-tests between the sets of experiments were used for pair-wise comparisons. Empirical Bayesian statistics were used to moderate the standard errors within each gene and Benjamini-Hochberg's method (Benjamini and Hochberg 1995) was used to adjust for multi-testing. A cut-off value of adjusted $p<0.05$ was used for statistical significance. The significantly expressed genes can be found in supplementary material S1.

8.4 Results and Discussion

Because most living cells are capable of using a large variety of compounds as carbon, energy and nitrogen sources, they contain complementary pathways that serve similar functions when they operate at the same time. The glyoxylate bypass can be seen as a bypass pathway of the TCA cycle, because the two pathways share a number of similar reactions. In prokaryotes these two pathways are both present in the cytosol, while in eukaryotes compartmentalisation separates them. The TCA cycle is located in the mitochondria, in contrast to the glyoxylate bypass that operates either in the cytosol or in microbodies. Although these pathways follow the same reactions they serve very different purposes. The TCA cycle serves as an oxidizing pathway where pyruvate is converted to carbon dioxide, whereas the glyoxylate bypass has the purpose of synthesizing precursor metabolites anaplerotically, e.g. net production of oxaloacetate from acetyl-CoA. The glyoxylate bypass basically consists of only two enzymes: isocitrate lyase (ICL, EC 4.1.3.1) and malate synthase (MS, EC 2.3.3.9) (Kornberg and Krebs 1957). ICL catalyses the cleavage of isocitrate to succinate and glyoxylate and hence, isocitrate is a branch point metabolite between the TCA cycle and the glyoxylate bypass. MS catalyses the condensation of acetyl-CoA and glyoxylate to form malate. This anaplerotic reaction enables a net synthesis of C_4 carboxylic acids from a carbon source of C_2 compounds like acetate or fatty acid derived acetyl-CoA (Kornberg 1966). In the present study the *icl* gene was over-expressed in order to stimulate the glyoxylate bypass flux and thereby produce more succinate and malate in *A. niger*.

8.4.1 Comparison WT and ICL over-expression strains

The wild-type strain and the ICL over-expression mutant were grown in batch cultures with glucose as carbon source. Metabolic fluxes were determined, as well as the global transcription response using DNA microarrays. Based on the data, 1,511 significantly changed genes were identified using a moderated t-test. The list of significantly changed genes is given in supplementary material S1.

The metabolic flux analysis showed that in the ICL over-expression strain the flux towards the PPP is reduced (Figure 8.1). The total flux through the glycolysis was increased. At the branch point towards serine synthesis a higher flux towards serine was measured in the ICL over-expression strain compared to the WT strain. Figure 8.1 is a simplified representation of the stoichiometric metabolic model. The complete model can be found in supplementary

material S2. The microarray data support the decreased flux in the PPP since the genes in the PPP were significantly down-regulated. Furthermore, genes encoding glycolytic enzymes were up-regulated whereas gluconeogenic genes were down-regulated, supporting the increased glycolytic flux (Figure 8.1). Glycolysis is known to be important for citrate production since most of the citrate is produced via this pathway (Cleland and Johnsen 1954; Martin and Wilsen 1951; Legisa and Mattey 1986). Only a slight increase in citrate yield was found in the ICL over-expression strain (0.05 C-mol/C-mol glucose in the WT and 0.14 C-mol/C-mol glucose in the ICL over-expression strain), indicating that the over-expression changed the flux distribution (Table 8.2). Looking at the fermentation profiles a higher citrate concentration was measured during the exponential growth phase (Figure 8.2).

Table 8.2 Biomass and organic acid yields expressed in C-mol/C-mol glucose consumed

	Biomass	Citric acid	Oxalic acid	Succinic acid	Pyruvic acid	Glycerol	Fumaric acid
WT	0.37	0.05	0.016	0.003	0.0012	0.0032	0
WT + mal	0.23	0.08	0.030	0	0	0.0032	0
ICL	0.22	0.14	0.000	0	0.0033	0	0.058
ICL+mal	0.58	0.09	0.000	0	0.0025	0.0059	0.003

WT = wild-type N402 strain, WT + mal = N402 strain with addition of 50 mM malonate, ICL = isocitrate lyase over-expression in the AB4.1 strain, ICL + mal = isocitrate lyase over-expression in the AB4.1 strain with addition of 50 mM malonate

For the TCA cycle a similar positive correlation between transcription and flux was not found. The flux through the TCA cycle was lower in the ICL over-expression strain compared to the wild-type strain, while expression of several of the TCA cycle genes was up-regulated. Over-expression of the *icl* was not confirmed by the gene expression data. The expression levels of *icl* and *ms* were unchanged (fold change is 1.1). This is likely to be an artefact as a higher ICL enzyme activity was observed in the over-expression strain (Table 8.3).

The fumarate reductase was found to be down-regulated, but nevertheless no succinate production was observed in the ICL over-expression strain (Table 8.2). Succinate production could result from up-regulation of the oxidative part of the TCA cycle and down-regulation of the gene encoding fumarate reductase. However, instead of producing succinate and malate, the estimated fluxes and measurements of the extracellular metabolite concentrations indicated that fumarate was over-produced. This suggests that instead of up-regulating the glyoxylate bypass by over-expressing the *icl* gene, the oxidative part of the TCA cycle is up-regulated, creating a bottleneck in the TCA cycle, leading to fumarate production.

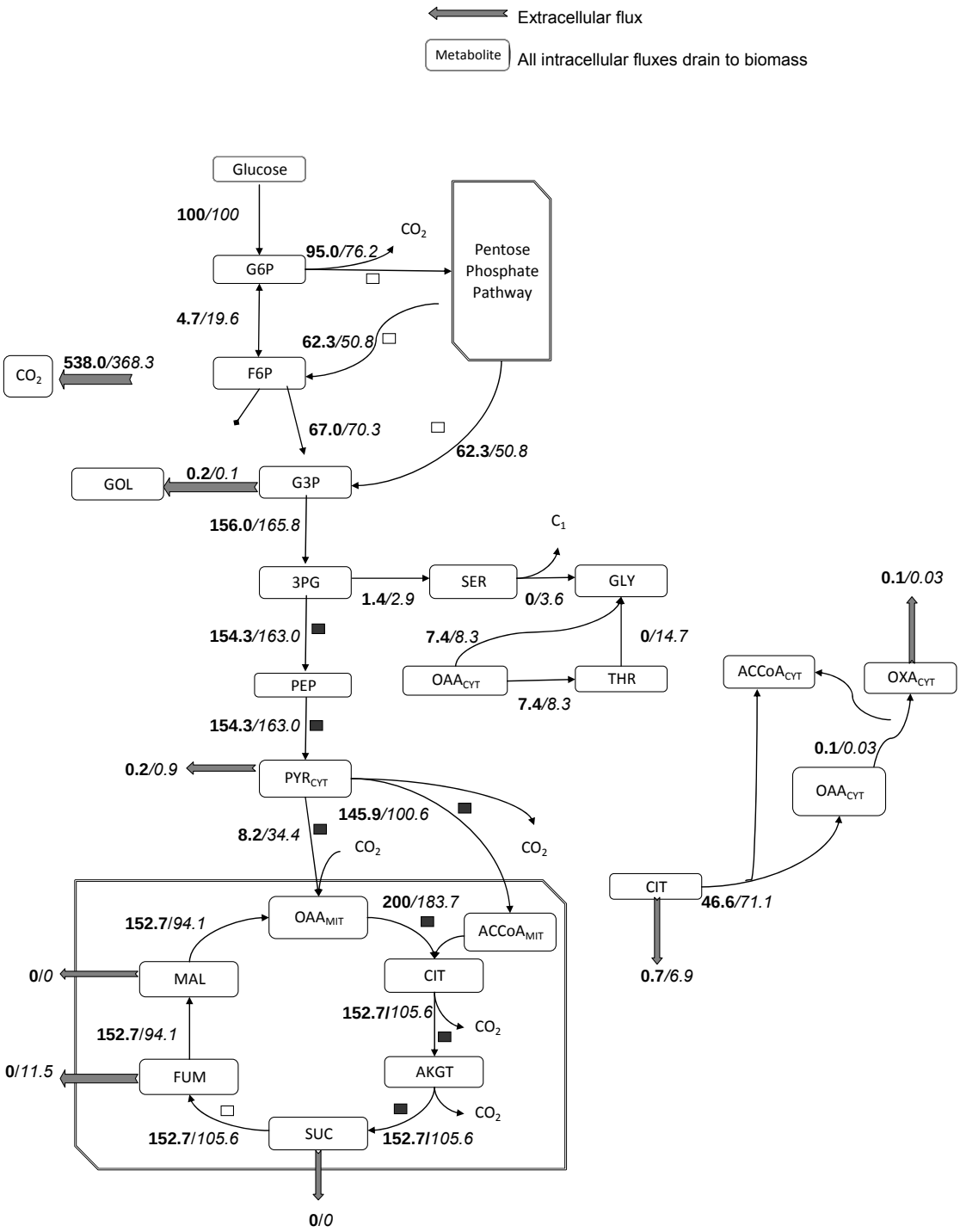

Figure 8.1 A simplified flux distribution model of the N402 and ICL over-expression strain (complete model see S2). The first number is the flux in the N402 strain and the second number (italic) is the flux in the ICL over-expression strain. G6P = glucose 6-phosphate, F6P = fructose 6-phosphate, GOL = glycerol, G3P = glyceraldehyde 3-phosphate, PEP = phosphoenolpyruvate, PYRcyt = cytosolic pyruvate, SER = serine, GLY = glycine, THR = threonine, OAAcyt = cytosolic oxaloacetate, CIT = citrate, ACCoAcyt = cytosolic acetyl-CoA, OXAcyt = cytosolic oxalate, ACCoAmit = mitochondrial acetyl-CoA, OAAcyt = mitochondrial oxaloacetate, AkGT = alfa-keto-glutarate, SUC = succinate, FUM = fumarate, MAL = malate.

■ = up-regulation of gene expression levels, □ = down-regulation of gene expression levels. Unmarked reactions did not have any significant change in gene expression.

In comparison to the WT, the ICL over-expression strain produced more fumarate and pyruvate, and less oxalate and glycerol (Figure 8.1 and Table 8.2) indicating a clear shift of flux distribution in the TCA cycle.

The *in vitro* enzyme activities measured in the ICL over-expression strain differed from the WT (Table 8.3). First, measurement of the ICL activity confirmed that the gene was over-expressed in the ICL strain as the activity was higher. Although the MDH activity was reduced, no malate or succinate was produced. The PYC activity was increased in the ICL over-expression strain, which corresponds with the increased gene expression and elevated flux through this pathway. The expression of the gene encoding pyruvate dehydrogenase was also up-regulated, but this reaction showed a decreased flux in the ICL over-expression strain. Comparing the pyruvate carboxylase and pyruvate dehydrogenase flux at the pyruvate branch point in the ICL over-expression strain showed that the pyruvate dehydrogenase flux was higher than the carboxylase flux. Compared to the WT strain the ratio between dehydrogenase and carboxylase flux was found to be changed, but the dehydrogenase flux was still most dominant. This suggests that the oxidative TCA cycle is active, as this pathway requires both oxaloacetate and acetyl-CoA. The reduced flux through the TCA cycle in the ICL over-expression strain may be caused by a feedback regulation mechanism exerted at the level of the fumarase reaction that converts fumarate to malate.

A slightly higher citrate production in the ICL over-expression strain is likely to be caused by an increased formation of oxaloacetate. The rate of the reaction catalysed by citrate synthase is controlled *in vivo* by the oxaloacetate concentration. Oxaloacetate first binds to the enzyme, followed by binding of acetyl-CoA (Kubicek and Rohr 1980; Papagianni 2007). Therefore, if more oxaloacetate is produced the production of citrate will also increase.

The measured gene expression data between the WT and ICL over-expression strain showed also pathway regulations outside the central carbon metabolism. The gene expression changes were mapped against the stoichiometric model developed by Andersen et al. (2008). These analyses showed that the protein degradation pathway was significantly down-regulated, whereas the purine and pyrimidine pathways were up-regulated in the ICL over-expression strain. Purines and pyrimidines make up the two groups of nitrogenous bases, that are a crucial part of both deoxyribonucleotides and ribonucleotides. Aside from DNA and RNA, purines are biochemically significant components in a number of other important cellular metabolites such as ATP, GTP, cyclic AMP, NADH, and coenzyme A.

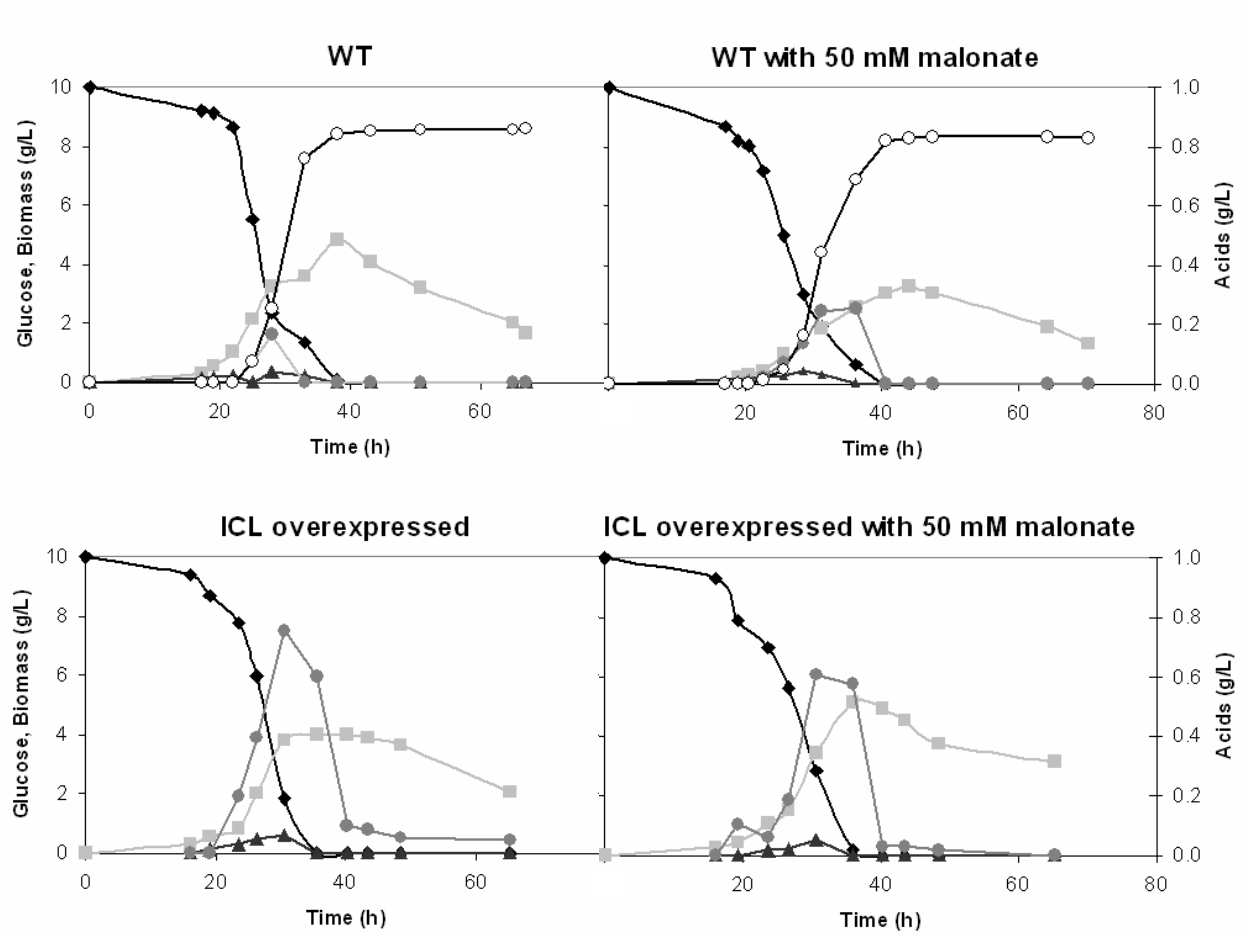

Figure 8.2 Fermentation profiles of the wild-type N402 strain and ICL over-expression strain with and without 50 mM malonate addition in glucose batches. ♦ = glucose, ■ = biomass, ● = citrate, ▲ = glycerol, ○ = oxalate

Since major changes were detected in the PPP and TCA cycle, which are pathways that are highly linked to redox reactions, it seems that the redox balance has been changed in the ICL over-expression strain. Fuhrer et al. (1980) showed that a remarkable constancy was found in the catabolic reduction charge (NADH/ (NADH + NAD)) and the anabolic reduction charge (NADPH/ (NADPH + NADP)) in *A. niger* grown at non-limited growth conditions. Furthermore, they observed that the ratio (NAD + NADH)/(NADP + NADPH) was constant over the whole culture time. In the growth phase of *A. niger*, the catabolic reduction charge has been found to be relatively high (0.10) and during citric acid accumulation this value was even higher. This may reflect the metabolic situation of growth-restricting conditions necessary for acidogenesis (Kubicek and Rohr 1977). Excessive NADH production under acidogenic conditions also requires high alternative oxidase activity (AOX) to maintain the redox balance and to limit the amount of ATP produced (Ruijter et al. 2002). Since a shift in organic acid production was detected in the ICL over-expression strain, a shift in the

catabolic reduction charge is expected. This shift may result in an up-regulation of the purine and pyrimidine pathways. It has been proven that the levels of pyridine nucleotides are highly interdependent and their well-balanced ratios are necessary for optimal operation of the metabolic pathways (Fuhrer et al. 1980), indicating that in the ICL over-expression strain a new physiological state was achieved. It was also observed that the expression levels of genes involved in nitrogen metabolism were up-regulated, which can be linked to the need of nitrogen incorporation in the pyridine nucleotides. Also gene expression levels of other pathways requiring nitrogen were up-regulated like pathways leading to several amino acids and vitamins, e.g. the biotin pathway. These pathways mainly lead to biomass formation, however, in our experiments the biomass yield was not increased in the ICL over-expression strain. This indicates that up-regulation does not result in increased fluxes through these pathways.

Table 8.3 Enzyme activities in U/mg measured in different *A. niger* strains

	ICL	MDH	CIT	PYC
WT	0.26	0.016	0.10	0.013
WT + mal	0.1	0.012	0.07	0.031
ICL	0.38	0.009	0.14	0.023
ICL+ mal	0.47	0.003	0.06	0.029

WT = wild-type N402 strain, WT + mal = N402 strain with addition of 50 mM malonate, ICL = isocitrate lyase over-expression in the AB4.1 strain, ICL + mal = isocitrate lyase over-expression in the AB4.1 strain with addition of 50 mM malonate.
ICL = isocitrate lyase, MDH = malate dehydrogenase, CIT = citrate synthase, PYC = pyruvate carboxylase

8.4.2 Effect of malonate addition for SDH inhibition

Malonate is known to be a competitive inhibitor of the succinate dehydrogenase. In rat and mammalian cells its inhibitory characteristics have been demonstrated (K_i values of 0.68 and 0.018 mM, respectively) (Armson et al. 1995; Hatefi and Stiggall 1976). Since the enzyme assay for SDH was not sufficiently sensitive for analysis in the cell extracts of *A. niger* (most likely due to instability of the co-factor FAD) the inhibition constant of malonate on SDH could not be determined. Instead several concentrations of malonate were tested and the effect of malonate on growth was assessed (data not shown). The fact that *A. niger* is unable to grow anaerobically suggests that SDH is an essential enzyme required for cellular propagation.

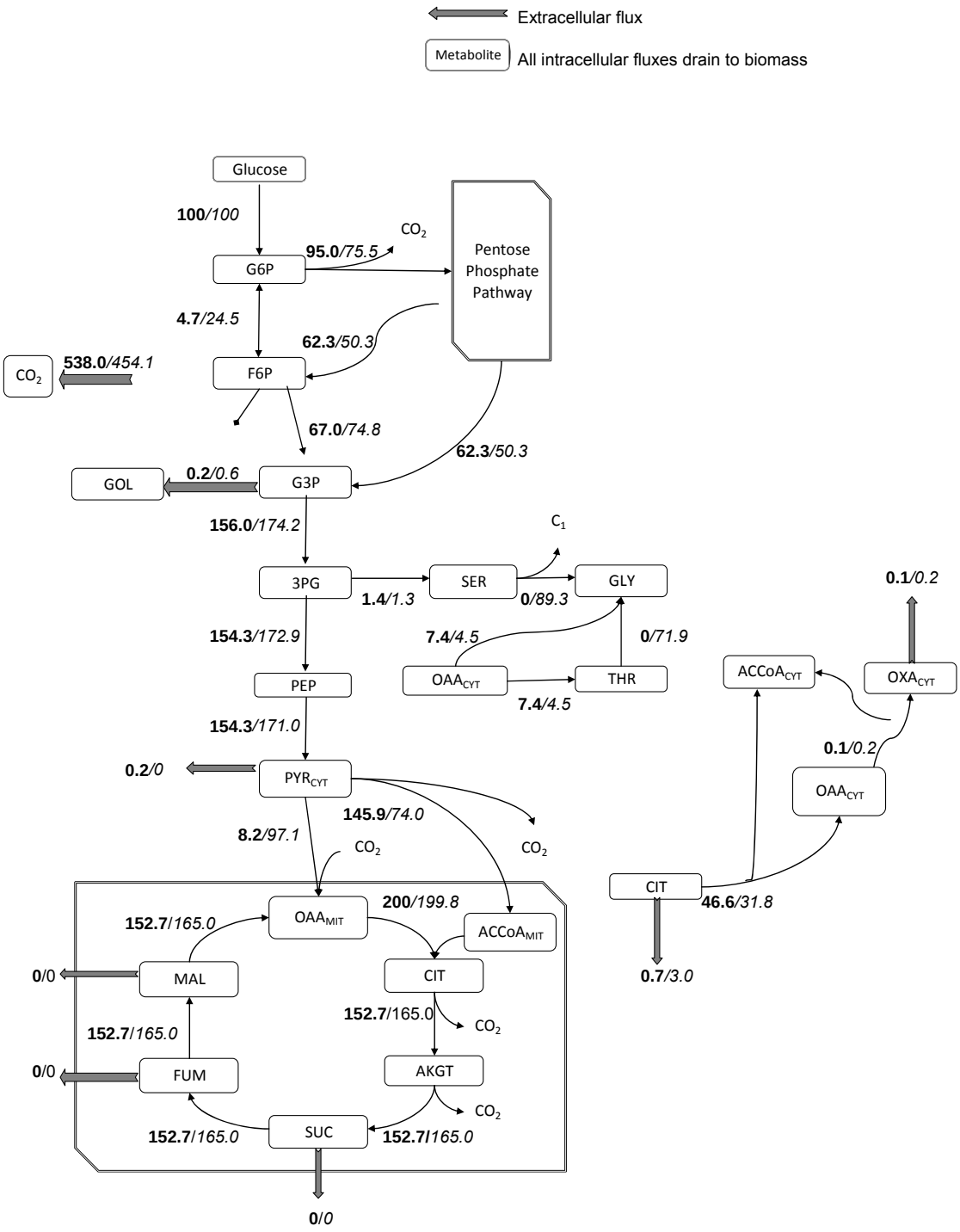

Figure 8.3 A simplified flux distribution model of the wild-type N402 strain with and without 50 mM malonate addition (complete model see S2). The first number is the flux in the N402 strain and the second number (italic) is the flux in the N402 strain with 50 mM malonate added. G6P = glucose 6-phosphate, F6P = fructose 6-phosphate, GOL = glycerol, G3P = glyceraldehyde 3-phosphate, PEP = phosphoenolpyruvate, PYR_{cyt} = cytosolic pyruvate, SER = serine, GLY = glycine, THR = threonine, OAA_{cyt} = cytosolic oxaloacetate, CIT = citrate, $ACCoA_{cyt}$ = cytosolic acetyl-CoA, OXA_{cyt} = cytosolic oxalate, $ACCoA_{mit}$ = mitochondrial acetyl-CoA, OAA_{cyt} = mitochondrial oxaloacetate, AkGT = alfa-keto-glutarate, SUC = succinate, FUM = fumarate, MAL = malate.

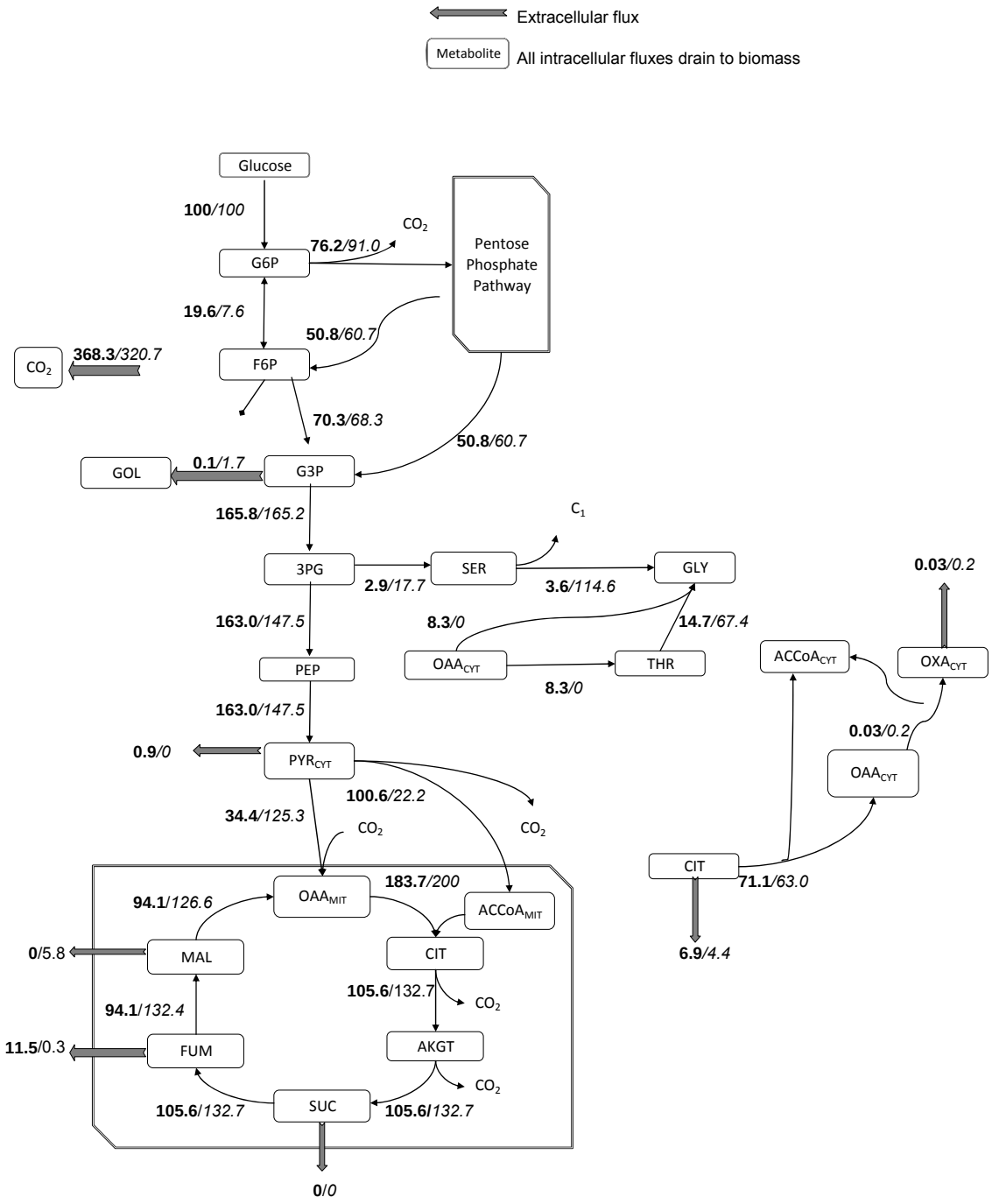

Figure 8.4 A simplified flux distribution model of the ICL over-expression strain with and without 50 mM malonate addition (complete model see S2). The first number is the flux in the ICL over-expression strain and the second number (italic) is the flux in the ICL over-expression strain with 50 mM malonate added. G6P = glucose 6-phosphate, F6P = fructose 6-phosphate, GOL = glycerol, G3P = glyceraldehyde 3-phosphate, PEP = phosphoenolpyruvate, PYR_{cyt} = cytosolic pyruvate, SER = serine, GLY = glycine, THR = threonine, OAA_{cyt} = cytosolic oxaloacetate, CIT = citrate, $ACCoA_{cyt}$ = cytosolic acetyl-CoA, OXA_{cyt} = cytosolic oxalate, $ACCoA_{mit}$ = mitochondrial acetyl-CoA, OAA_{cyt} = mitochondrial oxaloacetate, AkGT = alfa-keto-glutarate, SUC = succinate, FUM = fumarate, MAL = malate.

It was expected that inhibiting the SDH with malonate would inhibit the growth of *A. niger*. Indeed, it was observed that with increasing malonate concentrations the growth was limited. A malonate concentration of 50 mM was found to be suitable for partial inhibition of SDH without having a considerable effect on the growth of *A. niger*. This concentration is much higher than the K_i values in rat and mammals, suggesting that there is some inhibition of the SDH enzyme. In order to be sure that malonate was reaching the SDH inside the cell, the uptake of malonate was verified by measurement of the intracellular levels of malonate. Hereby the effect of inhibition of SDH in the WT and the ICL over-expression strain could be evaluated. The effect between the strains was found to differ significantly.

Malonate addition affected the fluxes in the PPP and the fluxes towards amino acids (Figure 8.3 and 8.4). When malonate was added in the WT strain the flux through the PPP was reduced and the flux towards amino acids was unchanged. In the ICL over-expression strain malonate addition caused an increase in the PPP flux. It was remarkable that in the ICL over-expression strain the flux towards amino acids was already higher compared to the WT strain. This flux increased even more when malonate was added. This increase in amino acid synthesis and PPP flux was accompanied by a significantly higher biomass yield of 0.58 C-mol biomass/C-mol glucose in the ICL over-expression strain when malonate was added, compared to 0.22 if no malonate was added (Table 8.2).

When malonate was added, the flux towards glycerol was increased while the extracellular pyruvate flux was decreased in both the WT and the ICL over-expression strain. This indicates that malonate addition regulates cell metabolism not only in the TCA cycle, but also in glycolysis.

At the pyruvate node, the flux ratio between pyruvate carboxylase (PYC) and pyruvate dehydrogenase (PDH) was changed. When malonate was added the flux through pyruvate carboxylase increased, and the flux ratio of PDH over PYC changed from 18 to 0.8 in the WT strain and from 3 to 0.2 in the ICL over-expression strain. This may indicate an increase in flux towards the reductive TCA cycle.

In the WT strain, the flux through the TCA was not significantly changed by adding malonate and the extracellular organic acid profiles were also not significantly changed, except for citrate and oxalate (Figure 8.3 and Table 8.2). The increase in citrate flux upon addition of malonate did not relate to the 1.5 fold decrease in enzyme activity (Figure 8.3 and Table 8.3). In the ICL over-expression strain, the malonate addition did not lead to an increased flux towards citrate, rather a decreased flux (Figure 8.4). When *icl* was over-expressed an almost

20 times increase in fumarate yield was detected (Table 8.2). This might be caused by a limitation in the conversion from fumarate to malate. When malonate was added, the flux control was shifted due to inhibition of the SDH activity. Therefore, instead of fumarate more malate was produced. The malate was most likely produced in the cytosol before it was shuttled towards the extracellular medium or towards the mitochondria in exchange for citrate. Since the citrate production was reduced the capacity of shuttling malate towards the mitochondria was decreased leading to more malate excretion into the medium.

The difference between the effect of malonate on the WT strain and ICL over-expression strain may be caused by a shift in flux control found in the metabolism. A strong flux control at the level of fumarase in the TCA cycle, caused by *icl* over-expression, was not present in the WT strain. The effect of SDH inhibition by malonate in the WT strain was therefore not effecting the fumarate and malate production, but instead increased the citrate and oxalate production.

8.5 Conclusion

Over-expression of the *icl* gene was hypothesised to up-regulate the glyoxylate bypass resulting in production of more succinate and malate. The glyoxylate bypass is known to be a parallel pathway to the TCA cycle and by up-regulation of the glyoxylate bypass the flux through the TCA cycle was expected to decrease. Even though flux analysis showed a decreased flux through the TCA cycle, more fumarate was produced instead of malate and succinate. This change in organic acid profiles was caused by regulation within the TCA cycle and not by the glyoxylate bypass.

A second method for stimulating the glyoxylate bypass was investigated. Malonate inhibits the SDH, which should lead to succinate production. The addition of malonate showed different cellular effects in both the WT and ICL over-expression strain. In the WT, the malonate addition resulted in more citrate and oxalate production, while in the ICL over-expression strain more malate was produced.

The combination of flux, gene expression, enzyme activity and metabolite production data gave a better understanding of the physiological behaviour of the cells and resulted in some unexpected outcomes. The hypothesized increase in glyoxylate bypass by over-expression of *icl* and its influence of succinate and malate showed distinct results. This shows that there is a coordinated regulation of fluxes through the glycolysis, the TCA cycle and different anapleorotic reactions, and redirection of the carbon fluxes therefore requires building better models for the overall regulation in these pathways.

8.6 References

Affymetrix 2007. GeneChip expression analysis technical manual - with specific protocols for using the GeneChip hybridisation, wash, and stain kit. *P/N 702232 Rev 2*.

Andersen MR, Vongsangnak W, Panagiotou G, Salazar MP, Lehmann L and Nielsen J 2008. A tri-species *Aspergillus* microarray: Comparative transcriptomics of three *Aspergillus* species. *PNAS* **105**:4387-4392.

Armson A, Grubb WB and Mendis AHW 1995. The effect of electron-transport (Et) inhibitors and thiabendazole on the fumarate reductase (FR) and succinate dehydrogenase (SDH) of *Strongyloides ratti* infective (L3) larvae. *International Journal for Parasitology* **25** (2):261-263.

Baker SE 2006. *Aspergillus niger* genomics: Past, present and into the future. *Medical Mycology* **44**:S17-S21.

Benjamini Y and Hochberg Y 1995. Controlling the false discovery rate - A practical and powerful approach to multiple testing. *Journal of the Royal Statistical Society Series B-Methodological* **57** (1):289-300.

Bolstad BM, Irizarry RA, Astrand M and Speed TP 2003. A comparison of normalisation methods for high density oligonucleotide array data based on variance and bias. *Bioinformatics* **19** (2):185-193.

Bradford MM 1976. Rapid and sensitive method for quantitation of microgram quantities of protein utilizing principle of protein-dye binding. *Analytical Biochemistry* **72** (1-2):248-254.

Christensen B and Nielsen J 1999. Isotopomer analysis using GC-MS. *Metabolic Engineering* **1** (4):282-290.

Cleland WW and Johnson MJ 1954. Tracer experiments on the mechanism of citric acid formation by *Aspergillus niger*. *Journal of Biological Chemistry* **208** (2):679-689.

Führer L, Kubicek CP and Rohr M 1980. Pyridine nucleotide levels and ratios in *Aspergillus niger*. *Canadian Jounal of Microbiology* **26** (405):411.

Gautier L, Cope L, Bolstad BM and Irizarry RA 2004. Affy - analysis of Affymetrix GeneChip data at the probe level. *Bioinformatics* **20** (3):307-315.

Grotkjaer T, Christakopoulos P, Nielsen J and Olsson L 2005. Comparative metabolic network analysis of two xylose fermenting recombinant *Saccharomyces cerevisiae* strains. *Metabolic Engineering* **7** (5-6):437-444.

Hatefi Y and Stiggall DL 1976. Metal-containing flavoprotein dehydrogenase. In *"The enzymes",* 3rd Ed , editors Boyer P D **13**:175-297.

Irizarry RA, Hobbs B, Collin F, Beazer-Barclay YD, Antonellis KJ, Scherf U and Speed TP 2003. Exploration, normalisation, and summaries of high density oligonucleotide array probe level data. *Biostatistics* **4** (2):249-264.

Kornberg HL and Krebs HA 1957. Synthesis of cell constituents from C2-units by a modified tricarboxylic acid cycle. *Nature* **179** (4568):988-991.

Kornberg HL 1966. Role and control of glyoxylate cycle in *Escherichia coli* - First Colworth Medal Lecture. *Biochemical Journal* **99** (1):1-11.

Kristiansen B, Mattey M and Linden J 1999. Biochemistry of cirtic acid accumulation by *A. niger* . In: Kristiansen B , Mattey M , Linden J , editors *Citric acid biotechnology* London, PA: Taylor & Francis.

Kubicek CP and Rohr M 1977. Influence of manganese on enzyme synthesis and citric acid accumulation in *Aspergillus niger*. *European Journal of Applied Microbiology* **4** (3):167-175.

Kubicek CP and Rohr M 1980. Regulation of citrate synthase from the citric acid-accumulating fungus, *Aspergillus niger*. *Biochimica et Biophysica Acta* **615** (2):449-457.

Legisa M and Mattey M 1986. Glycerol synthesis by *Aspergillus niger* under citric acid accumulating conditions. *Enzyme and Microbial Technology* **8** (10):607-609.

Martin SM and Wilson PW 1951. Uptake of C^{14}-O_2 by *Aspergillus niger* in the formation of citric acid. *Archives of Biochemistry and Biophysics* **32** (1):150-157.

Meijer S, Panagiotou G, Olsson L and Nielsen J 2007. Physiological characterisation of xylose metabolism in *Aspergillus niger* under oxygen-limited conditions. *Biotechnology and Bioengineering* **98** (2):462-475.

Nielsen ML, Albertsen L, Lettier G, Nielsen JB and Mortensen UH 2006. Efficient PCR-based gene targeting with a recyclable marker for *Aspergillus nidulans*. *Fungal Genetics and Biology* **43** (1):54-64.

Papagianni M 2007. Advances in citric acid fermentation by *Aspergillus niger*: Biochemical aspects, membrane transport and modelling. *Biotechnology Advances* **25** (3):244-263.

Pel HJ, de Winde JH, Archer DB, Dyer PS, Hofmann G, Schaap PJ, Turner G, de Vries RP, Albang R, Albermann K, Andersen MR, Bendtsen JD, Benen JAE, van den Berg M, Breestraat S, Caddick MX, Contreras R, Cornell M, Coutinho PM, Danchin EGJ, Debets AJM, Dekker P, van Dijck PWM, van Dijk A, Dijkhuizen L, Driessen AJM, d'Enfert C, Geysens S, Goosen C, Groot GSP, de Groot PWJ, Guillemette T, Henrissat B, Herweijer M, van den Hombergh

JPTW, van den Hondel CAMJ, van der Heijden RTJM, van der Kaaij RM, Klis FM, Kools HJ, Kubicek CP, van Kuyk PA, Lauber J, Lu X, van der Maarel MJEC, Meulenberg R, Menke H, Mortimer MA, Nielsen J, Oliver SG, Olsthoorn M, Pal K, van Peij NNME, Ram AFJ, Rinas U, Roubos JA, Sagt CMJ, Schmoll M, Sun JB, Ussery D, Varga J, Vervecken W, de Vondervoort PJJV, Wedler H, Wosten HAB, Zeng AP, van Ooyen AJJ, Visser J and Stam H 2007. Genome sequencing and analysis of the versatile cell factory *Aspergillus niger* CBS 513.88. *Nature Biotechnology* **25** (2):221-231.

R Development Core Team 2007. R: A language and environment for statistical computing. *(R Foundation for Statistical Computing, Vienna,Austria), http://www R-project org* .

Ruijter GJG, Kubicek CP and Visser J 2002. Production of organic acids by fungi. Source: In: *The Mycota, vol X Industrial applications* / K Esser, J W Bennet (ed) - Berlin, Germany : Springer :213-230.

Schmidt K, Carlsen M, Nielsen J and Villadsen J 1997. Modelling isotopomer distributions in biochemical networks using isotopomer mapping matrices. *Biotechnology and Bioengineering* **55**:831-840.

Smith CA, Want EJ, O'Maille G, Abagyan R and Siuzdak G 2006. XCMS: Processing mass spectrometry data for metabolite profiling using nonlinear peak alignment, matching, and identification. *Analytical Chemistry* **78** (3):779-787.

Smyth GK 2004. Linear models and empirical Bayes methods for assessing differential expression in microarray experiments. *Statistical Applications in Genetic and Molecular Biology* **3** (Article 3).

Vanhartingsveldt W, Mattern IE, Vanzeijl CMJ, Pouwels PH and Vandenhondel CAMJ 1987. Development of a homologous transformation system for *Aspergillus niger* based on the *pyrG* gene. *Molecular & General Genetics* **206** (1):71-75.

Werpy T and Petersen G 2004. Top value added chemicals from biomass. *http://www nrel gov/docs/fy04osti/35523 pdf* (27-03-2008).

Wiechert W 2001. C^{13} metabolic flux analysis. *Metabolic Engineering* **3** (3):195-206.

Zupke G and Stephanopoulos GN 1994. Modelling of isotope distributions and intracellular fluxes in metabolic networks using atom mapping matrices. *Biotechnology Progress* **10**:489-498.

Chapter 9

Creation of a cytosolic reductive TCA cycle in *Aspergillus niger* – Heterologous gene insertion of fumarase and fumarate reductase

Meijer S., Otero J., Olivares R., Andersen MR., Olsson L. and Nielsen J.
Biocentrum-DTU, Center for Microbial Biotechnology, Denmark

Aimed at *Biotechnology and Bioengineering*

9.1 Abstract

Metabolic engineering strategies were applied to shift the metabolism of *A. niger* towards more reduced organic acids like malate, fumarate and succinate instead of the citrate that is natively produced. The wild-type strain N402 and a strain unable to produce gluconic acid and oxalic acid (NW185) were compared. Additionally, the effect of the insertion of fumarase (*fum*) and fumarate reductase (*frds*) in the cytosol of both the N402 and NW185 strain was determined.
Although a major shift in glycolysis between the strains N402 and NW185 has been detected earlier, in this study only minor differences were observed in the organic acid profiles, whereas the main difference was found in anabolism, showing clear differences in energy and redox requirements.
The insertion of *fum* and *frds* in the cytosol of both strains led to major changes in the flux distribution and a significant increase in more reduced organic acids like malate, fumarate and succinate.

Keywords: NW185 strain, fumarase, fumarate reductase, redox state, organic acids

9.2 Introduction

Organic acids are valuable compounds that are widely used in the industry. They form important precursor molecules from which a lot of chemical compounds may be produced (Werpy and Petersen 2004). Some organic acids are used directly, e.g. in the food industry. In the last decades there has been a need to produce these organic acids more efficiently and environmentally friendly. With the increasing oil prices there is an increasing focus on developing sustainable biotech processes that can compete with traditional chemical synthesis. An example of an organic acid produced by a biological system is citrate, which is produced by fermentation of the filamentous fungus *Aspergillus niger*. This is an ancient production process that reaches high final product titers and yields, even competing with the natural extraction of citrate from lemons. More than 75 % of the citrate production is produced by biotechnological means (Kristiansen et al. 1998).

An economic forecast from 2004 predicted that also other organic acids like malic acid, fumaric acid and succinic acid are compounds that have high potential for biological production (Werpy and Petersen 2004). Ever since, there has been an interest in developing good hosts for production of these organic acids. Most attempts have been made in the model organism *E. coli* as *E. coli* is genetically easy to manipulate (Millard et al. 1996; Vermuri et al. 2002; Lin et al. 2005). Several groups have tried to design new production strategies in yeast and filamentous fungi. Arikawa et al. (1999) have studied the effect of single and multiple TCA cycle gene deletions on succinate production in *S. cerevisiae*. They observed that succinate was mainly formed by the cytosolic reactions of pyruvate carboxylase and malate dehydrogenase and the mitochondrial reactions of fumarase and fumarate reductase (reductive TCA cycle). In a medium optimisation study for improved succinate yields, it has been found that *P. simplisicum* has an organic acid transporter that favours succinate transport (Gallmetzer et al. 2002). This transporter is similar to the citrate transporter in *A. niger*, both resulting in an energy spilling process. *A. flavus* also produces succinate as a by-product in the malate production process, but due to its mycotoxin formation it is unsuitable for industrial applications.

In the present study, the focus was on organic acid production in the filamentous fungus *A. niger*. The proposed strategy was to test several strains under defined conditions and to assess the effect of different genetic changes on the transcript profiles and flux patterns in relation to organic acid production. We investigated a wild-type (WT) strain and a strain that is unable to produce gluconic acid and oxalic acid (NW185). A second strategy was to insert two genes, fumarate reductase from

S. cerevisiae (*frds*) and fumarase from *R. oryzae* (*fum*), for cytosol expression in *A. niger* (Enomoto et al. 2002; Friedberg et al. 1995). These genes are believed to form a reductive TCA cycle in the cytosol that should be able to produce cytosolic fumarate and succinate. In the native genome these enzymes are expressed in the mitochondria (Andersen et al. 2008). Our physiological studies have not indicated an active reductive TCA pathway.

A. niger has evolved to produce citrate. Firstly, malate is produced in the cytosol and then exchanged for mitochondrial citrate through an antiport mechanism over the mitochondrial membrane (Kubicek et al. 1988; Karaffa and Kubicek 2003). This observation, and the fact that *A. niger* is not able to grow anaerobically, made us believe that the reductive part of the TCA cycle is underdeveloped in this micro-organism. By a heterologous insertion of the reductive TCA cycle enzymes *frds* and *fum* in the WT and NW185 strain we aimed at diverting the flux towards these organic acids (malate, fumarate and succinate).

The *frds* gene from *S. cerevisiae* has been shown to irreversibly convert cytosolic fumarate to succinate. A possible problem of using this enzyme in the present study is that it uses non-covalently bound FAD as co-factor (Muratsubaki and Katsume 1985) and there is still a lack of knowledge of the FAD redox balance in *A. niger*. Additionally, it has been reported that FAD is oxygen sensitive, which might lead to a lack of this co-factor during aerobic fermentations. In this study, we did not insert the fumarase gene from *S. cerevisiae* since the kinetics of this enzyme favour the reaction from fumarate to malate (Peleg et al. 1990; Pines et al. 1997). Instead, the fumarase gene from *R. oryzae* was inserted, as this enzyme favours the reverse reaction. Because fumarase is normally a mitochondrial enzyme, the first 15 basepairs coding for the mitochondrial target sequence in *R. oryzae* were deleted (Friedberg et al. 1995). We supposed that oxygen limiting conditions will adequately mimic anaerobic fermentation conditions to stimulate the inserted reductive part of the TCA cycle and to stabilize the FAD^+ availability in the cells. $NaCO_3$ was used as base control, in order to stimulate carboxylation reactions. This has been shown to have an effect in other organic acid production processes like malate production in *A. flavus*, *A. paraciticus* and *A. oryzae* (Abe et al. 1962; Peleg et al. 1988). The consequence of adding $NaCO_3$ is that we have to run the fermentation at higher pH for the carbonate to be dissolved. At higher pH *A. niger* is likely to produce gluconic acid and, therefore, we included the NW185 strain that is unable to produce gluconic acid and oxalic acid in the study.

9.3 Material and Methods

9.3.1 Strains

As a reference strain the laboratory strain N402 (*cspA1* mutation) of *Aspergillus niger* was used. The NW185 strain (*cspA1, fwnA1, goxC17, prtF28* mutation) was kindly donated by Peter Schaap (Wageningen University, Holland). This strain is deficient in gluconic and oxalic acid production (Ruijter et al. 1999).

The fumarate reductase from *S. cerevisiae* (*frds*) and fumarase from *R. oryzae* (*fum*) were both fused to the *A. nidulans gpdA* promoter using fusion PCR. PCR was performed using the Expand High Fidelity PCR kit (Roche) according to the manufacturer's recommendations. The primers used are shown in Table 9.1.

Table 9.1 Primers used for fusion PCR of genes to be inserted in the cytosolic *A. niger* fraction

Primer name	Sequence
FumRs_up	CGT CTG TCC GCC CGG TGT AAC AAC TCT CCT CGT CTT TTC AG
FumRs_down	TTT AAT CCT TGG CAG AGA TCA TAT CTT C
FRDS_down2	TAT AGG ATC CGT TAC TTG CGG TCA
FRDS_up	CGT CTG TCC GCC CGG TGT ATG TCT CTC TCT CCC GTT GT
GpdA_up_ICL	GCT GAT TCT GGA GTG ACC CAG AG
GpdA_down_ICL	ACA CCG GGC GGA CAG ACG

The underlined letters are the overlapping genetic elements used for fusion PCR. The other letters are the actual primer sequences.

All PCR products were purified from agarose gels using illustra™ DNA and Gel band purification kit (GE Healthcare). 2-3 μg of the purified fusion PCR fragments were used to co-transform both genes, applying the protoplast and transformation procedures for *A. niger* as described previously for A*. nidulans* (Nielsen et al. 2006). In order to confirm gene insertion and expression a semi-quantitave reverse transcriptase PCR reaction was performed using the SuperScript III OneStep RT-PCR kit (Invitrogen) following the manufacturer's protocol. The primers used were GpdA_up and FumRs_down for the fumarase detection and GpdA_up and FRDS_down2 for the fumarate

reductase detection (Table 9.1). Both genes were shown to be expressed based on this RT-PCR reaction.

9.3.2 Cultivation conditions

Before spore harvesting with 0.01 % w/w Tween-80, the pre-culture plates were incubated for 4-7 days at 30 ºC. These culture plates consisted of a defined medium containing 10 g/L D-glucose, 50 ml salt solution, 1 ml trace element solution 1 and 18 g/L agar. Salt solution contained the following: 120 g/L $NaNO_3$, 10.4 g/L KCl, 10.4 g/L $MgSO_4 \cdot 7\ H_2O$ and 30.4 g/L KH_2PO_4. Trace element solution 1 contained the following: 22 g/L $ZnSO_4 \cdot 7\ H_2O$, 11 g/L H_3BO_3, 5 g/L $MnCl_2 \cdot 2\ H_2O$, 5 g/L $FeSO_4 \cdot 7\ H_2O$, 1.7 g/L $CoCl_2 \cdot 6\ H_2O$, 1.6 g/L $CuSO_4 \cdot 5\ H_2O$, 1.5 g/L $Na_2MoO_4 \cdot 2\ H_2O$ and 50 g/L Na_4EDTA. The spores were propagated on these culture plates at pH 6.5

Subsequently 10^9 spores were inoculated in 3 L Braun bioreactors with a working volume of 2L. The batch cultivations were carried out in a chemically defined medium adjusted initially to pH 2.5 containing 10 g/L glucose, 10 g/L $NaNO_3$, 3 g/L KH_2PO_4, 2 g/L $MgSO_4 \cdot 7\ H_2O$, 2 g/L NaCl, 0.2 g/L $CaCl_2 \cdot 2H_2O$, 0.5 ml/L antifoam (sb2121) and 1 ml/L trace element solution 2. Trace element solution 2 contained the following: 14.3 g/L $ZnSO_4 \cdot 7\ H_2O$, 2.5 g/L $CuSO_4 \cdot 5\ H_2O$, 0.5 g/L $NiCl_2 \cdot 6\ H_2O$, 7 g/L $MnCl_2 \cdot 2\ H_2O$ and 13.8 g/L $FeSO_4 \cdot 7\ H_2O$.

For the flux experiments the same cultivation conditions were used as in the other batch cultivations. The only changes in these cultivations were that 5 g/L 1-^{13}C glucose labelled substrate was used in a total volume of 200 mL.

In all cultivations the temperature was maintained constant at 30 ºC and the pH was controlled by automatic addition of 1 M $NaCO_3$ and 2 M HCl. Two Rushton four-blade disc turbines were used for homogeneous mixing. No baffles were used in the reactors thereby reducing the surface area available for biofilm formation. The initial aeration rate, agitation and pH were 0.2 vvm, 200 rpm and pH 2.5, respectively. They were gradually changed after germination (that takes place after approximately 15 hours) to 0.02 vvm, 700 rpm and pH 5, respectively. These parameters were kept constant throughout the rest of the batch cultivation. Air was used for sparging and the concentrations of oxygen and carbon dioxide in the exhaust gas were monitored by an acoustic gas analyser (Brüel & Kjær, Nærum, Denmark). The dissolved oxygen tension (DOT) was measured with an oxygen probe (Mettler Toledo sensors).

9.3.3 Sampling

Biomass samples were taken manually from the reactor. For dry weight measurements, a known cell culture volume was filtered through a pre-weighed nitrocellulose filter (pore size 45 µm, Pall Corporation). The filtrate was frozen immediately and later used for the determination of the concentrations of substrate and extracellular metabolites. The filter was washed with 0.9 % w/v NaCl, dried for 15 min in a microwave oven at 150 W and weighed again to determine the biomass concentration.

For determination of *in vitro* enzyme activities, flux analysis and microarray analysis, biomass samples were filtered through a nitrocellulose filter (pore size 45 µm, Pall Corporation) and washed with 0.9 % w/v NaCl. The filter cake (± 1 g) was immediately frozen in liquid nitrogen and stored at -80 ºC.

9.3.4 Substrate and extracellular metabolite quantification

High-performance liquid chromatography was used for the quantification of extracellular sugars and organic acids. Glucose, acetate, pyruvate, citrate, ethanol, succinate, fumarate, malate, glycerol and oxalate concentrations were measured on an Aminex HPX-87H cationic exchange column (BioRad, Hercules, California) eluted at 60 ºC with 5 mM H_2SO_4 at a flow rate of 0.6 mL/min. Metabolites were detected with both a refractive index detector and a UV detector.

9.3.5 Analysis of *in vitro* enzyme activities

The frozen samples were crushed on liquid nitrogen with a mortar. The crushed biomass (0.5 g) was solved in 2 ml of extraction buffer containing 25 mM MES-NaOH, 0.1 mM EDTA, 0.1 mM DTT, 0.1 mM phenylmethylsulfonyl fluoride and 0.1 mM NaN_3. This solution was transferred to 2 mL FastPrep tubes containing 0.5 mL glass beads (0.75-1 mm). The FastPrep tubes were processed 3 times 10 s on a FastPrep FP120 Instrument (Savant Instruments, New York), at speed setting 5, with cooling on ice in between each cycle. After disruption, the samples were centrifuged at 13,000 g at 4 ºC for 10-20 min, and the supernatants were analysed for enzyme activity.

Enzyme assays were performed at 30 °C using a HP8453 UV-visible light spectrophotometer. In order to test the linearity of the assays, the reactions were performed with 2-3 different dilutions of cell extract. The specific enzyme activities were expressed in micromoles $minute^{-1}$ $milligram^{-1}$ (U/mg). The amount of protein was determined by the Bradford method with bovine serum albumin as the standard (Bradford 1976). Four different enzyme activities were measured: citrate synthase

(CIT), malate dehydrogenase (MDH), isocitrate lyase (ICL) and pyruvate carboxylase (PYC) as described by Meijer et al. (2007).

9.3.6 Determination of intracellular flux distribution

9.3.6.1 Sample preparation and derivatisation for flux analysis

35-50 mg of biomass was dissolved in 600 µl 6M HCl and kept overnight at 105 ºC for hydrolysis. The hydrolysate was then centrifuged for 5 minutes at 15,000 rpm and the supernatant was transferred into new vials. The supernatant was dried for 3 hours at 105 ºC and dissolved in 200 µl milliQ water.

In the mean time, the resin bed for solid phase extraction was prepared by weighing 1 g of Dowex cation exchange resin and mixed it with 15 mL of 50 % w/w glycerol. One mL of resin solution was added to a syringe containing a frit on a SPE workstation. When the resin was settled at the bottom of the syringe, the excess of glycerol was drained and a second frit was added on top of the resin. Two mL of biomass hydrolysate was added on the SPE column. After the biomass had trickled through the column, 1 mL of 50 % v/v ethanol solution was added followed by 200 µl 1M NaOH solution, which washed the remaining unbound compounds off the column. Finally, the amino acids were eluted with 1 mL of solution containing 1 % w/v NaOH in saline (0.9 % w/v NaCl), ethanol and pyridine in a ratio of 9:5:1, respectively. The eluted amino acids were derivatised by ethylchloroformate (ECF) derivatisation and dimethylformamide dimethylacetal (DMF/DMA) derivatisation, respectively.

In the ECF derivatisation, 50 µl ECF was added to 500 µl amino acid solution and mixed in two sequential rounds of 30 s. Next, 200 µl propylacetate was added and finally 50 µl 1 M HCl. The upper organic layer was removed and analysed by GC-MS.

The DMF/DMA derivatisation required the addition of 300 µl 1M HCl to 500 µl amino acid solution followed by a 2-4 hours drying period at 105 ºC. 200 µl DMF/DMA and 200 µl acetonitrile were then added to dissolve the dried substance and mixed well for 30 s. This solution was kept at 100 ºC for 20 minutes and was subsequently transferred to -20 ºC for 10 minutes to ensure proper derivatisation. This solution was finally analysed by the GC-MS.

9.3.6.2 GC-MS analysis

GC-MS analysis was performed on an Agilent (Palo Alto, CA, USA) HP 6890 gas chromatograph coupled to a HP 5973 quadrupole mass selective detector in positive electron impact ionization

(EI^+) operated at an electron energy of 70 eV. The GC was equipped with a 4.0 mm i.d. Siltek gooseneck splitless deactivated liner (Restek, Bellefonte, PA, USA), and a Supelco (Bellefonte, PA, US) SLB-5 MS column, 15 m, 0.25 mm i.d., 0.25 µm film. Helium of a purity of 99.999 % was used as carrier gas at a constant linear gas velocity of 35 cm/s. Transfer line temperature was 280 ºC, quadrupole temperature 150 ºC and MS source 200 ºC. The GC-MS system was controlled from Agilent MSD Chemstation v. D.01.02.16. For both methods (ECF and DMF/DMA) 1 µL sample was injected in the splitless (30 sec, split 1:20) mode at 200 ºC using a hot needle. The MS scan range was m/z 40-400 with 2.88 s/scan. To avoid sample carry-over the syringe was cleaned using five times 5 µL acetone, then five times 5 µL dichloromethane and finally 3 times rinsing with 3 µL sample.

9.3.6.2.1 ECF derivatives

The oven temperature was initially held at 75 °C for one min. Hereafter, the temperature was raised with a gradient of 40 °C/min until 165 °C, after which the temperature increase was 4 °C/min until 190 °C and 40 °C/min up to 240 °C. Finally, the temperature was increased to 260 °C with a gradient of 4 °C/min and held constant for 4 minutes. The flow through the column was held constant at 1.3 mL He/min. The temperature of the inlet was 200 °C, of the interface 280 °C and of the quadrupole 105 °C.

9.3.6.2.2 DMF/DMA derivatives

Initially the oven temperature was held at 60 °C for one min. Hereafter, the temperature was raised with a gradient of 20 °C/min until 130 °C, after which the temperature increase was 4 °C/min until 150 °C and 40 °C/min up to 260 °C. Next, the temperature was held constant for 4.25 minutes. The flow through the column was held constant at 1 mL He/min. The temperature of the inlet was 230 °C, of the interface 270 °C and of the quadrupole 105 °C.

9.3.6.3 Metabolic network analysis

The flux analysis was based on the labelling patterns of derivatives of glucose and amino acids obtained from acid hydrolysis of the biomass. The mass spectra obtained from the GC-MS were converted into summed fractional labelling (SFL) patterns with the aid of the XCMS library operating within the R programming language environment (Smith et al. 2006). The SFL of a molecule or a fragment is identical to the sum of the fractional labelling of the carbon atoms contained in the molecule or fragment.

The metabolic network consisted of 52 reactions, 6 of them are reversible and 25 are balanced metabolites (Supplementary materials S2). The fluxes were determined using an in-house program code in Matlab V 7.0.4 (Grotkjær et al. 2005), which implements the metabolic network analysis framework from Wiechert (2001). The algorithm minimises the differences between measured

fluxes and calculated fluxes by least square minimisation, as well as measured and calculated SFL using the non-linear Levenberg-Marqueartd algorithm. Measured fluxes were weighed with a standard deviation of 10%. Multiple initial guesses were generated with a genetic algorithm to verify the existence of a global minimum. A sensitivity analysis was done by adding 10% of Gaussian noise to the measured SFL data in 50 simulations followed by calculating the standard deviation of the estimated fluxes.

9.3.7 Analysis of transcription data

9.3.7.1 Total RNA extraction

Total RNA was extracted from 40-50 mg frozen mycelia. The mycelia were transferred to pre-cooled 2 ml Eppendorf tubes containing steel balls (2x ∅2mm, 1x ∅5mm) and shaken in a Mixer Mill for 10 minutes at 4 °C. The resulting powder was used for total RNA extraction using the Qiagen RNA easy kit, according to the protocol for isolation of total RNA from plant and fungi.
The quality of the extracted total RNA of each sample was analysed using the Bioanalyser 2100 (Agilent technologies Inc., Santa Clara, CA, USA) and the quantity of the extracted total RNA was determined spectrophotometrically (Amersham Pharmacia Biotech, GE Healthcare Biosciences AB, Uppsala, Sweden). The total RNA was stored at -80 °C until further processing.

9.3.7.2 Biotin labelled cRNA and microarray processing

5 μg of total RNA was used for making 15 μg of fragmented biotin labelled cRNA that was hybridised to the 3AspergDTU gene chip (Affymetrix) according to the Affymetrix GeneChip Expression Analysis Technical Manual (Affymetrix 2007). The cRNA quality and quantity were analysed in the same way as the total RNA described above. A GeneChip fluidics Station FS-400 and a GeneChip scanner were used for hybridisation and scanning of the microarrays. The scanned probe array images were converted to .CEL files using the GeneChip Operating Software (Affymetrix). Affymetrix CEL-data files were pre-processed using the statistical language and environment R (R Development Core Team 2007). The probe intensities were normalised for background using the robust multiarray average (RMA) method (Irizarry et al. 2003) only using perfect match (PM) probes. Subsequently normalisation was performed using the quantiles algorithm (Bolstad et al. 2003). Gene expression values were calculated from the PM probes with the medianpolish summary method (Irizarry et al. 2003). All statistical pre-processing methods were used by invoking them through the Affymetrix package (Gautier et al. 2004).

Statistical analysis was applied to determine genes subject to differential transcriptional regulation. The limma package (Smyth 2004) was used for all statistical analysis. Moderated t-tests between

the sets of experiments were used for pairwise comparisons. A 2x2 ANOVA design was used to assess the effects of the strain, the insertion of the fumarate pathway and an additive effect. For all analyses, empirical Bayesian statistics were used to moderate the standard errors within each gene and Benjamini-Hochberg's method (Benjamini and Hochberg 1995) to adjust for multi-testing. A cut-off value of adjusted $p<0.05$ was for statistical significance. The complete list of significant genes is given as Supplementary materials S3.

9.4 Results and discussion

A physiological characterisation was made in order to map possible shift in metabolic behaviour towards production of more reduced organic acids comparing four different strains. The physiological state of these strains, fermented under the same conditions, was determined at different levels. Gene expression levels were compared to enzyme activities, metabolite concentrations and metabolic fluxes. The two strains compared in this study were the wild-type N402 strain and the mutated strain NW185 (unable to produce oxalate and gluconate). Furthermore, the effect of inserting two genes (*fum* and *frds*) on organic acid production was evaluated.

9.4.1 Comparison between N402 and NW185

The physiological state of N402 was significantly altered compared to NW185. Figure 9.1 gives an overview of the flux and gene expression changes in the central carbon metabolism of both strains. This figure is only a simplified representation of the stoichiometric metabolic model used for flux simulations. The complete model can be found in the supplementary material S2. The fluxes showed a correlation with the expression data in the upper part of the central carbon metabolism (PPP and upper part of glycolysis). Deviations were mainly found in the lower part of the glycolysis, where the flux is reduced in NW185 compared to N402. In line with the flux analysis, expression of genes involved in the lower part of the glycolysis and the oxidative part of the TCA cycle was significantly down-regulated in the NW185 strain (Figure 9.1).

At the pyruvate node a more pronounced change in flux pattern was detected between the two strains. The N402 strain obviously favoured flux through the pyruvate dehydrogenase (145.9 in the N402 strain and 17.0 in the NW185 strain), in contrast to the NW185 strain, which preferred the pyruvate carboxylase (8.2 in the N402 strain and 106.5 in the NW185 strain) (Figure 9.1). Looking at the enzyme activity of the pyruvate carboxylase (PYC), no difference could be detected in activity between the two strains (Table 9.2). Also the gene expression level was not significantly changed for this enzyme. Therefore, if the flux through PYC in NW185 was indeed higher compared to N402, post-translational modifications or metabolic regulation must be responsible for this increase. In case of a higher flux through this pathway would result in more oxaloacetate being formed. In the NW185 strain, this excess of oxaloacetate cannot be converted to oxalate, since this strain is unable to produce oxalate and therefore the oxaloacetate needs to be converted to other compounds. Since *A. niger* is well known for its organic acid production, it was expected that other

organic acids would be overproduced (Kubicek et al. 1989). However, none of the other TCA organic acids were produced significantly higher compared to the N402 strain (Table 9.3).

Table 9.2 Enzyme activities in U/mg measured in different *A. niger* strains

	ICL	MDH	CIT	PYC
WT	0.26	0.016	0.100	0.013
NW185	0.83	0.005	0.160	0.011
WT + FF	0.16	0.015	0.047	0.023
NW185 + FF	0.50	0.020	0.043	0.025

WT = wild-type N402 strain, NW185 = NW185 strain unable to produce gluconate and oxalate,
WT + FF = wild-type N402 strain with cytosolic fumarase and fumarate reductase genes inserted, NW185 + FF = NW185 strain with cytosolic fumarase and fumarate reductase genes inserted.
ICL = isocitrate lyase, MDH = malate dehydrogenase, CIT = citrate synthase, PYC = pyruvate carboxylase

The production profiles of organic acids derived from the TCA cycle differed only slightly between the two strains. The NW185 strain produced small amounts of fumarate (5 mg/L), while the N402 strain produced more citrate (1.2 g/L) (Figure 9.1 and Table 9.3). An increase in pyruvate excretion could be observed in the NW185 strain (0.2 g/L) (Table 9.3). This suggests that accumulation of intracellular pyruvate might occur, promoting the secretion of pyruvate. Another significant difference between the two strains was observed in the flux towards glycerol. The measured extracellular glycerol concentration was three times higher in the NW185 strain. The increase in both pyruvate and glycerol production indicates a metabolic limitation in the glycolysis leading to a higher excretion of these metabolites in the NW185 strain.

Looking at the enzyme activities, it was observed that the ICL activity was much higher in the NW185 strain than in the N402 strain (Table 9.2). Unfortunately, the flux through the glyoxylate cycle could not be determined with the method used. Therefore, it could not be verified if the higher enzyme activity was associated with a higher flux. However, a higher enzyme activity would suggest a higher flux through this pathway. Additionally, the expression data confirmed that ICL was up-regulated, giving an indication that the glyoxylate pathway was more active in the NW185 strain. All significantly expressed genes were plotted in the stoichiometric metabolic model from Andersen et al. (2008), which also showed an elevated ICL gene expression levels. The MDH activity was significantly lower in the NW185 strain. This does not seem to have an obvious effect on the flux through this enzyme, and moreover, the lower enzyme activity was not confirmed by the expression data (Table 9.2 and 9.3).

Table 9.3 Biomass and organic acid yields expressed in C-mol/C-mol glucose consumed

	Biomass	Citric acid	Oxalic acid	Succinic acid	Pyruvic acid	Glycerol	Fumaric acid
WT	0.37	0.14	0.0157	0.0029	0.0012	0.0032	0
NW185	0.49	0.08	0.0000	0.0024	0.0047	0.0096	0.001
WT + FF	0.29	0.10	0.0024	0.0096	0	0.0041	0.008
NW185 + FF	0.41	0.01	0.0000	0.0061	0.0042	0	0.020

WT = wild-type N402 strain, NW185 = NW185 strain unable to produce gluconate and oxalate, WT + FF = wild-type N402 strain with cytosolic fumarase and fumarate reductase genes inserted, NW185 + FF = NW185 strain with cytosolic fumarase and fumarate reductase genes inserted

It was found that over 1000 genes were significantly changed comparing the expression levels in N402 and NW185 (in S3, the 1000 most significantly changed genes are listed). Using the microarray data, pathway changes outside the central carbon metabolism could be detected. The surprisingly good correlation between the flux and microarray data in the central carbon metabolism, also seen in other micro-organisms (Cakir et al. 2007; Schilling et al. 2007), provided a good basis for elaborating on other parts of the metabolism based on the expression data. The significantly expressed genes were plotted in the stoichiometric model of Andersen et al. (2008) and showed that other parts of the metabolism were significantly changed as well (data not shown). For example the protein degradation pathway in the NW185 strain was up-regulated. The pyrimidine and purine synthesis together with amino acid pathways were down-regulated. At the same time down-regulation of RNA synthesis genes and ribosomal genes was detected in the NW185 strain. Also mitochondrial carriers were down-regulated. The combination of these gene expression changes indicate that the metabolic activity and, therefore, also the total energy requirement in the NW185 strain was reduced. This reduced energy requirement can again be correlated to the down-regulation of the TCA cycle that is coupled to the electron transport chain. The electron transport chain is the main regeneration pathway of redox equivalents, since *A. niger* is an absolute aerobic micro-organism needing its respiratory chain for survival. This reduced need for regeneration of redox equivalents is an indication that the redox balance was less disturbed in the NW185 or, that the NW185 strain needs less redox equivalents for maintaining its cellular state. This could have led to an increased biomass yield. The NW185 strain reached a biomass yield of 0.49 C-mol biomass / C-mol glucose, while the N402 strain reached only 0.37 C-mol biomass / C-mol glucose.

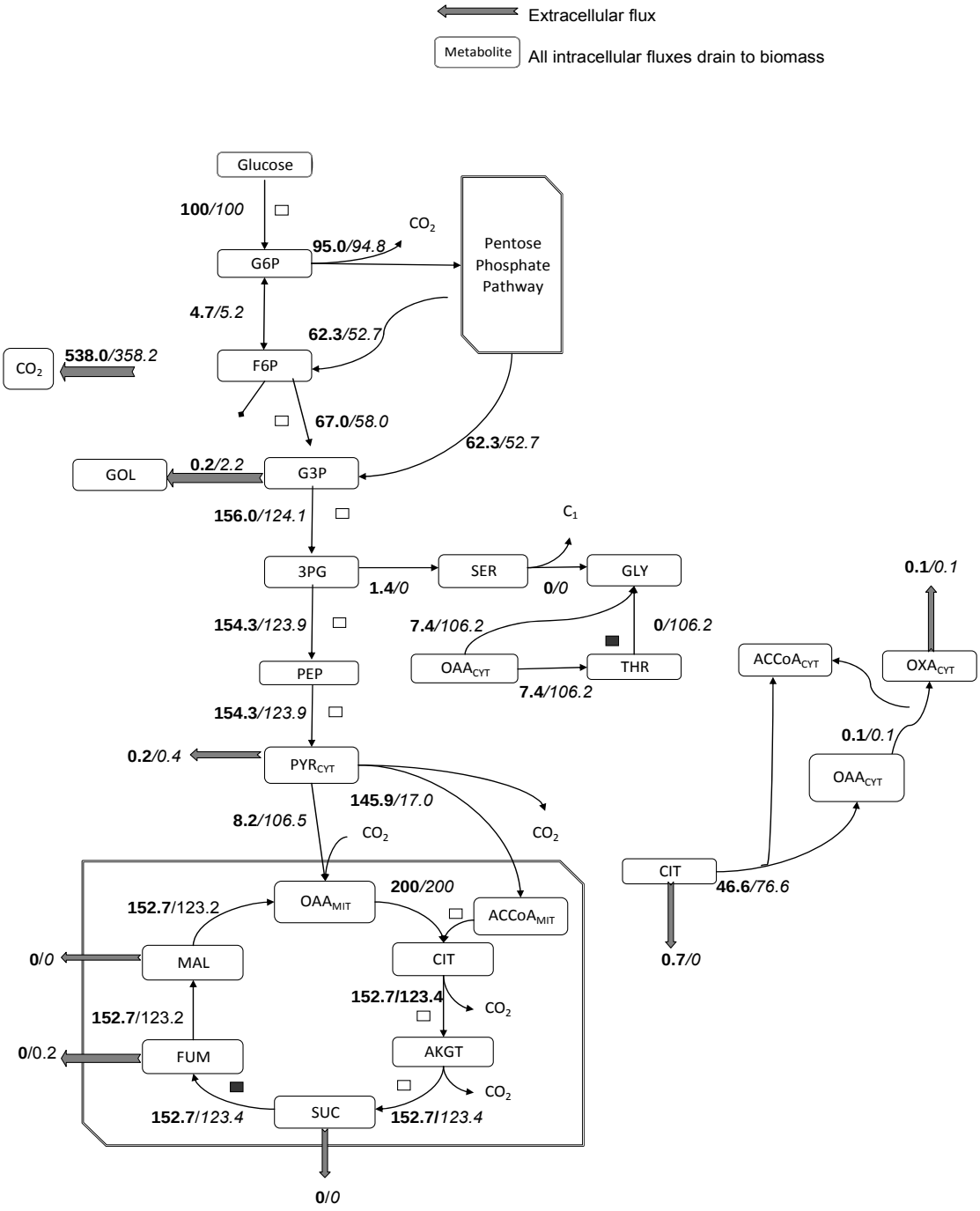

Figure 9.1 A simplified flux distribution model of the N402 and NW185 (complete model see S2). The first number is the flux in the N402 strain and the second number (italic) is the flux in the NW185 strain. G6P = glucose 6-phosphate, F6P = fructose 6-phosphate, GOL = glycerol, G3P = glyceraldehyde 3-phosphate, PEP = phosphoenolpyruvate, PYRcyt = cytosolic pyruvate, SER = serine, GLY = glycine, THR = threonine, OAAcyt = cytosolic oxaloacetate, CIT = citrate, ACCoAcyt = cytosolic acetyl-CoA, OXAcyt = cytosolic oxalate, ACCoAmit = mitochondrial acetyl-CoA, OAAcyt = mitochondrial oxaloacetate, AkGT = alfa-keto-glutarate, SUC = succinate, FUM = fumarate, MAL = malate.

■ = up-regulation of gene expression levels, □ = down-regulation of gene expression levels. Unmarked reactions did not have any significant change in gene expression.

9.4.2 Comparison of N402 with and without gene insertions

The fumarate reductase from *S. cerevisiae* and the fumarase from *R. oryzae* were inserted into the genome of *A. niger* N402. The gene insertions significantly changed the expression profiles of 965 genes (see S3). These insertions created a cytosolic pathway towards succinate in the cytosol of *A. niger*. Insertion of the genes resulted in a decreased flux towards the PPP and an increased flux through the glycolysis (Figure 9.2). The PPP is an essential pathway for NADPH regeneration, which is an important redox equivalent necessary for biomass production (Poulsen et al. 2005). Due to the reduction in the PPP flux the biomass yield in the strain with the genes inserted was reduced. For the strain without and with heterologous genes, respectively, the biomass yields were 0.37 and 0.29 C-mol biomass / C-mol glucose, respectively (Table 9.3). Furthermore, in the strain with the heterologous genes inserted there were increased fluxes from 3-phosphoglycerate towards serine biosynthesis (Figure 9.2). This resulted in a decreased flux through the lower part of the glycolysis. At the pyruvate node the pyruvate carboxylase reaction was clearly preferred when the two genes were inserted, probably the gene insertion provided a pathway where the carboxylated pyruvate could be further converted to malate, fumarate and succinate in the cytosol. Thus, the expression of *frds* and *fum* allowed for further conversion of malate to fumarate and succinate, instead of transporting malate into the mitochondria. Due to a drain of pyruvate into the new pathway, the flux towards extracellular pyruvate was decreased. As a response the malate transporter, transporting malate from the cytosol to the mitochondria, was up-regulated. Additionally, an increased expression level of the succinate thiokinase was observed, which also may have contributed to an increased succinate production.

Overall, the metabolic changes led to a three times increase in extracellular succinate levels. It was not determined if the majority of the succinate was built inside the mitochondria due to a shuttling of malate into the mitochondria and a higher expressed succinate thiokinase, or whether it was formed by the cytosolic pathway. Unfortunately, the enzyme activities of the inserted genes could not be determined due to unstable cofactors and separation difficulties between native and heterologous enzyme activity and kinetic properties. The overall production of reduced organic acids like fumarate and succinate was significantly increased in the strain with the gene insertions. This is in contradiction with the results obtained by Jongh (2006), who found more citrate and oxalate production when these genes were inserted. Even though the same strain was used, an explanation for the difference in results could be the substantial difference in cultivation conditions between the present study and the one by de Jongh. We used a more complete medium compared to the medium used by Jongh (2006). In our medium the pH was set to 5 instead of 3.5 and controlled with $NaCO_3$ instead of NaOH.

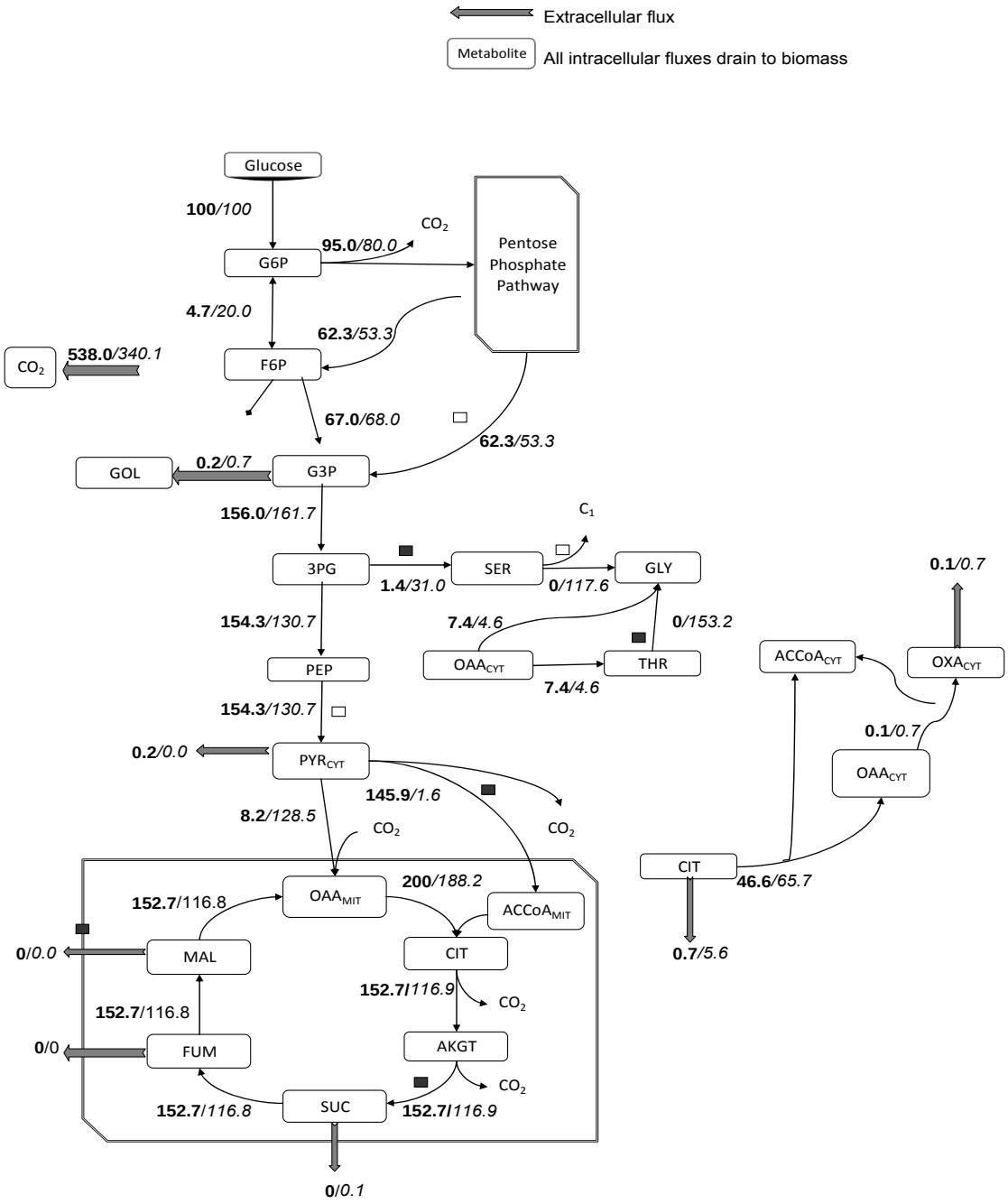

Figure 9.2 A simplified flux distribution model of the N402 and N402 with heterologous *fum* and *frds* inserted.(complete model see S2). The first number is the flux in N402 and the second number (italic) is the flux in N402 with heterologous *fum* and *frds* inserted. G6P = glucose 6-phosphate, F6P = fructose 6-phosphate, GOL = glycerol, G3P = glyceraldehyde 3-phosphate, PEP = phosphoenolpyruvate, PYRcyt = cytosolic pyruvate, SER = serine, GLY = glycine, THR = threonine, OAAcyt = cytosolic oxaloacetate, CIT = citrate, ACCoAcyt = cytosolic acetyl-CoA, OXAcyt = cytosolic oxalate, ACCoAmit = mitochondrial acetyl-CoA, OAAcyt = mitochondrial oxaloacetate, AkGT = alfa-keto-glutarate, SUC = succinate, FUM = fumarate, MAL = malate.

■ = up-regulation of gene expression levels, □ = down-regulation of gene expression levels. Unmarked reactions did not have any significant change in gene expression.

Also the aeration was lower in our study. We can conclude that the medium composition and fermentation conditions have a major influence on the physiological behaviour during the cultivations.

In this study the extracellular citrate concentration was not increased in the strains harbouring gene insertions (Table 9.3). Also the enzyme activity of CIT was not increased in comparison with the N402 strain (Table 9.2). Only an increased pyruvate carboxylase activity could be detected (0.013 and 0.023 U/mg protein, respectively). Therefore, we assume that malate was mainly converted towards fumarate and succinate in the cytosol and not transported into the mitochondria. This was confirmed by the increase in extracellular concentrations of these two compounds (Table 9.3), since the transport of malate into mitochondria would most likely produce more citrate (Jongh 2006).

9.4.3 Comparison of NW185 with and without gene insertions

The same genes as inserted in the N402 strain were inserted in the NW185 strain. The gene insertions had only a small effect on the gene expression levels of NW185. Only 5 genes were significantly changed in their expression level (see S3). These genes were not located in one specific part of the metabolism. In contrast, the fluxes were significantly changed, as well as the enzyme activities and extracellular metabolite concentrations.
The flux through the PPP was significantly decreased when the two heterologous genes were inserted in the genome of the NW185 strain. As a consequence the flux in the glycolysis was increased. Furthermore, insertion of the two heterologous genes led to an increased flux towards serine biosynthesis and a small decrease in flux through the pyruvate carboxylase reaction (Figure 9.3).

The pyruvate carboxylase enzyme activity measured in both NW185 strains was comparable and the gene expression of this enzyme was not found to be changed (Table 9.2 and Figure 9.3). Considering these results and the extracellular metabolite profiles, it is believed that the flux through this pathway was not decreased, but rather similar to the flux in the NW185 strain without gene insertions.

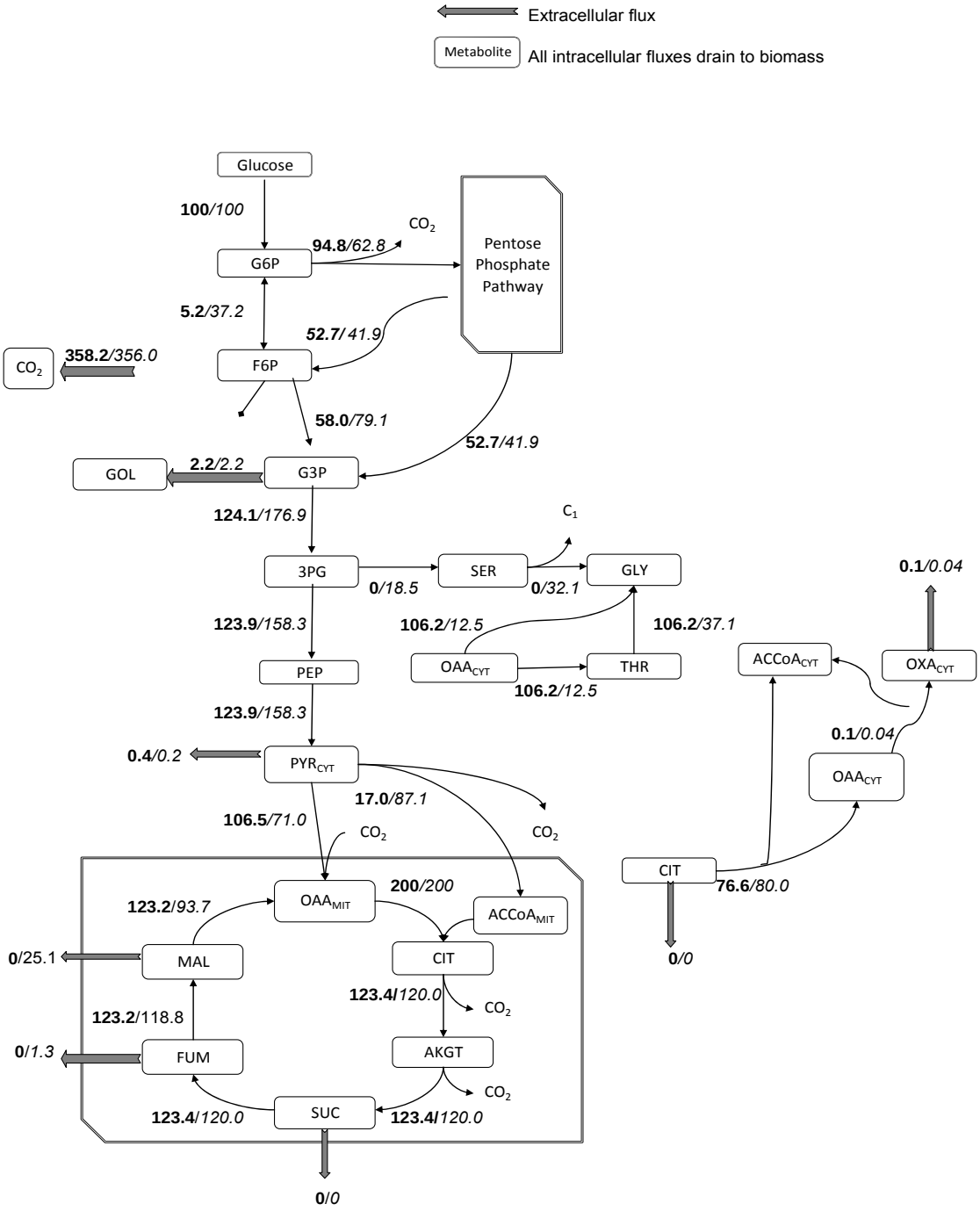

Figure 9.3 A simplified flux distribution model of the N402 and N402 with heterologous *fum* and *frds* inserted.(complete model see S2). The first number is the flux in N402 and the second number (italic) is the flux in N402 with heterologous *fum* and *frds* inserted. G6P = glucose 6-phosphate, F6P = fructose 6-phosphate, GOL = glycerol, G3P = glyceraldehyde 3-phosphate, PEP = phosphoenolpyruvate, PYRcyt = cytosolic pyruvate, SER = serine, GLY = glycine, THR = threonine, OAAcyt = cytosolic oxaloacetate, CIT = citrate, ACCoAcyt = cytosolic acetyl-CoA, OXAcyt = cytosolic oxalate, ACCoAmit = mitochondrial acetyl-CoA, OAAcyt = mitochondrial oxaloacetate, AkGT = alfa-keto-glutarate, SUC = succinate, FUM = fumarate, MAL = malate.

Looking at trends in the other enzyme activities measured, a large difference in MDH and CIT activity was observed (Figure 9.4). The MDH activity was significantly increased in the strain with the two heterologous genes. This higher activity leads to a larger flux towards extracellular malate, 25.1 compared to 0 (Figure 9.3). Also a significant change in the CIT activity was measured. The CIT activity was almost 4 times lower with gene insertions (Table 9.2). The extracellular flux towards citrate was estimated to be 0 for both strains, but a slightly lower extra-cellular citrate concentration was measured in the strain with the two genes inserted, correlating with the decreased enzyme activity. This indicates that the reductive TCA cycle is probably stimulated, resulting in a decrease in citrate production. In both NW185 strains (with and without genes inserted) the fluxes are mainly diverted towards malate and fumarate. Although no fluxes towards succinate could be estimated, the strain with the heterologous genes inserted showed a 3 times higher succinate yield based on the extracellular concentrations (Table 9.3), demonstrating an active reductive TCA cycle.

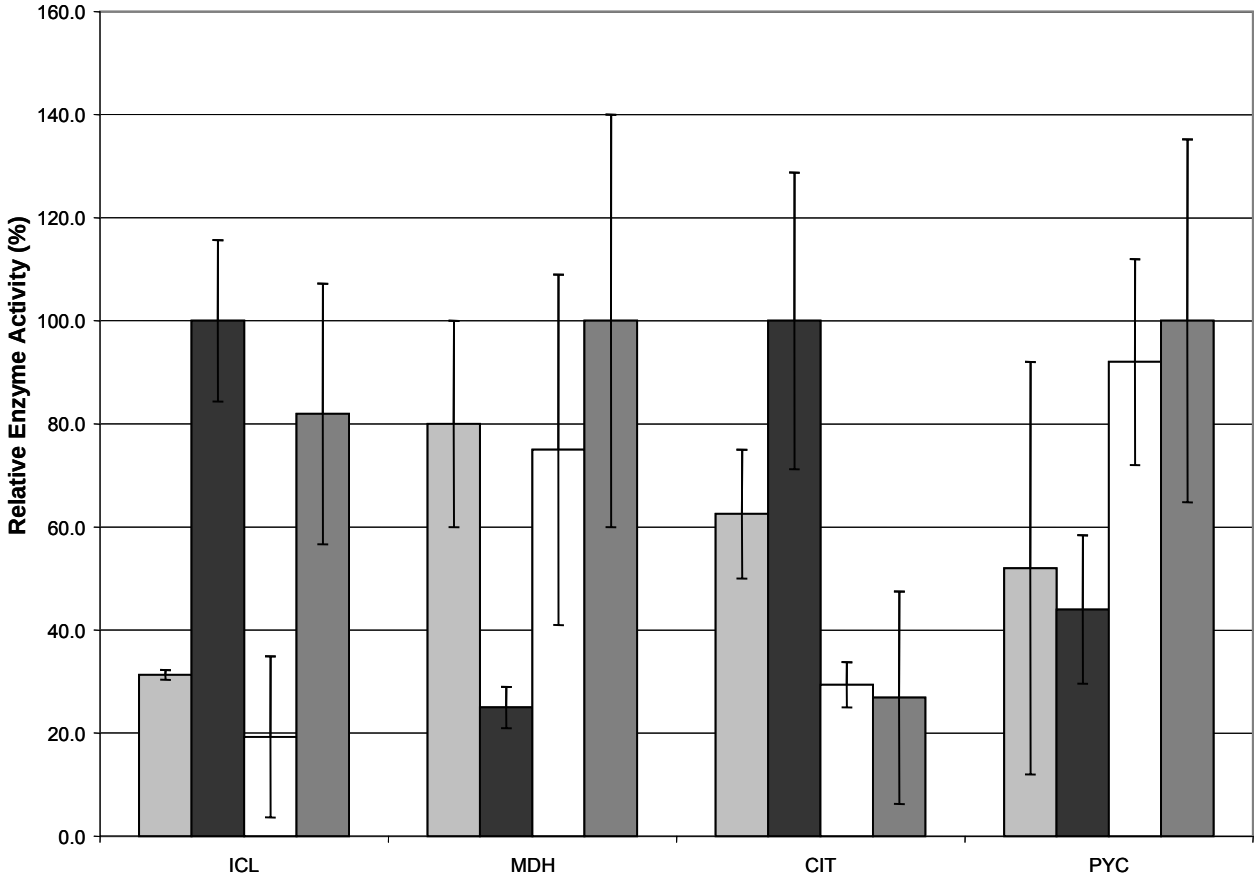

Figure 9.4 Relative enzyme activities and their standard deviations. ■ = WT N402, ■ = NW185, □ = N402 with the heterologous gene insertions of *fum* and *frds*, ■ = NW185 with the heterologous gene insertions of *fum* and *frds*. ICL = isocitrate lyase, MDH = malate dehydrogenase, CIT = citrate synthase, PYC = pyruvate carboxylase

9.4.4 Effect of gene insertions in both strains

The insertions of the two heterologous genes in both the N402 strain and the NW185 strain showed some resemblance but also some differences. In both the N402 and the NW185 strain the PPP was down-regulated as a consequence of the insertion of *fum* and *frds*. Furthermore, the flux towards serine biosynthesis was increased in both strains upon addition of the genes. The succinate yield was improved in both strains when the reductive part of the TCA cycle was expressed in the cytosol, indicating that both strains had a functional reductive TCA cycle pathway. However, the pyruvate carboxylase reaction was increased in the N402 strain upon addition of the genes, which was not observed in the NW185 strain. It was also observed that the citrate production in the “NW185 strains” was lower than in the “N402 strains”.

Overall, malate, fumarate and succinate production was higher in the strains with the genes inserted. This together with the fact that less citrate was produced in the NW185 strain with the two genes inserted indicates that significantly more reduced organic acids are produced. The insertion of the fumarate reductase and fumarase in the cytosol of *A. niger* has obviously diverted the flux towards the reductive part of the TCA cycle, thereby producing more reduced organic acids.

9.5 Conclusion

Major strain differences between N402 and NW185 (unable to produce gluconate and oxalate) were observed. The reduced need for regeneration of redox equivalents in the NW185 was a remarkable observation, but it did not result in more organic acid production. On the other hand, the insertion of the two heterologous genes (fumarate reductase and fumarase) shifted the metabolism towards organic acid production in the reductive part of the TCA cycle in both the NW185 strain and N402. Overall, a threefold higher succinate yield was achieved. A comparison between the four strains showed that the NW185 strain with the genes inserted was the best combination regarding malate, fumarate and succinate production. The metabolism was obviously redirected towards more reduced organic acids. It is believed that most of these acids are produced in the cytosol and not in the mitochondria.

The system level approach used in this study showed that a better cell factory for reduced organic acid production was created. The integration of the measurements at different cellular levels has contributed to defining and comparing the physiological states of the four strains. The correlation between expression data and flux data was evident in the primary metabolism, but more elaborate experiments are necessary for determining if this correlation also holds outside the primary metabolism.

9.6 References

Abe S, Furuya A, Saito T and Takayama K 1962. Method for procuding L-Malic acid by fermentation. *US Patent 3063910*.

Affymetrix 2007. GeneChip expression analysis technical manual - with specific protocols for using the GeneChip hybridisation, wash, and stain kit. *P/N 702232 Rev 2*.

Andersen MR, Vongsangnak W, Panagiotou G, Salazar MP, Lehmann L and Nielsen J 2008. A tri-species *Aspergillus* microarray: Comparative transcriptomics of three *Aspergillus* species. *PNAS* **105**:4387-4392.

Arikawa Y, Kuroyanagi T, Shimosaka M, Muratsubaki H, Enomoto K, Kodaira R and Okazaki M 1999. Effect of gene disruptions of the TCA cycle on production of succinic acid in *Saccharomyces cerevisiae*. *Journal of Bioscience and Bioengineering* **87** (1):28-36.

Benjamini Y and Hochberg Y 1995. Controlling the false discovery rate - A practical and powerful approach to multiple testing. *Journal of the Royal Statistical Society Series B-Methodological* **57** (1):289-300.

Bolstad BM, Irizarry RA, Astrand M and Speed TP 2003. A comparison of normalisation methods for high density oligonucleotide array data based on variance and bias. *Bioinformatics* **19** (2):185-193.

Cakir T, Kirdar B, Onsan ZI, Ulgen KO and Nielsen J 2007. Effect of carbon source perturbations on transcriptional regulation of metabolic fluxes in *Saccharomyces cerevisiae*. *Bmc Systems Biology* **1**:18.

Enomoto K, Arikawa Y and Muratsubaki H 2002. Physiological role of soluble fumarate reductase in redox balancing during anaerobiosis in *Saccharomyces cerevisiae*. *Fems Microbiology Letters* **215** (1):103-108.

Friedberg D, Peleg Y, Monsonego A, Maissi S, Battat E, Rokem JS and Goldberg I 1995. The *fumR* gene encoding fumarase in the filamentous fungus *Rhizopus oryzae* - Cloning, structure and expression. *Gene* **163** (1):139-144.

Gallmetzer M, Meraner J and Burgstaller W 2002. Succinate synthesis and excretion by *Penicillium simplicissimum* under aerobic and anaerobic conditions. *Fems Microbiology Letters* **210** (2):221-225.

Gautier L, Cope L, Bolstad BM and Irizarry RA 2004. Affy - analysis of Affymetrix GeneChip data at the probe level. *Bioinformatics* **20** (3):307-315.

Grotkjaer T, Christakopoulos P, Nielsen J and Olsson L 2005. Comparative metabolic network analysis of two xylose fermenting recombinant *Saccharomyces cerevisiae* strains. *Metabolic Engineering* **7** (5-6):437-444.

Irizarry RA, Hobbs B, Collin F, Beazer-Barclay YD, Antonellis KJ, Scherf U and Speed TP 2003. Exploration, normalisation, and summaries of high density oligonucleotide array probe level data. *Biostatistics* **4** (2):249-264.

Jongh Wd 2006. Organic acid production by *Aspergillus niger*. *Ph D thesis*:Center of Mircobial Biotechnology, Biocentrum-DTU, Technical University of Denmark, Denmark.

Karaffa L and Kubicek CP 2003. *Aspergillus niger* citric acid accumulation: do we understand this well working black box? *Applied Microbiology and Biotechnology* **61** (3):189-196.

Kristiansen B, Mattey M and Linden J 1998. Citric acid Biotechnology. *Published by Taylor and Francis*.

Kubicek CP, Schreferlkunar G, Wohrer W and Rohr M 1988. Evidence for a cytoplasmic pathway of oxalate biosynthesis in *Aspergillus niger*. *Applied and Environmental Microbiology* **54** (3):633-637.

Kubicek CP and Rohr M 1989. Citric acid fermentation. *Critical Reviews in Biotechnology* **4**:331-373.

Lin H, Bennett GN and San KY 2005. Metabolic engineering of aerobic succinate production systems in *Escherichia coli* to improve process productivity and achieve the maximum theoretical succinate yield. *Metabolic Engineering* **7** (2):116-127.

Meijer S, Panagiotou G, Olsson L and Nielsen J 2007. Physiological characterisation of xylose metabolism in *Aspergillus niger* under oxygen-limited conditions. *Biotechnology and Bioengineering* **98** (2):462-475.

Millard CS, Chao YP, Liao JC and Donnelly MI 1996. Enhanced production of succinic acid by overexpression of phosphoenolpyruvate carboxylase in *Escherichia coli*. *Applied and Environmental Microbiology* **62** (5):1808-1810.

Muratsubaki H and Katsume T 1985. Characterisation of fumarate reductase from baker's yeast - Essential sulfhydryl-group for binding of FAD. *Journal of Biochemistry* **97** (4):1201-1209.

Nielsen ML, Albertsen L, Lettier G, Nielsen JB and Mortensen UH 2006. Efficient PCR-based gene targeting with a recyclable marker for *Aspergillus nidulans*. *Fungal Genetics and Biology* **43** (1):54-64.

Peleg Y, Stieglitz B and Goldberg I 1988. Malic acid accumulation by *Aspergillus flavus*.1. Biochemical aspects of acid biosynthesis. *Applied Microbiology and Biotechnology* **28** (1):69-75.

Peleg Y, Rokem JS, Goldberg I and Pines O 1990. Inducible overexpression of the *fum1* gene in *Saccharomyces cerevisiae* - Localisation of fumarase and efficient fumaric acid bioconversion to L-malic acid. *Applied and Environmental Microbiology* **56** (9):2777-2783.

Pines O, Shemesh S, Battat E and Goldberg I 1997. Overexpression of cytosolic malate dehydrogenase (MDH2) causes overproduction of specific organic acids in *Saccharomyces cerevisiae*. *Applied Microbiology and Biotechnology* **48** (2):248-255.

Poulsen BR, Nohr J, Douthwaite S, Hansen LV, Iversen JJL, Visser J and Ruijter GJG 2005. Increased NADPH concentration obtained by metabolic engineering of the pentose phosphate pathway in *Aspergillus niger*. *Febs Journal* **272** (6):1313-1325.

R Development Core Team 2007. R: A language and environment for statistical computing. *(R Foundation for Statistical Computing, Vienna,Austria), http://www R-project org* .

Ruijter GJG, van de Vondervoort PJI and Visser J 1999. Oxalic acid production by *Aspergillus niger*: an oxalate-non-producing mutant produces citric acid at pH 5 and in the presence of manganese. *Microbiology-Sgm* **145**:2569-2576.

Schilling O, Frick O, Herzberg C, Ehrenreich A, Heinzle E, Wittmann C and Stulke J 2007. Transcriptional and metabolic responses of *Bacillus subtilis* to the availability of organic acids: Transcription regulation is important but not sufficient to account for metabolic adaptation. *Applied and Environmental Microbiology* **73** (2):499-507.

Smith CA, Want EJ, O'Maille G, Abagyan R and Siuzdak G 2006. XCMS: Processing mass spectrometry data for metabolite profiling using nonlinear peak alignment, matching, and identification. *Analytical Chemistry* **78** (3):779-787.

Smyth GK 2004. Linear models and empirical Bayes methods for assessing differential expression in microarray experiments. *Statistical Applications in Genetic and Molecular Biology* **3** (Article 3).

Vemuri GN, Eiteman MA and Altman E 2002. Succinate production in dual-phase *Escherichia coli* fermentations depends on the time of transition from aerobic to anaerobic conditions. *Journal of Industrial Microbiology & Biotechnology* **28** (6):325-332.

Werpy T and Petersen G 2004. Top value added chemicals from biomass. *http://www nrel gov/docs/fy04osti/35523 pdf* (27-03-2008).

Wiechert W 2001. C^{13} metabolic flux analysis. *Metabolic Engineering* **3** (3):195-206.

Chapter 10

Summary and future prospects

The overall objective of this study was to improve the organic acid production platform by *Aspergillus niger*. At first a shake flask medium optimization study was performed using a Design of Experiment set up (Chapter 4). The fractional factorial optimization could not define an optimum medium compostion due to large experimental variations. The hypothesis was that varying amounts of oxygen limitation caused these deviations. Therefore, a second study was performed analyzing the oxygen limitation effect on the physiology of *A. niger* (Chapter 5). This study showed that oxygen limitation affected the polyol production. This change in polyol profiles indicated that the redox balance was changed and that cells encountered a state of cellular stress. Only minor changes in organic acid profiles were detected. Intracellular metabolite analysis showed that some pathways were activated under oxygen limited conditions. This gave information about possible flux distributions and metabolic targets that might be interesting.

After these two physiological characterisation studies five different metabolic engineering strategies were pursued, aimed at increasing organic acid production with focus on succinic acid.

The first strategy was a complete deletion of the gene encoding succinate dehydrogenase (Chapter 6), but unfortunately no knock-out mutant could be obtained. It is possible that SDH is an essential gene, prohibiting growth when deleted. Another possibility is that the poor gene targeting performance obscured the results.

The second metabolic engineering strategy aimed at complete deletion of ATP: citrate lyase (Chapter 6). This enzyme was identified as a target by *in silico* stoichiometric metabolic model predictions in combination with pyruvate decarboxylase (PDC) and oxygen limitation. Because the physiological study on oxygen limitation showed no PDC activity under oxygen limitation, only ACL was deleted. This deletion resulted in a three-fold increase in succinate production on glucose, and the model predictioncs was hereby verified.

As a third strategy the regulatory enzyme AcuB was deleted and characterized in solid state and submerged fermentations (Chapter 7). AcuB is responsible for acetate metabolism through the glyoxylate pathway leading to succinate and malate. AcuB regulates the

enzymes involved in the glyoxylate pathway and was therefore thought to have an effect on organic acid production. However, the organic acid profiles were not significantly changed by *acuB* deletion. This indicates that deletion of this regulatory enzyme was not as effective as deleting *acl*, which is directly involved in the central carbon metabolism. It is believed that evolution resulted in a complex regulatory mechanism, where functions can be replaced by other regulatory pathways ensuring system robustness. This does not hold for enzymes in the central carbon metabolism, since these enzymes are conserved.

Over-expression of isocitrate lyase (ICL) was the fourth metabolic engineering strategy studied in this dissertation (Chapter 8). In contrast to AcuB, ICL has a direct influence on the glyoxylate pathway. ICL and malate synthase (MS) are the two enzyme that constitute this pathway. Instead of producing more succinate and malate, the fumarate production was significantly increase by *icl* over-expression. This change in organic acid profiles is thought to be caused by regulation within the TCA cycle and not by the glyoxylate bypass. For additional stimulation of the glyoxylate pathway malonate was added to the cultivations. Malonate inhibits the SDH, thereby interrupting the TCA cycle. The addition of malonate showed different cellular effects in both wild-type and *icl* over-expression strain. In the WT, the malonate addition resulted in more citrate and oxalate production, while in the ICL over-expression strain more malate was produced.

The fifth metabolic engineering strategy was the insertion of fumarase (*fum*) and fumarate reductase (*frds*) in the cytosol of both the wild-type and NW185 strain (Chapter 9). These two insertions created a reductive TCA cycle route towards succinate in the cytosol of *A. niger*. In both strain a three times higher succinate yield was achieved upon insertion of the genes. The combination of the NW185 strain and gene insertions led to a significant increase in malate, fumarate and succinate production. Therefore, the metabolism was redirected towards more reduced organic acids and it is believed that most of these acids were produced in the cytosol and not in the mitochondria.

The different metabolic engineering strategies tested in this dissertation have resulted in significant changes in the organic acid production profiles and show potential for using *A. niger* as production platform for formation of several organic acids. The system level approach used to characterize the strains has given us valuable new information. It was possible to link data retrieved from DNA microarrays, flux analyses, enzyme analyses and metabolite quantification methods. The integration of these results has given us a better understanding of the cellular mechanisms involved in organic acid production and has led to the discovery of new metabolic engineering targets.

Stoichiometric metabolic models were shown to be a useful tool for defining new targets. It is therefore believed that integration of the experimental results obtained by these studies will reveal new strategies redirecting carbon flux towards desired products. Probably, the simulations will predict multiple manipulations. Because the gene targeting methods are not very efficient in *A. niger*, more development is needed in this area. Strategies aimed at avoiding non-homologous end-joining must be investigated.

Transport mechanisms are another important aspect in unravelling the metabolic regulation of organic acid production. With the current sequencing projects more genes will be annotated and possible transporters might be identified. Transport of organic acids from mitochondria towards cytosol and vice versa will be a key element in understanding organic acid production. Localization of compounds must be verified in these studies, which poses a new challenge in separation technology for separating cellular compartments. Finally, the redox state and energy balance will be important for understanding the transport mechanisms and the general metabolic state of the cell. Further studies on this topic will improve our understanding of metabolism, leading to new metabolic engineering strategies and enhanced organic acid production.

Sammenfatning på dansk

Formålet med denne PhD afhandling var at forbedre organisk syreproduktion i *Aspergillus niger*. Indledningsvis blev et rystekolbeoptimeringsstudie udført. ”Fractional factorial optimization” gav ikke de ønskede resultater, da iltbegrænsningen forårsagede store eksperimentelle variationer. Den næste undersøgelse blev derfor koncentreret om iltbegrænsning i forbindelse med *A. niger* fysiologi. Denne undersøgelse påviste, at iltbegrænsning påvirker polyol produktion, mens den organiske syreproduktion var næsten upåvirket.

Efter disse to fysiologiske studier, blev teorier indenfor metabolic engineering anvendt til at undersøge mulighederne for at fremme ravsyreproduktion. Den første strategi var at fjerne hele succinate dehydrogenase (SDH) genet. Desværre viste det sig umuligt at konstruere denne deletions mutant.

Den næste strategi fokuserede på at fjerne al ATP: citrate lyase (ACL). Denne undersøgelse har resulteret i en tre gang større ravsyreproduktion på glukose. Det kan derfor konkluderes, at brugen af støkiometriske metabolome modeller er et godt værktøj til identificering af gener der kan fremme organisk syreproduktion.

I den tredje strategi blev det regulatoriske enzym AcuB slettet. Dette påvirkede desværre ikke i tilstrækkelig grad den organiske syreproduktion. Dette beviser, at fjernelse af dette regulatoriske enzym ikke var så effektiv som fjernelse af *acl*, som er direkte involveret i en central kulstofmetabolisme.

Over-udtryk af isocitrat lyase (ICL) var den fjerde metabolic engineering strategi som blev brugt i denne afhandling. I modsætning til AcuB, har ICL direkte indflydelse på glyoxylate syntesevejen. ICL og malat synthase (MS) er de to enzymer som opbygger denne syntesevej. I stedet for at fremme succinat- og malatproduktion, blev fumaratproduktionen betydeligt øget med *icl* over-udtryk. Med henblik på at stimulere glyoxylat syntesevejen, blev malonat tilføjet kultiveringen. Malonate inhiberer SDH, og bryder dermed Tricarboxylsyre (TCA) cyklussen. Hos wild-typen (WT) øger dette citrate and oxalate produktion, mens mere malat blev produceret i ICL stammen.

Den femte strategi var at tilføre fumarase (*fum*) og fumarate reduktase (*frds*) i cytosolen hos både WT og NW185 stammerne. Dette resulterede i en reduceret TCA cyklus mod succinate

i *A. niger* cytosol. Et tre gang så stort succinat afkast blev observeret i begge stammer. I NW185 stammen resulterede genindsætningen i øget malat, fumarat og succinat produktion.

De forskellige metabolic engineering strategier, der blev testede i denne afhandling har resulteret i signifikante ændringer i organisk syreproduktion og viser potentialet af *A. niger* til produktion af forskellige organiske syrer. Det var muligt at forbinde DNA microarray data, flux analyse, enzym analyse and metabolite kvantificeringsmetoder. Integrering af disse resultater har givet os bedre forståelse af cellular mekanismer involveret i organisk syreproduktion, samt indblik i nye metabolic engineering strategier.

Støkiometriske metabolome modeller har viste sig at være et brugbart værktøj til at finde nye mål. Desuden kan integrering af eksperimentelle resultater, som beskrevet i denne afhandling, bruges til at finde strategier til om-dirigering af kulstof fluxen væk fra uønskede produkter. Gen targeting metoderne er desværre ikke så effektive i *A. niger*, og yderligere forskning er derfor nødvendig indenfor dette område.

Transport mekanismer er endnu et vigtigt aspekt forbundet med metabolisk regulering af organisk syreproduktion. Med de nuværende sekventeringsprojekter vil flere gener blive annoterede og nye transportproteiner muligvis blive identificerede. Organisk syretransport fra mitochondria til cytosol og vice versa kan blive et bærende element i forståelsen af syreproduktion. Sidst men ikke mindst, vil redox niveau og energi balance være vigtige områder til forståelse af transport mekanismer, men også for den generelle metabolome tilstand i cellen. Dette åbner døre til forskellige muligheder, som vil forbedre vores forståelse for metabolisme og øge organisk syreproduktion ved hjælp af nye metabolic engineering strategier.

S1: Significantly expressed genes in Chapter 8

Identification of the significantly expressed genes, fold change in log2 ration between WT and ICL over-expression strain (positive number then expression level in ICL over-expression strain higher), p. value < 0.05, the general description is taken from the JGI annotation database.

JGI_ID	Fold change	p. value	General description
198539	21.8	5.3E-04	-
209252	-4.5	5.7E-04	Autophagy related protein, involved in membrane trafficking
45946	7.9	7.9E-04	-
213703	-5.3	9.9E-04	-
189002	-102.1	1.1E-03	-
46621	-4.5	1.1E-03	Hypothetical amylo-alpha-1,6-glucosidase. Glycogen debranching
213014	-4.5	1.2E-03	Flavin-containing monooxygenase
38103	-2.9	1.3E-03	Hypothetical Damage-specific DNA binding protein
170627	-5.0	1.4E-03	-
196377	3.2	1.4E-03	Mitochondrial/chloroplast ribosomal protein L2
52705	4.2	1.7E-03	Predicted protein shares amino acid sequence identity with the Saccharomyces cerevisiae TUF1 gene product; mitochondrial translation elongation factor Tu.
208272	-2.0	1.7E-03	Ubiquitin-like protein
57285	24.4	1.8E-03	Major facilitator superfamily
212412	6.1	1.8E-03	-
131354	-5.3	1.9E-03	-
53717	-2.5	1.9E-03	AAA ATPase
209058	5.6	1.9E-03	ATP sulfurylase
53518	-6.2	2.0E-03	Phosphoribosyltransferase
44868	-3.3	2.1E-03	-
170612	-2.5	2.1E-03	-
57159	-2.5	2.1E-03	-
136000	1.4	2.2E-03	-
184507	-2.1	2.2E-03	-
205766	-5.9	2.2E-03	Sugar (ANd other) transporter
213950	-2.3	2.3E-03	Peptidase M28
200887	4.7	2.3E-03	Hypothetical S-adenosylmethionine-dependent methyltransferase activity
184678	-4.8	2.3E-03	-
55052	-3.1	2.3E-03	Fungal specific transcription factor
210556	-2.6	2.4E-03	-
128721	-3.6	2.4E-03	-
209032	-7.3	2.5E-03	-
208048	105.1	2.5E-03	Nitrate reductase
210558	4.1	2.5E-03	Thiamine pyrophosphate-requiring enzyme
208078	5.6	2.6E-03	-
205484	-6.3	2.6E-03	-
210295	-3.2	2.6E-03	SNARE protein TLG1/Syntaxin 6
123074	2.3	2.7E-03	-

206645	-3.0	2.7E-03	Related to phosphatidylinositol/phosphatidylglycerol transfer protein
54541	-116.7	2.8E-03	Candidate oxidoreductase, Short-chain dehydrogenase/reductase
127436	-7.7	2.8E-03	Carbohydrate kinase
57039	3.3	2.9E-03	Aspartyl-tRNA synthetase, mitochondrial
208387	2.4	3.0E-03	RNA-binding protein LARP/SRO9 and related La domain proteins
136140	-5.6	3.0E-03	-
190740	3.6	3.1E-03	-
37080	-2.7	3.2E-03	pepE, extracellular aspartic protease
209660	3.6	3.2E-03	SWI-SNF chromatin-remodelling complex protein
50350	-7.3	3.3E-03	Hypothetical Fungal transcriptional regulatory protein, N-terminal
52970	-2.6	3.3E-03	-
54838	-74.1	3.3E-03	Major facilitator superfamily
49674	-4.9	3.3E-03	-
37678	-3.6	3.3E-03	-
202315	-2.3	3.3E-03	-
39215	3.0	3.4E-03	Ribosomal protein L6
120185	-1.7	3.4E-03	Hypothetical protein. May be a transcription factor due to a Zn-finger domain.
137527	3.1	3.5E-03	-
209255	3.6	3.5E-03	Mitochondrial substrate carrier
55785	3.8	3.5E-03	Protein kinase
42152	-13.6	3.5E-03	-
51685	21.5	3.5E-03	Related to Schizosaccharomyces pombe asparaginase (EC 3.5.1.1)
207376	2.1	3.6E-03	Predicted protein shares amino acid sequence identity to the Saccharomyces cerevisiae TIF34 gene product; subunit of the core complex of translation initiation factor 3(eIF3), which is essential for translation.
131516	-3.7	3.7E-03	-
203401	6.3	3.7E-03	Amidase
46405	-3.2	3.7E-03	-
142364	3.2	3.8E-03	-
55805	-2.6	3.8E-03	Hypothetical catalytic protein
41505	-9.7	3.8E-03	Permease of the major facilitator superfamily
46346	-5.4	3.8E-03	-
176433	-10.6	3.9E-03	-
129773	10.8	3.9E-03	-
55741	2.4	3.9E-03	Protein import receptor MAS20
54145	3.7	3.9E-03	-
133160	-2.5	4.0E-03	Beta subunit of farnesyltransferase
201957	-2.0	4.0E-03	Synaptobrevin/VAMP-like protein
205959	2.0	4.0E-03	-
38274	-3.9	4.0E-03	-
178744	-7.2	4.1E-03	Hypothetical Metal-dependent phosphohydrolase, HD region
120353	2.6	4.2E-03	Hypothetical protein with PPR repeat
55707	-2.4	4.2E-03	Nucleotide-sugar transporter
211162	-3.7	4.2E-03	Hypothetical 1,4-alpha-glucan branching enzyme
124156	-28.6	4.3E-03	Candidate NAD dependent formate dehydrogenase
200589	8.8	4.4E-03	8-amino-7-oxononanoate synthase (biotin synthesis)
54926	-3.8	4.5E-03	-
56366	-2.2	4.5E-03	-

188168	-2.8	4.5E-03	-
39625	-6.4	4.7E-03	-
42619	-2.9	4.7E-03	DSBA oxidoreductase
55980	4.5	4.7E-03	-
194595	-2.5	4.7E-03	Flavonol reductase/cinnamoyl-CoA reductase
55261	-2.4	4.8E-03	-
52996	2.7	4.9E-03	Related to ubiquinone biosynthesis methyltransferase COQ5 (S. cerevisiae)
208535	-3.0	4.9E-03	-
52668	-2.0	4.9E-03	(trpC) Anthranilate synthase. Trifunctional enzyme bearing the Gln amidotransferase (GATase) domain of anthranilate synthase, indole-glycerolphosphate synthase, and phosphoribosylanthranilate isomerase activities
205291	-2.5	4.9E-03	Isocitrate and isopropylmalate dehydrogenases
38286	3.4	5.0E-03	FOG: RRM domain
53978	-2.4	0.01	(mstA) high affinity monosaccharide transporter
133197	-5.6	0.01	Transcriptional coactivator
209315	4.4	0.01	-
56629	-2.1	0.01	Cullin 4 type protein
201918	1.9	0.01	Synaptic vesicle protein Synapsin
208898	7.6	0.01	NADP/FAD dependent oxidoreductase
56782	-27.3	0.01	Glycosyl hydrolase family 3 C terminal domain
37333	4.9	0.01	-
56635	2.9	0.01	Ribonucleotide reductase
182442	4.5	0.01	-
49490	2.2	0.01	-
208835	-2.6	0.01	Serine/threonine protein kinase Chk2 and related proteins
57101	2.0	0.01	-
197860	-2.7	0.01	-
196077	3.2	0.01	-
206447	2.3	0.01	Hypothetical Aminotransferase
203758	15.3	0.01	-
206414	7.6	0.01	-
42171	-5.3	0.01	Hypothetical isocitrate lyase and phosphorylmutase
193981	-8.5	0.01	Putative pyruvate decarboxylase joined with TPR repeat containing protein
40734	-15.3	0.01	Hypothetical aldehyde dehydrogenase. Specificity towards NAD or NADP is not deducible from sequence data
195172	-2.3	0.01	Hypothetical. N-acetyltransferase activity
199051	-2.2	0.01	Sugar transporter superfamily
200430	1.7	0.01	Sterol desaturase
211137	-2.0	0.01	GHMP kinase
56275	3.1	0.01	acnA, Homoaconitase (EC 4.2.1.36)
40329	-2.5	0.01	-
40484	-2.5	0.01	Peptidase M, neutral zinc metallopeptidases, zinc-binding site
39180	3.1	0.01	-
214665	-3.0	0.01	Hypothetical protease
51820	-1.9	0.01	Related to S. cerevisiae phosphatidyl serine synthase
209436	1.6	0.01	Putative cell polarity protein
175251	-5.5	0.01	-
44156	6.1	0.01	Related to mitochondrial translation elongation factor
41926	-2.3	0.01	Hypothetical G-protein with WD-40 repeat
52140	-2.6	0.01	Serine/threonine protein kinase

39360	-1.8	0.01	Zinc-binding oxidoreductase
198023	1.6	0.01	Actin/actin-like
46999	1.9	0.01	Related to prephenate dehydrogenase of Candida albicans
56195	2.1	0.01	Carbohydrate kinase, FGGY
39893	-2.9	0.01	Synaptic vesicle transporter SVOP
124912	-3.0	0.01	Choline kinase
211094	3.2	0.01	-
132154	2.5	0.01	Cytochrome P450
56202	1.6	0.01	-
127627	2.3	0.01	Candidate ribosomal protein S18
171442	-7.0	0.01	-
52586	-10.0	0.01	Hypothetical protein with TPR-like domain
48688	4.8	0.01	Adenosylmethionine-8-amino-7-oxononanoate transaminase
198685	2.0	0.01	-
51731	1.9	0.01	Molecular chaperones GRP170/SIL1, HSP70 superfamily
42523	3.5	0.01	Hypothetical Inositol monophosphatase
44347	2.3	0.01	Ribosomal protein L3
52717	1.9	0.01	Shares limited amino acid sequence identity with ribosomal protein L15, bacterial form.
208043	54.7	0.01	Nitrogen transporter
198660	2.1	0.01	Hypothetical translocase of outer mitochondrial membrane complex
53574	4.8	0.01	Candidate carbamoyl-phosphate synthase
55742	-3.7	0.01	aldA Aldehyde dehydrogenase (aldA) (EC 1.2.1.3)
48502	1.6	0.01	Hypothetical septin B-like protein
48505	-2.0	0.01	-
212582	3.6	0.01	-
40867	2.2	0.01	-
39679	5.8	0.01	Oxidoreductase, molybdopterin binding
184314	-2.7	0.01	-
40924	-2.7	0.01	-
40917	3.4	0.01	Predicted mechanosensitive ion channel
52919	4.2	0.01	Hypothetical. Intrpro: AMP-dependent synthetase and ligase
56336	-17.0	0.01	-
206719	2.0	0.01	Hypothetical protein with Zn-finger, Tim10/DDP type
200187	-3.1	0.01	pepC. Subtilisin like serine protease
119993	-2.1	0.01	Hypothetical Mg2+ transporter protein, CorA-like
55956	-2.2	0.01	Hypothetical subunit of the 26S proteasome regulatory complex
54662	2.1	0.01	Hypothetical SNF5/SMARCB1/INI1 protein - a key component of SWI/SNF-class complexes; KOG Class: Chromatin structure and dynamics; KOG Id: 1649; KOG Description: SWI-SNF chromatin remodelling complex, Snf5 subunit
196832	2.3	0.01	Hypothetical pseudouridylate synthase
201712	-1.9	0.01	-
125418	-2.6	0.01	Short-chain dehydrogenase/reductase SDR
124206	4.4	0.01	-
38222	2.7	0.01	-
211068	-9.5	0.01	-
54784	2.4	0.01	-
211595	1.5	0.01	Related to extracellular GH family 61 endo-1,4-beta-glucanase of Trichoderma reesei

53049	-1.7	0.01	Ras-related small GTPase, Rho type
209327	-4.0	0.01	Fungal transcriptional regulatory protein, N-terminal
54217	-2.4	0.01	Conserved Zn-finger protein
41983	-2.4	0.01	Amidohydrolase 2
52725	-3.9	0.01	Flavin-containing monooxygenase
52603	-3.0	0.01	Related to carboxypeptidase Y
42282	2.7	0.01	-
191636	-9.2	0.01	Hypothetical protein. Electronic annotation suggests pyridine nucleotide-disulphide oxidoreductase
202783	-2.2	0.01	Ras small GTPase,
188662	2.3	0.01	Nuclear transport factor 2
199618	-2.5	0.01	-
209093	2.5	0.01	-
192093	-10.7	0.01	Major facilitator superfamily
130834	-2.6	0.01	Fungal specific transcription factor
40968	1.6	0.01	-
55391	3.3	0.01	-
53297	3.6	0.01	-
38135	1.6	0.01	Esterase/lipase/thioesterase
36895	2.8	0.01	SAM-dependent methyltransferases
210297	-2.3	0.01	Signal transduction
54083	2.4	0.01	Hypothetical. Related to GCN5-related N-acetyltransferase
189635	-7.1	0.01	Monodehydroascorbate/ferredoxin reductase
120659	1.4	0.01	-
204514	-2.2	0.01	Nucleotide excision repair factor NEF2, RAD23 component
54071	-4.8	0.01	-
187475	-2.6	0.01	-
209263	5.2	0.01	-
171058	-2.7	0.01	-
54095	-44.5	0.01	Sugar (ANd other) transporter
41935	-5.8	0.01	-
210783	-4.0	0.01	Hypothetical. Probable peroxisomal membrane. Interpro suggests alkylhydroperoxide reductase
53357	3.0	0.01	Related to aldehyde dehydrogenase (EC 1.2.1.3). Sequence similarity to ALD2 of C. albicans
198287	-1.7	0.01	Ubiquitin-like protein
210274	4.8	0.01	NADP-dependent flavoprotein reductase
46341	-2.0	0.01	-
209597	-2.0	0.01	Protein kinase
44118	1.3	0.01	-
52629	2.4	0.01	-
176010	-5.8	0.01	Predicted esterase of the alpha-beta hydrolase superfamily
51482	-17.3	0.01	Major facilitator superfamily
54966	1.7	0.01	-
56031	-7.2	0.01	Fungal transcriptional regulatory protein
56788	-3.1	0.01	Hypothetical protease that contains peptidase M28 domain
39626	1.3	0.01	Hypothetical protein
56305	2.8	0.01	Aldehyde dehydrogenase family
56871	2.6	0.01	Mitochondrial carrier proteins
55027	-2.2	0.01	-
213288	-3.2	0.01	-
209231	-3.9	0.01	Aldo/keto reductase

200680	2.4	0.01	Eukaryotic translation initiation factor 3, subunit 7
190311	-9.8	0.01	2-nitropropane dioxygenase
187784	-3.8	0.01	Hypothetical. Monocarboxylate transporter like
56628	-12.1	0.01	Dak kinase
190051	-1.7	0.01	Fungal specific transcription factor
51725	-4.0	0.01	-
207660	1.6	0.01	Glycosyl transferase, family 48
178568	-2.5	0.01	-
205836	-4.3	0.01	-
184073	7.2	0.01	Related to NADPH-dependent alcohol dehydrogenase, Zinc containing
135849	-2.2	0.01	-
212140	-2.6	0.01	hypotetical cAMP-dependent protein kinase catalytic subunit
38226	-7.0	0.01	Related to Geranylgeranyl pyrophosphate synthase
35655	6.9	0.01	-
213851	-30.6	0.01	GTP cyclohydrolase II
49586	5.2	0.01	-
207636	-4.2	0.01	Hypothetical non-ribosomal peptide synthetase
140888	-3.0	0.01	Glutathione S-transferase
49737	-4.4	0.01	Hypothetical protein
201503	10.0	0.01	NAD-cytochrome b5 reductase
186114	3.9	0.01	-
38995	-5.3	0.01	Hypothetical, AAA+-type ATPase domain
55759	-2.1	0.01	-
57277	-1.6	0.01	yop1 (A. fumigatus), Protein involved in membrane traffic (YOP1/TB2/DP1/HVA22 family)
210041	2.8	0.01	ABC (ATP binding cassette) 1 protein
55510	2.8	0.01	Pyruvate dehydrogenase E1 B-subunit
53338	2.6	0.01	Related to dihydrolipoamide acetyltransferase, EC 2.3.1.12
212098	6.2	0.01	Hypothetical CAP20-like protein
210672	-10.7	0.01	Short-chain dehydrogenase/reductase SDR
50882	9.4	0.01	Hypothetical glucose-methanol-choline oxidoreductase (EC 1.99.1.1)
36035	-3.1	0.01	-
54817	26.2	0.01	Hypothetical oligopeptide transporter
170261	-11.4	0.01	Permease of the major facilitator superfamily
57355	-4.5	0.01	-
43721	-2.5	0.01	-
42720	2.4	0.01	-
188037	3.2	0.01	Lipoate-protein ligase A
52123	1.8	0.01	Mitochondrial import inner membrane translocase, subunit TIM23
212337	-9.7	0.01	Hypothetical protein. Contains four putative transmembrane helices
43123	2.3	0.01	Ferredoxin
129632	-2.3	0.01	-
190580	-1.7	0.01	Hypothetical protein prenyltransferase, alpha subunit
185619	1.4	0.01	Ribosomal protein
205518	5.6	0.01	NADH-dehydrogenase (ubiquinone)
47491	-2.2	0.01	-
174228	3.5	0.01	-
40771	2.0	0.01	Putative GroEL-like chaperone, ATPase
50042	2.5	0.01	-
206931	1.9	0.01	FOG: RCC1 domain

137851	-1.5	0.01	-
199601	2.2	0.01	-
48803	-2.6	0.01	-
170638	-1.9	0.01	-
198936	1.8	0.01	Hypothetical protein with PPR repeat
53423	-3.0	0.01	Related to 2-methylcitrate dehydratase of E. coli
54896	4.0	0.01	-
207572	-40.5	0.01	General substrate transporter
211078	1.5	0.01	Actin/actin-like
136845	2.4	0.01	Ribosomal protein
189135	10.7	0.01	Hypothetical carboxylesterase
55296	1.9	0.01	Hypothetical threonyl-tRNA synthetase kinase. HMMPfam indicates Threonyl-tRNA synthetase kinase activity
40740	-2.5	0.01	Hypothetical Short-chain dehydrogenase
170148	-4.5	0.01	Putative GH family 18 endo-chitinase
201122	-3.6	0.01	-
143749	-5.0	0.01	-
35440	1.5	0.01	Hypothetical phosphatidylserine decarboxylase (EC 4.1.1.65)
55947	4.6	0.01	Related to cytochrome P450
208150	3.3	0.01	FAD-dependent pyridine nucleotide-disulphide oxidoreductase
175519	-1.9	0.01	Hypothetical Cobalamin synthesis protein
197381	-2.7	0.01	GTPase Rab5/YPT51 and related small G protein superfamily GTPases
210798	3.5	0.01	Dienelactone hydrolase
198250	-9.3	0.01	2-enoyl-CoA hydratase/3-hydroxyacyl-CoA dehydrogenase/Peroxisomal 3-ketoacyl-CoA-thiolase, sterol-binding domain and related enzymes
51829	-1.6	0.01	Clathrin-associated protein medium chain
174759	-3.0	0.01	Cation efflux family
39630	1.6	0.01	Ribosomal protein S4
209875	3.6	0.01	-
55604	-19.9	0.01	-
204276	4.7	0.01	Zinc-containing alcohol dehydrogenase
210871	-8.7	0.01	3-hydroxyacyl-CoA dehydrogenase
203335	-2.1	0.01	-
212581	3.6	0.01	Acetohydroxy acid isomeroreductase
181179	-10.5	0.01	Catechol dioxygenase, N-terminal
209956	-3.5	0.01	-
55918	-2.6	0.01	Serine/threonine-specific protein phosphatase
48713	-5.3	0.01	DNA-binding SAP
209842	2.8	0.01	Phosphoribosyl pyrophosphate synthetase
183116	1.8	0.01	-
39912	1.9	0.01	DMQ mono-oxygenase
202289	1.5	0.01	-
55981	1.9	0.01	Cytochrome b5
190566	3.6	0.01	Predicted endoplasmic reticulum membrane protein Lec35
37420	2.7	0.01	-
137661	1.8	0.01	-
175118	-2.1	0.01	Mob1/phocein family
45363	3.5	0.01	-
56736	3.1	0.01	Haloacid dehalogenase-like hydrolase
56298	2.3	0.01	Putative mannosyl-oligosaccharide glucosidase, GH family 63
209768	3.4	0.01	Hypothetical protein of the Ribonuclease III supefamily

180792	2.8	0.01	Glutathione S-transferase
46100	1.9	0.01	-
197567	-1.6	0.01	Candidate vacuolar H+-transporting two-sector ATPase, C subunit
50833	-2.2	0.01	-
120372	-2.9	0.01	Phosphoinositide-specific phospholipase C (PLC)
42186	-5.7	0.01	-
50154	-6.1	0.01	Hypothetical ribulose-phosphate 3-epimerase
143917	-4.2	0.01	Upstream transcription factor
53053	13.2	0.01	Uroporphyrin III methyltransferase
52986	2.6	0.01	Lipoprotein
136397	-3.0	0.01	-
48817	-3.2	0.01	Transcription initiation factor IIA, gamma subunit
138063	2.2	0.01	-
136883	-1.8	0.01	-
206611	-2.3	0.01	Hypothetical Acyl-CoA-binding protein
40937	2.2	0.01	Hypothetical phosphoglycerate mutase; EC 5.4.2.1
37999	2.1	0.01	-
52796	2.6	0.01	Mitochondrial import inner membrane translocase, subunit Tim44
56137	3.1	0.01	-
41118	1.4	0.01	-
142899	1.5	0.01	-
143893	4.3	0.01	-
213656	-2.4	0.01	C2 domain
209919	-1.6	0.01	Tryptophanyl-tRNA synthetase
36379	2.1	0.01	Calcium-binding EF-hand
207169	-2.6	0.01	Receptor-activated Ca2+-permeable cation channels
208321	-3.7	0.01	Peroxisomal membrane protein MPV17 and related proteins
47444	2.3	0.01	-
176127	2.1	0.01	Predicted hydrolase related to dienelactone hydrolase
53082	-2.5	0.01	Related to histone 1 protein, H1, with a predicted H1/H5 domain, histone linker N- terminal, and winged helix DNA binding. The protein is essential for chromatin stucture and links nucleosomes in higher order structures; KOG Class: Chromatin structure and dynamics; KOG Id: 4012; KOG Description: Histone H1
39105	-3.5	0.01	-
213757	-3.0	0.01	Gamma-glutamyltranspeptidase
177781	-1.7	0.01	GCN5-related N-acetyltransferase
209754	-13.8	0.01	2-nitropropane dioxygenase
35897	-2.0	0.01	COP9 signalosome, subunit CSN7
211774	3.9	0.01	Amino acid/polyamine transporter I
56530	-3.8	0.01	Fungal specific transcription factor
52517	2.6	0.01	Peptidase S10, serine carboxypeptidase
189708	-5.2	0.01	-
172399	2.2	0.01	-
190892	2.2	0.01	Predicted sugar transporter
44184	-2.3	0.01	-
196275	2.2	0.01	-
52219	2.3	0.01	Glycoside hydrolase, family 28
57271	2.8	0.01	-
38426	1.9	0.01	Short-chain dehydrogenase/reductase
184312	-10.4	0.01	Glutathione S-transferase
52269	4.8	0.01	-

40514	-1.7	0.01	-
180337	2.7	0.01	Hypothetical. KOG suggests transcription regulation/DEAD box
203198	-3.9	0.01	-
197415	-5.1	0.01	Putative extracellular proteins sharing 38% amino acid sequence identity with Aspergillus oryzae glutaminase A (PMID: 10952006)
210048	-2.1	0.01	-
197883	3.2	0.01	Plasma membrane H+-transporting ATPase
198312	1.8	0.01	Reticulon-like protein
206339	-8.4	0.01	Haem peroxidase, plant/fungal/bacterial
42805	-4.3	0.01	-
46852	-2.1	0.01	Tyrosine specific protein phosphatase
171357	1.4	0.01	-
212792	1.8	0.01	-
209960	1.8	0.01	Porin, eukaryotic type
54125	-2.4	0.01	-
183782	1.7	0.01	Deduced protein shares amino acid sequence identity with Saccharomyces cerevisiae GCD10 gene product comprising a subunit of tRNA (1-methyladenosine) methyltransferase with Gcd14p; required for the modification of the adenine at position 58 in tRNAs, especially tRNAi-Met.
52947	-1.7	0.01	Peptidase C19
54056	2.6	0.01	Hypothetical protein kinase
183937	2.9	0.01	Hypothetical biphenyl-2,3-diol 1,2-dioxygenase III-related protein. Glyoxalase/Bleomycin resistance protein
183900	-5.1	0.01	-
49486	2.5	0.01	-
55365	-3.5	0.01	-
185461	-31.5	0.01	-
39573	-2.4	0.01	-
170262	-1.8	0.01	Aldo/keto reductase family proteins
192940	1.8	0.01	-
212230	-2.0	0.01	AAA ATPase
36773	-7.5	0.01	Hypothetical enoyl-CoA hydratase. (EC 4.2.1.17) HMM predicts secretion.
191260	-3.4	0.01	-
55511	4.3	0.01	Beta-ketoacyl synthase
193196	1.7	0.01	-
214565	-1.3	0.01	Mitochondrial F1F0-ATP synthase
44450	-5.2	0.01	-
210989	3.8	0.01	Amino acid/polyamine transporter I
190603	-1.8	0.01	4-hydroxyphenylpyruvate dioxygenase (Phenylalanin degradation)
201697	-2.5	0.01	Signal transduction protein with FHA domain
206203	-2.1	0.01	Zinc-containing alcohol dehydrogenase
201858	-2.0	0.01	H+-transporting two-sector ATPase
53706	3.3	0.01	Related to C-4 methylsterol monooxygenase
44367	-2.3	0.01	-
50189	2.1	0.01	Hypothetical protein, Contains WD40 repeat
54633	-2.8	0.01	Hypothetical protein containing Zn-finger, C2H2 type domain
128477	2.3	0.01	-
208631	-5.7	0.01	Predicted pyroglutamyl peptidase
191505	-3.0	0.01	Possible hexose transporter
55524	-2.5	0.01	Hypothetical transmembrane protein
56247	-2.8	0.01	Phospholipase D. Active site motif

46523	1.6	0.01	-
171996	-2.0	0.01	beta-1,6-N-acetylglucosaminyltransferase, contains WSC domain
127717	1.5	0.01	-
213629	-2.0	0.01	Drebrins and related actin binding proteins
210450	-1.5	0.01	AMP-dependent synthetase and ligase
127683	-2.1	0.01	Flavoprotein
208493	-2.0	0.01	-
56872	1.7	0.01	-
53446	2.5	0.01	-
182426	2.0	0.01	Hypothetical, ABC transporter
47821	-1.7	0.01	Ras small GTPase, Ras type
56395	-8.8	0.01	2-nitropropane dioxygenase
54814	9.7	0.01	D-xylulose 5-phosphate/D-fructose 6-phosphate phosphoketolase
46760	3.3	0.01	-
52139	-10.3	0.01	Peripheral-type benzodiazepine receptor
190721	1.5	0.01	Putative transcription factor
57366	2.3	0.01	-
55723	4.9	0.01	-
44808	-10.0	0.01	Acetyl-CoA acetyltransferase
55177	-1.5	0.01	-
173033	-9.6	0.01	Translation initiation factor 4F
52216	2.0	0.01	-
190197	5.1	0.01	(apsC) aminopeptidase C.
127495	4.3	0.01	-
176378	-5.4	0.01	Short-chain dehydrogenase/reductase
37809	-2.3	0.01	-
213466	-3.8	0.01	Peptidase
56753	7.4	0.01	Aromatic-ring hydroxylase
202202	-1.8	0.01	Hypothetical. Ca2+-binding actin-bundling protein (fimbrin/plastin)
207067	-6.9	0.01	HAD-superfamily hydrolase,
184327	11.4	0.01	Hypothetical cytochrome P450. Sequence similarity to an Aspergillus flavus cytochrome P450
197162	15.3	0.01	Sugar (ANd other) transporter
57253	-2.4	0.01	Ubiquitin-conjugating enzyme
203868	5.6	0.01	Aromatic-ring hydroxylase
210935	2.4	0.01	Candidate eukaryotic translation initiation factor 3
48625	1.9	0.01	-
56462	2.7	0.01	Candidate serine hydroxymethyltransferase (EC 2.1.2.1)
210213	15.2	0.01	Major facilitator superfamily
214748	2.2	0.01	Acyl-CoA synthetase
42464	-4.0	0.01	Candidate Peptidyl-prolyl cis-trans isomerase
142826	3.8	0.01	Ribosomal protein L27
210065	2.7	0.01	Transmembrane protein
47520	-5.3	0.01	Hypothetical protein
203483	2.0	0.01	-
44186	-7.3	0.01	Hypothetical protein. HMMPfam predicts short-chain dehydrogenase/reductase activity, but no similarity to proteins with confirmed activities are found. Signalp predicts secretion.
191512	3.2	0.02	Hypothetical enoyl-CoA hydratase (EC 4.2.1.17)
51852	-4.1	0.02	Phox-like
36316	7.1	0.02	-

57173	2.0	0.02	Hypothetical fungal transcription factor
143379	-11.8	0.02	Candidate mismatched base pair and cruciform DNA recognition protein
56523	-3.3	0.02	Related to leucine aminopeptidase
214265	-2.8	0.02	Putative polyubiquitin
56966	9.4	0.02	-
198624	2.4	0.02	Ribosomal protein S6
56739	2.9	0.02	Ornithine-N5-oxygenase
46429	-6.8	0.02	Glycosyl hydrolases family 35
35601	-2.1	0.02	-
55356	-1.5	0.02	Glucose-repressible alcohol dehydrogenase transcriptional effector CCR4 and related proteins
208447	1.7	0.02	Translation initiation factor 3
190964	1.7	0.02	Predicted member of the intramitochondrial sorting protein family
55609	3.5	0.02	-
138144	5.0	0.02	Ribosomal L32p protein
199912	-2.2	0.02	Oxysterol-binding protein
42357	-2.4	0.02	-
40460	-3.7	0.02	FAD-dependent oxidoreductase
177616	-2.3	0.02	Sugar transporter superfamily
209716	-1.9	0.02	Cu2+/Zn2+ superoxide dismutase SOD1
47416	3.2	0.02	Hypothetical protein, contains DENN domain
54451	-2.1	0.02	Hypothetical. Interpro: UTP-glucose-1-phosphate uridylyltransferase
42051	-1.7	0.02	-
210666	2.3	0.02	-
172548	-2.1	0.02	-
136082	-3.9	0.02	-
54354	2.4	0.02	-
177282	-3.4	0.02	-
191243	-2.4	0.02	Candidate amidase B (EC 3.5.1.4)
52343	-1.4	0.02	Hypothetical transcription factor TFIIB
43300	-3.5	0.02	Hypothetical dehydrogenase
183410	-1.8	0.02	-
213557	-2.7	0.02	Short-chain dehydrogenase/reductase
55055	-1.9	0.02	Hypothetical protein containing Zn-finger, C2H2 type domain
35857	2.6	0.02	-
44470	-1.9	0.02	Fungal specific transcription factor
52374	2.2	0.02	Hypothetical protein with ankyrin and DNA-binding domains
202252	-6.6	0.02	Putative extracellular tannase and feruloyl esterase
53232	1.6	0.02	Related to dihydrolipoamide dehydrogenase of Schizosaccharomyces pombe; EC 1.8.1.4
44662	2.6	0.02	-
54378	3.8	0.02	Related to alpha-1,3-glucan synthase
55566	11.3	0.02	Hydroxymethylglutaryl-coenzyme A synthase
52868	1.5	0.02	Hypothetical protein transporter of the TRAM (translocating chain-associating membrane) superfamily
141873	4.5	0.02	Carbon-nitrogen hydrolase
40088	1.6	0.02	Hypothetical protein with predicted Structure-specific recognition protein (SSRP) domain
202206	-1.6	0.02	Gamma-glutamyl phosphate reductase
213093	-2.0	0.02	Proteasome/cyclosome, regulatory subunit

177406	-4.9	0.02	-
211915	2.2	0.02	Ribosomal protein L23
170709	-5.5	0.02	Aldehyde dehydrogenase
202139	-3.1	0.02	Ubiquitin-like protein
187304	3.6	0.02	Ergosterol biosynthesis ERG4/ERG24 family
127809	1.3	0.02	Hypothetical extracellular thaumatin domain protein
47870	-1.8	0.02	-
205810	1.8	0.02	Calnexin
177851	2.0	0.02	FOG: WD40 repeat
191821	-1.9	0.02	Hypothetical. Predicted transporter (major facilitator superfamily
41928	1.5	0.02	-
128744	-2.9	0.02	-
173139	-11.7	0.02	Methionine synthase, vitamin-B12 independent
212637	-2.6	0.02	Hypothetical protein containing fungal specific transcription factor and fungal transcriptional regulatory protein domains.
41950	2.2	0.02	-
207638	-2.0	0.02	Golgi-associated protein/Nedd4 WW domain-binding protein
37382	3.4	0.02	Mitochondrial/chloroplast ribosomal protein L54/L37
49427	-2.0	0.02	-
119946	-1.7	0.02	AAA ATPase
130735	-2.4	0.02	-
39372	-4.6	0.02	-
209145	-3.8	0.02	Interferon-related protein PC4 like
55534	1.6	0.02	-
189874	2.0	0.02	Short-chain dehydrogenase/reductase
54140	2.3	0.02	Hypothetical myosin assembly protein/sexual cycle protein in A. niger
51779	4.2	0.02	-
46666	1.6	0.02	Pyridoxal/pyridoxine/pyridoxamine kinase
55693	-2.4	0.02	-
197817	3.3	0.02	E3 binding
49258	-3.8	0.02	Hypothetical aldehyde dehydrogenase. May be a succinate-semialdehyde dehydrogenase
211385	-1.8	0.02	-
51257	2.2	0.02	Deduced translation product shares amino acid sequence identity with the Saccharomyces cerevisiae NOP14 gene product; a aucleolar protein that forms a complex with Noc4p and mediates maturation and nuclear export of 40S ribosomal subunits; also present in the small subunit processome complex, which is required for processing of pre-18S rRNA.
53140	-2.0	0.02	FMN-dependent dehydrogenase
173978	1.5	0.02	-
206560	1.3	0.02	Microtubule-associated protein
178051	-1.6	0.02	Related to A. nidulans CreC
42034	31.0	0.02	Formate/nitrite transporter
56606	2.5	0.02	Mitochondrial/chloroplast ribosomal protein
195925	2.1	0.02	Transcription factor containing homeobox and Zn-finger
53893	3.4	0.02	Phosphatidylethanolamine binding protein
199928	-4.9	0.02	Predicted hydrolase
198862	2.8	0.02	Ribosomal protein S11
120939	4.0	0.02	-
201294	1.6	0.02	-

119891	-1.5	0.02	Inorganic pyrophosphatase
206461	-2.1	0.02	-
52861	-2.0	0.02	Uncharacterised conserved protein XAP-5
195095	2.5	0.02	Related to zink transporter of A. fumigatus
125824	-2.8	0.02	-
52387	-1.8	0.02	Hypothetical H+-transporting two-sector ATPase
127816	-2.4	0.02	SNARE protein
56053	4.0	0.02	-
133626	2.0	0.02	Hypothetical DnaJ domain protein
206779	-1.9	0.02	Core histone H2A/H2B/H3/H4
53381	2.4	0.02	Cytochrome b5 domain
208917	-6.5	0.02	-
209830	12.5	0.02	Hypothetical FAD/FMN-containing dehydrogenase
211145	2.7	0.02	-
173724	2.5	0.02	-
189339	1.2	0.02	-
51267	2.9	0.02	Oligosaccharyltransferase subunit
205553	2.0	0.02	Insulinase-like
128153	2.5	0.02	Hypothetical Sec61 protein translocation complex, beta subunit
52574	1.5	0.02	-
39772	1.7	0.02	Kinesin-like protein
171583	-2.2	0.02	-
45789	1.3	0.02	Hypothetical copper amine oxidase
188782	-1.8	0.02	Amino acid transporters
46527	1.5	0.02	-
125912	-2.9	0.02	-
211906	-1.7	0.02	-
52105	-25.2	0.02	Amidohydrolase
134406	-2.8	0.02	-
51717	2.3	0.02	Hypothetical Mitochondrial phosphate carrier protein
211641	-1.9	0.02	-
41530	3.8	0.02	Hypothetical glycosylphosphatidylinositol anchor synthesis protein
200274	1.9	0.02	TATA-binding protein
189204	-3.2	0.02	Hypothetical DNA repair protein (RAD4 like)
54719	-1.9	0.02	Protein kinase
202514	-2.2	0.02	-
200255	1.4	0.02	Hypothetical cation efflux protein
190212	-1.8	0.02	Splicing coactivator SRm160/300, subunit SRm300
44253	-1.9	0.02	-
191350	2.3	0.02	-
205431	-2.0	0.02	Molecular chaperones HSP70/HSC70, HSP70 superfamily
55041	2.8	0.02	-
208113	-1.6	0.02	Mitochondrial substrate carrier
209236	1.9	0.02	Ribonuclease HII
210981	-2.6	0.02	Putative extracellular GH family 3 beta-glucosiadse
212641	-2.5	0.02	Hypothetical protein with esterase/lipase/thioesterase and signal peptide motifs
36108	-1.7	0.02	Protein kinase PCTAIRE and related kinases
55190	-1.5	0.02	-
54651	-10.4	0.02	Hypothetical 3-ketoacyl-CoA-thiolase
181863	1.7	0.02	-
50560	-3.3	0.02	Predicted ubiquitin regulatory protein
37318	1.5	0.02	-

46776	-2.7	0.02	TatD-related DNase
184246	2.9	0.02	-
124989	1.4	0.02	U4/U6 small nuclear ribonucleoprotein Prp4 (contains WD40 repeats)
56853	1.6	0.02	Deduced translation product shares amino acid sequence identity with the Saccharomyces cerevisiae PNO1 gene product; an essential nucleolar protein required for pre-18S rRNA processing; in yeast Pno1p interacts with Dim1p, an 18S rRNA dimethyltransferase, and also with Nob1p, which is involved in proteasome biogenesis; contains a KH domain.
179558	-1.7	0.02	-
205670	-14.8	0.02	Glycoside hydrolase, family 3
126807	1.6	0.02	Preprotein translocase subunit
212837	2.3	0.02	UTP--glucose-1-phosphate uridylyltransferase
192694	-3.1	0.02	Zinc-containing alcohol dehydrogenase
204313	1.5	0.02	-
122081	-4.6	0.02	-
191038	-1.6	0.02	Amino acid/polyamine transporter
45504	-2.1	0.02	-
39277	-9.2	0.02	-
203770	1.8	0.02	Protein kinase
173727	-2.1	0.02	-
53188	-1.9	0.02	-
211011	-3.3	0.02	-
203739	2.0	0.02	Hypothetical ubiquinol cytochrome c reductase, subunit QCR7
206266	3.1	0.02	Cytochrome P450
179623	2.3	0.02	WD40 repeat protein
197132	2.7	0.02	-
189398	-2.9	0.02	Protein of unknown function UPF0075
38830	2.5	0.02	-
119858	-4.4	0.02	Related to alpha-glucosidase; glycoside hydrolase, family 31
213343	2.3	0.02	Predicted 3-hydroxy-3-methylglutaryl-CoA (HMG-CoA) reductase
205376	1.4	0.02	-
214072	-2.6	0.02	SCF ubiquitin ligase, Skp1 component
212646	2.3	0.02	-
55164	-7.0	0.02	-
209397	-2.9	0.02	-
128007	-2.6	0.02	Membrane protein involved in organellar division
206911	-1.9	0.02	Hypothetical protein tyrosine phosphatase
206304	2.5	0.02	Hypothetical RAS GTPase
36238	-2.2	0.02	Hypothetical protein; KOG Class: Chromatin structure and dynamics; KOG Id: 4191; KOG Description: Histone acetyltransferases PCAF/SAGA/ADA, subunit TADA3L/NGG1
210029	2.0	0.02	Candidate translational cofactor elongation factor-1 gamma
119390	-1.8	0.02	Hypothetical vacuolar assembly/sorting protein PEP5/VPS11
57172	-6.3	0.02	-
50015	-2.5	0.02	Hypothetical, DNA-binding
40813	2.0	0.02	Hypothetical protein containing basic-leucine zipper transcription factor domain
213414	1.8	0.02	Predicted transporter (ABC superfamily)
52503	-1.9	0.02	Peptidase C19
119363	1.4	0.02	-
44905	1.8	0.02	-

186735	3.3	0.02	-
206990	-2.1	0.02	HMG box-containing protein
53675	-2.0	0.02	Predicted protein shares amino acid sequence identity with the Saccharomyces cerevisiae SKI3 gene product; a protein involved in exosome mediated 3' to 5' mRNA degradation and translation inhibition of non-poly(A) mRNAs; forms complex with Ski2p and Ski8p; required for repressing propagation of dsRNA viruses.
196788	-1.7	0.02	Hypothetical CCAAT-binding factor; KOG Class: Transcription; KOG Id: 0869; KOG description: CCAAT-binding factor, subunit A (HAP3)
55573	7.8	0.02	Candidate pyruvate decarboxylase
54391	3.2	0.02	Hypothetical homoserine O-acetyltransferase (EC 2.3.1.31).
212490	2.1	0.02	Cell division/GTP binding protein
38375	-19.2	0.02	Major facilitator superfamily
49162	1.5	0.02	Major facilitator superfamily
206713	-2.1	0.02	-
213947	-2.0	0.02	Hypothetical protein with RRM domain
207006	-1.6	0.02	-
57261	-1.5	0.02	Hypothetical Chaperone DnaJ
207705	-1.8	0.02	Hypothetical 26S proteasome, regulatory subunit
213834	-1.5	0.02	Permease for cytosine/purines
127896	-1.9	0.02	-
54934	1.7	0.02	-
143899	-2.0	0.02	-
214608	1.6	0.02	Candidate endo-1,4-beta-glucanase; glucan 1,4-beta-glucosidase; glycoside hydrolase, family 5; cellulose-binding region, fungal
203604	1.8	0.02	Aminoacyl-tRNA synthetase
55758	-1.5	0.02	Zn-finger, AN1-like
198565	1.9	0.02	-
193227	1.7	0.02	-
188256	-4.9	0.02	Hypothetical. Interpro: eukaryotic cysteine peptidase active site
206723	-3.4	0.02	-
54707	-2.4	0.02	Involved in autophagocytosis
53390	1.5	0.02	-
56133	-3.0	0.02	ABC superfamily
51896	1.4	0.02	Hypothetical. KOG suggests role in cell division
170127	3.2	0.02	-
179224	-2.0	0.02	TIP120 family protein, Cullin-associated NEDD8-dissociated protein
55560	-5.8	0.02	mannitol-1-phosphate 5-dehydrogenase
121874	-1.5	0.02	Putative extracellular carboxylesterase, type B
193894	-2.7	0.02	-
190578	-1.8	0.02	-
209184	-2.4	0.02	Oxysterol-binding protein
173461	-2.1	0.02	-
54957	1.7	0.02	Putative GroEL-like chaperone, ATPase
134540	1.5	0.02	Fungal transcriptional regulatory protein, N-terminal
36938	-1.2	0.02	Hypothetical. KOG: Collagens (type IV and type XIII)
122116	-4.7	0.02	Metacaspase involved in regulation of apoptosis
185119	-1.5	0.02	Hypothetical protein , contains FHA domain
56454	3.0	0.02	-
52740	2.7	0.02	Myosin class II heavy chain
193151	2.1	0.02	-

208463	1.9	0.02	-
44729	-26.1	0.02	Zinc-containing alcohol dehydrogenase superfamily
180728	-1.9	0.02	-
50898	3.8	0.02	Hypothetical permease. 10 predicted transmembrane domains. May have Xanthine/uracil transporter activity
181975	1.6	0.02	Hypothetical Alkaline phytoceramidase
45871	2.0	0.02	-
183812	2.0	0.02	Major facilitator superfamily
45900	-1.7	0.02	Hypothetical. KOG suggests Carbonic anhydrase. Simil suggests DNA polymerase subunit
54557	-2.2	0.02	-
176547	1.5	0.02	RNA recognition motif (RRM)
181231	-1.8	0.02	-
210131	1.7	0.02	-
35976	4.5	0.02	Major facilitator superfamily
133729	2.8	0.02	RNA-binding protein
177953	-1.6	0.02	Hypothetical Zn finger protein with RING domain
213441	5.7	0.02	Squalene monooxygenase
179884	-1.9	0.02	Protein kinase
56378	-2.2	0.02	-
36700	2.1	0.02	AAA ATPase
184522	2.0	0.02	Hypothetical DNA polymerase
204610	3.1	0.02	Ribosomal protein L7/L12
180715	1.7	0.02	Hypothetical ubiquitin-dependent hydrolase
52571	1.5	0.02	Ribosomal protein S17
45769	-2.3	0.02	Hypothetical FAD/FMN-containing dehydrogenase with signal peptide motif
47307	-3.0	0.02	Methyltransferases
185138	-1.5	0.02	Candidate GCN5-related histone actyltransferase (GNAT)
214611	1.9	0.02	Candidate multidrug resistance ABC transporter
213627	1.9	0.02	Dynamin GTPase effector
56568	-5.1	0.02	Hypothetical aldehyde dehydrogenase (EC 1.2.1.3).
47390	-2.6	0.02	-
207831	-8.1	0.02	Glucose-methanol-choline oxidoreductase
180069	-8.5	0.02	Major facilitator superfamily
45394	1.5	0.02	-
170610	-1.4	0.02	Cytochrome P450
47683	-2.0	0.02	-
54097	9.4	0.02	Flavohemoglobon
134658	-1.7	0.02	Hypothetical 3-methyladenine DNA glycosidase
184977	3.1	0.02	Mitochondrial substrate carrier
50449	1.6	0.02	Hypothetical RNA procesing protein
52803	2.8	0.02	Mitochondrial substrate carrier
201822	6.0	0.02	Methylmalonate semialdehyde dehydrogenase
41315	2.4	0.02	Hypothetical Protein involved in inorganic phosphate transport
173004	-1.2	0.02	Predicted hydrolase related to dienelactone hydrolase
203924	2.1	0.02	Putative protein transport protein SEC61 subunit alpha. Probable endoplasmic reticulum
122948	-1.5	0.02	-
53084	-1.9	0.02	Ubiquitin-conjugating enzymes, 16 kDa
46152	1.6	0.02	-
212507	-4.0	0.02	-
52653	-2.9	0.02	Phosphotyrosyl phosphatase activator
211901	3.2	0.02	-

199159	-3.9	0.02	-
52344	-7.2	0.02	-
46991	1.8	0.02	Peptidase S16, lon protease
132806	-5.0	0.02	-
197549	-21.4	0.02	Sugar (ANd other) transporter
40043	3.1	0.02	-
52874	-3.3	0.02	Serine/threonine protein kinase
125779	4.0	0.02	-
120053	-4.8	0.02	Fungal specific transcription factor
39998	1.9	0.02	Hypothetical subunit of oligosaccharyltransferase
180255	-2.6	0.02	neutral zinc metallopeptidases
54972	1.9	0.02	FAD binding domain
44695	2.4	0.02	-
56235	1.9	0.02	Peptidase C50, separase
43265	-72.1	0.02	-
54021	1.5	0.02	-
51373	-4.5	0.02	-
175181	-3.2	0.02	Phox-like
39760	-1.5	0.02	-
36048	-1.3	0.02	-
212162	1.6	0.02	-
175900	2.4	0.02	GCN5-related N-acetyltransferase
51738	-1.4	0.02	-
54080	4.0	0.02	-
44000	3.6	0.02	Hypothetical Isochorismatase hydrolase
49063	-6.0	0.02	Hypothetical fatty acid omega-hydroxylase
193955	-1.6	0.02	beta-1,6-N-acetylglucosaminyltransferase, contains WSC domain
51069	1.6	0.03	Hypothetical protein with predicted SET, AWS & WW domains; KOG Class: Intracellular trafficking, secretion, and vesicular transport; KOG Id: 4442; KOG description: Clathrin coat binding
196638	1.6	0.03	60S acidic ribosomal protein P0
42079	-2.8	0.03	-
178656	1.6	0.03	-
53856	-2.3	0.03	Protein phosphatase
52108	2.5	0.03	-
42733	2.9	0.03	Dihydroxy-acid dehydratase
209138	1.6	0.03	Transcription elongation factor
180771	-1.5	0.03	-
210632	1.4	0.03	tRNA synthetase anti-codon binding domain
186860	-7.2	0.03	Aminotransferase class-III
213042	-7.8	0.03	MOSC N-terminal beta barrel domain
211200	-2.6	0.03	Snf7 family protein
55287	-2.3	0.03	Metallophosphoesterase
55463	-1.3	0.03	-
175686	2.2	0.03	Myosin class II heavy chain
48373	2.2	0.03	Uncharacterised conserved protein similar to ATP/GTP-binding protein
180608	-5.9	0.03	-
120524	1.3	0.03	Fungal specific transcription factor
53788	4.4	0.03	Nucleoside phosphatase
128495	-3.0	0.03	-
48357	-1.8	0.03	-
140924	1.7	0.03	-

184532	-2.1	0.03	-
196241	1.7	0.03	-
140013	3.6	0.03	-
208365	-2.5	0.03	Hypothetical. KOG: aldo/keto reductase
38566	-1.8	0.03	Hypothetical. RNA splicing. Related to S. cerev.TRL, tRNA ligase, required for tRNA splicing
174315	-4.1	0.03	-
193828	-1.4	0.03	-
203350	1.5	0.03	-
37976	3.2	0.03	-
121695	-5.1	0.03	AMP-dependent synthetase and ligase
207741	-1.4	0.03	Hypothetical transcription initiation factor TFIIE, beta subunit
35810	1.7	0.03	DEAD/DEAH box helicase
180548	-4.1	0.03	-
200652	1.6	0.03	C-3 sterol dehydrogenase/3-beta-hydroxysteroid dehydrogenase and related dehydrogenases
42784	6.5	0.03	-
189430	-2.6	0.03	Hypothetical 2-nitropropane dioxygenase. (EC 1.13.11.32)
195992	-2.5	0.03	Hypothetical cyclic-AMP phosphodiesterase
57150	-2.2	0.03	-
48279	1.6	0.03	-
186792	-4.5	0.03	-
44995	1.3	0.03	Hypothetical protein with Zn-finger, Tim10/DDP type
53811	-1.7	0.03	Related to profilin an actin bindin protein involved in cytoskeleton dynamics
196559	-2.1	0.03	-
43654	-1.8	0.03	-
206734	1.3	0.03	Hypothetical. Interpro: H+-transporting two-sector ATPase
125918	2.1	0.03	RNA-binding proteins
54733	2.0	0.03	Eukaryotic transcription factor with helix-loop-helix DNA-binding domain
36622	-1.3	0.03	Hypothetical protein with predicted SET domain & TPR repeat; KOG Class: Chromatin structure and dynamics; KOG Id: 2084; KOG Description: Predicted histone tail methylase containing SET domain
56243	-1.6	0.03	Electron transfer flavoprotein
212044	1.3	0.03	Mitochondrial ADP/ATP carrier proteins
201534	-2.2	0.03	-
128714	-2.8	0.03	Candidate Rad54 homolog (first part); Related to Vac14 homolog (second part)
55273	4.1	0.03	ABC transporter protein. Induced at low pH (2.5).
120468	-2.0	0.03	Fungal specific transcription factor
212036	-1.5	0.03	Tyrosine specific protein phosphatase and dual specificity protein phosphatase
206143	-4.5	0.03	-
186006	-5.5	0.03	-
52348	-1.8	0.03	-
56941	1.3	0.03	-
136905	-2.3	0.03	-
180730	1.9	0.03	-
208826	-2.6	0.03	-
214216	-1.6	0.03	Calmodulin
43767	1.5	0.03	-

46856	2.0	0.03	DEAD/DEAH box helicase
206496	1.7	0.03	Molecular chaperone of the GrpE family
40531	1.3	0.03	Citron-like
200874	8.7	0.03	Transmembrane amino acid transporter protein
194814	-2.1	0.03	-
122135	-2.3	0.03	-
196625	1.8	0.03	Hypothetical. KOG: putative COPII vesicle protein
35666	1.8	0.03	FAD linked oxidase
44921	-1.9	0.03	-
174413	-4.9	0.03	Candidate galactose-1-phosphate uridyl transferase
47364	-4.2	0.03	Candidate catalase
179989	-2.4	0.03	-
203210	1.9	0.03	-
212525	2.0	0.03	Candidate DNA replication licensing factor
45992	3.7	0.03	(chsC) Class-III chitin synthase C
46311	-1.5	0.03	Members of tubulin/FtsZ family
44596	1.6	0.03	GCN5-related N-acetyltransferase
53008	2.5	0.03	Hypothetical aminopeptidase
186010	1.6	0.03	-
52361	2.8	0.03	-
200845	-3.6	0.03	Phospholipase D/Transphosphatidylase
56548	3.6	0.03	Generic methyltransferase
174264	1.6	0.03	-
53636	2.5	0.03	DNA-directed DNA polymerase B
53686	1.3	0.03	Aldo/keto reductase family proteins
48843	3.0	0.03	rRNA processing protein
42089	1.5	0.03	Predicted translation product shares amino acid sequence identity with the Saccharomyces cerevisiae SEN1 gene product; a nuclear protein, putative helicase required for processing of tRNAs, rRNAs, and small nuclear RNAs; potential Cdc28p substrate.
204742	1.6	0.03	Hypothetical protein involved in chromatin remodelling
143435	1.5	0.03	-
38788	-3.2	0.03	Amino acid/polyamine transporter
173677	-14.5	0.03	Hypothetical. Ketopantoate reductase pyrimidin base metabolism
206783	11.4	0.03	-
213169	2.1	0.03	GHMP kinase
51832	2.8	0.03	-
35583	1.9	0.03	Deduced amino acid sequence shares identity with the Saccharomyces cerevisiae NCL1 gene product; an S-adenosyl-L-methionine-dependent tRNA: m5C-methyltransferase; methylates cytosine to m5C at several positions in tRNAs and intron-containing pre-tRNAs.
170910	-2.1	0.03	Glucose/ribitol dehydrogenase
183972	1.4	0.03	Major facilitator superfamily
191568	-9.5	0.03	Predicted glutathione S-transferase
177836	1.5	0.03	-
128905	2.9	0.03	Protein kinase
50147	1.5	0.03	Hypothetical Amino acid/polyamine transporter II
207105	1.5	0.03	-
53033	1.5	0.03	Related to beta-1,3-glucanosyltransferase
40602	1.5	0.03	-
211789	15.7	0.03	-
200493	5.5	0.03	Imidazoleglycerol-phosphate dehydratase

37023	-1.5	0.03	-
178686	-1.9	0.03	Fungal transcriptional regulatory protein
208354	1.7	0.03	-
49311	-10.2	0.03	Hypothetical, similarities to sialidase superfamily
53473	-3.7	0.03	-
56299	-1.5	0.03	-
53696	1.6	0.03	Major facilitator superfamily
39857	1.4	0.03	-
119945	1.7	0.03	-
205426	-2.4	0.03	Peptidase
202677	2.3	0.03	-
205095	-6.5	0.03	Short-chain dehydrogenase/reductase
120073	2.3	0.03	Serine/threonine protein kinase
181938	-1.9	0.03	Ypt/Rab-specific GTPase-activating protein GYP7 and related proteins
196738	2.6	0.03	Signaling protein
172823	1.7	0.03	Related to zink transporter of A. fumigatus. Seven putative transmembrane domains and PFam domains for zink transport.
51930	-1.6	0.03	Gen A8; hypothetical Cyanovirin-N protein
121710	-2.2	0.03	Amidases
46980	1.8	0.03	ABC transporter
208679	1.5	0.03	-
135865	1.3	0.03	-
214413	-2.0	0.03	Vacuolar protein sorting-associated protein
56457	-2.8	0.03	(cmkB) calcium/calmodulin dependent protein kinase B - high homology to cmkB in A. nidulans
205452	1.6	0.03	Hypothetical translation initiation factor 4F
44892	1.4	0.03	-
138876	1.4	0.03	beta-mannosidase A
193056	-2.0	0.03	-
201912	-1.7	0.03	-
128279	1.9	0.03	-
191935	1.5	0.03	-
176923	2.1	0.03	-
41302	1.4	0.03	-
206219	4.6	0.03	ERG2 and sigma1 receptor-like protein
184233	1.6	0.03	-
185018	-1.9	0.03	-
187701	-4.1	0.03	Electron transporter activity
180923	-10.4	0.03	Major facilitator superfamily
47908	2.2	0.03	Short-chain dehydrogenase/reductase SDR
211941	2.9	0.03	Predicted protein shares amino acid sequence identity with the Saccharomyces cerevisiae TRM2 gene product; a tRNA methyltransferase, 5-methylates the uridine residue at position 54 of tRNAs and may also have a role in tRNA stabilization or maturation; previously thought to be an endo-exonuclease.
196499	-8.3	0.03	Major facilitator superfamily
51836	1.4	0.03	Zn-finger, CCHC type
56841	2.5	0.03	Putative transmembrane GH family 47 mannosyl-oligosaccharide 1,2-alpha-mannosidase
49344	2.6	0.03	Putative GH family 76 endo-1,6-alpha-mannanase
47312	1.6	0.03	Kinesin-like protein
129990	2.3	0.03	FOG: PPR repeat
195339	1.3	0.03	-

213924	-1.8	0.03	-
172886	-2.0	0.03	-
39962	-2.1	0.03	Phosphoinositide 3-kinase, C2
195119	1.2	0.03	Esterase/lipase/thioesterase
198750	21.0	0.03	Ammonium transporter
52406	3.3	0.03	Beta-ketoacyl synthase
40477	-2.2	0.03	Hypothetical. Some similarity to alkylhydroperoxidase
45821	2.1	0.03	(pelB) extracellular pectin lyase B
49775	-1.4	0.03	-
54127	1.3	0.03	-
119842	1.4	0.03	Zn-finger-like, PHD finger
39899	1.4	0.03	Hypothetical Signal recognition particle, subunit Srp68
136326	-2.7	0.03	-
205686	1.5	0.03	-
130307	-3.1	0.03	RNA-binding protein required for biogenesis of the ribosomal 60S subunit
44628	-2.3	0.03	-
188766	1.3	0.03	-
55655	1.8	0.03	-
124929	-1.6	0.03	Metallophosphoesterase
55493	3.0	0.03	Related to serine protease
49158	-2.2	0.03	Hypothetical NADH:flavin oxidoreductase/NADH oxidase-like protein
127656	-1.9	0.03	Calcium-binding EF-hand
180223	2.6	0.03	Mitochondrial substrate carrier
211361	-2.9	0.03	-
40805	1.6	0.03	-
209060	1.3	0.03	-
190584	-1.5	0.03	-
176070	-6.9	0.03	ATP-dependent DNA ligase
52362	1.8	0.03	Candidate 40S ribosomal protein S0.
48684	-3.6	0.03	-
171513	-1.5	0.03	GCN5-related N-acetyltransferase
205428	-60.4	0.03	-
36654	1.5	0.03	Hypothetical. Initiation factor 2B domain and NUDIX hydrolase domain
185751	-1.6	0.03	Hypothetical lysophospholipase
125201	-4.2	0.03	Esterase/lipase/thioesterase
50844	-3.5	0.03	Hypothetical Fungal specific transcription factor
197123	-2.0	0.03	Rab GDI protein
178195	2.0	0.03	Hypothetical protein with an ARM repeat fold
205572	-2.0	0.03	Hypothetical protein containing Zn-finger, C2H2 type and U1-like domains
190030	-3.9	0.03	Aldo/keto reductase family proteins
47488	1.7	0.03	DEAD/DEAH box helicase
53339	2.8	0.03	Malate dehydrogenase
180990	-4.3	0.03	Zinc-binding oxidoreductase
35726	3.7	0.03	-
52713	-1.7	0.03	Glucosamine 6-phosphate synthetases, contain amidotransferase and phosphosugar isomerase domains
189779	6.1	0.03	-
137999	-2.1	0.03	Predicted coiled-coil protein
44558	-2.3	0.03	-
205450	-2.0	0.03	-

52275	-3.8	0.03	-
46302	2.9	0.03	Serine/threonine protein kinase
189606	2.6	0.03	Fungal specific transcription factor
44704	2.0	0.03	Predicted translation product shares amino acid sequence identity with the Saccharomyces cerevisiae PAP2 gene product; the catalytic subunit of TRAMP (Trf4/Pap2p-Mtr4p-Air1p/2p), a nuclear poly (A) polymerase complex involved in RNA quality control; catalyses polyadenylation of unmodified tRNAs, and snoRNA and rRNA precursors; disputed role as a DNA polymerase (yeast).
38790	1.4	0.03	Hypothetical protein.
54742	1.8	0.03	-
176572	1.6	0.03	-
214187	-5.3	0.03	-
205005	-4.4	0.03	Putative soluble Fumarate reductase/succinate dehydrogenase flavoprotein, N-terminal
55487	-2.2	0.03	-
178864	4.0	0.03	Protein involved in ubiquinone biosynthesis
186794	2.0	0.03	Related to pseudouridine synthase.
183189	1.6	0.03	-
197120	1.7	0.03	Ribosomal protein L29
38223	1.3	0.03	-
202801	2.1	0.03	citA citrate synthase
40316	1.5	0.03	AAA ATPase
199085	-2.1	0.03	Putative GH family 16 GPI-glucanosyltransferase
38822	1.3	0.03	Predicted gene product shares amino acid sequence identity with the Saccharomyces cerevisiae UTP20 gene product; a component of the small-subunit (SSU) processome, which is involved in the biogenesis of the 18S rRNA.
54428	1.5	0.03	-
205944	-1.8	0.03	-
197539	-1.1	0.03	Transcription factor of the Forkhead/HNF3 family
49138	2.0	0.03	AAA ATPase
211648	1.6	0.03	ATP-dependent RNA helicase
175987	-4.1	0.03	Carbon-nitrogen hydrolase
56228	-3.7	0.03	-
200777	-1.7	0.03	Hypothetical mitotic spindle checkpoint protein
52614	-4.6	0.03	FAD-binding protein DIMINUTO
210170	-1.3	0.03	-
36739	4.2	0.03	-
55790	-1.5	0.03	Putative allergen produced in response to stress or pathogen infection
132415	1.4	0.03	WD40 protein
56242	-1.4	0.03	-
213815	-12.7	0.03	Cytoskeletal protein A
55611	1.6	0.03	Putative eIF2 alpha subunit, similar to Gcn3p of S. cerevisiae. possibly involved in translation initiation and protein biosynthesis.
136603	-2.0	0.03	Hypothetical transcription initiation factor. A putative YEATS domain is present in the sequence
56633	-3.2	0.03	-
129862	-1.6	0.03	Glycosyl transferase, family 25
194528	-1.9	0.03	-
139340	2.9	0.03	-
47046	2.1	0.03	Hypothetical Ras GTPase
41998	-3.5	0.03	-
190360	1.8	0.03	-

208486	-1.6	0.03	Peptidase S10
48500	1.8	0.03	-
46099	4.9	0.03	-
39964	2.5	0.03	Conserved ATP/GTP binding protein
174983	1.6	0.03	Predicted methyltransferase
176363	-11.3	0.03	-
50062	1.3	0.03	Hypothetical TGc (transglutaminase/protease-like) domain-containing protein involved in cytokinesis
57417	-1.9	0.03	-
201412	-3.9	0.03	-
185301	-2.5	0.03	Hypothetical carboxylesterase
47141	1.5	0.03	-
45817	2.3	0.03	beta-1,6-N-acetylglucosaminyltransferase, contains WSC domain
40956	2.7	0.03	-
130150	-1.4	0.03	Serine/threonine protein kinase
193903	1.5	0.03	Predicted nucleolar protein involved in ribosome biogenesis
182597	-1.5	0.03	Zn-finger transcription factor
42045	-2.0	0.03	Ankyrin repeat
48560	-2.0	0.03	Glutathione S-transferase
206802	2.8	0.03	Serine/threonine protein kinase
56664	-8.0	0.03	Exoinulinase
211484	-2.1	0.04	TATA box binding protein (TBP)-associated factor, RNA polymerase II
212420	2.1	0.04	Hypothetical ribosomal protein
172476	-2.6	0.04	-
190129	3.2	0.04	-
39748	1.6	0.04	-
43857	-2.3	0.04	Amino acid permease
173527	1.4	0.04	Related to the extracellular pectin lyase C
54860	35.8	0.04	Purine nucleoside permease
196801	-2.2	0.04	Seems like two proteins have been combined in one model
38920	-2.5	0.04	-
48810	1.8	0.04	-
121960	-1.7	0.04	-
200605	-37.0	0.04	(abfB) alpha-L-arabinofuranosidase B
191214	3.9	0.04	Hypothetical. Helicase domain
211010	-1.9	0.04	Protein kinase
52239	-2.6	0.04	-
37575	-2.2	0.04	-
49003	2.7	0.04	-
36779	1.5	0.04	Hypothetical dihydroorotate dehydrogenase (EC 1.3.3.1)
187898	-1.6	0.04	Predicted glycosyltransferase
211766	-15.7	0.04	SAM (and some other nucleotide) binding motif
40151	1.5	0.04	Caspase-1, p20
180211	-10.0	0.04	Alpha/beta hydrolase
178365	-6.0	0.04	Hypothetical aspartic protea
197786	-1.5	0.04	(dapB) dipeptidylpeptidase
40078	1.8	0.04	Predicted metalloprotease with chaperone activity
187366	-4.3	0.04	AMP-binding enzyme
183511	-5.6	0.04	Fungal transcriptional regulatory protein

196062	2.5	0.04	Deduced translation product shares amino acid sequence identity with the Saccharomyces cerevisiae NOP1 gene product; a nucleolar protein, component of the small subunit processome complex, which is required for processing of pre-18S rRNA; has similarity to mammalian fibrillarin.
194861	1.2	0.04	Hypothetical shikimate/quinate 5-dehydrogenase
35846	1.5	0.04	-
172596	-2.1	0.04	-
56429	1.3	0.04	-
186797	-1.4	0.04	-
53994	1.8	0.04	-
207173	-2.1	0.04	FYVE finger-containing protein
211899	-2.4	0.04	Protein kinase
46407	2.4	0.04	DEAD/DEAH box helicase
47735	-2.9	0.04	Uncharacterised conserved protein predicted to be involved in protein sorting
196160	-2.8	0.04	-
51602	-2.3	0.04	-
170573	2.2	0.04	-
191708	2.2	0.04	-
206020	3.5	0.04	Hypothetical. involved in rRNA processing. associates with trans-acting ribosome biogenesis factors (yeast); similar to beta-transducin superfamily.
54073	12.0	0.04	-
188553	-18.1	0.04	Acyl-CoA dehydrogenase
36331	-6.9	0.04	-
192427	-2.0	0.04	-
179151	1.2	0.04	Aminotransferase
210597	-1.4	0.04	cAMP-dependent protein kinase
184098	1.6	0.04	-
210994	1.6	0.04	-
119438	-1.4	0.04	Phosphoprotein involved in cytosol to vacuolar targeting and autophagocytosis
212289	1.9	0.04	Candidate 6,7-dimethyl-8-ribityllumazine synthase
55704	-3.1	0.04	(tpsA) trehalose-6-phosphate synthase A
54208	-1.8	0.04	AAA ATPase
211598	-3.7	0.04	-
39109	-2.5	0.04	-
48067	1.8	0.04	Hydroxyindole-O-methyltransferase and related SAM-dependent methyltransferases
123950	-2.0	0.04	Protein phosphatase 2C-like
199609	-2.4	0.04	Fungal transcriptional regulatory protein
54575	1.6	0.04	-
53463	3.5	0.04	Cation efflux family
121846	1.6	0.04	-
176596	1.9	0.04	Cytochrome P450
52961	1.4	0.04	PolyC-binding proteins alphaCP-1 and related KH domain proteins
56345	-2.8	0.04	Major facilitator superfamily
181821	-1.7	0.04	-
55077	1.5	0.04	DNA-binding protein of the nucleobindin family
133804	2.0	0.04	Microfibrillar-associated protein
207217	-5.7	0.04	Glycogen synthase
51264	2.5	0.04	-
187486	-20.7	0.04	-
55640	-1.4	0.04	-

193639	1.9	0.04	-
184760	1.6	0.04	-
47578	4.0	0.04	Nucleolar GTPase/ATPase p130
57028	-2.4	0.04	Aldehyde dehydrogenase
55090	-1.8	0.04	This subunit of TFIIF is required for recruitment of RNA polymerase onto the promoter; this gene is known as "TFG2" in S.cerevisiae
40461	-3.0	0.04	-
187803	1.6	0.04	Hypothetical ribosomal protein
141681	-4.1	0.04	-
47983	2.4	0.04	-
50979	2.5	0.04	Related to alpha-L-arabinofuranosidase
37025	-1.5	0.04	Predicted K+/H+-antiporter
139686	-1.7	0.04	-
123216	1.8	0.04	FAD linked oxidase, N-terminal
207131	2.1	0.04	Nucleolar GTPase/ATPase p130
173825	3.1	0.04	Candidate Alpha-1,2 glucosyltransferase alg10
52207	-3.2	0.04	-
51140	1.8	0.04	Hypothetical Signal recognition particle, subunit Srp72
39373	-1.8	0.04	-
55773	-2.6	0.04	-
210957	-7.2	0.04	-
57395	1.3	0.04	Glycosyl transferase, family 39
213531	1.8	0.04	Mitochondrial import translocase, subunit Tom70
55193	-2.4	0.04	-
35745	1.7	0.04	-
192901	-1.3	0.04	-
135590	-6.6	0.04	Predicted RNA binding protein
196122	1.5	0.04	Putative extracellular GH family 16 cell wall glucanse
136122	2.3	0.04	Hypothetical Ubiquinol cytochrome c reductase assembly protein CBP3
49039	1.9	0.04	Hypothetical protein containing Sec23/Sec24 domains involved in vesicle coating
193610	-23.5	0.04	Carboxylesterases
179383	-2.1	0.04	-
38116	1.8	0.04	Related to ATP-dependent RNA helicases of the DEAD-box protein family.
200271	-1.3	0.04	Zn-finger-like, PHD finger
177364	-1.3	0.04	Mitochondrial substrate carrier
136009	-3.1	0.04	-
120082	-1.6	0.04	Predicted hydrolase involved in interstrand cross-link repair
50698	1.5	0.04	Hypothetical. Calcium/actin binding
48814	-12.1	0.04	-
179991	-2.8	0.04	-
56607	-2.3	0.04	Armadillo/beta-catenin-like repeats
184012	1.8	0.04	Amino acid transporters
40780	-2.6	0.04	-
141890	1.5	0.04	-
174055	5.9	0.04	Putative tRNA acetyltransferase,
136205	3.5	0.04	-
208174	-1.4	0.04	-
212069	1.5	0.04	-
37700	-1.6	0.04	-
177700	1.5	0.04	Inner centromere protein (INCENP), C-terminal domain

180578	1.7	0.04	-
197463	1.8	0.04	Mitochondrial large ribosomal subunit
138508	1.4	0.04	Hypothetical Cytochrome c oxidase assembly protein/Cu2+ chaperone COX17
210766	2.2	0.04	-
44033	-1.6	0.04	(apsA) Peptidase M1
53274	1.9	0.04	-
52489	1.7	0.04	Putative extracellular protein
35368	1.3	0.04	Isopenicillin N synthase
204359	1.2	0.04	-
52186	3.3	0.04	Hypothetical beta-keto-reductase
194765	1.3	0.04	Putative GH family 61 endo-1,4-beta-glucanase
182877	1.6	0.04	-
207193	3.7	0.04	Amino acid/polyamine transporter
42949	1.7	0.04	-
56203	1.5	0.04	Cell division/GTP binding protein
35401	1.4	0.04	3-hydroxyacyl-CoA dehydrogenase, NAD-binding
42764	1.4	0.04	-
39069	1.5	0.04	-
205537	-1.5	0.04	Hypothetical. Sequence identity with S. cerevisiae LSM7 gene; involved in mRNA decay; possibly involved in processing tRNA, snoRNA, and rRNA.
36528	1.5	0.04	-
180635	3.2	0.04	-
182245	1.4	0.04	Hypothetical protein. PFam identifies short-chain dehydrogenase activity.
190444	1.4	0.04	-
54488	-1.8	0.04	-
211979	-1.7	0.04	-
124451	-4.8	0.04	Esterase/lipase/thioesterase
48629	1.8	0.04	-
208677	4.5	0.04	-
210217	6.4	0.04	large beta-ketoacyl synthase probably involved in polyketide synthesis (aurasperone??)
183335	-2.9	0.04	Hypothetical. Glutathione-dependent formaldehyde-activating, GFA domain (Interpro)
171186	1.7	0.04	-
207758	-3.2	0.04	26S proteasome regulatory complex, subunit PSMD9
51164	1.6	0.04	-
180846	1.9	0.04	beta-1,6-N-acetylglucosaminyltransferase, contains WSC domain
48389	18.5	0.04	Predicted transporter (major facilitator superfamily
213733	-2.5	0.04	Predicted ubiquitin regulatory protein, contains UAS and UBX domains
182927	3.2	0.04	H+/oligopeptide symporter
40392	2.3	0.04	Hypothetical protein sharing amino acid sequence identity with the Saccharomyces cerevisiae ECM16 gene encoding an essential DEAH-box ATP-dependent RNA helicase specific to the U3 snoRNP; predominantly nucleolar in distribution; required for 18S rRNA synthesis.
213937	-2.0	0.04	26S proteasome subunit
200308	2.1	0.04	-
56906	1.7	0.04	Predicted translation product shares amino acid sequence identity with the Saccharomyces cerevisiae PWP2 gene product; conserved 90S pre-ribosomal component essential for proper endonucleolytic cleavage of the 35 S rRNA precursor at A0, A1, and A2 sites; contains eight WD-repeats.

187248	-1.5	0.04	-
128935	1.4	0.04	Major facilitator superfamily
55598	2.5	0.04	-
185038	1.3	0.04	-
143030	1.5	0.04	Haloacid dehalogenase-like hydrolase
45757	-3.3	0.04	-
186597	1.6	0.04	-
172198	2.8	0.04	Putative cytochrome P450 monooxygenase
203777	-2.7	0.04	Hypothetical mitochondrial substrate carrie
214112	3.0	0.04	-
46653	-2.6	0.04	-
212771	-35.4	0.04	-
45282	-3.3	0.04	-
171903	1.9	0.04	ABC transporter
45867	2.6	0.04	-
38997	1.6	0.04	-
54229	1.7	0.04	-
184932	1.6	0.04	Hypothetical protein containing ferric reductase-like transmembrane component and helix-turn-helix, Fis-type domain components.
185630	3.0	0.04	Helicase, C-terminal
190033	-2.0	0.04	Putative proline racemase
121523	-2.1	0.04	-
205564	2.0	0.04	Candidate. DNA-directed RNA polymerase
210481	-8.5	0.04	Predicted dehydrogenase
209129	-1.8	0.04	-
42052	2.1	0.04	-
188780	-2.7	0.04	-
57403	-4.2	0.04	-
57296	-1.9	0.04	Nuclear protein ES2
206692	2.3	0.04	Adenylosuccinate lyase
119606	-2.7	0.04	Trehalose-6-phosphate synthase component TPS1 and related subunits
195287	-3.8	0.04	-
49515	5.4	0.04	-
47166	-3.2	0.04	-
42934	-4.0	0.04	-
55985	-1.6	0.04	Protein synthesis factor
44492	1.4	0.04	ABC transporter
194066	1.8	0.04	-
190335	-2.4	0.04	Protein kinase
53986	-12.8	0.04	-
124202	2.7	0.04	tRNA(1-methyladenosine) methyltransferase, subunit GCD14
187778	-9.7	0.04	Fungal transcriptional regulatory protein, N-terminal
188704	1.8	0.04	Hypothetical signal peptidase. Signalp predictions suggests that it is anchored to a membrane.
190193	2.3	0.04	-
194077	1.7	0.04	Valyl-tRNA synthetase
42132	-1.7	0.04	Hypothetical lipase
53046	-2.1	0.04	Hypothetical protein containing fungal specific transcription factor domain.
121949	-3.0	0.04	-
183274	1.7	0.04	TatD-related DNase
208336	3.0	0.04	Hypothetical. Possible role in carbohydrate metabolism
38054	-11.8	0.04	Hypothetical Short-chain dehydrogenase/reductase SDR

208699	2.0	0.04	Predicted translation product shares amino acid sequence identity with the Saccharomyces cerevisiae RSC9 gene product; one of 15 subunits of the 'Remodel the Structure of Chromatin' (RSC) complex; DNA-binding protein involved in the synthesis of rRNA and in transcriptional repression and activation of genes regulated by the Target of Rapamycin (TOR) pathway.
41754	1.9	0.04	-
41165	3.5	0.04	Putative GH family 16 GPI_glucanosyltransferase
182754	-1.9	0.04	-
198577	-6.9	0.04	Carnitine O-acyltransferase
43556	1.8	0.04	-
214402	-1.4	0.04	Zn-finger, C2H2 type
170608	-8.2	0.04	Hypothetical PHD zinc finger
184563	-2.4	0.04	-
56159	-1.6	0.04	Related to phenylalanine-tRNA ligase of Candida albicans
192754	1.3	0.04	-
173081	1.2	0.04	Hypothetical protein. Transport activity is a probable function due to 12 predicted transmembrane domains.
181060	1.6	0.04	Predicted protein shares amino acid sequence identity with the Saccharomyces cerevisiae UTP4 gene product; a nucleolar protein, component of the small subunit (SSU) processome containing the U3 snoRNA that is involved in processing of pre-18S rRNA.
49535	-10.4	0.04	FMN-dependent alpha-hydroxy acid dehydrogenase
55417	-11.6	0.04	Serine/threonine protein kinase, active site
205270	3.9	0.04	-
212893	-5.2	0.04	Glycoside hydrolase
127054	1.4	0.04	-
186640	-1.3	0.04	Hypothetical isoprenylcysteine carboxyl methyltransferase
56498	-8.8	0.04	Isoflavone reductase
172670	-1.6	0.04	-
136791	-2.1	0.04	Predicted short chain-type dehydrogenase
49404	-1.7	0.04	-
189824	-1.3	0.04	-
193777	-2.9	0.04	DEAD/DEAH box helicase
192050	-2.4	0.04	Na+:Ca2+ antiporter
214512	1.4	0.04	RNA-binding protein musashi/mRNA cleavage and polyadenylation factor I complex
47411	-1.4	0.04	Short-chain dehydrogenase/reductase
199734	3.1	0.04	Coproporphyrinogen III oxidase
38678	-1.3	0.04	-
37042	1.6	0.04	-
54890	2.0	0.04	Carbamoyl-phosphate synthase
189342	-1.8	0.04	Sugar transporter
39731	-4.3	0.04	-
50029	-4.1	0.04	-
209244	-2.9	0.04	Oxidoreductase
44753	-1.3	0.04	Esterase/lipase/thioesterase
212567	-3.8	0.04	-
56350	-2.6	0.04	-
142990	-1.5	0.04	mRNA splicing factor
194112	-1.4	0.04	Lipase essential for autophagy
42932	1.6	0.04	Rhodopsin-like GPCR superfamily
53697	-1.9	0.04	Hypothetical protein containing Zn-finger protein, C2H2 type domain

42826	1.5	0.04	Putative growth response protein
55212	1.5	0.04	(pelD) extracellular pectin lyase D
178954	1.3	0.04	Fungal transcriptional regulatory protein, N-terminal
52857	-1.5	0.04	NEDD8-activating complex, APP-BP1/UBA5 component
52637	-1.3	0.04	Histone H3
187878	-4.1	0.04	Related to hogA MAP kinase
52779	1.3	0.04	-
171548	-2.1	0.04	-
213237	-2.9	0.04	-
51412	-3.0	0.04	-
42787	2.1	0.04	-
207996	15.2	0.04	Permeases for cytosine/purines, uracil, thiamine, allantoin
119587	2.0	0.04	Glycosyl hydrolases family 18
53946	-1.7	0.04	-
135680	1.6	0.04	Methyltransferases
48610	1.6	0.04	-
46101	1.5	0.04	-
48631	1.3	0.04	-
52154	1.7	0.04	-
182017	-1.6	0.04	Short-chain dehydrogenase/reductase
54982	2.6	0.04	Hypothetical protein with homeobox domain
176406	1.8	0.04	Deduced amino acid sequence shares identity with the Saccharomyces cerevisiae NHP2 gene product; a nuclear protein related to mammalian high mobility group (HMG) proteins, essential for function of H/ACA-type snoRNPs, which are involved in 18S rRNA processing.
42728	-2.5	0.04	Related to vacuolar ATP synthase subunit D
210454	3.9	0.04	Molecular chaperones mortalin/PBP74/GRP75, HSP70 superfamily
46084	1.2	0.04	-
212182	-6.4	0.04	-
127270	1.2	0.04	-
187819	1.4	0.04	Glucose dehydrogenase/choline dehydrogenase/mandelonitrile lyase (GMC oxidoreductase family)
138217	-2.0	0.04	Predicted RNA-binding protein (RRM superfamily)
54762	1.6	0.04	Adenosine monophosphate deaminase
37289	-1.5	0.04	Non voltage-gated ion channels (DEG/ENaC family)
54187	-1.6	0.04	-
36826	2.3	0.04	-
54411	-17.9	0.04	Short-chain dehydrogenase/reductase SDR
187108	1.3	0.04	-
124393	-3.9	0.04	Peroxisomal NUDIX hydrolase
210291	-2.9	0.04	-
55229	-2.7	0.04	Alpha/beta hydrolase
211589	1.5	0.04	Candidate tif5 gene encoding translation initiation factor eIF5.
143583	-2.9	0.04	-
37296	1.9	0.04	-
35473	-4.7	0.04	Protein containing a zinc finger C2H2-type domain; it is similar to S.cerevisiae CRZ1 (YNL027W) calcineurin-responsive transcription factor
212155	1.7	0.04	Ribosomal protein S2
188240	-1.8	0.04	-
47972	-1.2	0.04	-
36822	-1.3	0.04	Hypothetical regulatory subunit of the 20S preoteasome
213490	15.3	0.04	-

53547	2.5	0.04	-
47866	1.6	0.04	Putative GroEL-like chaperone, ATPase
54207	-5.3	0.04	MaoC-like dehydratase
202416	1.4	0.04	40S ribosomal protein S3
48964	-1.6	0.04	-
41820	-2.1	0.04	-
173769	-2.1	0.04	-
41756	1.6	0.04	Amidohydrolase
55526	1.7	0.04	Fungal chitin synthase
214466	1.5	0.04	Hypothetical. KOG suggests function in ER-Golgi transport
54960	-1.7	0.04	-
52676	1.2	0.04	60s ribosomal protein gene RPL5.
55451	-3.1	0.04	-
180549	5.6	0.04	-
43417	2.7	0.04	-
44401	2.2	0.04	-
204315	-2.7	0.04	Hypothetical. Interpro suggests Cupin domain. Sugar isomerase activity ?
132036	2.6	0.04	-
197480	-9.2	0.04	Enoyl-CoA hydratase/isomerase
51934	1.3	0.04	RuvB-like helicase 2
47358	2.9	0.04	Predicted protein shares amino acid sequence identity with the Saccharomyces cerevisiae UTP10 gene product; a nucleolar protein, component of the small subunit (SSU) processome containing the U3 snoRNA that is involved in processing of pre-18S rRNA.
129162	1.6	0.04	-
178237	1.6	0.04	-
55131	-6.3	0.04	-
43285	-2.7	0.04	Fungal transcriptional regulatory protein
184613	1.3	0.04	Fungal transcriptional regulatory protein
43664	1.3	0.04	Esterase/lipase/thioesterase
55910	-2.1	0.04	FAD dependent oxidoreductase
213737	1.5	0.04	-
52020	1.4	0.04	Ribosomal protein
46134	-2.2	0.04	FAD-linked oxidase
171426	-1.6	0.04	Related to aldehyde dehydrogenase (EC 1.2.1.3). Sequence similarity to aldH of A. fumigatus
210182	4.7	0.04	-
56149	-2.4	0.05	Metallophosphoesterase
45331	1.4	0.05	-
130814	-2.8	0.05	-
180718	-10.9	0.05	AAA+-type ATPase
201398	-11.5	0.05	-
194754	-1.7	0.05	-
206638	2.7	0.05	Aconitate hydratase
179964	1.5	0.05	Hypothetical ATP-dependent helicase with DEAD/DEAH box domain
52004	1.7	0.05	oxidoreductase
179508	1.4	0.05	Major facilitator superfamily
54734	2.3	0.05	Putative extracellular serine carboxypeptidase
49380	-2.5	0.05	-
50479	1.4	0.05	-
204381	-4.0	0.05	Voltage-gated shaker-like K+ channel, subunit beta/KCNAB
174932	-1.6	0.05	-
143320	-1.9	0.05	Hypothetical inosine triphosphate pyrophosphatase

54717	2.8	0.05	-
187802	-2.1	0.05	-
56167	-2.0	0.05	TRIHA 14-3-3 protein homologue, putative kinase regulator
207503	6.6	0.05	Ammonium Transporter Family
195335	2.2	0.05	General substrate transporter
185012	1.5	0.05	Hypothetical WD-40 repeat protein
45718	1.3	0.05	-
38610	-1.7	0.05	Possible Translation initiation factor 2B, beta subunit (eIF-2Bbeta/GCD7)
186204	1.3	0.05	-
185165	1.4	0.05	-
209757	4.2	0.05	-
191085	-2.5	0.05	-
128523	2.4	0.05	Mitochondrial ribosomal protein S27
174948	2.2	0.05	Hypothetical fumarylacetoacetate hydrolase
46809	2.1	0.05	Amino acid transporters
53524	2.6	0.05	-
209439	2.7	0.05	Candidate HMG-CoA reductase
195098	2.0	0.05	-
39038	-1.3	0.05	Transcription factor Engrailed, contains HOX domain
206983	-1.9	0.05	-
197350	1.6	0.05	Ribosomal protein S9
172934	-1.7	0.05	ABC transporter
40884	1.9	0.05	Hypothetical nitric-oxide synthase (EC 1.14.13.39)
45500	1.3	0.05	G-like protein containing WD-40 repeat
38759	-1.5	0.05	-
210938	-1.5	0.05	-
52945	4.7	0.05	ER chaperone encoding bipA gene, kar2
53173	-6.1	0.05	-
55656	2.2	0.05	-
211990	1.8	0.05	-
176395	-3.2	0.05	WD40 repeat-containing protein
189450	1.7	0.05	Heat shock protein DnaJ
54079	6.3	0.05	-
40277	1.3	0.05	-
43469	1.7	0.05	Actin-binding, actinin-type
131188	2.0	0.05	Glucose dehydrogenase/choline dehydrogenase/mandelonitrile lyase (GMC oxidoreductase family)
55738	5.5	0.05	Multifunctional pyrimidine synthesis protein CAD (pyrABCN)
41616	-1.6	0.05	Proteinase inhibitor I25, cystatin
178612	-2.0	0.05	-
52164	2.0	0.05	Putative RNA polymerase II regulator
171112	1.6	0.05	Hypothetical FAD-dependent pyridine nucleotide-disulphide oxidoreductase
187460	1.5	0.05	-
205183	-2.0	0.05	AAA+-type ATPase
189328	-15.6	0.05	-
136869	2.3	0.05	Hypothetical lysin. Extracellular. Peptidoglycan-binding domain and peptidase-like domain
190389	2.2	0.05	Insulinase-like
42579	-18.8	0.05	Hypothetical. Related to 15-hydroxyprostaglandin dehydrogenase

56469	1.4	0.05	Hypothetical protein with WD40-like region
40039	1.5	0.05	Peptidase, eukaryotic cysteine peptidase active site
56449	1.9	0.05	-
192711	1.5	0.05	-
173430	-11.0	0.05	Major facilitator superfamily
189424	1.7	0.05	Putative glycosyl transferase
178649	-2.2	0.05	Nucleolar GTPase/ATPase p130
37552	-3.8	0.05	-
199512	-1.8	0.05	Hypothetical proteasome component
37992	-2.7	0.05	-
55909	2.8	0.05	GTP binding protein
208484	-2.3	0.05	Signal transduction
189666	-2.7	0.05	Aminoacyl-tRNA synthetase
50657	6.3	0.05	Predicted hydrolases or acyltransferases (alpha/beta hydrolase superfamily)
53726	1.7	0.05	-
39481	-2.1	0.05	Aldehyde dehydrogenase
132000	-1.5	0.05	Peptidyl-prolyl cis-trans isomerase
51992	3.1	0.05	-
49499	2.5	0.05	-
54939	4.5	0.05	Amino acid/polyamine transporter
38493	-2.2	0.05	Candidate V-Snare
209506	-2.7	0.05	Hypothetical alkaline phosphatase
133782	1.4	0.05	Hypothetical protein with a MOSC domain
37300	-11.4	0.05	-
142108	2.7	0.05	-
44595	3.9	0.05	Sterol desaturase, methylsterol monooxygenase; C-4 sterol methyl oxidase
207079	2.3	0.05	Zinc-binding oxidoreductase
43055	-7.9	0.05	-
52764	2.3	0.05	AAA ATPase
43993	1.2	0.05	Fungal specific transcription factor
143389	-2.3	0.05	Serine/threonine protein kinase
188800	-2.3	0.05	Flavoprotein monooxygenase
206952	-1.6	0.05	-
53467	1.8	0.05	-
40065	-1.9	0.05	-
51912	2.0	0.05	Argininosuccinate lyase
53361	-14.9	0.05	-
192623	-1.6	0.05	Hypothetical DNA helicase
48618	-2.1	0.05	Esterase/lipase/thioesterase
39094	-2.2	0.05	Sugar (ANd other) transporter
52017	-9.1	0.05	-
38188	-1.6	0.05	N-methyltransferase
54566	1.7	0.05	Hypothetical tyrosyl-tRNA synthetase. Shows similarity with N. crassa tyrosyl-tRNA synthetase
178117	2.2	0.05	Serine/threonine protein kinase
57223	1.4	0.05	NRPS
181710	1.8	0.05	Major facilitator superfamily
38174	-2.9	0.05	-
46394	2.1	0.05	Hypothetical methionine aminopeptidase
211517	5.0	0.05	-
54806	2.3	0.05	-
42536	1.4	0.05	-

127247	-2.0	0.05	COP9 signalosome, subunit
141918	2.0	0.05	-
206105	1.6	0.05	-
43317	1.9	0.05	-
123901	-1.5	0.05	-
173627	-2.4	0.05	HypB/UreG, nucleotide-binding
45820	9.2	0.05	-
56689	-2.8	0.05	-
46226	1.4	0.05	Splicing coactivator SRm160/300, subunit SRm300
177916	2.0	0.05	-
124374	1.4	0.05	-
210373	-28.2	0.05	Cyanate lyase
52532	-2.3	0.05	-
203982	-1.9	0.05	-
46117	3.0	0.05	-
57034	-21.2	0.05	Short-chain acyl-CoA dehydrogenase

S2: Stoichiometric metabolic model of *Aspergillus niger*

REACTIONS

In this section all model reactions are presented and their corresponding carbon atom transitions (the order of the metabolites is the same as in the stoichiometry row, e.g. ab + cd <-> bacd).
The reaction declaration ends with a declaration of net and exchange fluxes.

Glucose uptake

v1: GLC <-> G6P
abcdef <-> abcdef
net = 100; exch = 0.0;

EMP-pathway

v2: G6P <-> F6P
abcdef <-> abcdef
net 0.0 200.0;

v3: F6P <-> G3P + G3P
abcdef <-> cba + def
net 0.0 200.0; exch = 0.0;

v4: G3P <-> 3PG
abc <-> abc
net 0.0 200.0; exch = 0.0;

v5: 3PG <-> PEP
abc <-> abc
net 0.0 200.0; exch = 0.0;

v6: PEP <-> PYRCYT
abc <-> abc
net 0.0 200.0; exch = 0.0;

PP-pathway

v7: G6P <-> CO + R5P
abcdef <-> a + bcdef
net 0.0 300.0; exch = 0.0;

v8: R5P + R5P <-> S7P + G3P
abcde + fghij <-> fgabcde + hij
net 0.0 300.0;

v9: S7P + G3P <-> F6P + E4P
abcdefg + hij <-> abchij + defg
net 0.0 300.0;

v10: R5P + E4P <-> F6P + G3P
abcde + fghi <-> abfghi + cde
net 0.0 300.0;

Formation of AcCoA in the cytosol

v11: ICIT <-> ACCOACYT + OAACYT
abcdef <-> ba + fedc
net 0.0 200.0; exch = 0.0;

Anaplerotic reaction

v12: PYRCYT + CO <-> OAACYT
abc + d <-> abcd
net -300.0 300.0; exch = 0.0;

Oxalate formation

v13: OAACYT <-> OXACYT + ACCOACYT
abcd <-> ab + cd
net 0.0 200.0; exch = 0.0;

TCA-cycle

v14: PYRMIT <-> ACCOAMIT + CO
abc <-> bc + a
net 0.0 200.0; exch = 0.0;

v15: OAAMIT + ACCOAMIT <-> ICIT

abcd + ef <-> dcabfe
net 0.0 200.0; exch = 0.0;

v16: ICIT <-> AKGT + CO
abcdef <-> abcef + d
net 0.0 200.0; exch = 0.0;

v17: AKGT <-> CO + SUC
abcde <-> a + bcde
net 0.0 200.0; exch = 0.0;

v18: SUC <-> FUM
abcd <-> abcd
net 0.0 200.0; exch = 0.0;

v19: FUM <-> MAL
abcd <-> abcd
net 0.0 200.0; exch = 0.0;

Scrambling in reaction v20 and v21 with variable scrambling fraction

v20: MAL + MAL <-> OAAMIT + OAAMIT
abcd + efgh <-> abcd + hgfe
net 0.0 300.0;

Transport reactions Mitochondria-Cytosol

v21: OAACYT <-> OAAMIT
abcd <-> abcd
net -200 200.0;

v22: ACCOACYT <-> ACCOAMIT
ab <-> ab
net 0.0 200.0;exch = 0.0;

v23: PYRCYT <-> PYRMIT
abc <-> abc
net 0.0 200.0;exch = 0.0;

Specialties around Glyceraldehyde-3-P

v24: 3PG <-> SER
abc <-> abc
net 0.0 200.0; exch = 0.0;

v25: SER <-> GLY + C1
abc <-> ab + c
net 0.0 200.0; exch = 0.0;

v26: OAACYT <-> GLY + ACCOACYT
abcde <-> cde + ab
net 0.0 200.0; exch = 0.0;

v27: OAACYT <-> THR
abcd <-> abcd
net 0.0 200.0; exch = 0.0;

v28: THR <-> GLY + ACCOACYT
abcd <-> ab + cd
net 0.0 200.0; exch = 0.0;

C1 Metabolism

v29: GLY <-> CO + C1
ab <-> a + b
net 0.0 200.0; exch = 0.0;

Polyol Metabolism

v30: G3P <-> GOL
abc <-> abc
net 0.0 200.0; exch = 0.0;

Drain of intermediates to BIOMASS

v31: G6P <-> G6POUT
abcdef <-> abcdef
net 0.0 200.0; exch = 0.0;

v32: F6P <-> F6POUT
abcdef <-> abcdef
net 0.0 200.0; exch = 0.0;

v33: R5P <-> R5POUT
abcde <-> abcde
net 0.0 200.0; exch = 0.0;

v34: E4P <-> E4POUT
abcd <-> abcd
net 0.0 200.0; exch = 0.0;

v35: G3P <-> G3POUT
abc <-> abc
net 0.0 200.0; exch = 0.0;

v36: PEP <-> PEPOUT
abc <-> abc
net 0.0 200.0; exch = 0.0;

v37: PYRMIT <-> PYRMITOUT
abc <-> abc
net 0.0 200.0; exch = 0.0;

v38: PYRCYT <-> PYRCYTOUT
abc <-> abc
net 0.0 200.0; exch = 0.0;
v39: OAACYT <-> OAACYTOUT
ab <-> ab
net 0.0 200.0; exch = 0.0;

v40: AKGT <-> AKGTOUT
abcde <-> abcde
net 0.0 200.0; exch = 0.0;

v41: ACCOACYT <-> ACCOACYTOUT
ab <-> ab
net 0.0 200.0; exch = 0.0

v42: ACCOAMIT <-> ACCOAMITOUT

ab <-> ab
net 0.0 200.0; exch = 0.0

v43: SER <-> SEROUT
abc <-> abc
net 0.0 200.0; exch = 0.0;

v44: GLY <-> GLYOUT
ab <-> ab
net 0.0 200.0; exch = 0.0;

v45: C1 <-> C1OUT
a <-> a
net 0.0 200.0; exch = 0.0;

Secretion to Medium

v46: ICIT <-> ICITOUT
abcdef <-> abcdef
net 0.0 200.0; exch = 0.0;

v47: SUC <-> SUCOUT
abcd <-> abcd
net 0.0 200.0; exch = 0.0;

v48: MAL <-> MALOUT
abcd <-> abcd
net 0.0 200.0; exch = 0.0;

v49: FUM <-> FUMOUT
abcd <-> abcd
net 0.0 200.0; exch = 0.0;

v50: OXACYT <-> OXACYTOUT
abcd <-> abcd
net 0.0 200.0; exch = 0.0;

v51: GOL <-> GOLOUT
abc <-> abc
net 0.0 200.0; exch = 0.0;

v52: CO <-> COOUT

a <-> a

net 0.0 800.0; exch = 0.0;

LABELED METABOLITES

Here comes a specification of the labeled metabolites and their fractional labelling

GLC: 99.0 1.1 1.1 1.1 1.1 1.1;

EXTERNAL METABOLITES

Here other metabolites that should not be balanced are stated by their name

G6POUT
F6POUT
R5POUT
E4POUT
G3POUT
PEPOUT
PYRMITOUT
OAACYTOUT
AKGTOUT
ACCOACYTOUT
ACCOAMITOUT
SEROUT
GLYOUT
C1OUT
PYRCYTOUT
ICITOUT
SUCOUT
MALOUT
FUMOUT
OXACYTOUT
GOLOUT
COOUT

S3: Significantly expressed genes in Chapter 9

Identification of the first 1000 most significantly expressed genes between WT N402 and NW185 strain, fold change in log2 ratio (positive number then expression level in NW185 strain higher), p. value < 0.05, the general description is taken from the JGI annotation database.

JGI_ID	Fold change	p.value	General description
55604	9.5	3.2E-09	-
189002	12.6	3.2E-09	-
208150	-9.7	6.8E-09	FAD-dependent pyridine nucleotide-disulphide oxidoreductase
54541	13.9	1.1E-08	Candidate oxidoreductase, Short-chain dehydrogenase/reductase
52269	-5.1	1.1E-08	-
209784	-6.5	1.1E-08	Mitochondrial aspartate/glutamate carrier protein
197162	-8.3	1.1E-08	Sugar (ANd other) transporter
184012	-6.1	1.1E-08	Amino acid transporters
171442	6.7	1.1E-08	-
127436	6.0	1.1E-08	Carbohydrate kinase
56782	12.2	1.1E-08	Glycosyl hydrolase family 3 C terminal domain
50981	13.3	1.1E-08	Putative AMP-dependent synthetase and ligase, Acyl-CoA synthetase
44729	10.0	1.1E-08	Zinc-containing alcohol dehydrogenase superfamily
208043	-11.6	1.1E-08	Nitrogen transporter
124156	10.9	1.1E-08	Candidate NAD dependent formate dehydrogenase
54073	-9.5	1.8E-08	-
42152	8.9	1.8E-08	-
38375	9.8	1.8E-08	Major facilitator superfamily
203401	-9.3	1.8E-08	Amidase
131354	6.6	1.8E-08	-
176433	7.4	1.9E-08	-
56336	9.2	2.1E-08	-
54838	12.6	2.5E-08	Major facilitator superfamily
209754	8.3	2.5E-08	2-nitropropane dioxygenase
205428	13.4	2.5E-08	-
190162	-5.6	2.5E-08	Amino acid transporters
51685	-8.6	2.8E-08	Related to Schizosaccharomyces pombe asparaginase (EC 3.5.1.1)
54095	10.6	2.9E-08	Sugar (ANd other) transporter
180923	7.4	2.9E-08	Major facilitator superfamily
56628	8.8	3.6E-08	Dak kinase
55670	13.4	4.2E-08	Sugar (ANd other) transporter
198250	8.6	5.2E-08	2-enoyl-CoA hydratase/3-hydroxyacyl-CoA dehydrogenase/Peroxisomal 3-ketoacyl-CoA-thiolase, sterol-binding domain and related enzymes
186735	-5.9	5.2E-08	-
205484	5.2	5.6E-08	-
54717	-5.1	6.2E-08	-
53338	-4.3	6.2E-08	Related to dihydrolipoamide acetyltransferase, EC 2.3.1.12

189779	-7.3	6.2E-08	-
124797	12.6	6.2E-08	Major facilitator superfamily
56137	-5.3	6.6E-08	-
209255	-4.6	6.7E-08	Mitochondrial substrate carrier
199928	5.3	8.0E-08	Predicted hydrolase
173139	6.0	8.0E-08	Methionine synthase, vitamin-B12 independent
53978	5.3	8.2E-08	(mstA) high affinity monosaccharide transporter
208583	9.8	8.3E-08	-
177169	8.3	9.0E-08	Hypothetical extracellular gluconolactonase
37760	-6.1	9.2E-08	-
208048	-13.6	9.2E-08	Nitrate reductase
206266	-5.8	9.2E-08	Cytochrome P450
190311	6.8	9.5E-08	2-nitropropane dioxygenase
173677	8.5	9.5E-08	Hypothetical. Ketopantoate reductase pyrimidin base metabolism
209058	-6.0	1.1E-07	ATP sulfurylase
183511	6.0	1.1E-07	Fungal transcriptional regulatory protein
57285	-13.3	1.2E-07	Major facilitator superfamily
55566	-8.8	1.2E-07	Hydroxymethylglutaryl-coenzyme A synthase
43265	11.8	1.2E-07	-
210213	-10.2	1.2E-07	Major facilitator superfamily
206339	9.4	1.2E-07	Haem peroxidase, plant/fungal/bacterial
44808	6.3	1.4E-07	Acetyl-CoA acetyltransferase
57002	-6.8	1.5E-07	Hypothetical alpha-amylase
184678	4.8	1.5E-07	-
182306	-5.7	1.5E-07	-
54411	8.9	1.6E-07	Short-chain dehydrogenase/reductase SDR
197480	6.0	1.6E-07	Enoyl-CoA hydratase/isomerase
52105	7.9	1.7E-07	Amidohydrolase
207572	12.6	1.8E-07	General substrate transporter
213014	5.2	1.8E-07	Flavin-containing monooxygenase
52586	6.1	1.8E-07	Hypothetical protein with TPR-like domain
200605	13.9	1.8E-07	(abfB) alpha-L-arabinofuranosidase B
56664	11.2	2.0E-07	Exoinulinase
210871	6.5	2.0E-07	3-hydroxyacyl-CoA dehydrogenase
175251	5.6	2.0E-07	-
54860	-8.3	2.0E-07	Purine nucleoside permease
54329	11.1	2.0E-07	-
186207	5.8	2.0E-07	-
181999	-6.1	2.0E-07	Arylamine N-acetyltransferase
121987	8.5	2.0E-07	-
55742	4.4	2.3E-07	aldA Aldehyde dehydrogenase (aldA) (EC 1.2.1.3)
180718	6.1	2.3E-07	AAA+-type ATPase
38054	7.8	2.3E-07	Hypothetical Short-chain dehydrogenase/reductase SDR
212771	9.3	2.3E-07	-
210730	18.1	2.4E-07	Related to Thermomyces lanuginosus triacylglycerol lipase
48743	7.6	2.6E-07	Hypothetical enoyl-CoA hydratase
210108	8.9	2.6E-07	AMP-dependent synthetase and ligase
207067	6.7	2.6E-07	HAD-superfamily hydrolase,
45814	-3.8	2.7E-07	-
56395	9.1	2.7E-07	2-nitropropane dioxygenase
51813	-6.5	2.7E-07	Amino acid/polyamine transporter
44156	-5.6	2.7E-07	Related to mitochondrial translation elongation factor
194529	5.1	2.7E-07	-

170891	8.5	2.7E-07	-
132154	-4.5	2.7E-07	Cytochrome P450
194335	-6.3	2.8E-07	Amino acid/polyamine transporter
207831	5.7	2.9E-07	Glucose-methanol-choline oxidoreductase
46101	-8.7	2.9E-07	-
42171	5.4	3.0E-07	Hypothetical isocitrate lyase and phosphorylmutase
53574	-5.9	3.2E-07	Candidate carbamoyl-phosphate synthase
38226	5.2	3.3E-07	Related to Geranylgeranyl pyrophosphate synthase
213113	11.2	3.4E-07	Hypothetical cytochrome b5
184312	7.6	3.4E-07	Glutathione S-transferase
187304	-3.4	3.5E-07	Ergosterol biosynthesis ERG4/ERG24 family
42733	-4.6	3.6E-07	Dihydroxy-acid dehydratase
119858	5.6	3.7E-07	Related to alpha-glucosidase; glycoside hydrolase, family 31
52796	-3.8	3.7E-07	Mitochondrial import inner membrane translocase, subunit Tim44
38000	9.3	3.7E-07	Acetoacetyl-CoA synthase
201398	9.4	3.7E-07	-
170261	3.8	3.7E-07	Permease of the major facilitator superfamily
208631	5.3	3.8E-07	Predicted pyroglutamyl peptidase
40734	7.0	3.8E-07	Hypothetical aldehyde dehydrogenase. Specificity towards NAD or NADP is not deducible from sequence data
202252	4.3	3.8E-07	Putative extracellular tannase and feruloyl esterase
48891	-6.5	4.0E-07	Putative extracellular protein
200874	-6.6	4.0E-07	Transmembrane amino acid transporter protein
48724	6.0	4.1E-07	Isocitrate lyase
35965	-5.0	4.1E-07	-
188553	9.0	4.1E-07	Acyl-CoA dehydrogenase
47354	9.6	4.1E-07	-
53518	5.5	4.2E-07	Phosphoribosyltransferase
190132	-11.4	4.2E-07	Iron/ascorbate family oxidoreductases
56643	10.3	4.3E-07	Major facilitator superfamily
49321	5.7	4.3E-07	-
35778	5.2	4.3E-07	Hypothetical long chain fatty alcohol oxidase
188168	5.2	4.3E-07	-
53423	3.2	4.6E-07	Related to 2-methylcitrate dehydratase of E. coli
57034	10.1	4.8E-07	Short-chain acyl-CoA dehydrogenase
52919	-5.4	4.8E-07	Hypothetical. Intrpro: AMP-dependent synthetase and ligase
176294	8.3	4.8E-07	-
172439	11.3	4.9E-07	-
55417	7.4	5.3E-07	Serine/threonine protein kinase, active site
54651	7.8	5.3E-07	Hypothetical 3-ketoacyl-CoA-thiolase
46405	5.9	5.4E-07	-
193610	6.3	5.4E-07	Carboxylesterases
177616	5.7	5.4E-07	Sugar transporter superfamily
180211	5.3	5.8E-07	Alpha/beta hydrolase
174330	11.0	6.0E-07	Major facilitator superfamily
213815	7.6	6.1E-07	Cytoskeletal protein A
42186	6.6	6.3E-07	-
210373	10.5	6.3E-07	Cyanate lyase
206020	-5.1	6.3E-07	Hypothetical. involved in rRNA processing. associates with trans-acting ribosome biogenesis factors (yeast); similar to beta-transducin superfamily.
205670	5.2	6.3E-07	Glycoside hydrolase, family 3
205005	8.1	6.3E-07	Putative soluble Fumarate reductase/succinate dehydrogenase flavoprotein, N-terminal

211162	4.7	6.4E-07	Hypothetical 1,4-alpha-glucan branching enzyme
56053	-5.2	6.8E-07	-
200589	-8.7	6.8E-07	8-amino-7-oxononanoate synthase (biotin synthesis)
172579	12.5	6.8E-07	-
203198	4.1	6.9E-07	-
174228	-5.3	7.2E-07	-
143749	7.7	7.3E-07	-
53949	9.0	7.8E-07	Major facilitator superfamily
43683	-13.8	7.8E-07	Hypothetical argininosuccinate synthase (EC 6.3.4.5)
44103	6.3	7.8E-07	-
210981	5.3	7.8E-07	Putative extracellular GH family 3 beta-glucosiadse
51764	10.8	8.1E-07	Glycosyl hydrolases family 35
181888	7.6	8.2E-07	Carboxyl transferase
190129	-5.6	8.3E-07	-
54145	-4.1	8.4E-07	-
55052	5.6	8.5E-07	Fungal specific transcription factor
54207	7.1	8.6E-07	MaoC-like dehydratase
132806	11.7	8.6E-07	-
41505	4.9	9.3E-07	Permease of the major facilitator superfamily
204610	-3.6	9.3E-07	Ribosomal protein L7/L12
212876	-3.2	9.4E-07	Ribosomal protein S5
54784	-3.0	9.5E-07	-
177282	4.1	9.8E-07	-
53053	-7.0	9.9E-07	Uroporphyrin III methyltransferase
207996	-6.5	9.9E-07	Permeases for cytosine/purines, uracil, thiamine, allantoin
38851	11.8	9.9E-07	homogentisate 1,2-dioxygenase
39400	8.8	1.0E-06	-
209842	-4.9	1.0E-06	Phosphoribosyl pyrophosphate synthetase
209327	4.1	1.1E-06	Fungal transcriptional regulatory protein, N-terminal
47696	4.9	1.1E-06	-
213793	5.9	1.1E-06	Candidate succinate-semialdehyde dehydrogenase
205368	6.5	1.1E-06	Peptidase
44193	5.1	1.1E-06	-
176070	4.7	1.1E-06	ATP-dependent DNA ligase
206792	-4.9	1.1E-06	RNA polymerase subunit
40461	3.0	1.2E-06	-
53847	13.2	1.2E-06	-
36331	4.3	1.2E-06	-
207853	8.2	1.2E-06	Predicted dehydrogenase
187949	8.7	1.2E-06	Esterase/lipase/thioesterase
142364	-3.8	1.2E-06	-
181179	7.2	1.2E-06	Catechol dioxygenase, N-terminal
197549	7.5	1.2E-06	Sugar (ANd other) transporter
41762	-4.3	1.2E-06	Hypothetical RNA helicase
40740	5.6	1.2E-06	Hypothetical Short-chain dehydrogenase
40460	4.2	1.2E-06	FAD-dependent oxidoreductase
183812	-2.4	1.2E-06	Major facilitator superfamily
121695	4.7	1.2E-06	AMP-dependent synthetase and ligase
205766	7.3	1.2E-06	Sugar (ANd other) transporter
55437	-3.4	1.3E-06	-
123450	-3.2	1.4E-06	Hypothetical neutral amino acid permease
143560	7.4	1.4E-06	Hypothetical, maybe secreted.
125004	-4.6	1.4E-06	-
210672	8.1	1.5E-06	Short-chain dehydrogenase/reductase SDR

52705	-5.0	1.5E-06	Predicted protein shares amino acid sequence identity with the Saccharomyces cerevisiae TUF1 gene product; mitochondrial translation elongation factor Tu.
38924	10.5	1.5E-06	Glycoside hydrolase, family 43
204381	4.7	1.5E-06	Voltage-gated shaker-like K+ channel, subunit beta/KCNAB
196275	-3.4	1.5E-06	-
122081	5.5	1.5E-06	-
55306	6.6	1.5E-06	Aminotransferase class-III
205959	-2.6	1.5E-06	-
55296	-2.6	1.6E-06	Hypothetical threonyl-tRNA synthetase kinase. HMMPfam indicates Threonyl-tRNA synthetase kinase activity
43508	3.7	1.6E-06	-
44096	4.8	1.6E-06	-
43929	3.6	1.6E-06	Hypothetical dehydrogenase
212893	5.3	1.6E-06	Glycoside hydrolase
208535	3.4	1.6E-06	-
55205	6.8	1.7E-06	Hypothetical short chain dehydrogenase
175986	3.4	1.7E-06	-
55007	8.3	1.8E-06	Related to 3-ketoacyl-CoA thiolase
55164	6.8	1.8E-06	-
43953	-5.2	1.8E-06	-
172390	3.3	1.8E-06	Manganese and iron superoxide dismutase
205291	5.6	1.8E-06	Isocitrate and isopropylmalate dehydrogenases
53424	8.1	1.8E-06	-
44497	-3.2	1.8E-06	-
40924	2.7	1.8E-06	-
214881	4.2	1.8E-06	Short-chain dehydrogenase/reductase
189328	6.2	1.8E-06	-
170709	5.6	1.8E-06	Aldehyde dehydrogenase
143580	-3.5	1.8E-06	40s ribosomal protein s10
209315	-5.4	1.8E-06	-
57039	-3.1	1.9E-06	Aspartyl-tRNA synthetase, mitochondrial
198539	-12.0	1.9E-06	-
55738	-7.1	1.9E-06	Multifunctional pyrimidine synthesis protein CAD (pyrABCN)
210944	6.4	1.9E-06	Cytochrome P450
55785	-4.1	2.0E-06	Protein kinase
55510	-4.3	2.0E-06	Pyruvate dehydrogenase E1 B-subunit
180570	5.0	2.0E-06	Short-chain dehydrogenase/reductase SDR
47549	6.0	2.0E-06	-
49535	6.4	2.0E-06	FMN-dependent alpha-hydroxy acid dehydrogenase
120053	5.3	2.1E-06	Fungal specific transcription factor
209244	4.8	2.1E-06	Oxidoreductase
188426	7.6	2.1E-06	-
124451	6.7	2.1E-06	Esterase/lipase/thioesterase
56031	6.5	2.2E-06	Fungal transcriptional regulatory protein
49576	6.6	2.2E-06	Glucose/ribitol dehydrogenase
209960	-2.2	2.2E-06	Porin, eukaryotic type
40569	6.0	2.3E-06	ATPases associated with various cellular activities (AAA)
42464	4.2	2.3E-06	Candidate Peptidyl-prolyl cis-trans isomerase
206496	-3.1	2.3E-06	Molecular chaperone of the GrpE family
55680	6.2	2.4E-06	Coenzyme A transferase
52415	6.5	2.4E-06	Glycoside hydrolase, family 38
52239	5.2	2.4E-06	-
42357	3.3	2.4E-06	-

210295	3.6	2.4E-06	SNARE protein TLG1/Syntaxin 6
124202	-3.3	2.4E-06	tRNA(1-methyladenosine) methyltransferase, subunit GCD14
55131	4.1	2.4E-06	-
57355	3.4	2.4E-06	-
49063	6.0	2.4E-06	Hypothetical fatty acid omega-hydroxylase
209252	5.0	2.4E-06	Autophagy related protein, involved in membrane trafficking
45688	7.5	2.4E-06	-
141681	3.5	2.4E-06	-
43221	-4.5	2.5E-06	Amino acid transporters
37300	3.8	2.5E-06	-
180223	-4.0	2.5E-06	Mitochondrial substrate carrier
44916	6.2	2.5E-06	Candidate extracellular phospholipase C
53576	-2.7	2.7E-06	Candidate 60s ribosomal protein gene RPP1.
212044	-2.2	2.7E-06	Mitochondrial ADP/ATP carrier proteins
42852	-5.6	2.7E-06	Survival protein SurE
131149	6.8	2.7E-06	-
48811	4.9	2.7E-06	(xlnR) Transcriptional activator xlnR
180635	-4.3	2.7E-06	-
55468	-3.2	2.7E-06	-
52362	-3.4	2.7E-06	Candidate 40S ribosomal protein S0.
136397	3.8	2.8E-06	-
206611	2.5	2.8E-06	Hypothetical Acyl-CoA-binding protein
206645	3.5	2.8E-06	Related to phosphatidylinositol/phosphatidylglycerol transfer protein
42184	3.9	2.9E-06	pgaX Exopolygalacturonase precursor (ExoPG) (Galacturan 1,4-alpha-galacturonidase)
198715	-3.0	2.9E-06	Related to tef1B; elongation factor 1 beta
197817	-3.9	3.0E-06	E3 binding
45610	9.9	3.1E-06	Sugar (ANd other) transporter
187254	6.1	3.1E-06	-
120939	-4.3	3.1E-06	-
202416	-2.6	3.1E-06	40S ribosomal protein S3
128421	4.6	3.1E-06	FOG: WD40 repeat
47417	6.8	3.2E-06	Short-chain dehydrogenase/reductase
208677	-4.1	3.2E-06	-
57101	-2.7	3.2E-06	-
56339	-7.0	3.2E-06	Related to sulphate permease. Has 11 transmembrane domains and several sulphate transporter domains.
48373	-3.8	3.2E-06	Uncharacterised conserved protein similar to ATP/GTP-binding protein
207002	-5.0	3.2E-06	Hypothetical. InterPro suggests role in chromosome condensation
125764	6.7	3.2E-06	-
53845	9.0	3.2E-06	-
45887	7.7	3.2E-06	Hypothetical glucose-methanol-choline oxidoreductase (EC 1.99.1.1)
39346	3.7	3.2E-06	Hypothetical protein containing Ada, metal-binding and helix-turn-helix, AraC type domains.
36596	5.2	3.3E-06	Esterase/lipase/thioesterase
37678	4.1	3.3E-06	-
178744	5.6	3.3E-06	Hypothetical Metal-dependent phosphohydrolase, HD region
55391	-4.6	3.3E-06	-
206033	6.4	3.3E-06	-
202059	5.4	3.4E-06	Isochorismatase hydrolase

47429	-3.2	3.4E-06	(dphE) Methyltransferase required for synthesis of diphthamide, which is a modified histidine residue of translation elongation factor 2.
45208	-3.3	3.4E-06	Hypothetical Ribosome biogenesis protein RPF1, contains IMP4 domain
49737	3.9	3.5E-06	Hypothetical protein
46100	-5.2	3.5E-06	-
42787	-3.3	3.5E-06	-
212337	6.5	3.5E-06	Hypothetical protein. Contains four putative transmembrane helices
181938	2.7	3.5E-06	Ypt/Rab-specific GTPase-activating protein GYP7 and related proteins
172786	7.1	3.5E-06	Major facilitator superfamily
202490	9.8	3.6E-06	Cellulase (glycosyl hydrolase family 5)
196077	-4.2	3.6E-06	-
51482	5.9	3.7E-06	Major facilitator superfamily
51478	3.1	3.7E-06	(faeB) feruloyl esterase
135002	-2.7	3.7E-06	-
48688	-5.3	3.7E-06	Adenosylmethionine-8-amino-7-oxononanoate transaminase
53339	-2.8	3.8E-06	Malate dehydrogenase
39109	2.4	3.9E-06	-
187366	5.0	4.0E-06	AMP-binding enzyme
57271	-3.5	4.0E-06	-
56498	4.6	4.0E-06	Isoflavone reductase
56022	4.0	4.0E-06	Cytochrome P450
47847	-4.2	4.0E-06	Predicted translation product shares amino acid sequence identity with the Saccharomyces cerevisiae POL5 gene product; a protein with sequence similarity to the human MybBP1A and weak sequence similar to B-type DNA polymerases, not required for chromosomal DNA replication; required for the synthesis of rRNA.
46429	4.2	4.0E-06	Glycosyl hydrolases family 35
40929	-5.2	4.0E-06	Fungal transcriptional regulatory protein
201122	5.3	4.0E-06	-
198624	-3.6	4.0E-06	Ribosomal protein S6
194112	3.2	4.0E-06	Lipase essential for autophagy
183900	3.9	4.0E-06	-
128988	3.2	4.0E-06	Ankyrin
180885	6.9	4.0E-06	Fungal transcriptional regulatory protein
52653	2.9	4.1E-06	Phosphotyrosyl phosphatase activator
39560	7.2	4.1E-06	-
206434	12.2	4.1E-06	Related to glucose transporter
200680	-3.2	4.1E-06	Eukaryotic translation initiation factor 3, subunit 7
202801	-3.4	4.1E-06	citA citrate synthase
196819	-2.9	4.1E-06	RNA polymerase
205686	-2.6	4.2E-06	-
186114	-6.4	4.2E-06	-
211094	-4.4	4.3E-06	-
191636	4.4	4.4E-06	Hypothetical protein. Electronic annotation suggests pyridine nucleotide-disulphide oxidoreductase
46134	2.9	4.4E-06	FAD-linked oxidase
39788	-2.8	4.4E-06	Permease for cytosine/purines, uracil, thiamine, allantoin
37080	4.1	4.4E-06	pepE, extracellular aspartic protease
56553	10.7	4.5E-06	-
206738	5.1	4.5E-06	Esterase/lipase/thioesterase
128861	6.6	4.5E-06	Acyl-CoA dehydrogenase

45681	7.3	4.5E-06	Short chain dehydrogenase
54926	3.6	4.5E-06	-
196147	-3.0	4.5E-06	-
139340	-4.5	4.5E-06	-
53893	-4.5	4.7E-06	Phosphatidylethanolamine binding protein
194300	3.7	4.7E-06	Candidate Ribonuclease III
209231	5.2	4.7E-06	Aldo/keto reductase
185434	7.5	4.8E-06	Short chain dehydrogenase
36779	-2.8	4.9E-06	Hypothetical dihydroorotate dehydrogenase (EC 1.3.3.1)
51717	-3.8	4.9E-06	Hypothetical Mitochondrial phosphate carrier protein
212412	-5.6	4.9E-06	-
170262	2.9	4.9E-06	Aldo/keto reductase family proteins
49515	-4.1	4.9E-06	-
129773	-4.3	4.9E-06	-
53381	-2.8	5.0E-06	Cytochrome b5 domain
176830	-3.4	5.1E-06	WD40 repeat nucleolar protein putatively involved in ribosome biogenesis
174161	-2.4	5.1E-06	snRNP A' protein
46760	-4.3	5.1E-06	-
176483	9.1	5.1E-06	12 kDa heat shock protein
182005	-4.7	5.1E-06	Amino acid permease
170612	2.9	5.1E-06	-
38274	4.4	5.3E-06	-
203604	-2.3	5.3E-06	Aminoacyl-tRNA synthetase
47307	3.3	5.4E-06	Methyltransferases
37420	-4.4	5.4E-06	-
180608	5.0	5.4E-06	-
198599	-4.1	5.4E-06	-
46346	5.7	5.4E-06	-
172955	2.8	5.5E-06	Hydantoinase/oxoprolinase
37998	3.5	5.5E-06	Hypothetical protein. Is very likely associated with degradation of aromatic compounds based on Pfam and protein similarity
198565	-3.1	5.6E-06	-
54939	-3.4	5.6E-06	Amino acid/polyamine transporter
55209	-6.7	5.6E-06	Isocitrate dehydrogenase, alpha subunit
39803	6.4	5.7E-06	Yippee-type zinc-binding protein
209263	-7.1	5.7E-06	-
120073	-3.6	5.7E-06	Serine/threonine protein kinase
51373	3.5	5.8E-06	-
56753	-5.0	5.8E-06	Aromatic-ring hydroxylase
129399	2.5	5.9E-06	Putative pyruvate carboxylase
52361	-2.5	6.0E-06	-
43055	5.1	6.0E-06	-
210297	2.3	6.0E-06	Signal transduction
41928	-2.8	6.0E-06	-
184233	-2.7	6.1E-06	-
193981	4.5	6.1E-06	Putative pyruvate decarboxylase joined with TPR repeat containing protein
170910	3.5	6.1E-06	Glucose/ribitol dehydrogenase
214665	3.2	6.4E-06	Hypothetical protease
190106	2.5	6.5E-06	2-nitropropane dioxygenase family
40771	-3.0	6.7E-06	Putative GroEL-like chaperone, ATPase
196874	8.9	6.7E-06	Aldehyde dehydrogenase
181451	6.5	6.8E-06	Hypothetical 3-methylcrotonyl-CoA carboxylase, subunit

			beta
56227	11.9	6.8E-06	Major facilitator superfamily
199462	-2.3	6.9E-06	Related to ribosomal protein RPL26.
176411	6.3	6.9E-06	Haloacid dehalogenase-like hydrolase
173997	-5.8	6.9E-06	Deduced translation product shares amino acid sequence identity with the Saccharomyces cerevisiae NSR1 gene product; a nucleolar protein that binds nuclear localisation sequences, required for pre-rRNA processing and ribosome biogenesis.
53910	-4.3	7.0E-06	Fatty acid desaturase
213414	-2.4	7.0E-06	Predicted transporter (ABC superfamily)
211531	-6.6	7.0E-06	-
178256	4.8	7.0E-06	Related to histidine kinase
213288	3.4	7.0E-06	-
119939	3.8	7.1E-06	Fungal specific transcription factor
56770	4.9	7.1E-06	Peptidase S16
48827	3.7	7.1E-06	-
208898	-6.8	7.1E-06	NADP/FAD dependent oxidoreductase
211789	-7.1	7.1E-06	-
175855	-3.1	7.1E-06	Major facilitator superfamily
176012	-3.5	7.2E-06	-
179385	2.6	7.3E-06	Major facilitator superfamily
210666	-2.5	7.4E-06	-
185842	5.6	7.5E-06	Cytochrome b5
209386	-2.6	7.6E-06	Ribosomal protein S17
51512	4.6	7.7E-06	Cytochrome P450
211185	-3.4	7.7E-06	-
206955	4.1	7.7E-06	Transthyretin and related proteins
48713	3.8	7.7E-06	DNA-binding SAP
125644	5.1	7.7E-06	Short-chain dehydrogenase/reductase SDR
127191	-2.4	7.8E-06	-
197015	-5.7	7.8E-06	Cytochrome c
205884	-2.3	7.8E-06	-
52344	4.7	7.8E-06	-
39459	-4.4	7.8E-06	-
176378	4.9	7.9E-06	Short-chain dehydrogenase/reductase
51952	4.7	7.9E-06	-
204514	1.7	7.9E-06	Nucleotide excision repair factor NEF2, RAD23 component
53361	7.9	8.0E-06	-
52571	-2.7	8.0E-06	Ribosomal protein S17
46099	-7.0	8.1E-06	-
210454	-4.8	8.1E-06	Molecular chaperones mortalin/PBP74/GRP75, HSP70 superfamily
127671	-4.2	8.2E-06	-
55759	3.3	8.2E-06	-
212140	3.2	8.3E-06	Hypotetical cAMP-dependent protein kinase catalytic subunit
125201	7.1	8.5E-06	Esterase/lipase/thioesterase
40356	-4.3	8.6E-06	Predicted DNA-directed RNA polymerase
213737	-1.9	8.6E-06	-
129990	-3.3	8.6E-06	FOG: PPR repeat
123758	5.5	8.6E-06	-
172596	2.3	8.7E-06	-
40329	2.0	8.7E-06	-
39630	-2.2	8.7E-06	Ribosomal protein S4
186860	5.1	8.7E-06	Aminotransferase class-III

57352	-2.7	8.8E-06	Ribosomal protein S6e
55609	-6.3	8.8E-06	-
54125	3.5	8.8E-06	-
201503	-6.1	8.8E-06	NAD-cytochrome b5 reductase
176363	7.2	8.8E-06	-
122999	-5.9	8.8E-06	Major facilitator superfamily
38832	6.2	8.8E-06	Cytochrome P450
205431	2.4	8.9E-06	Molecular chaperones HSP70/HSC70, HSP70 superfamily
48629	-2.2	8.9E-06	-
55305	-3.0	9.0E-06	-
46090	6.6	9.0E-06	-
45282	3.6	9.1E-06	-
179623	-3.4	9.1E-06	WD40 repeat protein
54294	2.8	9.1E-06	-
125779	-3.6	9.1E-06	-
52335	-4.5	9.1E-06	Related to protein arginine N-methyltransferase (E. nidulans)
212567	4.2	9.1E-06	-
122116	5.4	9.1E-06	Metacaspase involved in regulation of apoptosis
47866	-3.0	9.2E-06	Putative GroEL-like chaperone, ATPase
128477	-2.8	9.2E-06	-
48505	3.0	9.2E-06	-
197381	2.7	9.2E-06	GTPase Rab5/YPT51 and related small G protein superfamily GTPases
212915	-5.1	9.2E-06	Hypothetical alpha-1,3-glucan synthase
53668	3.7	9.3E-06	-
130294	-4.1	9.3E-06	Hypothetical ATP-dependent RNA helicase
52441	-2.8	9.4E-06	Putative GroEL-like chaperone, ATPase
49896	6.1	9.4E-06	Mandelate racemase
48646	6.9	9.4E-06	Hypothetical enoyl-CoA hydratase (EC 4.2.1.17)
54106	5.9	9.5E-06	-
189170	8.2	9.6E-06	Related to alpha keto acid dehydrogenase complex of Aspergillus fumigatus; EC 2.3.1.12
188037	-2.7	9.6E-06	Lipoate-protein ligase A
47380	-2.3	9.7E-06	NRPS
45820	-6.4	9.7E-06	-
186253	-2.9	9.7E-06	-
44666	5.2	9.7E-06	-
42981	6.3	9.7E-06	Lanthionine synthetase C-like protein
44770	3.5	9.9E-06	-
42238	-8.7	9.9E-06	Guanine-specific ribonuclease N1 and T1
195992	4.6	9.9E-06	Hypothetical cyclic-AMP phosphodiesterase
54083	-3.2	9.9E-06	Hypothetical. Related to GCN5-related N-acetyltransferase
47533	-2.2	9.9E-06	Amino acid permease
40917	-2.7	9.9E-06	Predicted mechanosensitive ion channel
40260	-3.5	9.9E-06	Major facilitator superfamily
52996	-3.5	9.9E-06	Related to ubiquinone biosynthesis methyltransferase COQ5 (S. cerevisiae)
43123	-3.1	9.9E-06	Ferredoxin
189635	6.9	9.9E-06	Monodehydroascorbate/ferredoxin reductase
54174	5.3	9.9E-06	Dihydroxy-acid dehydratase
137527	-3.3	1.0E-05	-
210041	-2.3	1.0E-05	ABC (ATP binding cassette) 1 protein
206469	-2.6	1.0E-05	-
137752	-2.2	1.0E-05	60S ribosomal protein L18A

133810	-2.7	1.1E-05	FAD dependent oxidoreductase
140924	-3.8	1.1E-05	-
120955	4.3	1.1E-05	-
184314	2.6	1.1E-05	-
206859	-2.5	1.1E-05	40S ribosomal protein S14
193903	-2.9	1.1E-05	Predicted nucleolar protein involved in ribosome biogenesis
176127	-7.1	1.1E-05	Predicted hydrolase related to dienelactone hydrolase
188240	3.7	1.1E-05	-
50403	-4.5	1.1E-05	Kinesin-like protein
205848	-5.0	1.1E-05	Sulfate/bicarbonate/oxalate exchanger SAT-1 and related transporters (SLC26 family)
56308	-4.3	1.1E-05	ABC transporter
44216	-3.9	1.1E-05	-
128739	2.8	1.1E-05	Hypothetical. RNA binding motif
37610	-5.0	1.1E-05	-
54001	-3.6	1.1E-05	Putative Hsp60
51857	6.7	1.1E-05	-
50029	5.0	1.1E-05	-
43594	4.9	1.1E-05	Hypothetical. SignalP suggests secreted
172823	-2.5	1.1E-05	Related to zink transporter of A. fumigatus. Seven putative transmembrane domains and PFam domains for zink transport.
180069	5.6	1.1E-05	Major facilitator superfamily
55524	2.4	1.1E-05	Hypothetical transmembrane protein
49311	5.6	1.1E-05	Hypothetical, similarities to sialidase superfamily
196583	-3.3	1.1E-05	Candidate rpl12 gene, component of the large (60S) ribosomal subunit
55741	-2.4	1.1E-05	Protein import receptor MAS20
55365	3.6	1.1E-05	-
140013	-3.4	1.1E-05	-
176395	5.2	1.1E-05	WD40 repeat-containing protein
56477	7.3	1.1E-05	Epoxide hydrolase
54071	3.5	1.1E-05	-
45992	-3.9	1.1E-05	(chsC) Class-III chitin synthase C
207169	3.5	1.1E-05	Receptor-activated Ca2+-permeable cation channels
56462	-4.7	1.1E-05	Candidate serine hydroxymethyltransferase (EC 2.1.2.1)
208447	-3.5	1.1E-05	Translation initiation factor 3
48002	6.4	1.2E-05	Amidohydrolase
36773	4.1	1.2E-05	Hypothetical enoyl-CoA hydratase. (EC 4.2.1.17) HMM predicts secretion.
55451	3.4	1.2E-05	-
43674	-1.7	1.2E-05	Ribonuclease II
202202	2.0	1.2E-05	Hypothetical. Ca2+-binding actin-bundling protein (fimbrin/plastin)
194591	5.6	1.2E-05	-
47358	-5.1	1.2E-05	Predicted protein shares amino acid sequence identity with the Saccharomyces cerevisiae UTP10 gene product; a nucleolar protein, component of the small subunit (SSU) processome containing the U3 snoRNA that is involved in processing of pre-18S rRNA.
43791	-6.0	1.2E-05	Generic methyltransferase
174644	4.3	1.2E-05	Ubiquitin-conjugating enzymes
211901	-3.3	1.2E-05	-
207158	7.2	1.2E-05	Prohibitins and stomatins of the PID superfamily
209012	8.1	1.2E-05	Proteins containing the FAD binding domain
53946	3.3	1.2E-05	-

185301	4.6	1.2E-05	Hypothetical carboxylesterase
137631	5.5	1.2E-05	-
53084	2.2	1.2E-05	Ubiquitin-conjugating enzymes, 16 kDa
39990	6.7	1.2E-05	Carbamoyl-phosphate synthetase large chain
56215	-6.7	1.2E-05	Hypothetical Hydroxymethylglutaryl-coenzyme A synthase
56167	2.4	1.2E-05	TRIHA 14-3-3 protein homologue, putative kinase regulator
48625	-2.3	1.2E-05	-
211906	1.9	1.2E-05	-
207426	-4.9	1.3E-05	-
120372	4.2	1.3E-05	Phosphoinositide-specific phospholipase C (PLC)
210989	-4.8	1.3E-05	Amino acid/polyamine transporter I
194595	2.6	1.3E-05	Flavonol reductase/cinnamoyl-CoA reductase
189927	-6.1	1.3E-05	Monocarboxylate transporter
35976	-3.8	1.3E-05	Major facilitator superfamily
55693	2.4	1.3E-05	-
190740	-2.8	1.3E-05	-
172934	3.3	1.3E-05	ABC transporter
38549	7.2	1.3E-05	-
48817	2.7	1.3E-05	Transcription initiation factor IIA, gamma subunit
54957	-2.4	1.3E-05	Putative GroEL-like chaperone, ATPase
190030	4.0	1.3E-05	Aldo/keto reductase family proteins
55193	3.0	1.3E-05	-
56084	3.3	1.3E-05	-
52186	-2.9	1.3E-05	Hypothetical beta-keto-reductase
46776	3.0	1.3E-05	TatD-related DNase
50151	9.1	1.4E-05	Hypothetical Glutathione-dependent formaldehyde-activating, GFA
201109	-3.0	1.4E-05	Putative GroEL-like chaperone, ATPase
37942	7.1	1.4E-05	Hypothetical Cytochrome P450 monooxygenase
187314	3.3	1.4E-05	-
45912	6.6	1.4E-05	FMN-dependent alpha-hydroxy acid dehydrogenase
212502	-4.2	1.4E-05	Hypothetical nucleosome assembly protein
188497	-4.2	1.4E-05	Fungal specific transcription factor
172399	-2.7	1.4E-05	-
55805	3.3	1.4E-05	Hypothetical catalytic protein
178365	7.0	1.4E-05	Hypothetical aspartic protea
52783	3.0	1.4E-05	Alternative splicing factor SRp55/B52/SRp75 (RRM superfamily)
197079	-3.2	1.4E-05	-
36238	1.9	1.4E-05	Hypothetical protein; KOG Class: Chromatin structure and dynamics; KOG Id: 4191; KOG Description: Histone acetyltransferases PCAF/SAGA/ADA, subunit TADA3L/NGG1
170848	9.4	1.4E-05	-
203483	-2.3	1.5E-05	-
207730	-3.3	1.5E-05	60S ribosomal protein L7A
176010	5.0	1.5E-05	Predicted esterase of the alpha-beta hydrolase superfamily
39372	4.3	1.5E-05	-
185692	-2.9	1.5E-05	Mitochondrial substrate carrier
198577	4.4	1.5E-05	Carnitine O-acyltransferase
133729	-4.8	1.5E-05	RNA-binding protein
35657	-3.0	1.5E-05	-
56966	-5.2	1.5E-05	-
210935	-3.2	1.5E-05	Candidate eukaryotic translation initiation factor 3
207710	3.1	1.5E-05	MAP kinase

188804	3.8	1.5E-05	-
208835	3.4	1.5E-05	Serine/threonine protein kinase Chk2 and related proteins
53446	-3.4	1.5E-05	-
35307	-2.3	1.5E-05	-
170148	4.5	1.5E-05	Putative GH family 18 endo-chitinase
39511	-4.7	1.5E-05	-
174831	6.1	1.6E-05	Ribonuclease T2
207217	5.8	1.6E-05	Glycogen synthase
137560	4.1	1.6E-05	-
209521	3.9	1.6E-05	-
192202	6.7	1.6E-05	Transketolase, C-terminal domain
50189	-2.3	1.6E-05	Hypothetical protein, Contains WD40 repeat
37620	9.6	1.6E-05	gdhB, NAD dependent glutamate dehydrogenase
55967	-2.2	1.6E-05	Cytochrome P450
51887	3.1	1.6E-05	-
50833	2.0	1.6E-05	-
49148	-4.9	1.6E-05	-
208321	3.5	1.6E-05	Peroxisomal membrane protein MPV17 and related proteins
55560	5.4	1.6E-05	Mannitol-1-phosphate 5-dehydrogenase
183352	-1.9	1.6E-05	Aromatic-ring hydroxylase
47227	-6.0	1.6E-05	3-oxoacyl-(acyl-carrier-protein) synthase
54383	3.7	1.6E-05	Splicing coactivator SRm160/300, subunit SRm300
57366	-3.3	1.7E-05	-
37382	-4.0	1.7E-05	Mitochondrial/chloroplast ribosomal protein L54/L37
52676	-2.4	1.7E-05	60s ribosomal protein gene RPL5.
214825	-5.2	1.7E-05	Glycosyl transferase, group 1
214265	4.4	1.7E-05	Putative polyubiquitin
55501	6.3	1.7E-05	Cytochrome P450
43264	4.8	1.7E-05	-
214402	2.5	1.7E-05	Zn-finger, C2H2 type
43857	2.6	1.7E-05	Amino acid permease
207193	-5.4	1.7E-05	Amino acid/polyamine transporter
46473	6.3	1.7E-05	Hypothetical short chain dehydrogenase
46523	-2.7	1.7E-05	-
49003	-2.4	1.7E-05	-
42079	3.5	1.7E-05	-
128007	2.1	1.8E-05	Membrane protein involved in organellar division
55161	6.1	1.8E-05	Hypothetical Alpha/beta hydrolase. Involded in aromatic compound metabolism
136049	4.4	1.8E-05	Hypothetical protein with WD-40 and NACHT domain
45871	-2.7	1.8E-05	-
175089	5.7	1.8E-05	NAD dependent epimerase
133888	-3.0	1.8E-05	Putative Zinc transporter ZIP, Zn /Fe
142826	-4.5	1.8E-05	Ribosomal protein L27
46272	-4.0	1.8E-05	Putative Ribosomal protein S8
47586	3.3	1.8E-05	Fungal specific transcription factor
42344	1.8	1.8E-05	Hypothetical esterase/lipase
198750	-8.4	1.8E-05	Ammonium transporter
191806	-2.7	1.8E-05	40S ribosomal protein S28
44695	-3.6	1.8E-05	-
127378	3.9	1.8E-05	-
52603	3.4	1.8E-05	Related to carboxypeptidase Y
172668	3.5	1.8E-05	Aldehyde dehydrogenase
35486	6.1	1.8E-05	-

55529	-3.6	1.8E-05	Candidate ATP-dependent RNA helicase of the DEAD-box protein family
56078	-3.2	1.8E-05	Deduced protein shares amino acid sequence identity with the Saccharomyces cereivisiae YRG054W gene product; eukaryotic initiation factor (eIF) 2A; associates specifically with both 40S subunits and 80 S ribosomes, and interacts genetically with both eIF5b and eIF4E; homologous to mammalian eIF2A.
206982	4.4	1.8E-05	-
125824	3.6	1.8E-05	-
56702	-2.4	1.8E-05	Ribosomal protein L7Ae/L30e/S12e/Gadd45
212718	-5.2	1.9E-05	Hypothetical protein. PFam suggests Oligopeptide transporter activity. 12 transmembrane domains are predicted
205095	4.4	1.9E-05	Short-chain dehydrogenase/reductase
49344	-3.3	1.9E-05	Putative GH family 76 endo-1,6-alpha-mannanase
177847	5.5	1.9E-05	ABC transporter
57253	2.2	1.9E-05	Ubiquitin-conjugating enzyme
210217	-3.7	1.9E-05	Large beta-ketoacyl synthase probably involved in polyketide synthesis (aurasperone??)
214305	3.5	1.9E-05	Hypothetical Vesicle transport protein (v-SNARE)
50457	-3.9	1.9E-05	Nuclear GTP binding protein
56788	3.5	1.9E-05	Hypothetical protease that contains peptidase M28 domain
35583	-2.5	1.9E-05	Deduced amino acid sequence shares identity with the Saccharomyces cerevisiae NCL1 gene product; an S-adenosyl-L-methionine-dependent tRNA: m5C-methyltransferase; methylates cytosine to m5C at several positions in tRNAs and intron-containing pre-tRNAs.
201783	5.5	1.9E-05	-
127635	3.4	1.9E-05	-
121949	3.3	1.9E-05	-
52874	3.8	1.9E-05	Serine/threonine protein kinase
213185	-3.5	1.9E-05	Pyruvate carboxylase (EC 6.4.1.1)
44450	3.7	1.9E-05	-
180548	3.5	1.9E-05	-
48704	-3.1	1.9E-05	-
130735	2.7	2.0E-05	-
211766	8.6	2.0E-05	SAM (and some other nucleotide) binding motif
209822	-5.7	2.0E-05	Hypothetical ribosomal protein L1
127816	1.7	2.0E-05	SNARE protein
54961	10.0	2.0E-05	Hypothetical cysteine dioxygenase (EC 1.13.11.20)
184073	-6.2	2.0E-05	Related to NADPH-dependent alcohol dehydrogenase, Zinc containing
209685	5.4	2.0E-05	Acyl-CoA dehydrogenase
199933	-3.0	2.0E-05	Hypothetical Ribosomal protein S21e
212420	-3.1	2.0E-05	Hypothetical ribosomal protein
194767	5.0	2.0E-05	-
170127	-4.0	2.0E-05	-
55229	2.8	2.0E-05	Alpha/beta hydrolase
42523	-3.2	2.0E-05	Hypothetical Inositol monophosphatase
39215	-3.6	2.0E-05	Ribosomal protein L6
211616	2.4	2.0E-05	Peptidase
187878	4.0	2.0E-05	Related to hogA MAP kinase
210558	-3.7	2.0E-05	Thiamine pyrophosphate-requiring enzyme
183116	-2.5	2.0E-05	-
180337	-4.5	2.0E-05	Hypothetical. KOG suggests transcription regulation/DEAD box

190193	-3.3	2.0E-05	-
53525	-2.6	2.0E-05	Ribosomal protein L32e
213531	-1.8	2.0E-05	Mitochondrial import translocase, subunit Tom70
190860	-3.4	2.0E-05	Threonine dehydratase
56332	-3.9	2.1E-05	Prolyl-4-hydroxylase
51877	4.5	2.1E-05	Isopenicillin N synthase
41935	4.5	2.1E-05	-
40825	5.1	2.1E-05	Geranylgeranyl pyrophosphate synthase/Polyprenyl synthetase
213350	3.1	2.1E-05	-
44347	-2.4	2.1E-05	Ribosomal protein L3
197679	-5.5	2.1E-05	Amino acid/polyamine transporter
196638	-4.1	2.1E-05	60S acidic ribosomal protein P0
179170	6.6	2.1E-05	-
50197	7.6	2.1E-05	Hypothetical protein. PFam suggests a Enoyl-CoA hydratase/isomerase function
207027	8.2	2.1E-05	Oxidoreductase, N-terminal
38275	7.6	2.1E-05	-
203758	-12.4	2.1E-05	-
214897	4.1	2.1E-05	-
36035	4.6	2.1E-05	-
38174	2.3	2.2E-05	-
203246	-3.2	2.2E-05	40S ribosomal protein S24
55190	2.9	2.2E-05	-
176406	-5.4	2.2E-05	Deduced amino acid sequence shares identity with the Saccharomyces cerevisiae NHP2 gene product; a nuclear protein related to mammalian high mobility group (HMG) proteins, essential for function of H/ACA-type snoRNPs, which are involved in 18S rRNA processing.
55964	6.6	2.2E-05	-
42808	12.2	2.2E-05	-
42805	4.4	2.2E-05	-
39108	2.7	2.2E-05	Predicted NUDIX hydrolase FGF-2 and related proteins
207638	2.2	2.2E-05	Golgi-associated protein/Nedd4 WW domain-binding protein
203335	5.1	2.2E-05	-
120052	-4.7	2.2E-05	Related to SPB1
207776	3.3	2.2E-05	Voltage-gated shaker-like K+ channe
43391	8.9	2.2E-05	Dehydrogenase E1 component
202653	-1.9	2.2E-05	Putative Ribosomal protein 60S
51124	3.3	2.3E-05	-
52539	4.9	2.3E-05	-
208093	-1.9	2.3E-05	-
193894	2.9	2.3E-05	-
41702	5.3	2.3E-05	Major facilitator superfamily
53246	1.6	2.3E-05	-
206038	5.5	2.3E-05	-
50499	13.1	2.3E-05	Related to 2-deoxy-D-gluconate 3-dehydrogenase
42446	3.7	2.3E-05	Zinc transporter ZIP
208365	3.1	2.3E-05	Hypothetical. KOG: aldo/keto reductase
199618	3.7	2.3E-05	-
41761	-2.3	2.3E-05	Predicted RNA-binding protein
39748	-2.3	2.4E-05	-
181825	-2.1	2.4E-05	Nuclear cap-binding complex, subunit NCBP1/CBP80
200208	3.6	2.4E-05	N-methyl-D-aspartate receptor glutamate-binding subunit
197269	5.8	2.4E-05	-

187486	6.8	2.4E-05	-
54016	-3.4	2.4E-05	Hypothetical high-affinity nickel transport protein
48843	-5.8	2.4E-05	rRNA processing protein
193012	2.9	2.4E-05	Ubiquitin-protein ligase
121560	4.4	2.4E-05	-
200276	-2.3	2.4E-05	40S ribosomal protein S13
197559	-3.2	2.4E-05	60S ribosomal protein L22
206509	4.3	2.4E-05	-
55252	-2.2	2.4E-05	Ribosomal protein S7
53232	-1.6	2.4E-05	Related to dihydrolipoamide dehydrogenase of Schizosaccharomyces pombe; EC 1.8.1.4
171186	-6.1	2.4E-05	-
171113	2.2	2.5E-05	Fatty acid desaturase
135680	-2.0	2.5E-05	Methyltransferases
176795	4.1	2.5E-05	Hypothetical phenylalanine ammonia-lyase
187076	-3.9	2.5E-05	-
213213	-2.6	2.5E-05	Ribosomal protein L36E
183718	1.5	2.5E-05	Predicted membrane protein
173652	-3.8	2.5E-05	-
38529	4.0	2.5E-05	-
171440	2.3	2.5E-05	Fungal specific transcription factor
45363	-3.6	2.5E-05	-
128721	2.2	2.5E-05	-
52257	3.1	2.5E-05	Ankyrin repeat
51992	-5.4	2.5E-05	-
46653	2.7	2.6E-05	-
212055	-2.3	2.6E-05	40S ribosomal protein S12
210632	-1.7	2.6E-05	tRNA synthetase anti-codon binding domain
200417	-2.5	2.6E-05	60S ribosomal protein L28
53197	-5.4	2.6E-05	Hypothetical IMP dehydrogenase
210783	4.1	2.6E-05	Hypothetical. Probable peroxisomal membrane. Interpro suggests alkylhydroperoxide reductase
188662	-2.7	2.6E-05	Nuclear transport factor 2
176941	-5.6	2.6E-05	RNA polymerase
188673	5.7	2.6E-05	AMP-dependent synthetase and ligase
214112	-5.5	2.6E-05	-
200967	-2.8	2.6E-05	-
56457	2.4	2.7E-05	(cmkB) calcium/calmodulin dependent protein kinase B - high homology to cmkB in A. nidulans
188691	5.0	2.7E-05	-
128111	3.2	2.7E-05	-
206692	-4.2	2.7E-05	Adenylosuccinate lyase
206105	-2.9	2.7E-05	-
184977	-3.8	2.7E-05	Mitochondrial substrate carrier
211004	9.9	2.7E-05	Glycosyl transferase, family 20
208493	2.6	2.7E-05	-
192136	-3.0	2.7E-05	Hypothetical protein shares amino acid sequence identity with the Saccharomyces cerevisiae RRS1 gene product; an essential protein that binds ribosomal protein L11 and is required for nuclear export of the 60S pre-ribosomal subunit during ribosome biogenesis
35670	4.5	2.8E-05	GCN5-related N-acetyltransferase
56033	-2.1	2.8E-05	Prolyl-4-hydroxylase

54662	-1.8	2.8E-05	Hypothetical SNF5/SMARCB1/INI1 protein - a key component of SWI/SNF-class complexes; KOG Class: Chromatin structure and dynamics; KOG Id: 1649; KOG Description: SWI-SNF chromatin remodelling complex, Snf5 subunit
122321	10.1	2.8E-05	Major facilitator superfamily
36031	-1.8	2.8E-05	Putative GroEL-like chaperone, ATPase
53784	2.6	2.8E-05	Ras small GTPase, Rab type
52118	8.2	2.8E-05	-
191597	4.8	2.8E-05	Short chain dehydrogenase
179383	2.3	2.8E-05	-
56247	2.6	2.8E-05	Phospholipase D. Active site motif
54557	2.3	2.8E-05	-
39817	-2.7	2.8E-05	Hypothetical glutathione-dependent formaldehyde-activating protein
36316	-3.7	2.8E-05	-
197459	-1.9	2.8E-05	Translation initiation factor
44432	4.9	2.8E-05	Helix loop helix transcription factor EB
55644	-2.3	2.9E-05	Putative Ribosomal protein S4/9
198674	-2.5	2.9E-05	60S ribosomal protein L10A
213042	6.1	2.9E-05	MOSC N-terminal beta barrel domain
42169	5.9	2.9E-05	-
35952	3.2	2.9E-05	-
207376	-3.1	2.9E-05	Predicted protein shares amino acid sequence identity to the Saccharomyces cerevisiae TIF34 gene product; subunit of the core complex of translation initiation factor 3(eIF3), which is essential for translation.
174968	4.4	2.9E-05	-
202504	-3.1	2.9E-05	40S ribosomal protein S19
197350	-3.4	2.9E-05	Ribosomal protein S9
193991	6.2	2.9E-05	-
40623	2.9	2.9E-05	-
213629	2.1	2.9E-05	Drebrins and related actin binding proteins
211941	-3.0	3.0E-05	Predicted protein shares amino acid sequence identity with the Saccharomyces cerevisiae TRM2 gene product; a tRNA methyltransferase, 5-methylates the uridine residue at position 54 of tRNAs and may also have a role in tRNA stabilization or maturation; previously thought to be an endo-exonuclease.
175113	4.8	3.0E-05	Predicted Yippee-type zinc-binding protein
173033	4.9	3.0E-05	Translation initiation factor 4F
201412	5.2	3.0E-05	-
211539	3.1	3.0E-05	-
206447	-3.4	3.0E-05	Hypothetical Aminotransferase
46218	-2.5	3.0E-05	Predicted kinase
199510	4.0	3.0E-05	Sugar transporter superfamily
50782	5.7	3.0E-05	Cytidine deaminase, homotetrameric
207758	2.4	3.1E-05	26S proteasome regulatory complex, subunit PSMD9
177222	2.2	3.1E-05	Hypothetical protein. May be involved in protein-protein interactions due to a predicted TPR-like domain
39988	4.6	3.1E-05	-
188987	3.2	3.1E-05	-
43297	9.9	3.1E-05	Glyoxylate/hydroxypyruvate reductase (D-isomer-specific 2-hydroxy acid dehydrogenase superfamily)
49674	4.7	3.1E-05	-
43695	3.7	3.1E-05	-
143899	4.7	3.1E-05	-

174332	-2.4	3.2E-05	Zn-finger, C2H2 type
197786	2.0	3.2E-05	(dapB) dipeptidylpeptidase
46410	-4.0	3.2E-05	Predicted protein involved in nuclear export of pre-ribosomes
43311	4.5	3.2E-05	Hypothetical carboxylesterase
213502	-5.6	3.2E-05	Dihydroxy-acid dehydratase
175410	-3.3	3.2E-05	Peptidase
171242	-5.3	3.2E-05	-
133197	2.8	3.2E-05	Transcriptional coactivator
45864	-5.7	3.2E-05	Deduced gene product shares amino acid sequence identity with the Saccharomyces cerevisiae NIP7 gene product; a nucleolar protein required for 60S ribosome subunit biogenesis, constituent of 66S pre-ribosomal particles.
207677	-3.0	3.2E-05	Deduced amino acid sequence shares identity with the Saccharomyces cerevisiae MRP49 gene product; a mitochondrial ribosomal protein of the large subunit.
186794	-2.2	3.2E-05	Related to pseudouridine synthase.
173835	2.2	3.2E-05	-
51810	6.1	3.2E-05	Glutathione S-transferase
212182	5.4	3.2E-05	-
212180	-2.3	3.2E-05	Putative GroEL-like chaperone, ATPase
198936	-1.9	3.2E-05	Hypothetical protein with PPR repeat
178649	2.3	3.2E-05	Nucleolar GTPase/ATPase p130
53770	4.4	3.3E-05	Hypothetical GPI anchor protein
38790	-4.0	3.3E-05	Hypothetical protein.
136905	2.1	3.3E-05	-
130434	-4.2	3.3E-05	Protein required for normal rRNA processing
129632	3.4	3.3E-05	-
170573	-3.9	3.3E-05	-
127683	2.1	3.3E-05	Flavoprotein
212884	2.2	3.3E-05	-
211361	2.9	3.3E-05	-
50014	-2.1	3.3E-05	RNA polymerase III (C) subunit
44753	1.9	3.3E-05	Esterase/lipase/thioesterase
212637	4.0	3.3E-05	Hypothetical protein containing fungal specific transcription factor and fungal transcriptional regulatory protein domains.
55041	-7.3	3.3E-05	-
37809	2.3	3.3E-05	-
50713	2.1	3.4E-05	Putative Zinc-containing alcohol dehydrogenase superfamily
212646	-2.3	3.4E-05	-
47390	1.8	3.4E-05	-
41394	5.3	3.4E-05	-
54217	3.5	3.4E-05	Conserved Zn-finger protein
41757	-2.3	3.4E-05	-
39893	5.2	3.4E-05	Synaptic vesicle transporter SVOP
209032	4.9	3.4E-05	-
55723	-4.0	3.4E-05	-
208354	-2.5	3.4E-05	-
55936	-4.1	3.4E-05	Related to N. crassa RNA polymerase, beta subunit
43930	5.9	3.4E-05	-
190605	-2.6	3.4E-05	-
183410	1.8	3.4E-05	-
55895	-2.3	3.5E-05	-
180348	4.8	3.5E-05	Peptidase S26
35556	6.1	3.5E-05	Hypothetical amidase (EC 3.5.1.4)
173461	2.2	3.5E-05	-

50898	-5.4	3.5E-05	Hypothetical permease. 10 predicted transmembrane domains. May have Xanthine/uracil transporter activity
206586	1.8	3.5E-05	Vacuolar assembly/sorting protein
42962	-3.2	3.5E-05	Adenine nucleotide translocator
38222	-2.2	3.5E-05	-
40484	4.2	3.5E-05	Peptidase M, neutral zinc metallopeptidases, zinc-binding site
175896	-4.2	3.5E-05	Glucose-6-phosphate/phosphate and phosphoenolpyruvate/phosphate antiporter
52938	3.3	3.5E-05	Esterase/lipase/thioesterase
46856	-3.2	3.5E-05	DEAD/DEAH box helicase
133565	3.5	3.5E-05	-
200493	-5.2	3.5E-05	Imidazoleglycerol-phosphate dehydratase
176865	2.7	3.5E-05	Hypothetical GPI anchor protein
211641	1.4	3.6E-05	-
196377	-3.6	3.6E-05	Mitochondrial/chloroplast ribosomal protein L2
39551	4.1	3.6E-05	Protein-L-isoaspartate(D-aspartate) O-methyltransferase
52046	-5.2	3.6E-05	Shares amino acid sequence identity with Saccharomyes cerevisiae EBP2 encoding an essential protein required for the maturation of 25S rRNA and 60S ribosomal subunit assembly; localises to the nucleolus; constituent of 66S pre-ribosomal particles.
127627	-2.7	3.6E-05	Candidate ribosomal protein S18
46999	-2.1	3.6E-05	Related to prephenate dehydrogenase of Candida albicans
174680	-2.0	3.7E-05	Candidate glucosyltransferase
206881	-1.8	3.7E-05	40S ribosomal protein S7
181216	4.1	3.7E-05	Kinesin light chain
55773	3.0	3.7E-05	-
52971	3.9	3.7E-05	Protein kinase
124393	4.5	3.7E-05	Peroxisomal NUDIX hydrolase
136845	-3.1	3.7E-05	Ribosomal protein
56736	-3.1	3.8E-05	Haloacid dehalogenase-like hydrolase
51412	2.2	3.8E-05	-
185461	8.4	3.8E-05	-
47290	-3.6	3.8E-05	Mitochondrial substrate carrier
174284	3.6	3.8E-05	-
176409	-5.3	3.8E-05	Hypothetical citrate synthase
209363	3.3	3.8E-05	-
185262	5.1	3.9E-05	-
50719	-4.5	3.9E-05	-
48814	7.6	3.9E-05	-
129172	1.6	3.9E-05	-
191450	3.0	3.9E-05	-
54566	-1.6	3.9E-05	Hypothetical tyrosyl-tRNA synthetase. Shows similarity with N. crassa tyrosyl-tRNA synthetase
54707	2.6	3.9E-05	Involved in autophagocytosis
54391	-3.5	3.9E-05	Hypothetical homoserine O-acetyltransferase (EC 2.3.1.31).
46991	-3.8	3.9E-05	Peptidase S16, lon protease
201439	-6.2	3.9E-05	Related to molecular chaperone DnaJ.
186614	-2.2	3.9E-05	-
172145	4.0	3.9E-05	-
197622	-2.3	3.9E-05	Putative GroEL-like chaperone, ATPase
137182	-3.0	3.9E-05	60S ribosomal protein L14
53140	2.7	3.9E-05	FMN-dependent dehydrogenase
41013	2.3	4.0E-05	-
52140	3.2	4.0E-05	Serine/threonine protein kinase

206235	-2.1	4.0E-05	40S ribosomal protein S8
40254	-5.0	4.0E-05	Hypothetical glucose oxidase (EC 1.1.3.4)
134353	3.3	4.0E-05	-
54483	-2.9	4.0E-05	Related to squalene synthetase (EC 2.5.1.21). Involved in lipid biosynthesis.
39541	-5.3	4.0E-05	Predicted protein shares amino acid sequence identity with the Saccharomyces cerevisiae UTP22 gene product; a possible U3 snoRNP protein involved in maturation of pre-18S rRNA, based on computational analysis of large-scale protein-protein interaction data.
48809	-2.9	4.0E-05	-
38758	3.7	4.0E-05	Fungal specific transcription factor
201957	2.1	4.0E-05	Synaptobrevin/VAMP-like protein
55027	1.8	4.1E-05	-
56776	6.2	4.1E-05	-
44662	-3.0	4.1E-05	-
202682	-2.3	4.1E-05	-
173346	2.4	4.1E-05	DEAD/DEAH box helicase
54575	-2.3	4.1E-05	-
40922	4.2	4.1E-05	Predicted dehydrogenase
35655	-4.2	4.1E-05	-
52998	-2.3	4.1E-05	Hypothetical protein. Pfam suggests activity similar to the SAM-dependent methyltransferase/cell division protein FtsJ
209716	1.9	4.1E-05	Cu2+/Zn2+ superoxide dismutase SOD1
211346	3.8	4.2E-05	-
206831	1.6	4.2E-05	Histone acetyltransferase complex
196832	-2.7	4.2E-05	Hypothetical pseudouridylate synthase
51832	-6.0	4.2E-05	-
43122	-3.2	4.2E-05	Hypothetical. Sequence similarity to S cerevisiae RRP15; Nucleolar, constituent of pre-60S ribosomal particles; required for processing of the 27S pre-rRNA
36700	-1.7	4.2E-05	AAA ATPase
119946	2.4	4.2E-05	AAA ATPase
136205	-3.4	4.2E-05	-
56454	-5.6	4.3E-05	-
54966	-2.0	4.3E-05	-
125912	4.4	4.3E-05	-
49486	-3.0	4.4E-05	-
143917	3.5	4.4E-05	Upstream transcription factor
52769	-4.6	4.4E-05	-
52748	-2.4	4.4E-05	Hypothetical. Sequence identity to protein component of the large (60S) ribosomal subunit
45989	-3.5	4.4E-05	Hypothetical UDP-glucose 4-epimerase
187754	2.1	4.5E-05	-
52536	3.8	4.5E-05	Ubiquitin-conjugating enzyme
202623	-1.9	4.5E-05	Hypothetical protein containing a Golgi phosphoprotein 3 domain
170610	2.3	4.5E-05	Cytochrome P450
136267	2.6	4.5E-05	Kinesin light chain
184532	2.9	4.5E-05	-
53238	3.1	4.5E-05	Candidate sterol 3-beta-glucosyltransferease
191568	5.6	4.6E-05	Predicted glutathione S-transferase
52717	-2.9	4.6E-05	Shares limited amino acid sequence identity with ribosomal protein L15, bacterial form.
47806	-2.1	4.6E-05	-
207173	2.2	4.6E-05	FYVE finger-containing protein

41983	2.6	4.6E-05	Amidohydrolase 2
139419	-4.8	4.6E-05	KRR1-interacting protein involved in 40S ribosome biogenesis
192151	6.2	4.6E-05	-
55704	2.6	4.7E-05	(tpsA) trehalose-6-phosphate synthase A
41591	-2.1	4.7E-05	-
201401	-2.6	4.7E-05	60S ribosomal protein L7
183782	-2.1	4.7E-05	Deduced protein shares amino acid sequence identity with Saccharomyces cerevisiae GCD10 gene product comprising a subunit of tRNA (1-methyladenosine) methyltransferase with Gcd14p; required for the modification of the adenine at position 58 in tRNAs, especially tRNAi-Met.
188287	2.4	4.7E-05	Hypothetical silent information regulator protein of the Sir2 family
213827	10.2	4.7E-05	Permease of the major facilitator superfamily
52617	7.6	4.7E-05	Aromatic-ring hydroxylase
207187	3.5	4.7E-05	Hypothetical protein with predicted Appr-1-p domain; KOG Class: Chromatin structure and dynamics; KOG Id: 2633; KOG Description: Hismacro and SEC14 domain-containing proteins
51912	-4.2	4.7E-05	Argininosuccinate lyase
52111	4.9	4.7E-05	Hypothetical beta-galactosidase. extracellular GH family 2
44202	-3.7	4.7E-05	G-protein containing WD40 repeats
206812	2.9	4.7E-05	-
133728	2.9	4.7E-05	-
212792	-2.6	4.7E-05	-
39731	3.0	4.7E-05	-
172733	-3.8	4.8E-05	Predicted membrane protein
211917	4.6	4.8E-05	Dual specificity phosphatase, catalytic domain
52969	-5.9	4.8E-05	Importin-beta, N-terminal
36379	-2.4	4.8E-05	Calcium-binding EF-hand
41518	3.5	4.8E-05	-
197959	-4.4	4.8E-05	Hypothetical. Sequence identity with S cerevisiae NOP53 gene (nuclear); involved in biogenesis of 60S subunit of ribosome.
187288	-2.3	4.8E-05	-
54041	3.4	4.8E-05	-
47225	-7.2	4.9E-05	-
40333	5.4	4.9E-05	-
39277	4.4	4.9E-05	-
190177	-4.4	4.9E-05	Predicted protein shares amino acid sequence identity with the Saccharomyces cerevisiae UTP13 gene product; a nucleolar protein, component of the small subunit (SSU) processome containing the U3 snoRNA that is involved in processing of pre-18S rRNA.
40780	3.2	5.0E-05	-
54128	4.1	5.0E-05	-
53524	-3.6	5.0E-05	-
191332	-1.9	5.0E-05	Serine/threonine kinase receptor-associated protein
55348	4.2	5.1E-05	-
187802	3.1	5.1E-05	-
52578	-2.2	5.1E-05	-
178568	2.3	5.1E-05	-
180990	4.8	5.2E-05	Zinc-binding oxidoreductase
143583	3.8	5.2E-05	-
206219	-4.6	5.2E-05	ERG2 and sigma1 receptor-like protein
130155	-1.7	5.2E-05	-
214206	2.6	5.2E-05	Nucleoside transporter

Identification of the most significantly expressed genes between N402 and N402 with *fum* and *frds* inserted, fold change in log2 ratio (positive number then expression level in N402 strain with gene insertions higher), p. value < 0.05, the general description is taken from the JGI annotation database.

JGI_ID	Fold change	p.value	General description
170261	2.9	1.7E-05	Permease of the major facilitator superfamily
49576	5.5	3.9E-05	Glucose/ribitol dehydrogenase
54383	4.0	3.9E-05	Splicing coactivator SRm160/300, subunit SRm300
180570	4.0	3.9E-05	Short-chain dehydrogenase/reductase SDR
56336	-3.5	4.5E-05	-
179170	6.8	4.6E-05	-
40825	5.2	4.6E-05	Geranylgeranyl pyrophosphate synthase/Polyprenyl synthetase
176795	4.4	4.6E-05	Hypothetical phenylalanine ammonia-lyase
35307	2.1	7.9E-05	-
131354	-2.2	8.2E-05	-
194591	4.7	9.5E-05	-
41998	3.2	9.5E-05	-
54080	-2.3	9.5E-05	-
48762	-4.1	9.5E-05	-
40740	3.2	1.1E-04	Hypothetical Short-chain dehydrogenase
41662	1.6	1.1E-04	-
52586	2.5	2.0E-04	Hypothetical protein with TPR-like domain
191345	3.1	2.3E-04	Related to carbonic anhydrase, protection against oxidative damage
119587	-2.1	2.3E-04	Glycosyl hydrolases family 18
194452	6.4	3.2E-04	-
177169	-2.7	3.5E-04	Hypothetical extracellular gluconolactonase
198715	1.6	4.5E-04	Related to tef1B; elongation factor 1 beta
54541	3.0	5.7E-04	Candidate oxidoreductase, Short-chain dehydrogenase/reductase
47386	2.8	5.7E-04	-
132154	-1.7	5.7E-04	Cytochrome P450
179001	-1.3	5.8E-04	Dihydroxy-acid dehydratase
37743	4.3	6.8E-04	-
127639	2.8	6.8E-04	-
173139	1.8	6.8E-04	Methionine synthase, vitamin-B12 independent
189022	4.7	7.8E-04	-
44428	4.0	7.8E-04	-
41394	3.8	7.8E-04	-
43594	3.0	7.8E-04	Hypothetical. SignalP suggests secreted
213612	-2.5	8.0E-04	Nucleolar GTPase
189398	1.6	8.2E-04	Protein of unknown function UPF0075
136267	1.9	8.5E-04	Kinesin light chain
42291	-1.5	8.6E-04	-
205291	-2.5	8.6E-04	Isocitrate and isopropylmalate dehydrogenases
52219	-2.0	9.0E-04	Glycoside hydrolase, family 28
44546	3.1	9.5E-04	-
179491	-1.5	1.0E-03	Serine/threonine protein kinase
52239	-2.3	1.0E-03	-
192151	4.3	1.2E-03	-

179385	-1.4	1.2E-03	Major facilitator superfamily
140548	-1.5	1.2E-03	Cytochrome P450
39667	3.0	1.2E-03	-
127335	-1.8	1.2E-03	-
35478	-1.3	1.3E-03	-
136326	-1.3	1.3E-03	-
55077	-1.4	1.4E-03	DNA-binding protein of the nucleobindin family
179673	4.2	1.4E-03	Ankyrin
126670	2.3	1.4E-03	-
133728	1.9	1.4E-03	-
42784	-2.4	1.4E-03	-
52111	-3.3	1.5E-03	Hypothetical beta-galactosidase. extracellular GH family 2
175401	4.5	1.5E-03	-
54636	3.0	1.6E-03	-
140623	-1.2	1.6E-03	Cytochrome P450
199928	-1.3	1.7E-03	Predicted hydrolase
54079	-2.6	1.7E-03	-
207067	-2.0	1.7E-03	HAD-superfamily hydrolase,
51794	2.9	1.7E-03	Extracellular ribonuclease M
42602	1.6	1.7E-03	Cytochrome P450
172476	-1.2	1.7E-03	-
208150	1.4	1.7E-03	FAD-dependent pyridine nucleotide-disulphide oxidoreductase
45103	5.0	1.7E-03	-
182162	3.1	1.8E-03	Hypothetical alpha-amylase
125836	-1.9	1.8E-03	-
171880	5.5	1.8E-03	Multicopper oxidase
193010	3.7	1.8E-03	Ferric reductase-like transmembrane component
43055	2.4	1.8E-03	-
39856	1.9	1.8E-03	-
35902	-1.3	1.8E-03	Fungal specific transcription factor
45042	-1.4	1.8E-03	-
41171	-1.6	1.8E-03	-
45928	3.4	1.8E-03	-
55305	1.4	1.8E-03	-
210217	-2.0	1.8E-03	Large beta-ketoacyl synthase probably involved in polyketide synthesis (aurasperone??)
202949	3.6	1.8E-03	Hypothetical. Has similarity to beta-1,6-N-acetylglucosaminyltransferase (KOG), contains WSC domain
44776	-1.1	1.8E-03	-
214441	1.0	1.9E-03	Hypothetical. KOG: acetyl-CoA acetyltransferase
182167	-1.2	1.9E-03	-
177882	-1.4	1.9E-03	-
175986	-1.3	1.9E-03	-
209075	-1.2	2.0E-03	Hypothetical mannosyltransferase activity
178804	-1.2	2.0E-03	Putative 2-dehydropantoate 2-reductase activity
55131	1.6	2.1E-03	-
52629	-1.2	2.1E-03	-
56664	-3.0	2.1E-03	Exoinulinase
55278	-3.5	2.1E-03	Hypothetical protein containing helix-turn-helix, Fis-type domain
54717	1.1	2.1E-03	-
55208	-2.4	2.1E-03	-
208525	5.3	2.3E-03	-

193984	1.9	2.3E-03	C4-dicarboxylate transporter/malic acid transport protein
194529	-1.4	2.3E-03	-
188240	-1.8	2.4E-03	-
56966	-2.6	2.4E-03	-
40876	3.4	2.4E-03	-
55402	-1.2	2.4E-03	-
209514	-1.7	2.4E-03	Myb, DNA-binding
133197	1.5	2.6E-03	Transcriptional coactivator
183352	-0.9	2.6E-03	Aromatic-ring hydroxylase
53015	4.6	2.7E-03	-
193767	2.0	2.7E-03	Predicted methyltransferase
129107	-1.1	2.7E-03	Hypothetical protein. Is likely to be involved in protein-protein interaction due to the presence of four TPR repeats.
53522	-1.1	2.7E-03	Hypothetical microtubule-associated protein essential for anaphase spindle elongation
42357	-1.2	2.7E-03	-
177244	-1.6	2.8E-03	-
212618	4.0	3.2E-03	-
180923	-1.4	3.2E-03	Major facilitator superfamily
194300	-1.5	3.2E-03	Candidate Ribonuclease III
176875	-1.1	3.3E-03	Receptor-activated Ca2+-permeable cation channels (STRPC family)
173803	1.9	3.3E-03	-
120113	1.6	3.3E-03	-
47364	1.1	3.3E-03	Candidate catalase
49158	-1.2	3.3E-03	Hypothetical NADH:flavin oxidoreductase/NADH oxidase-like protein
125323	2.9	3.3E-03	-
174497	-1.0	3.3E-03	-
40178	1.0	3.4E-03	-
186554	2.9	3.5E-03	Monooxygenase, FAD-binding
173689	1.1	3.6E-03	Protein kinase
37742	1.8	3.6E-03	Rhodopsin-like GPCR superfamily
37533	-1.7	3.7E-03	Unknown. SignalP predicts Anchor
186748	-1.8	3.7E-03	-
136363	-1.5	3.7E-03	-
54129	-1.2	3.7E-03	Isoflavone reductase
44405	-1.2	3.7E-03	Hypothetical DNA excision repair protein
178173	2.6	3.8E-03	-
195378	-1.0	3.8E-03	RNA polymerase II transcription initiation/nucleotide excision repair factor
206475	-1.3	3.8E-03	-
213113	-2.9	3.8E-03	Hypothetical cytochrome b5
195375	3.9	3.9E-03	Multicopper oxidase
118995	1.6	3.9E-03	WD40 repeat-containing protein
40885	-1.5	3.9E-03	beta-1,6-N-acetylglucosaminyltransferase, contains WSC domain
56215	-2.9	3.9E-03	Hypothetical Hydroxymethylglutaryl-coenzyme A synthase
193384	2.9	3.9E-03	-
140802	1.3	3.9E-03	Monocarboxylate transporter
207820	-0.7	3.9E-03	Major facilitator superfamily
202289	-0.9	3.9E-03	-
210798	-1.9	3.9E-03	Dienelactone hydrolase
41719	-1.0	4.0E-03	Hypothetical FAD/FMN-containing dehydrogenase
214466	-1.0	4.0E-03	Hypothetical. KOG suggests function in ER-Golgi transport

44401	-1.6	4.0E-03	-
192821	2.9	4.0E-03	Helicase-like transcription factor HLTF/DNA helicase RAD5, DEAD-box superfamily
192595	2.9	4.1E-03	-
36284	-1.1	4.1E-03	Hypothetical protein containing cytochrome c heme-binding site and Zn-finger, C2H2 type domains
40478	-2.8	4.1E-03	Aromatic-ring hydroxylase
183201	-0.7	4.2E-03	-
144154	-1.1	4.2E-03	-
189328	2.0	4.2E-03	-
134478	1.3	4.3E-03	-
119939	-1.5	4.3E-03	Fungal specific transcription factor
130000	3.0	4.3E-03	Vacuolar sorting protein VPS1, dynamin, and related proteins
214038	-0.9	4.3E-03	DEAD/DEAH box helicase
172955	-1.1	4.3E-03	Hydantoinase/oxoprolinase
173461	-1.1	4.3E-03	-
54174	-2.2	4.3E-03	Dihydroxy-acid dehydratase
192439	1.1	4.3E-03	ATP binding protein
122060	1.1	4.3E-03	-
55742	1.0	4.3E-03	aldA Aldehyde dehydrogenase (aldA) (EC 1.2.1.3)
172823	-1.0	4.4E-03	Related to zink transporter of A. fumigatus. Seven putative transmembrane domains and PFam domains for zink transport.
38570	-2.0	4.4E-03	Fibronectin type III domain
210119	-2.3	4.4E-03	Major facilitator superfamily
53002	1.1	4.4E-03	-
54966	-1.0	4.4E-03	-
180211	1.4	4.6E-03	Alpha/beta hydrolase
46858	3.0	4.6E-03	Hypothetical alcohol dehydrogenase; EC 1.1.1.1
45270	-1.2	4.6E-03	-
56311	-1.7	4.6E-03	Hypothetical Glucose-methanol-choline oxidoreductase
170984	-1.2	4.7E-03	-
36316	-1.8	4.7E-03	-
171113	-1.0	4.7E-03	Fatty acid desaturase
118832	-1.1	4.7E-03	ABC transporter
130814	-1.4	4.7E-03	-
207505	-0.9	4.7E-03	(pmrA) Secretory pathway Ca2+-ATPase
35683	-1.0	4.7E-03	-
55781	-1.1	4.8E-03	-
182202	-1.5	4.8E-03	DUF821 domain protein. Putative lipopolysaccharide-modifying enzyme;
52449	-1.3	4.8E-03	Transcription coactivator
35358	1.3	4.9E-03	CCAAT-binding transcription factor,
55296	-0.8	4.9E-03	Hypothetical threonyl-tRNA synthetase kinase. HMMPfam indicates Threonyl-tRNA synthetase kinase activity
43788	-1.4	4.9E-03	-
53945	-1.6	5.0E-03	Haem peroxidase, plant/fungal/bacterial
53909	-3.9	0.01	-
40617	-1.3	0.01	-
212637	-1.9	0.01	Hypothetical protein containing fungal specific transcription factor and fungal transcriptional regulatory protein domains.
134276	3.1	0.01	FOG: RRM domain
57420	-1.2	0.01	-
53233	-2.5	0.01	Hypothetical short chain dehydrogenase

190964	1.9	0.01	Predicted member of the intramitochondrial sorting protein family
35983	1.2	0.01	Conserved hypothetical ATP binding protein
186640	1.0	0.01	Hypothetical isoprenylcysteine carboxyl methyltransferase
50713	1.0	0.01	Putative Zinc-containing alcohol dehydrogenase superfamily
39373	0.9	0.01	-
132378	0.6	0.01	Amino acid transporters
181601	-0.9	0.01	-
175222	-1.0	0.01	Cell cycle-associated protein
128988	-1.1	0.01	Ankyrin
192367	-1.2	0.01	Uncharacterised conserved protein, contains TBC domain
44775	-1.3	0.01	-
210117	-1.4	0.01	-
182627	-1.6	0.01	-
38000	-2.2	0.01	Acetoacetyl-CoA synthase
182754	1.1	0.01	-
144008	-1.6	0.01	-
173989	-0.8	0.01	-
180295	-2.3	0.01	FAD-dependent oxidoreductase
52459	-1.1	0.01	-
211641	0.6	0.01	-
46090	2.5	0.01	-
190385	1.8	0.01	-
183718	-0.7	0.01	Predicted membrane protein
53918	-1.5	0.01	Fungal transcriptional regulatory protein
49896	-2.3	0.01	Mandelate racemase
206384	3.9	0.01	Related to aspartic protease
214715	2.8	0.01	Hypothetical. KOG suggests chitinase. SignalP suggests secretion
55721	2.5	0.01	Sulfatase
137681	1.6	0.01	Scytalone dehydratase
204381	-1.3	0.01	Voltage-gated shaker-like K+ channel, subunit beta/KCNAB
40613	-1.2	0.01	-
45912	-2.6	0.01	FMN-dependent alpha-hydroxy acid dehydrogenase
181053	3.1	0.01	ABC transporter
56390	2.8	0.01	Related to aspartate transaminase D-chain S. cerevisiae
214022	1.4	0.01	Adenosine kinase
53262	-1.0	0.01	-
211267	-1.1	0.01	Kinesin, motor region
51779	-2.6	0.01	-
49598	-1.7	0.01	Pyridine nucleotide-disulphide oxidoreductase, class-II
175034	-1.1	0.01	-
47399	-0.9	0.01	Aminoacyl-tRNA synthetase, class I
170610	-1.1	0.01	Cytochrome P450
129458	-1.2	0.01	-
36722	2.8	0.01	-
209480	-0.8	0.01	SNF2 family
48971	-1.0	0.01	-
174284	-1.6	0.01	-
206792	1.3	0.01	RNA polymerase subunit
171422	2.7	0.01	-
181735	-1.0	0.01	Fungal specific transcription factor
52107	-2.0	0.01	Chitinase
44975	2.0	0.01	Zinc-containing alcohol dehydrogenase

42184	-1.2	0.01	pgaX Exopolygalacturonase precursor (ExoPG) (Galacturan 1,4-alpha-galacturonidase)
42615	-1.5	0.01	-
44770	-1.3	0.01	-
213911	-3.5	0.01	Aldehyde dehydrogenase
52520	-2.3	0.01	Hypothetical Short-chain dehydrogenase/reductase
56643	2.4	0.01	Major facilitator superfamily
50823	0.9	0.01	Hypothetical Acetyl-CoA acetyltransferase
190362	-0.9	0.01	General substrate transporter
53471	-1.1	0.01	-
50154	2.0	0.01	Hypothetical ribulose-phosphate 3-epimerase
48666	0.7	0.01	-
202682	1.0	0.01	-
55650	-1.3	0.01	-
121359	-0.8	0.01	Glycosyl hydrolase family 20
51436	-1.1	0.01	-
179383	-1.0	0.01	-
203184	-2.2	0.01	O-methyltransferase, family 2
191636	1.4	0.01	Hypothetical protein. Electronic annotation suggests pyridine nucleotide-disulphide oxidoreductase
56753	-1.7	0.01	Aromatic-ring hydroxylase
39893	-2.2	0.01	Synaptic vesicle transporter SVOP
175357	-1.0	0.01	Sugar transporter superfamily
179947	3.1	0.01	Proline oxidase
44117	2.8	0.01	Ankyrin-repeat protein
50719	2.0	0.01	-
42378	1.6	0.01	Esterase/lipase/thioesterase
54208	-0.6	0.01	AAA ATPase
130155	-0.8	0.01	-
54785	-1.2	0.01	-
42470	-1.2	0.01	-
46699	-0.8	0.01	Hypothetical late Golgi protein sorting complex, subunit
213409	2.1	0.01	Monooxygenase, FAD-binding
134398	-0.9	0.01	Putative GH family 43 protein with 47% sequence identity to an Aspergillus nidulans endo-arabinanase (PMID: 16844780)
44909	-1.2	0.01	Flavin-containing monooxygenase
53517	-1.3	0.01	-
38610	1.2	0.01	possible Translation initiation factor 2B, beta subunit (eIF-2Bbeta/GCD7)
192136	1.2	0.01	Hypothetical protein shares amino acid sequence identity with the Saccharomyces cerevisiae RRS1 gene product; an essential protein that binds ribosomal protein L11 and is required for nuclear export of the 60S pre-ribosomal subunit during ribosome biogenesis
172651	-1.0	0.01	Vacuolar sorting protein 9 (VPS9) domain
53994	-1.6	0.01	-
36700	-0.8	0.01	AAA ATPase
40477	-2.5	0.01	Hypothetical. Some similarity to alkylhydroperoxidase
144038	-1.2	0.01	-
192694	1.4	0.01	Zinc-containing alcohol dehydrogenase
171978	-0.7	0.01	FOG: Zn-finger
176123	-1.2	0.01	-
196499	1.8	0.01	Major facilitator superfamily
45712	1.5	0.01	-
170609	1.6	0.01	-
56145	1.5	0.01	-

133512	1.3	0.01	-
184563	1.2	0.01	-
204582	-0.8	0.01	-
50140	-0.8	0.01	Related to 2,2-dialkylglycine decarboxylase of Burkholderia (4.1.1.64)
170624	-1.2	0.01	-
177616	-1.3	0.01	Sugar transporter superfamily
56475	-2.2	0.01	Aldo/keto reductase
41637	3.3	0.01	Calcium-binding EF-hand
39581	1.9	0.01	Peptidase C19, ubiquitin carboxyl-terminal hydrolase 2
207776	-1.3	0.01	Voltage-gated shaker-like K+ channe
42282	-1.3	0.01	-
176373	1.8	0.01	-
133870	-2.2	0.01	Hypothetical alpha-1,6-mannanase. GH family 76
124156	1.3	0.01	Candidate NAD dependent formate dehydrogenase
36028	0.9	0.01	Aminotransferase, class IV
209397	1.0	0.01	-
37608	-0.6	0.01	-
52284	-0.9	0.01	Hypothetical protein containing an ATP-dependent DNA ligase I motif
193872	-0.9	0.01	AAA ATPase
44792	-1.0	0.01	-
43224	-1.1	0.01	Fungal transcriptional regulatory protein
210291	1.2	0.01	-
36502	-1.7	0.01	Hypothetical cytochrome p-450
119444	2.3	0.01	Hypothetical protein. Possibly a DNA-dependent ATPase (SNF2 related)
137708	1.8	0.01	-
36079	1.1	0.01	-
45131	0.9	0.01	Hypothetical aldehyde dehydrogenase (EC 1.2.1.3).
52362	1.0	0.01	Candidate 40S ribosomal protein S0.
177916	-1.2	0.01	-
36162	0.8	0.01	-
43351	-1.1	0.01	-
180970	1.3	0.01	-
180635	1.2	0.01	-
170891	1.7	0.01	-
213970	1.4	0.01	-
170230	-2.1	0.01	-
199159	1.4	0.01	-
45514	-0.7	0.01	Hypothetical G-protein with WD-40 repeat
118624	-1.0	0.01	Putative polyketide synthase
52916	1.7	0.01	-
52676	0.9	0.01	60s ribosomal protein gene RPL5.
48772	-1.1	0.01	Protein kinase
213187	-0.6	0.01	Vesicle coat protein clathrin,
51410	-0.8	0.01	-
185291	-1.1	0.01	-
126473	1.9	0.01	-
55967	-0.8	0.01	Cytochrome P450
56240	-0.8	0.01	-
208591	-0.9	0.01	Serine carboxypeptidase
210141	-0.9	0.01	Peptidase
52565	-0.9	0.01	-

172232	-0.9	0.01	Hypothetical alpha-galactosidase; EC 3.2.1.22;
36613	-1.7	0.01	-
182426	-1.3	0.01	Hypothetical, ABC transporter
49639	-2.0	0.01	Short-chain dehydrogenase/reductase
173132	-0.9	0.01	WD domain, G-beta repeat
209822	2.1	0.01	Hypothetical ribosomal protein L1
180653	-0.8	0.01	-
54235	1.1	0.01	Chorismate synthase
40603	-1.2	0.01	-
37678	1.1	0.01	-
136603	0.9	0.01	Hypothetical transcription initiation factor. A putative YEATS domain is present in the sequence
214408	-0.9	0.01	Nucleic acid-binding OB-fold
212893	-1.3	0.01	Glycoside hydrolase
50306	1.8	0.01	Hypothetical ThiamineS, sulfur metabolism
200680	0.9	0.01	Eukaryotic translation initiation factor 3, subunit 7
214822	-0.6	0.01	-
121206	-0.8	0.01	Prolyl-tRNA synthetase
53410	-0.9	0.01	-
144147	-1.1	0.01	-
120638	-1.1	0.01	Fungal transcriptional regulatory protein
39128	-1.2	0.01	Hypothetical protein related to cytochrome P450 3A7
53065	-0.6	0.01	-
38790	1.6	0.01	Hypothetical protein.
181803	-1.4	0.01	-
195098	-1.5	0.01	-
43753	1.2	0.01	Hypothetical protein with predicted C-5 cytosine-specific DNA methylase and a peptidase domain; Interpro Id: 1525; Interpro description:C-5 cytosine-specific DNA methylase; GO Desc.: DNA binding and DNA methylation
39356	-1.1	0.01	-
210108	-1.7	0.01	AMP-dependent synthetase and ligase
37370	-0.8	0.01	-
209263	2.1	0.01	-
191243	1.0	0.01	Candidate amidase B (EC 3.5.1.4)
133158	-0.9	0.01	Fungal transcriptional regulatory protein
214651	2.4	0.01	Mannitol dehydrogenase
39268	-1.0	0.01	Fungal specific transcription factor
210981	-1.2	0.01	Putative extracellular GH family 3 beta-glucosiadse
172825	-1.8	0.01	-
40476	-2.2	0.01	-
191749	0.8	0.01	-
205501	-0.8	0.01	Hypothetical cell division cycle protein
183410	-0.7	0.01	-
209660	-1.6	0.01	SWI-SNF chromatin-remodelling complex protein
192085	1.9	0.01	-
173997	1.7	0.01	Deduced translation product shares amino acid sequence identity with the Saccharomyces cerevisiae NSR1 gene product; a nucleolar protein that binds nuclear localisation sequences, required for pre-rRNA processing and ribosome biogenesis.
199092	0.8	0.01	-
128516	-1.1	0.01	-
173704	-1.2	0.01	Major facilitator superfamily
47354	-1.9	0.01	-
56941	-0.8	0.01	-

122527	-0.9	0.01	Permease of the major facilitator superfamily
41808	-1.0	0.01	-
176070	1.1	0.01	ATP-dependent DNA ligase
194896	-0.8	0.01	Hypothetical amine oxidase
42844	-0.9	0.01	-
35824	2.1	0.01	-
130434	1.6	0.01	Protein required for normal rRNA processing
56298	-1.3	0.01	Putative mannosyl-oligosaccharide glucosidase, GH family 63
137752	0.7	0.01	60S ribosomal protein L18A
142587	-1.0	0.01	-
137102	1.0	0.01	-
38235	1.9	0.01	U3 small nucleolar ribonucleoprotein (snoRNP)
173835	-0.8	0.01	-
39623	-0.9	0.01	-
183116	-0.9	0.01	-
55324	-2.0	0.01	Putative extracellular tyrosinase
209842	1.1	0.01	Phosphoribosyl pyrophosphate synthetase
172691	-0.8	0.01	Serine/threonine protein kinase
45278	5.0	0.01	L-kynurenine hydrolase
178656	-0.8	0.01	-
140721	-0.9	0.01	-
40115	-2.5	0.01	Hypothetical protein with four predicted transmembrane domains
127191	-0.7	0.01	-
47312	-0.9	0.01	Kinesin-like protein
189874	-1.4	0.02	Short-chain dehydrogenase/reductase
214112	2.0	0.02	-
52421	-0.7	0.02	Peptidase M18, aminopeptidase I
208679	-1.4	0.02	-
50457	1.3	0.02	Nuclear GTP binding protein
45693	-1.4	0.02	-
214735	-1.6	0.02	Non-ribosomal peptide synthetase
42198	1.5	0.02	-
56566	-3.3	0.02	Major facilitator superfamily
209830	-3.0	0.02	Hypothetical FAD/FMN-containing dehydrogenase
35655	-1.6	0.02	-
131829	3.1	0.02	-
38152	1.7	0.02	-
54662	-0.6	0.02	Hypothetical SNF5/SMARCB1/INI1 protein - a key component of SWI/SNF-class complexes; KOG Class: Chromatin structure and dynamics; KOG Id: 1649; KOG Description: SWI-SNF chromatin remodelling complex, Snf5 subunit
37967	-1.7	0.02	-
49420	2.4	0.02	-
198577	1.4	0.02	Carnitine O-acyltransferase
127124	-0.5	0.02	-
171532	-1.1	0.02	-
55089	2.0	0.02	The basic-leucine zipper (bZIP) transcription factors of eukaryotes are proteins that contain a basic region mediating sequence-specific DNA-binding followed by a leucine zipper region required for dimerization
181179	1.6	0.02	Catechol dioxygenase, N-terminal
206859	0.8	0.02	40S ribosomal protein S14

213194	-1.0	0.02	Putative growth response protein
128882	-1.0	0.02	Predicted transporter (major facilitator superfamily)
206697	-1.2	0.02	Exocyst component protein and related proteins
42016	1.6	0.02	-
46999	-0.8	0.02	Related to prephenate dehydrogenase of Candida albicans
170910	-1.0	0.02	Glucose/ribitol dehydrogenase
173677	-1.3	0.02	Hypothetical. Ketopantoate reductase pyrimidin base metabolism
121987	-1.4	0.02	-
52754	1.3	0.02	Nucleolar protein NOP52/RRP1
211162	-0.9	0.02	Hypothetical 1,4-alpha-glucan branching enzyme
52257	-1.1	0.02	Ankyrin repeat
124027	-1.2	0.02	-
187859	-1.1	0.02	Kelch motif
49726	1.7	0.02	Related to the IMP3 gene product of Saccharomyces cerevisiae comprising a component of the SSU processome, which is required for pre-18S rRNA processing
38814	-0.6	0.02	-
134125	-1.1	0.02	Peptidase family M20/M25/M40
53788	-1.5	0.02	Nucleoside phosphatase
207380	0.8	0.02	Protein kinase
143580	0.8	0.02	40s ribosomal protein s10
53494	0.6	0.02	-
174132	-0.7	0.02	-
42449	-0.9	0.02	-
54127	-1.3	0.02	-
213343	-1.3	0.02	Predicted 3-hydroxy-3-methylglutaryl-CoA (HMG-CoA) reductase
50029	-1.5	0.02	-
54128	-1.6	0.02	-
209757	-1.5	0.02	-
53037	1.6	0.02	HEAT repeat-containing protein
38222	-0.8	0.02	-
46333	-0.8	0.02	RNA polymerase II transcription initiation factor TFIIA
209244	-1.1	0.02	Oxidoreductase
119822	-1.2	0.02	Nucleolar GTPase/ATPase p130
43664	-1.0	0.02	Esterase/lipase/thioesterase
209597	1.3	0.02	Protein kinase
120572	-0.7	0.02	N-methyltransferase
208923	-0.9	0.02	-
138440	-1.0	0.02	-
172914	-0.5	0.02	Peptidase, eukaryotic cysteine peptidase active site
45949	-0.6	0.02	-
176830	0.9	0.02	WD40 repeat nucleolar protein putatively involved in ribosome biogenesis
129111	-1.7	0.02	Hydantoinase/oxoprolinase
212044	0.5	0.02	Mitochondrial ADP/ATP carrier proteins
202623	-0.7	0.02	Hypothetical protein containing a Golgi phosphoprotein 3 domain
180613	-1.0	0.02	Hypothetical guanine nucleotide exchange factor
185623	1.0	0.02	-
143871	-1.9	0.02	Glycoside hydrolase, starch-binding
181710	-0.9	0.02	Major facilitator superfamily
47549	-1.4	0.02	-

50038	1.9	0.02	Hypothetical, Identity with cerev. Nob 1, nuclear protein involved in proteasome maturation and synthesis of 40S ribosomal subunits
208129	1.4	0.02	Glycine cleavage H-protein
37001	1.0	0.02	-
173284	-1.4	0.02	-
37764	-1.8	0.02	-
47113	1.8	0.02	-
47267	1.2	0.02	Hypothetical. Sequence identity with S.cerevisiae LCP5 gene product involved in maturation of 18S rRNA.
207134	0.7	0.02	-
57395	-0.7	0.02	Glycosyl transferase, family 39
124912	-0.9	0.02	Choline kinase
54199	-1.0	0.02	-
207532	-1.2	0.02	-
43746	-1.4	0.02	Hypothetical ribonuclease T1
52177	-1.7	0.02	Glycosyl transferase family 4
48103	-1.0	0.02	WD40 repeat-containing protein
211532	-1.1	0.02	Cytochrome P450
39083	1.0	0.02	-
211078	-0.6	0.02	Actin/actin-like
188287	-0.9	0.02	Hypothetical silent information regulator protein of the Sir2 family
40959	-0.6	0.02	-
196476	1.6	0.02	Phospho-2-dehydro-3-deoxyheptonate aldolase
180928	1.4	0.02	-
207718	1.1	0.02	Zn-finger, U1-like
181522	0.9	0.02	-
45500	-0.6	0.02	G-like protein containing WD-40 repeat
56504	-0.9	0.02	Hypothetical protein with RCC1 domain
181032	-0.9	0.02	Fungal specific transcription factor
36000	-1.6	0.02	-
180563	-1.6	0.02	-
178371	1.0	0.02	Splicing coactivator SRm160/300,
205776	-0.9	0.02	Predicted membrane protein
174907	1.1	0.02	Mitochondrial carrier protein
55728	-1.0	0.02	DNA topoisomerase II - ATPase-like, with high homology (topB)
47812	-0.7	0.02	OPT oligopeptide transporter protein
50075	1.3	0.02	DeoxyUTP pyrophosphatase
176989	-1.1	0.02	-
119367	-1.3	0.02	-
144060	-1.4	0.02	Related to Tar1 of K. lactis
204276	-2.3	0.02	Zinc-containing alcohol dehydrogenase
172647	1.5	0.02	Major facilitator superfamily
40922	1.5	0.02	Predicted dehydrogenase
202059	1.3	0.02	Isochorismatase hydrolase
42619	-1.0	0.02	DSBA oxidoreductase
46429	-1.1	0.02	Glycosyl hydrolases family 35
56195	-1.2	0.02	Carbohydrate kinase, FGGY
191214	-1.6	0.02	Hypothetical. Helicase domain
189637	-1.7	0.02	-
172079	1.8	0.02	-
48827	1.0	0.02	-
48109	-0.9	0.02	Myosin class II heavy chain

40924	-0.6	0.02	-
194286	-0.7	0.02	Flavin-containing monooxygenase FMO
48067	-2.4	0.02	Hydroxyindole-O-methyltransferase and related SAM-dependent methyltransferases
214657	3.8	0.02	-
36407	-1.9	0.02	-
181915	0.9	0.02	NB-ARC / TPR repeat
196617	0.9	0.02	GCN5-related N-acetyltransferase
187232	-0.9	0.02	-
188256	1.7	0.02	Hypothetical. Interpro: eukaryotic cysteine peptidase active site
55229	-0.9	0.02	Alpha/beta hydrolase
200255	-0.9	0.02	Hypothetical cation efflux protein
138063	-1.8	0.02	-
44094	-0.8	0.02	-
197549	1.5	0.02	Sugar (ANd other) transporter
173711	0.9	0.02	-
56137	0.7	0.02	-
42826	-0.5	0.02	Putative growth response protein
202202	-0.6	0.02	Hypothetical. Ca2+-binding actin-bundling protein (fimbrin/plastin)
53547	-1.6	0.02	-
185434	-1.9	0.02	Short chain dehydrogenase
207027	-2.6	0.02	Oxidoreductase, N-terminal
204746	0.9	0.02	Phosphoribosyl pyrophosphate synthetase
36288	0.9	0.02	-
195287	-1.2	0.02	-
45506	1.7	0.02	-
44487	-0.6	0.02	-
55156	-1.1	0.02	FOG: Zn-finger
44492	-0.7	0.02	ABC transporter
210672	-1.7	0.02	Short-chain dehydrogenase/reductase SDR
208917	1.7	0.02	-
198685	-0.7	0.03	-
136048	-1.0	0.03	Cytochrome c heme-binding site
210734	-0.9	0.03	Hypothetical protein with predicted histone deacetylase domain, which catalyses the removal of acetyl group of acetylated lysine residues in histones; KOG Class: Chromatin structure and dynamics; KOG Id: 1343; KOG Description: Histone deacetylase complex,
40878	1.3	0.03	Related to alpha-1,3-glucan synthase
208722	-0.7	0.03	-
205821	-1.0	0.03	HPr serine phosphorylation site
45893	-0.5	0.03	Putative glucosyltransferase
187212	-0.7	0.03	-
56449	-0.8	0.03	-
54864	2.6	0.03	Aromatic-ring hydroxylase
187934	0.8	0.03	Major facilitator superfamily
209129	1.2	0.03	-
207689	-1.4	0.03	Peptidase M20
35964	-2.1	0.03	Chitin synthase
209012	-2.3	0.03	Proteins containing the FAD binding domain
44615	0.7	0.03	-
171334	0.6	0.03	NADH:flavin oxidoreductase/NADH oxidase
180093	-1.7	0.03	-

122402	0.9	0.03	-
211773	-1.3	0.03	-
179092	-1.2	0.03	Serine/threonine protein kinase
184876	0.6	0.03	-
134406	-1.0	0.03	-
36826	1.6	0.03	-
35734	-0.7	0.03	-
181551	-1.3	0.03	GPCR, family 2, secretin-like
54294	0.8	0.03	-
138876	-1.3	0.03	beta-mannosidase A
56267	0.8	0.03	-
129373	-0.6	0.03	-
52229	-0.8	0.03	Zinc-containing alcohol dehydrogenase
181068	-0.9	0.03	Ras GTPase-activating protein family - IQGAP
55524	0.7	0.03	Hypothetical transmembrane protein
183186	2.1	0.03	Hypothetical Isoflavone reductase
36961	1.8	0.03	-
45817	-0.8	0.03	beta-1,6-N-acetylglucosaminyltransferase, contains WSC domain
141246	-1.8	0.03	-
171092	1.0	0.03	Monooxygenase involved in coenzyme Q (ubiquinone) biosynthesis
119858	-0.9	0.03	Related to alpha-glucosidase; glycoside hydrolase, family 31
119850	-0.8	0.03	-
185564	-0.9	0.03	Short-chain dehydrogenase/reductase SDR
55041	2.4	0.03	-
214397	1.6	0.03	Candidate aminotransferase, classes I and II
44464	-0.5	0.03	-
209060	-0.6	0.03	-
214831	-1.8	0.03	HPr serine phosphorylation site
182715	1.8	0.03	Hypothetical alpha-1,3-glucanase
188089	-0.9	0.03	Hypotehtical protein with galactose oxidase and transmembrane domains
182952	-0.6	0.03	-
176406	1.6	0.03	Deduced amino acid sequence shares identity with the Saccharomyces cerevisiae NHP2 gene product; a nuclear protein related to mammalian high mobility group (HMG) proteins, essential for function of H/ACA-type snoRNPs, which are involved in 18S rRNA proces
42098	-0.7	0.03	-
214017	-0.7	0.03	MEKK and related serine/threonine protein kinases
46980	-0.7	0.03	ABC transporter
52969	2.0	0.03	Importin-beta, N-terminal
38463	-0.7	0.03	-
197269	1.8	0.03	-
202416	0.6	0.03	40S ribosomal protein S3
41167	0.5	0.03	-
176469	0.5	0.03	-
35439	-0.7	0.03	Hypothetical part of the anaphase-promoting complex
39297	-0.9	0.03	Hypothetical carboxylesterase
51449	-1.6	0.03	Hypothetical. Monocarboxylate transporter. Signal P suggests secretion
181768	-0.7	0.03	Short-chain dehydrogenase
55805	-0.9	0.03	Hypothetical catalytic protein
125779	-0.9	0.03	-
170688	-1.4	0.03	-

178329	-0.8	0.03	Hypothetical protein with bromodomain & bromo adjacent region
195145	-0.8	0.03	-
188878	-0.8	0.03	Flavin-containing monooxygenase
36173	-1.0	0.03	DEAD/DEAH box helicase
54123	-2.2	0.03	-
187802	1.1	0.03	-
208123	-1.2	0.03	Eukaryotic translation initiation factor
56792	-0.8	0.03	Hypothetical GPI anchor protein
43317	-1.0	0.03	-
180050	-0.9	0.03	-
43031	-0.9	0.03	-
46719	1.4	0.03	Candidate multiple RNA-binding domain-containing protein.
187304	-0.5	0.03	Ergosterol biosynthesis ERG4/ERG24 family
130233	-0.6	0.03	-
40159	-1.0	0.03	-
52987	-1.5	0.03	-
176664	-0.8	0.03	Transcriptional activator FOSB/c-Fos and related bZIP transcription factors
177034	-0.6	0.03	-
52756	-1.0	0.03	-
180728	0.5	0.03	-
190721	-0.8	0.03	Putative transcription factor
206020	0.9	0.03	Hypothetical. involved in rRNA processing. associates with trans-acting ribosome biogenesis factors (yeast); similar to beta-transducin superfamily.
39220	1.3	0.03	-
185508	1.0	0.03	-
192063	-0.7	0.03	-
53033	-0.8	0.03	Related to beta-1,3-glucanosyltransferase
44216	1.0	0.03	-
184226	-0.5	0.03	Cell-cycle nuclear protein, contains WD-40 repeats
172670	1.0	0.03	-
210620	1.0	0.03	Predicted protein shares amino acid sequence similarity with the Saccharomyces cerevisiae UTP6 gene product
141681	0.8	0.03	-
56414	-1.0	0.03	-
45907	-1.4	0.03	-
45252	-0.7	0.03	-
129139	-0.8	0.03	Hypothtetical actin regulatory protein
208463	-0.7	0.03	-
39772	-0.7	0.03	Kinesin-like protein
52046	1.7	0.03	Shares amino acid sequence identity with Saccharomyes cerevisiae EBP2 encoding an essential protein required for the maturation of 25S rRNA and 60S ribosomal subunit assembly; localises to the nucleolus; constituent of 66S pre-ribosomal particles.
37965	-0.6	0.03	-
214849	-1.7	0.03	FAD-dependent pyridine nucleotide-disulphide oxidoreductase
52334	-0.6	0.03	-
40158	-0.7	0.03	Cytochrome P450
173432	-0.8	0.03	-
179912	-0.8	0.03	Putative extracellular carboxylesterase, type B
170414	1.0	0.03	Short chain dehydrogenase
194701	0.8	0.03	-

52402	0.8	0.03	-
184495	-0.8	0.03	-
185579	-0.8	0.03	-
187731	-1.2	0.03	-
119417	-1.1	0.03	Uso1/p115 like vesicle tethering protein
51125	1.8	0.03	-
189824	-0.7	0.03	-
191996	-1.2	0.03	Hypothetical flavin-containing amine oxidase
43917	-0.8	0.03	Peptidase S10, serine carboxypeptidase
55609	1.6	0.03	-
53082	1.3	0.03	Related to histone 1 protein, H1, with a predicted H1/H5 domain, histone linker N- terminal, and winged helix DNA binding. The protein is essential for chromatin stucture and links nucleosomes in higher order structures; KOG Class: Chromatin structure and
36612	-0.6	0.03	-
43907	-0.7	0.03	-
128111	-1.0	0.03	-
119238	-1.2	0.03	Fungal Zn(2)-Cys(6) binuclear cluster domain
205702	-1.4	0.03	Voltage-gated potassium channel activity
177282	-0.8	0.03	-
180223	0.8	0.03	Mitochondrial substrate carrier
188352	1.2	0.03	TetB, Synaptic vesicle transporter SVOP and related transporters (major facilitator superfamily
43466	-0.5	0.03	-
194006	0.8	0.03	-
170262	0.7	0.03	Aldo/keto reductase family proteins
45864	1.8	0.03	Deduced gene product shares amino acid sequence identity with the Saccharomyces cerevisiae NIP7 gene product; a nucleolar protein required for 60S ribosome subunit biogenesis, constituent of 66S pre-ribosomal particles.
140013	-0.9	0.03	-
123434	1.5	0.03	Iron/ascorbate family oxidoreductases
201697	0.8	0.03	Signal transduction protein with FHA domain
56235	-1.0	0.03	Peptidase C50, separase
45504	0.7	0.03	-
172198	-1.3	0.03	Putative cytochrome P450 monooxygenase
212736	-1.9	0.03	aglC, alpha-galactosidase; degradation of melibiose; EC 3.2.1.22; SwissProt ID AGALC_ASPNG; secreted alpha-galactosidase
170231	-0.7	0.03	-
188160	2.3	0.03	-
206713	0.5	0.03	-
36656	-0.5	0.03	Peptidase S15
133280	-0.8	0.03	Phosphatidylinositol-specific phospholipase C
214738	-1.9	0.03	Iron/ascorbate family oxidoreductases
120917	-0.6	0.03	-
55164	-1.3	0.03	-
206783	-2.1	0.03	-
38046	-0.4	0.03	Inner centromere protein
54125	-0.9	0.03	-
53546	-1.7	0.03	Putative Aconitate hydratase
214844	0.9	0.03	-
183599	0.8	0.03	Hypothetical sulfhydryl oxidase
40895	-1.1	0.03	von Willebrand factor and related coagulation proteins
57286	-0.8	0.03	RFX family transcription factor

194806	-1.0	0.03	Fungal specific transcription factor
42065	-1.3	0.04	-
133729	1.3	0.04	RNA-binding protein
55008	-0.7	0.04	Hypothetical HSP90 co-chaperone CPR7/Cyclophilin
53576	0.6	0.04	Candidate 60s ribosomal protein gene RPP1.
46056	-0.6	0.04	-
209577	-0.9	0.04	-
205026	1.5	0.04	-
125186	-1.2	0.04	Dehydrogenase
39998	-1.3	0.04	Hypothetical subunit of oligosaccharyltransferase
189922	-1.6	0.04	Cytochrome P450
52980	-1.7	0.04	-
209956	1.3	0.04	-
56167	0.6	0.04	TRIHA 14-3-3 protein homologue, putative kinase regulator
46227	-0.7	0.04	-
186514	-0.9	0.04	Chitinase
184760	-1.3	0.04	-
180802	-0.8	0.04	-
171940	-0.6	0.04	-
35670	-1.3	0.04	GCN5-related N-acetyltransferase
188517	0.9	0.04	-
170255	-0.5	0.04	Eukaryotic glutathione synthase
52241	-0.6	0.04	Glyoxalase
42146	-0.6	0.04	-
190884	-0.8	0.04	Cys/Met metabolism pyridoxal-phosphate-dependent enzymes
40615	-1.5	0.04	-
170954	-1.8	0.04	Transcription factor, MADS-box
50979	-2.1	0.04	Related to alpha-L-arabinofuranosidase
193602	0.8	0.04	-
52023	-1.2	0.04	Adenylosuccinate lyase
144063	-0.8	0.04	-
52418	1.2	0.04	Sugar transporter superfamily
141060	-0.4	0.04	Chloroperoxidase
52773	1.7	0.04	ABC transporter, transmembrane region
42932	1.2	0.04	Rhodopsin-like GPCR superfamily
121738	0.9	0.04	Na+/H+ antiporter
174228	-0.9	0.04	-
41246	-1.6	0.04	Fungal transcriptional regulatory protein, N-terminal
41128	1.0	0.04	-
136103	-0.7	0.04	-
209327	-0.7	0.04	Fungal transcriptional regulatory protein, N-terminal
196638	1.2	0.04	60S acidic ribosomal protein P0
46018	1.0	0.04	Amidohydrolase 2
57312	0.7	0.04	Related to C. albicans seryl-tRNA synthase (EC 6.1.1.11)
41387	-0.8	0.04	-
183143	1.0	0.04	-
187553	-0.8	0.04	-
178411	-0.9	0.04	-
194526	-2.0	0.04	Putative extracellular HpcH/HpaI aldolase
56391	-0.9	0.04	-
35594	-1.0	0.04	-
37314	-0.4	0.04	-
181863	-0.7	0.04	-

210854	1.8	0.04	-
185299	-2.0	0.04	Glycosyl transferase, group 1
121662	-0.6	0.04	Predicted transcriptional regulator
171186	1.7	0.04	-
209711	-1.1	0.04	-
172191	-0.8	0.04	-
43882	-0.5	0.04	Fungal specific transcription factor
174680	-0.6	0.04	Candidate glucosyltransferase
208602	-0.6	0.04	Candidate Ubiquinol cytochrome c oxidoreductase, subunit QCR9
174379	-1.4	0.04	Putative GH family 43 protein classified as beta-xylosidase (PTHR22925:SF4) and alpha-L-arabinanase (SSF75005)
193764	1.3	0.04	RNA polymerase II, large subunit
129910	1.5	0.04	Cytochrome P450
56345	1.1	0.04	Major facilitator superfamily
201349	0.7	0.04	Hypothetical protein with predicted histone deacetylase domain, which catalyses the removal of the acetyl group at acetylated lysine residues in histones; KOG Class: Chromatin structure and dynamics; KOG Id: 1343; KOG Description: Histone deacetylase comp
49207	-0.6	0.04	-
38580	-0.9	0.04	-
37992	-1.1	0.04	-
194381	-1.8	0.04	Putative polyketide synthase
41676	0.5	0.04	-
56078	-0.9	0.04	Deduced protein shares amino acid sequence identity with the Saccharomyces cereivisiae YRG054W gene product; eukaryotic initiation factor (eIF) 2A; associates specifically with both 40S subunits and 80 S ribosomes, and interacts genetically with both eIF5
45220	0.6	0.04	-
38774	0.6	0.04	Amidohydrolase-like
56389	-0.9	0.04	alpha/beta hydrolase fold
53315	2.1	0.04	-
53760	1.8	0.04	Glucose/ribitol dehydrogenase
144129	-1.0	0.04	-
39819	0.6	0.04	-
202429	-0.7	0.04	-
206654	-0.8	0.04	Fungal transcriptional regulatory protein
176564	-0.8	0.04	-
36770	-0.7	0.04	Major facilitator superfamily
207437	-0.6	0.04	Myb, DNA-binding
200072	-0.6	0.04	-
128638	1.4	0.04	Putative polyketide synthase
52590	-1.6	0.04	Putative alpha-1,3-glucanase, family 71
126969	-1.1	0.04	CDP-alcohol phosphatidyltransferase/Phosphatidylglycerol-phosphate synthase
173423	2.0	0.04	-
174620	1.1	0.04	-
171442	0.6	0.04	-
50449	-0.4	0.04	Hypothetical RNA procesing protein
174819	-0.5	0.04	-
44376	-0.6	0.04	-
209300	-0.8	0.04	-
191756	-1.5	0.04	-
170237	-2.5	0.04	Arylacetamide deacetylase
50781	1.6	0.04	Related to Mitochondrial transport protein amc-1

208535	0.6	0.04	-
50103	1.1	0.04	Hypothetical, Nucleolar GTPase/ATPase
42654	-0.8	0.04	Hypothetical protein containing Zn-finger and Homeobox domains
52574	-0.6	0.04	-
44103	-1.1	0.04	-
38673	-0.6	0.04	Hypothetical Shugoshin_N, nuclear.
208323	-0.6	0.04	-
36936	-0.6	0.04	-
182100	3.2	0.04	Hypothetical alpha-arabinanase (GH family 43)
201083	0.6	0.04	Phosphatidylinositol transfer protein SEC14
139753	-0.7	0.04	-
131182	-0.8	0.04	-
213492	-1.5	0.04	Glycosyltransferase, family 2
126001	-0.7	0.04	-
213629	-0.6	0.04	Drebrins and related actin binding proteins
54890	1.4	0.04	Carbamoyl-phosphate synthase
52705	0.9	0.04	Predicted protein shares amino acid sequence identity with the Saccharomyces cerevisiae TUF1 gene product; mitochondrial translation elongation factor Tu.
139686	0.7	0.04	-
121949	-0.9	0.04	-
52706	-0.7	0.04	Nucleoside phosphatase
49148	1.3	0.04	-
206715	-0.9	0.04	Putative calcium-dependent, mannose-binding lectin implicated in substrate-specific glycoprotein secreting pathway
213656	-1.2	0.04	C2 domain
37775	-1.0	0.04	Hypothetical protein containing Zn-finger, C2H2 type domain
212954	-1.3	0.04	-
204764	1.3	0.04	-
41530	-1.2	0.04	Hypothetical glycosylphosphatidylinositol anchor synthesis protein
211774	-1.5	0.04	Amino acid/polyamine transporter I
36409	-1.6	0.04	Ankyrin repeat
186422	-0.7	0.04	Sterol O-acyltransferase/Diacylglycerol O-acyltransferase
51800	1.0	0.04	Predicted protein shares amino acid sequence identity with the Saccharomyces cerevisiae TMA19 gene product
39626	0.5	0.04	Hypothetical protein
173978	-0.4	0.04	-
35780	-0.6	0.04	-
209988	-0.4	0.04	-
39012	-0.5	0.04	-
192619	-1.0	0.04	Serine carboxypeptidase
36287	0.9	0.04	Candidate anbA gene
37502	-1.0	0.04	-
42764	-1.4	0.04	-
38264	1.0	0.04	-
139793	-1.1	0.04	Fungal specific transcription factor
41595	-0.8	0.04	-
43621	-0.6	0.04	SAM (and some other nucleotide) binding motif
50981	-1.1	0.04	Putative AMP-dependent synthetase and ligase, Acyl-CoA synthetase
214443	-1.3	0.04	Putative Zinc transporter ZIP, Zn /Fe
51242	-0.5	0.04	CPSF A subunit

188782	1.5	0.04	Amino acid transporters
123724	0.5	0.04	-
130472	-0.8	0.04	Fungal specific transcription factor
52639	-1.1	0.04	SAM (and some other nucleotide) binding motif
173684	2.6	0.04	-
45703	-0.6	0.04	-
49539	-0.8	0.04	Candidate nimA
210220	-1.3	0.04	Short-chain dehydrogenase/reductase SDR
188056	-1.6	0.04	Cytochrome P450
55116	-1.6	0.04	Hypothetical short chain dehydrogenase
41809	-1.8	0.04	Major facilitator superfamily
39459	1.0	0.04	-
119945	-0.5	0.04	-
211367	-0.8	0.04	-
47819	-1.1	0.04	-
183336	-0.5	0.04	-
37022	-0.7	0.04	-
51512	-1.1	0.04	Cytochrome P450
124393	-1.3	0.04	Peroxisomal NUDIX hydrolase
35600	-0.6	0.04	-
43379	-0.6	0.04	-
210062	0.5	0.04	-
42083	-0.5	0.04	-
189853	0.8	0.04	-
206534	-1.2	0.04	Zinc-binding oxidoreductase
182904	-0.4	0.04	-
124797	-1.4	0.04	Major facilitator superfamily
124998	1.4	0.04	-
211845	-1.1	0.04	Glycosyl transferase, family 15
123304	-1.1	0.04	Amino acid/polyamine transporter
175633	-1.1	0.04	Cytochrome P450
53197	1.5	0.04	Hypothetical IMP dehydrogenase
37320	0.9	0.04	Shares amino acid sequence identity to Saccharomyces cerevisiae FAL1 encoding a nucleolar protein required for maturation of 18S rRNA; member of the eIF4A subfamily of DEAD-box ATP-dependent RNA helicases.
186889	-0.9	0.04	-
55422	-0.9	0.04	Related to vesicle coat complex COPII, subunit Sec23/24
211789	-1.6	0.04	-
196062	1.7	0.04	Deduced translation product shares amino acid sequence identity with the Saccharomyces cerevisiae NOP1 gene product; a nucleolar protein, component of the small subunit processome complex, which is required for processing of pre-18S rRNA; has similarity t
143583	-1.2	0.04	-
188497	-1.1	0.05	Fungal specific transcription factor
212470	-0.5	0.05	Peptidase C19
55540	0.7	0.05	-
44861	0.5	0.05	-
197559	0.9	0.05	60S ribosomal protein L22
176395	-1.2	0.05	WD40 repeat-containing protein
52769	1.4	0.05	-
56474	-1.2	0.05	-
212624	-0.6	0.05	-
38375	-0.9	0.05	Major facilitator superfamily

46410	1.1	0.05	Predicted protein involved in nuclear export of pre-ribosomes
57320	-0.8	0.05	-
53694	-0.8	0.05	-
46834	1.1	0.05	Major facilitator superfamily
196058	-0.8	0.05	Transcription factor/CCAAT displacement protein
183896	-0.6	0.05	Fungal specific transcription factor
193766	1.7	0.05	-
52416	0.6	0.05	-
179558	-0.7	0.05	-
182005	1.0	0.05	Amino acid permease
35440	-0.6	0.05	Hypothetical phosphatidylserine decarboxylase (EC 4.1.1.65)
49383	-0.6	0.05	-
195249	-0.8	0.05	-
176332	1.1	0.05	-
120694	0.6	0.05	Candidate Ferric reductase
53078	-0.6	0.05	-
52322	-2.7	0.05	-
38230	-1.0	0.05	Acyl-CoA synthetase
38316	-1.4	0.05	Non-ribosomal peptide synthetase
49258	0.9	0.05	Hypothetical aldehyde dehydrogenase. May be a succinate-semialdehyde dehydrogenase
190726	-0.6	0.05	-
206452	-0.7	0.05	klpA Kinesin family protein, motor region, KAR3
188804	-0.9	0.05	-
39613	0.7	0.05	Putative extracellular GH afmily 3 beta-glucosidase
56739	-1.5	0.05	Ornithine-N5-oxygenase
52163	-0.5	0.05	Actin/actin-like
181426	-0.5	0.05	WD40 repeat-containing protein
38291	-0.5	0.05	-
126879	-0.4	0.05	-
51281	1.5	0.05	3-hydroxyanthranilate oxygenase HAAO
123881	-1.1	0.05	-
183990	-1.2	0.05	Major facilitator superfamily
206990	0.6	0.05	HMG box-containing protein
56469	-0.7	0.05	Hypothetical protein with WD40-like region
46394	-0.8	0.05	Hypothetical methionine aminopeptidase
47077	-1.2	0.05	Oxidoreductase
36465	0.8	0.05	Hypothetical protein with predicted histone-fold; KOG Class: Transcription; KOG Id: 0871; KOG description: Class 2 transcription repressor NC2, beta subunit (Dr1)
55011	-0.8	0.05	51kDa subunit of NADH:ubiquinone reductase (complex I); NADH dehydrogenase [Aspergillus niger]
55417	-1.1	0.05	Serine/threonine protein kinase, active site
171166	-0.7	0.05	Major facilitator superfamily
134668	1.9	0.05	-
193651	-0.5	0.05	Zn-finger, C-x8-C-x5-C-x3-H type
41492	0.8	0.05	-
175768	1.4	0.05	HORMA domain
50549	0.9	0.05	Hypothetical. G-protein. WD40 repeat-containing
51478	0.6	0.05	(faeB) feruloyl esterase
37730	1.3	0.05	-
207862	0.6	0.05	This domain is found in a number of fungal transcription factors. The N-terminal region of a number of fungal transcriptional regulatory proteins contains a Cys-rich motif that is involved in zinc-dependent binding of DNA.

177198	-1.1	0.05	-
54806	-1.3	0.05	-
38807	-0.8	0.05	Protoporphyrinogen oxidase

Identification of the most significantly expressed genes between NW185 and NW185 with *fum* and *frds* inserted, fold change in log2 ratio (positive number then expression level in NW185 strain with gene insertions higher), p. value < 0.05, the general description is taken from the JGI annotation database.

JGI_ID	Fold change	p.value	General description
135002	-1.5	0.01	-
51515	4.4	0.03	Short-chain dehydrogenase/reductase SDR
55205	2.8	0.03	Hypothetical short chain dehydrogenase
43953	-1.9	0.04	-
45814	1.0	0.04	-